Advanced Propellant Chemistry

A symposium cosponsored by the Division of Fuel Chemistry of the American Chemical Society and the Propellants and Combustion Technical Committee of the American Institute of Aeronautics and Astronautics. Presented at the 149th Meeting of the American Chemical Society, Detroit, Mich., April 6–7, 1965.

Richard T. Holzmann, *Symposium Chairman*

ADVANCES IN CHEMISTRY SERIES 54

AMERICAN CHEMICAL SOCIETY

WASHINGTON, D.C. 1966

Publication Date: January 1, 1966 | doi: 10.1021/ba-1966-0054.fw001

Publication Date: January 1, 1966 | doi: 10.1021/ba-1966-0054.fw001

Library of Congress Catalog Card 66-22356

PRINTED IN THE UNITED STATES OF AMERICA

Publication Date: January 1, 1966 | doi: 10.1021/ba-1966-0054.fw001

Advances in Chemistry Series

Robert F. Gould, ***Editor***

AMERICAN CHEMICAL SOCIETY PUBLICATIONS

Publication Date: January 1, 1966 | doi: 10.1021/ba-1966-0054.fw001

FOREWORD

ADVANCES IN CHEMISTRY SERIES was founded in 1949 by the American Chemical Society as an outlet for symposia and collections of data in special areas of topical interest that could not be accommodated in the Society's journals. It provides a medium for symposia that would otherwise be fragmented, their papers distributed among several journals or not published at all. Papers are refereed critically according to ACS editorial standards and receive the careful attention and processing characteristic of ACS publications. Papers published in ADVANCES IN CHEMISTRY SERIES are original contributions not published elsewhere in whole or major part and include reports of research as well as reviews since symposia may embrace both types of presentation.

PREFACE

Advanced propellant chemistry embodies all aspects of chemistry which are normally used commercially to bring a product to market. New molecules must be synthesized, characterized, and produced on a scale adequate to effect a proper evaluation. Various military departments place as much emphasis on safety as on increased energy since rockets must be capable of safe handling by service personnel under combat conditions. Thus, questions of long term storage stability become paramount as the product advances to its end-use stage. In addition, the propellants must be safe with respect to impact, heat, and penetration by projectiles. On the other hand, in the test phase less stringent safety requirements are needed since in the hands of highly trained scientific personnel, much more hazardous ingredients can be tolerated.

In this symposium both the chemical and propulsion companies are heavily represented, but this was not always true. Increased government support of propulsion research since 1958 necessitated the involvement of major segments of the chemical industry. Before this time, most propulsion research was conducted by propulsion companies as an essential aspect of product improvement and competitive marketing. The competition, in the more basic research areas, between propellant chemists and industrial chemists working on propellant ingredients has tended to improve the quality of both.

Many of the great advances in modern inorganic chemistry in the past few decades have been a direct result of federal support in the areas of explosives and propellants. Aside from the transuranium elements, the chemistry of boron, beryllium, and fluorine have been elucidated because of this support. Research in fluorine chemistry was stimulated by the interest of the Atomic Energy Commission, and recent propellant work has shown it to be a "mild" reagent compared with other chemicals. One no longer needs to rely solely on the disruptive electrochemical and jet fluorinations; fluorine has been tamed and can be handled as easily as other halogens. The resurgence of boron hydride chemistry owing to AEC interest in volatile uranium compounds and military interest in the energy of these molecules, has revealed a chemical potential which as yet is barely tapped. Nonvacuum line, aqueous chemistry of the boron hydrides and fluorine itself will most assuredly lead to industrial applications of great magnitude in the next decades.

Publication Date: January 1, 1966 | doi: 10.1021/ba-1966-0054.pr001

In Advanced Propellant Chemistry; Holzmann, R.;
Advances in Chemistry; American Chemical Society: Washington, DC, 1966.

The chemistry reported in this volume was selected to give the uninitiated an appreciation of the scope of propellant research. The areas of thermochemistry, combustion research, polymer modification, materials research, etc., have intentionally been excluded since other forums have existed for them.

I would like to acknowledge publicly the many chemists and engineers who have made these papers possible but who will never receive acknowledgment owing to the nature of their contributions. Inadequately stated, their devotion to the public interest and to chemistry have made this work possible.

RICHARD T. HOLZMANN

Washington, D. C.
July 1965

Publication Date: January 1, 1966 | doi: 10.1021/ba-1966-0054.pr001

The Nature of an Advanced Propellant

RICHARD T. HOLZMANN[1]

Advanced Research Projects Agency, Washington, D.C.

Although propellant chemistry research concerns itself with everything from the synthesis and characterization of new molecules to their formulation and combustion in a rocket motor or engine, advanced propellant chemistry is primarily directed towards the search for new oxidizers. This intense effort is dictated by the greater contribution to energy which can be made by a small improvement here since the oxidizer normally comprises 70–80% by weight of the propellant combination. A semitheoretical approach to the ultimate energy achievable in propellants is presented.

Publication Date: January 1, 1966 | doi: 10.1021/ba-1966-0054.ch001

The propellant chemist knows what is needed to make a truly advanced propellant—the energy of the cryogenics (fluorine/hydrogen), the density of solids, and the ability to tailor properties to the mission at hand. The energetics are a direct consequence of the simplified specific impulse relationship:

$$I_s = \frac{F}{\dot{w}} = \frac{\text{thrust}}{\text{weight rate of flow}}$$

which is a major aspect of propellant performance expressed in units of pound per pound per second, or more commonly, just seconds. The overall efficiency of the rocket system, in turn, depends on the combined efficiencies of the combustion chamber (where the propellants are burned) and the nozzle (where the thermal energy is converted to kinetic energy). As a rough approximation in screening potential propellant combinations, it is frequently considered that specific impulse is proportional to:

$$\sqrt{\frac{\Delta H}{\bar{M}}}$$

[1] Present Address: Aerojet-General Corp., Chemical Products Division, Azusa, Calif.

In Advanced Propellant Chemistry; Holzmann, R.;
Advances in Chemistry; American Chemical Society: Washington, DC, 1966.

Thus, simply stated, a high heat release yielding low molecular weight products is most desirable.

The total figure of merit of propellant system performance is usually taken to be specific impulse multiplied by propellant bulk density to some exponent which may range from 0.05 to 1.0. The actual value of the exponent depends upon a complex relationship among the propellant, its properties, the mission, and design criteria. Thus, the high density of the propellant in a volume-limited application such as an air-launched missile is extremely important whereas for an upper-stage it is not nearly so critical.

The mission similarly influences the essential properties of the propellant ingredients. The military require rocket motors or engines which will withstand operational thermal cycling and handling. In addition, they must be safe under combat conditions in that they will not detonate in a fire or when struck by bullets, for example. They must be capable of storage for years—ideally under hermetically sealed conditions. There are many who presume that a more energetic advanced propellant necessarily must be less safe owing to the explosion hazard. They are confusing the thermodynamic and kinetic parameters. On the other hand, rockets for space applications do not have the serious restrictions inherent in a military mission, and thus cryogenics find a notable use. Consequently, advanced propellant chemistry is not generally concerned with cryogenics but rather with conferring the energetics of the cryogenics on earth-storable liquids and solids. With some levity then, one may strive to make hydrogen and fluorine liquid or solid at room temperature! This leads directly to the context of this symposium.

The first several papers concern themselves with a theoretical approach to extremely advanced oxidizers; the next group examine oxidizers primarily by studying important physical and combustion characteristics in propellants. Two papers follow on binders which act as fuels as well as conferring desirable physical properties on solid propellants. At this point there is no coverage of the light metal hydride fuels.

The next five papers explore the physical, combustion and detonation properties of liquid systems. The balance of the symposium is concerned primarily with the more energetic oxidizers based upon nitrogen-fluorine and oxygen-fluorine bonding. It is from this area that the most significant improvements will one day come, for with the oxidizer comprising 70–80% of the propellant combination, a relatively small improvement here is magnified as compared with the fuel. The use of metals, mentioned above, in both solid propellants and in liquid slurries, has been widely publicized and will not be discussed here. Their use, incidentally, originated in explosives technology and is commonplace at the present time.

Publication Date: January 1, 1966 | doi: 10.1021/ba-1966-0054.ch001

As broad as the coverage of this symposium appears, there is much propellant chemistry which has not been included. The experimental determination of thermodynamic properties such as heats of formation and equilibrium constants as well as the calculations of theoretical performance have been presented at other symposia. The applied chemistry related to modifying polymers, and hence mechanical and burning properties of solids, have other forums. The actual firing of solid motors and determination of thrust and efficiency have been omitted while the research into combustion instability and the transition from deflagration to detonation are only alluded to.

Publication Date: January 1, 1966 | doi: 10.1021/ba-1966-0054.ch001

The Advanced Propellant

The ideal advanced propellant is then one which yields a high heat release in the chamber and converts this to translational kinetic energy in the nozzle while generating low molecular weight "perfect" gases. This latter requirement is rarely satisfied owing to the presence of HF, CO, CO_2 and H_2O in the metal-free systems and to condensed metal oxides in the metal systems. This two-phase flow problem with a metallized propellant can easily result in a 5% efficiency loss. Therefore, although the metals have an extremely attractive heat release, a penalty of 5% is imposed from the start, even presuming perfect combustion efficiency. Everything considered, a performance of 92% is close to maximum efficiency. The metal-free liquid bipropellant systems, however, are capable of achieving 97–98% of theoretical performance.

Low molecular weight "perfect" gases clearly point the way to hydrogen, which accounts for the extreme performance of a nuclear propulsion unit. In this system, the reactor merely heats the lightweight gas. Although methane and ammonia have also been considered for nuclear applications, decomposed methane has a molecular weight of 5.4, ammonia of 7 while hydrogen has a molecular weight of 2. If too high temperatures are employed, molecular hydrogen will dissociate into atoms and absorb additional energy. In a chemical propulsion system the hydrogen will come, in the case of solids, from the binder and NH_4ClO_4 and, in liquids, from N_2H_4 and its derivatives or pentaborane or diborane—the latter being space-storable but not earth-storable. Much of the simple theoretical comparisons of oxidizers are therefore based on combustion with N_2H_4 or B_5H_9 for liquids and on more complex systems for solids.

Barrère (*1*) has published the performance calculations shown in Tables I and II.

It can be seen that future storable liquid propellant systems are in the 300–315 sec. range while future solid systems are around 290 sec.

Table I. Storables

		Propellant Composition	I_s	I_{sd}
Solid	Present	Ammonium perchlorate Al + plastic	267	455
	Future	Ammonium perchlorate LiBe + plastic	290	377
Liquid	Present	HNO_3–UDMH	276	348
		HNO_3–N_2H_4	283	362
		N_2O_4–UDMH	285	336
		N_2O_4–N_2H_4	292	356
		H_2O_2–UDMH	278	345
		H_2O_2–N_2H_4	282	355
	Future	ClO_3F–N_2H_4	295	360
		N_2O_4–B_5H_9	306	337
		H_2O_2–B_5H_9	312	311
		ClF_3–N_2H_4	294	444
Hybrid	Present	H_2O_2–Al + plastic	289	435
		HNO_3–Al + plastic	273	414
		NO_2ClO_4–N_2H_4	295	428
	Future	ClF_3–LiH	293	445
		ClF_3–Li	318	369
		N_2O_4–BeH_2	351	530
		H_2O_2–BeH_2	375	566

Table II. Cryogenics

	Propellant Composition	I_s	I_{sd}
Liquid	O_2–H_2	391	109
	O_2–N_2H_4	335	365
	F_2–H_2	410	185
	F_2–N_2H_4	363	476
	O_2–F_2–UDMH	345	398
	F_2–LiH	363	476
	F_2–O_2–plastic	343	412
Hybrid	F_2–BeH_2	395	604
	O_2–BeH_2	371	486
	F_2–AlH_3	353	551

Table III

	b.p. °C.	I_{sp} N_2H_4	I_{sp} B_5H_9
N_2F_4	−74	333	333
OF_2	−145	345	359

Barrère's analysis did not mention N_2F_4 or OF_2 since these are "soft" cryogenics, in that their boiling points are low. Their performance is excellent, however, as Table III shows.

The performance of F_2, OF_2, and NF_3 or N_2F_4 shows where the synthesis potential of rocket oxidizers is.

An attempt has been made here to determine the relative value of an oxidizing group as a propellant with a model fuel, N_2H_4. Hydrazine was chosen for simplicity and availability of calculations. The ΔH_f has been chosen in most cases by analogy. For example, to obtain one point

Publication Date: January 1, 1966 | doi: 10.1021/ba-1966-0054.ch001

for an —O, one may use one-third of +30 kcal./mole, the ΔH_f of O_3. For another point, one-half of —3.48 kcal./mole, the ΔH_f of $O_2(l)$. In this manner a series of curves were generated (Figure 1). Inherent then in any calculation of this type is the nature of the group to which the oxidizing group of interest is bonded. Several conclusions which can be drawn from such a curve would have been approximated "intuitively" by the synthesis chemist by reason of his background knowledge.

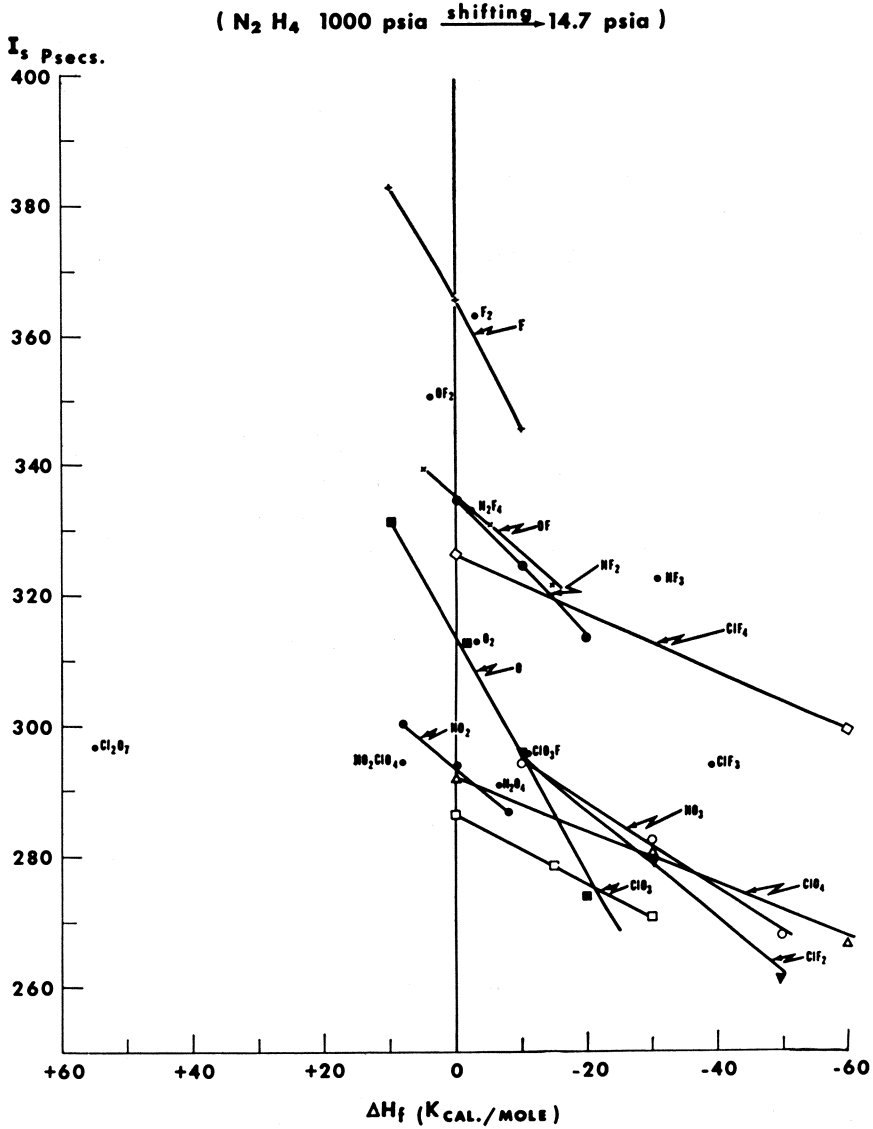

Figure 1. Oxidizer group contributions

Table IV. Relative Order of Oxidizing Power

—F	—ClF_2
—OF	—NO_3
—NF_2	—ClO_4
—ClF_4	—NO_2
—O	—ClO_3

If one chooses a constant ΔH_f, an index of oxidizing power may be obtained. For a $\Delta H_f = -10$ kcal./mole, the order in Table IV is observed.

If one chooses a target I_{sp}, there appear to be certain groups which, if embodied in an oxidizer, would have difficulty in attaining the objective. If 310 sec. is chosen as the target, the groups in Table V would not be expected to reach the objective unless combined with the highly energetic groups above them in Table IV.

Table V. Oxidizer Groups Not Expected to Yield 310 secs.

—ClF_2
—NO_3
—ClO_4
—NO_2
—ClO_3

The steepest slopes observed are those for —F and —O indicating the dramatic contribution to impulse by a slight increase in ΔH_f. In general, then, —N compounds have a more positive slope than —Cl compounds, demonstrating the relatively better performance of N as a carrier atom over Cl.

The value of such a curve (*see* Table VI) may be tested by locating the known oxidizers relative to the group contribution curves.

Table VI. Correlation of Known Oxidizers with Group Contributions

Oxidizer	*Location*	*Correlation*
F_2	on F	excellent
OF_2	midway between OF and F	excellent
N_2F_4	on NF_2	excellent
O_2	on O	excellent
NF_3	. . .	poor
ClF_3	midway between ClF_4 and ClF_2	good
ClO_3F	above ClF_2, much above ClO_3	poor
N_2O_4	close to NO_2	good
NO_2ClO_4	between NO_2 and extrapolated ClO_4	good
Cl_2O_7	far removed from extrapolated ClO_4 and ClO_3	poor

Hypothetical oxidizers may be tested in the same way. However, the question arises as to what ΔH_f to choose, and this is the primary limitation. Having the curve, would one have chosen ΔH_f $Cl_2O_7 = +55$ kcal./mole or ΔH_f $NF_3 = -29$ kcal./mole?

Publication Date: January 1, 1966 | doi: 10.1021/ba-1966-0054.ch001

In conclusion, it appears that the most desirable oxidizer is one which packs in the maximum fluorine bonded to itself (F_2), bonded to oxygen (OF_2, O_2F_2, O_3F_2, O_4F_2), or bonded to nitrogen (NF_3, N_2F_4, N_2F_2) in decreasing order of energy. The fuel must pack in the working fluid hydrogen while both should have high heats of formation and yield products with low heats of formation. With the covalent liquids and gases our ability to predict heats of formation is quite good; with ionic solids the unknown contributions from lattice energy preclude this.

Literature Cited

(1) Barrère, M., Office Nationale d'Etudes et de Recherche Aerospatiales, *Missiles Rockets* **15**, 32 (1964).

RECEIVED May 10, 1965.

Publication Date: January 1, 1966 | doi: 10.1021/ba-1966-0054.ch001

2

The Feasibility of Predicting Properties of N, F Oxidizers by Quantum Chemical Calculations

JOYCE J. KAUFMAN, LOUIS A. BURNELLE, and JON R. HAMANN

Research Institute for Advanced Studies, Martin Co., Baltimore, Md.

Publication Date: January 1, 1966 | doi: 10.1021/ba-1966-0054.ch002

In this research on N, F compounds we examined such properties as relative stabilities, possible existence of new species, ionization potentials, electron affinities, π-bonding, and charge distributions through extended Hückel LCAO-MO calculations and through analysis of the calculated wave functions and energy levels. It has been possible to: (1) predict the order of the N—F bond lengths in NF_2, NF_3, trans-N_2F_2 *and* cis-N_2F_2 *and of the N—N bond lengths in* cis- *and* trans-N_2F_2 *(before knowing experimental results); (2) predict the greater stability of* cis-N_2F_2 *relative to* trans-N_2F_2*; (3) reproduce the experimental ionization potential of NF_2; (4) predict the order of the symmetric N—F stretch frequencies in NF_2, NF_3,* trans-N_2F_2, N_2F_4, *and* cis-N_2F_2*; (5) verify the supposition of π-bonding in NF_2 and NF leading to a greater N—F bond dissociation energy in these species than in NF_3.*

This research conducts a quantum chemical investigation of energetic N, F compounds to provide insight into the fundamental bonding and behavior of these species. This insight is necessary for guiding and planning the overall experimental research project in the oxidizer field.

Our original theoretical interest in N, F compounds was stimulated by the observation of an apparently anomalous pattern in bond dissociation energies of some of these compounds. In 1961 at an American Chemical Society Symposium on Chemical Bonding in Inorganic Systems, C. B. Colburn of Rohm and Haas at Huntsville mentioned that while the N—H dissociation energies in NH_3 were $D(H_2N—H) > D(HN—H) > D(N—H)$, in NF_3 the order was $D(F_2N—F) < D(FN—F)$. At that time we postulated that the reason must largely be caused by the fact that

In Advanced Propellant Chemistry; Holzmann, R.;
Advances in Chemistry; American Chemical Society: Washington, DC, 1966.

although there is virtually no π-bonding in NF_3, there must be a considerable amount of F → N π-bonding in NF_2 which is planar (*15*). (Our subsequent calculations have confirmed this F → N π-bonding in NF_2.) π-Bonding in NF_2 would increase the N–F bond strength over that in NF_3. The close agreement of ionization potentials of NF_2 and NH_2 were also predicted as being caused by F → N π-bonding in NF_2 and NF_2^+. (Incidentally, it seemed likely that there would also be F → N π-bonding in N–F, which has also been corroborated subsequently by our calculations.)

In this class of compounds, there are many interesting properties whose solutions, using approximate wave functions, may yield sufficiently accurate results to permit interpretation of the desired phenomena. For this reason we have performed calculations using the semiempirical "extended Hückel method," modified to include a seemingly more justifiable physical interpretation of the matrix elements as well as iterative processes which introduce a measure of self-consistency. We shall discuss this method in detail later, present some results of the calculations, and show their good agreement with experimental results.

Publication Date: January 1, 1966 | doi: 10.1021/ba-1966-0054.ch002

Calculational Techniques

Good, rigorous SCF calculations on polyatomic molecules are long, difficult, and tedious to program and inevitably expensive in computer time. What we needed was a simple semiempirical approximate method for three-dimensional molecular orbital calculations.

In recent years increasing use has been made of an extended Hückel-type LCAO-MO method for calculating wave functions and energies of three-dimensional molecules (as opposed to molecules having separable π-systems). This extended Hückel-type method is based on a technique apparently originally introduced by Wolfsberg and Helmholz (*23*) and used over the years by Longuet-Higgins (*18*), extensively by Lipscomb and co-workers, (*8, 9, 12, 16, 17*) especially by Hoffman (*8, 9, 10, 11*) as well as by Ballhausen and Gray (*1*). From a molecular orbital ϕ_i built up as a linear combination of atomic orbitals χ_r

$$\phi_i = \sum_r \chi_r C_{ri} \tag{1}$$

and by applying the variation principle for the variation of energy, the following set of equations for the expansion coefficients is obtained.

$$(\alpha_r + ES_{rr})c_r + \sum_{r \neq s} (\beta_{rs} - ES_{rs})c_s = 0 \tag{2}$$

$s = 1, 2 \ldots M$ where M is the number of atomic orbitals

E = energy

$$S_{rs} = \int \chi_r^* \chi_s dv = \text{overlap integral} \tag{3}$$

$$H_{rr} = \alpha_r = \int \chi_r^* \mathcal{H} \chi_r dv = \text{Coulomb integral} \tag{4}$$

$$H_{rs} = \beta_{rs} = \int \chi_r^* \mathcal{H} \chi_s dv = \text{Resonance integral } (r \neq s) \tag{5}$$

$\mathcal{H}$ is an effective one-electron Hamiltonian representing the kinetic energy, the field of the nuclei, and the smoothed-out distribution of the other electrons.

The diagonal elements are set equal to the effective valence state ionization potentials of the orbitals in question. The off-diagonal elements, H_{rs}, can be evaluated in several ways as follows:

(1) In the early work on the boron hydrides the relationship

$$H_{rs} = K'S_{rs} \tag{6}$$

with $K' = -21$ e.v. was used. However, one was forced to use inordinately high values of K' owing to the requirement that K' be smaller than any diagonal matrix element $(L - H + R)$ (*18*).

(2) A better approximation was to set

$$H_{rs} = 0.5K(H_{rr} + H_{ss})S_{rs} \tag{7}$$

and to use K = (1.75–2.00) (*W-H*) (*23*)

(3) A similar expression,

$$H_{rs} = K''(H_{rr} \cdot H_{ss})^{-1/2} S_{rs} \tag{8}$$

which differs only in second order and has certain computational advantages, has also been used (*1*).

(4) Cusachs reported (*4*) that the repulsive terms in the *W-H* model which assumes that electron repulsion and nuclear repulsion cancel nuclear-electron attraction, consist of one-electron antibonding terms only. Cusachs noted Ruedenberg's observation that the two-center kinetic energy integral is proportional to the square of the overlap integral rather than the first power. Cusachs used this to develop the approximation:

$$H_{rs} = \frac{(H_{rr} + H_{ss})}{2} S_{rs}(2 - |S_{rs}|) \tag{9}$$

which contains no undetermined parameters and avoids collapse.

(5) At Istanbul Fukui (*5*) also reported a new scheme

$$H_{rs} = \left\{ \frac{1}{2}(H_{rr} + H_{ss}) + K \right\} S_{rs} \tag{10}$$

for approximating the off-diagonal elements.

Since the valence state ionization potentials are known to be functions of the electron population at that atom, we have introduced iterative schemes for calculating H_{rr} such as Equations 11 and 12:

$$\alpha_{r_a}{}^R = H_{r_a r_a}{}^R = H_{r_a r_a}{}^{R-1} - (m_{r_a} - q_{r_a}{}^{R-1})W \tag{11}$$

where R is the iteration cycle number, r_a refers to orbital a on atom r, m_{r_a} is the occupation number for that orbital in the ground state, q_{r_a} is some function of the population in that orbital, and W is an empirical constant.

$$\alpha_{r_a}{}^R = H_{r_a r_a}{}^R = H_{r_a r_a}{}^{R-1} + A_{r_a q r_a}{}^{R-1} + B_{r_a}(q_{r_a}{}^{R-1})^2 \quad (12)$$

which follows a Glockler-type equation and where $\alpha^0{}_r$ is equal to the valence state ionization potential. The iterative cycles are continued until

$$|q_{r_a}{}^{R-1} - q_{r_a}{}^R| < \text{constant}$$

The off-diagonal elements can be constructed in accordance with any of the schemes indicated earlier.

Results

Extended Hückel-type calculation on N, F compounds have led to a number of interesting and fruitful observations.

Comparison of Theoretical Indicies with Empirical Data. MOLECULAR GEOMETRIES. Table A shows our original calculations which were performed using Sanborn's (*22*) estimate for the geometry of N_2F_2 in which N—F and N—N bond distances were considered to be the same for both the cis and trans isomers.

Table A

Compound	*N—F Distance, A.*	*N—F Symmetric Stretch cm.*$^{-1}$	*Calculated N—F Overlap Population*
NF_2	1.365	1074	0.37
NF_3	1.371	1031	0.36
trans-N_2F_2	1.397	1010	0.34
cis-N_2F_2	1.409 (*2*)	896	0.32
	1.384*		

* Kuczkowski, R. L., Wilson, E. B., *J. Chem. Phys.* 39, 1030 (1963).

Our calculational results based on overlap population indicate clearly that the N—F distance in *trans*-N_2F_2 should be shorter than that in *cis*-N_2F_2, and this point was verified experimentally by S. Bauer at Cornell (*2*). He sent us his student's unpublished results on electron diffraction measurements of NF compounds and asked for our theoretical interpretation of the different N—F bond lengths. The fact that our calculated N—F overlap populations, even when using the original Sanborn estimate of identical N—F bond lengths for *cis*- and *trans*-N_2F_2, could predict correctly the order of the experimentally measured bond distances before we knew Bauer's results is very encouraging. The situation seems to be similar to that explored years ago in Hückel calculations of aromatic hydrocarbons. In condensed ring systems it is possible to perform an original Hückel LCAO-MO π-electron calculation assuming all bond lengths are equal. From the resulting differences in calculated bond orders it is possible to predict that certain bonds in the rings differ in length from the others. Refined calculations can then be made using differing values of β in order to predict more closely other properties of

the molecules. The correlation of overlap population with bond length even seems to enable one to evaluate the validity of experimental measurements. For example, the calculated N—F overlap population in *cis*-N_2F_2 of 0.32 compared to 0.34 for *trans*-N_2F_2 would indicate that the N—F distance of 1.409 A. for *cis*-N_2F_2 as measured by Bauer is more reasonable compared with 1.398 A. for *trans*-N_2F_2 than is the value of 1.384 A. measured by another investigator. Bauer also observed differences in the N—N distances in *cis*- and *trans*-N_2F_2, and these differences are also reproduced by our original calculations.

	N=N Distance, A.	*Calculated N—N Overlap Population*
cis-N_2F_2	1.209	1.16
trans-N_2F_2	1.224	1.09

MOLECULAR STABILITIES. Bauer noted that the shorter N=N distance in *cis*-N_2F_2 is entirely compatible with the greater thermochemical stability of the *cis*-N_2F_2. The order of N—F dissociation energies is also compatible with the order of their calculated overlap populations. Our calculated total energies for *cis*- and *trans*-N_2F_2 confirm the experimental order of thermal stabilities.

$$cis\text{-}N_2F_2 > trans\text{-}N_2F_2$$

IONIZATION POTENTIALS AND ELECTRON AFFINITIES. For NF_2 we have also performed a Pariser-Parr-Pople-type SCF open-shell calculation (*20, 21*) (including electron repulsion) for the π-orbitals only of NF_2, assuming that the unpaired electron and a pair of electrons on each fluorine were in a π-orbital with a node in the plane of the molecule (*13*). We reasoned that if we were fortunate enough to make reasonable approximations for the core, the appropriate valence state ionization potentials, and the electron repulsion integrals, we might arrive at a nearly correct value for the calculated ionization potential of NF_2 which we could check with the experimentally measured value. Applying the usual correction factor necessary for π-electron ionization potentials calculated by the Pople-SCF method, we calculated the ionization potential of NF_2 as 11.83 e.v., in excellent agreement with the experimentally measured value of 11.8 e.v. When dealing with open-shell species, the ionization potential is no longer equal to the negative of the orbital energy of the highest occupied molecular orbital but instead must be calculated from the differences in the total energies of the species and its positive ion. (The same holds true in calculating electron affinities.) This is because, owing to the coupling terms between open and closed shells in the species, one solves two pseudo-eigenvalue equations. Without applying any correction factors, we calculated the electron affinity of NF_2 as 1.64 e.v.; this quantity is as yet unmeasured.

Publication Date: January 1, 1966 | doi: 10.1021/ba-1966-0054.ch002

INFRARED FREQUENCIES. One might reasonably expect to find some form of correlation between the N—F stretching frequencies and the calculated N—F overlap populations. Table A includes a tabulation of the experimental N—F symmetric stretch frequencies for NF_2, NF_3, and *cis*- and *trans*-N_2F_2 which, in fact, have the same order as the overlap populations.

Calculational Details. The results of our extended Hückel calculations using Equation 9 for constructing the off-diagonal elements of the Hamiltonian matrix are collected in the Appendix together with the results of the Pariser-Parr-Pople SCF π-orbital calculations. The input geometries for these calculations were obtained as follows: *cis*- and *trans*-N_2F_2 from Sanborn (*22*); NF_2 and N_2F_4 from Bauer (*2*); NF_3 from the review of Hoffman and Neville (*7*); and the bond distance in NF itself was taken as 1.36 A. The input values for the diagonal elements of the Hamiltonian matrix were obtained as averages of the valence state ionization potentials (VSIP) for the appropriate processes (*19*) where the VSIP were derived from the tables of promotion energies of Hinze and Jaffé (*6*). The inner shell electrons were excluded in all the calculations, and the orbital exponents were obtained from Slater's rules. Finally, all of the calculations reported in this paper were done without iterating to internal consistency because our initial parameters were sufficiently well chosen to make iteration unnecessary.

The following properties of the resulting eigenvalues and eigenvectors are of particular interest.

(1) There is indeed a significant π-contribution to the total overlap population in NF.

(2) The results of the extended Hückel calculation indicate that the highest occupied molecular orbital (HOMO) (which is singly occupied) was indeed a π-type orbital in the NF_2 radical. This supports the validity of computing the ionization potential from the Pople-SCF π-electron energies. Furthermore, the energy of the HOMO (11.52 e.v.) is quite close to the experimental value.

(3) The extended Hückel calculations also indicate that the HOMO in N_2F_2 is not a π-type orbital; however, lying immediately above and below the HOMO are two π-type orbitals. This property, if confirmed by further calculations, should be significant in evaluating the ionization potential and electron affinity of this molecule.

(4) The coefficients of the atomic orbitals in the π-type molecular orbitals of the extended Hückel treatment are reasonably close to those of both the Hückel and Pople-SCF π-electron calculations on NF_2, *cis*- and *trans*-N_2F_2. The deviations tend to increase with increasing orbital energy.

(5) It is significant that the results do not vary greatly when the off-diagonal Hamiltonian elements are constructed by the alternative procedures.

Publication Date: January 1, 1966 | doi: 10.1021/ba-1966-0054.ch002

Conclusions

In conclusion, quantum chemistry is entering a most exciting and fruitful era. For three-dimensional polyatomic molecules, MO calculations on several levels of approximation are now possible. It is in areas in which the experimental research programs must start from little experimental data, just as in certain aspects of this field of high energy compounds, where quantum chemistry is able to make some of its most significant contributions.

In this research we have found that for general descriptions of bonding in N, F compounds an extended Hückel treatment leads to results consistent with the properties and behavior of known N, F compounds. Furthermore, certain other, as yet uninterpreted properties of these systems can be gleaned from the calculational results.

Although this extended Hückel method is rather simple and has proved fairly useful for predicting certain properties of some molecules, it suffers from the same defects as the regular Hückel procedure for conjugated organic molecules. These defects involve the difficulty of defining precisely the one-electron Hamiltonian. The molecular calculation should be formulated strictly in terms of the complete many-electron Hamiltonian in which the interelectronic repulsions are included explicitly. For this reason we have recently derived (*14*) and we are in the process of testing a semirigorous molecular orbital theory for three-dimensional molecules which is correctly based on the many-electron Hamiltonian but which has been simplified to make the calculations tractable following closely the reasoning applied by Pople to π-system calculations.

Finally, we are performing more rigorous SCF Gaussian calculations on the N,F systems (*3*).

Publication Date: January 1, 1966 | doi: 10.1021/ba-1966-0054.ch002

Acknowledgment

Research reported here was supported in part by the Advanced Research Projects Agency through the U. S. Army Research Office, Durham, N. C. This research was also supported in part by the Air Force Office of Scientific Research of the Office of Aerospace Research, under Contract No. AF49(638)-1220, to whom special thanks are due for support which enabled us to develop the general techniques and the three-dimensional Hückel program.

The authors should like to thank R. Daudel, Director, Centre de Mécanique Ondulatoire Appliquèe and O. Chalvet and G. Bessis of the Centre for the use of their Pople-SCF program. The authors are also indebted to Mr. Sol James, Chief of Automatic Computations, Martin Co.,

Computing Center for arranging to have some of the computations run there and to Joe Rachuba and Jane Flinn of the Martin Co., Computing Center for their assistance in writing the programs.

Literature Cited

(1) Ballhausen, C. J., Gray, H. B., *Inorg. Chem.* **1**, 111 (1962).
(2) Bauer, S., private communication.
(3) Burnelle, L., Kaufman, Joyce J., unpublished results.
(4) Cusachs, L. C., Sanibel Conference in Quantum Chemistry, January 1964.
(5) Fukui, K., NATO International Conference in Quantum Chemistry, Istanbul, Turkey, August 1964.
(6) Hinze, J., Jaffé, H. H., *J. Am. Chem. Soc.* **84**, 540 (1962).
(7) Hoffman, C. J., Neville, R. G., *Chem. Rev.*, **62**, 1 (1962).
(8) Hoffman, R., Lipscomb, W. N., *J. Chem. Phys.* **36**, 2179 (1962).
(9) Hoffman, R., Lipscomb, W. N., *J. Chem. Phys.* **37**, 2872 (1963).
(10) Hoffman, R., *J. Chem. Phys.* **39**, 1397 (1963).
(11) Hoffman, R., *J. Chem. Phys.* **40**, 2745 (1964).
(12) Jordan, T., Smith, W. H., Lohr, L. L., Jr., Lipscomb, W. N., *J. Am. Chem. Soc.*, **85**, 846 (1963).
(13) Kaufman, Joyce J., Hamann, J. R., "Abstracts of Papers," 148th Meeting ACS, September 1964, p. 6k.
(14) Kaufman, Joyce J., *J. Chem. Phys.*, **43**, S152 (1965).
(15) Kaufman, Joyce J., *J. Chem. Phys.* **37**, 759 (1962).
(16) Lohr, L. L., Jr., Lipscomb, W. N., *J. Chem. Phys.* **38**, 1607 (1963).
(17) Lohr, L. L., Jr., Lipscomb, W. N., *J. Am. Chem. Soc.* **85**, 240 (1963).
(18) Longuet-Higgins, H. C., Roberts, M. de V., *Proc. Roy. Soc.* (*London*) **A224**, 336 (1964).
(19) Mortimer, F. S. *et. al.*, Shell Development Co., *Quart. Tech. Rept.* No. **2** (March–May 1963); No. **3** (June–Aug. 1963); No. **5** (Dec. 1963–Feb. 1964).
(20) Pariser, R. and Parr, R. G., *J. Chem. Phys.*, **21**, 466, 767, (1953).
(21) Pople, J. A., *Trans. Faraday Soc.* **49**, 1375 (1953).
(22) Sanborn, R. H., *J. Chem. Phys.* **33**, 1855 (1960).
(23) Wolfsberg, M., Helmholz, L., *J. Chem. Phys.* **20**, 837 (1952).

RECEIVED April 27, 1965.

Publication Date: January 1, 1966 | doi: 10.1021/ba-1966-0054.ch002

Appendix

Table I. Extended Hückel Population Analysis

		Gross Atomic Population			*Overlap Population*		
Molecule		*N*		*F*		*N—F*	*N—N*
NF		4.50		7.50		0.35	
NF_2		3.96		7.52		0.37	
NF_3		3.32		7.56		0.36	
cis-N_2F_2		4.43		7.57		0.32	1.16
trans-N_2F_2		4.45		7.55		0.34	1.09
N_2F_4	N_1	3.87	F_1N_1	7.57	N_1—F_1N_1	0.34	0.66
	N_2	3.85	F_2N_1	7.56	N_1—F_2N_1	0.35	
			F_3N_2	7.58	N_2—F_3N_2	0.33	
			F_4N_2	7.57	N_2—F_4N_2	0.35	

Table II. π-Charges and Bond Orders

	Charges				Bond Orders			
	N		F		N—F		N—N	
Molecule	Hückel	Pople-SCF	Hückel	Pople-SCF	Hückel	Pople-SCF	Hückel	Pople-SCF
NF_2	1.0351	1.0187	1.9824	1.9907	0.1302	0.0957	...	...
N_2F_2	1.0096	1.0064	1.9904	1.9936	0.0974	0.0799	0.9904	0.9936

Table III. Extended Hückel Eigenvalues and Eigenvectors of NF_2

Molecular Orbitals		1	2	3	4
Eigenvalues (e.v.)		−41.46582747	−39.11192751	−23.87838674	−18.95929813
		Eigenvectors			
Atom	Quant. No. nlm				
N	200	0.26890495	−0.00000031	0.68127143	0.00000024
N	210	0.04274096	−0.00000009	−0.14397342	−0.00000003
N	211	0.	−0.	0.	−0.
N	211	0.00000004	0.08173175	0.00000006	−0.25532335
F_1	200	0.61710469	−0.69142177	−0.27182823	−0.06533920
F_1	210	0.00133079	−0.00738304	−0.26360615	−0.55525872
F_1	211	0.	−0.	0.	−0.
F_1	211	0.00140294	0.01565981	0.29079434	0.31316931
F_2	200	0.61710647	0.69142030	−0.27182828	0.06533903
F_2	210	0.00133076	0.00738303	−0.26360653	0.55526017
F_2	211	0.	−0.	0.	−0.
F_2	211	−0.00140304	0.01565983	−0.29079416	0.31316811

Table III. Continued

Molecular Orbitals		5	6	7	8
Eigenvalues (e.v.)		−18.70496464	−18.69909930	−18.24296069	−17.96356463
		Eigenvectors			
Atom	Quant. No. nlm				
N	200	0.	0.07547101	0.	−0.00000050
N	210	0.	−0.15537082	0.	0.00000059
N	211	0.21584626	−0.	−0.00000010	−0.
N	211	0.	−0.00000039	0.	−0.05946571
F_1	200	−0.	0.02348994	−0.	0.00343920
F_1	210	0.	−0.45456994	0.	0.36782390
F_1	211	0.66856693	−0.	−0.70840468	−0.
F_1	211	−0.	−0.50372230	−0.	0.60986723
F_2	200	−0.	0.02349009	−0.	−0.00343908
F_2	210	0.	−0.45456936	0.	−0.36782340
F_2	211	0.66856716	−0.	0.70840453	−0.
F_2	211	0.	0.50372438	0.	0.60986606

Publication Date: January 1, 1966 | doi: 10.1021/ba-1966-0054.ch002

Table III. Continued

Molecular Orbitals		9	10	11	12
Eigenvalues (e.v.)		−15.37721109	−11.51998711	−3.64191455	−0.54148036
		Eigenvectors			
Atom	*Quant No. nlm*				
N	200	0.49855894	0.	0.00000000	0.65705351
N	210	−0.59137409	0.	−0.00000000	0.87249788
N	211	−0.	0.98622740	−0.	−0.
N	211	0.00000005	0.	1.07171333	−0.00000000
F_1	200	−0.03992490	−0.	0.29035559	−0.36097327
F_1	210	0.43072518	0.	−0.30643348	0.24388471
F_1	211	−0.	−0.24652848	−0.	−0.
F_1	211	−0.19655681	−0.	0.24875469	−0.42268667
F_2	200	−0.03992497	−0.	−0.29035556	−0.36097327
F_2	210	0.43072445	0.	0.30643347	0.24388472
F_2	211	−0.	−0.24652839	−0.	−0.
F_2	211	0.19655732	0.	0.24875469	0.42268666

Total Energy = −436.32645798 e.v.

Table IV. Extended Hückel Eigenvalues and Eigenvectors of *cis*-N_2F_2

Molecular Orbitals		1	2	3	4
Eigenvalues (e.v.)		−40.92794323	−39.86583614	−27.92094755	−20.99939609
		Eigenvectors			
Atom	*Quant. No. nlm*				
N_1	200	0.18054599	−0.12866304	0.52806269	−0.38251179
N_1	210	0.	0.	0.	0.
N_1	211	−0.03064538	0.02246994	0.05332141	0.16028737
N_1	211	−0.02651485	0.03145184	0.08020350	−0.01687188
N_2	200	0.18054667	0.12866174	0.52806306	0.38251097
N_2	210	0.	0.	0.	0.
N_2	211	0.03064547	0.02246973	−0.05332129	0.16028795
N_2	211	−0.02651509	−0.03145159	0.08020362	0.01687131
F_1N_1	200	0.62621006	−0.66837937	−0.28016359	0.16008468
F_1N_1	210	0.	0.	0.	0.
F_1N_1	211	0.00402782	0.00588550	0.08061097	−0.15762668
F_1N_1	211	−0.00573286	0.00527768	0.13578303	−0.48372064
F_2N_2	200	0.62621439	0.66837559	−0.28016350	−0.16008446
F_2N_2	210	0.	0.	0.	0.
F_2N_2	211	−0.00402793	0.00588559	−0.08061115	−0.15762714
F_2N_2	211	−0.00573310	−0.00527788	0.13578355	0.48372234

Publication Date: January 1, 1966 | doi: 10.1021/ba-1966-0054.ch002

Table IV. Continued

Molecular Orbitals		5	6	7	8
Eigenvalues (e.v.)		−18.70123744	−18.56238723	−18.39924836	−18.36191201
		Eigenvectors			
Atom	*Quant No. nlm*				
N_1	200	−0.01862621	−0.	−0.	−0.12380677
N_1	210	−0.	0.13760109	0.09131082	0.
N_1	211	0.12370565	−0.	−0.	−0.12491000
N_1	211	−0.02823217	−0.	−0.	−0.22527447
N_2	200	−0.01862583	−0.	−0.	−0.12380761
N_2	210	−0.	0.13760258	−0.09130856	0.
N_2	211	−0.12370570	−0.	−0.	0.12490901
N_2	211	−0.02823243	0.	0.	−0.22527525
F_1N_1	200	0.00237933	−0.	−0.	−0.04343987
F_1N_1	210	−0.	0.67615765	0.69546393	0.
F_1N_1	211	0.54367374	0.	0.	0.37041809
F_1N_1	211	−0.40078846	−0.	−0.	0.45509648
F_2N_2	200	0.00237917	0.	0.	−0.04343939
F_2N_2	210	−0.	0.67616914	−0.69545280	0.
F_2N_2	211	−0.54367744	−0.	−0.	−0.37042528
F_2N_2	211	−0.40078893	0.	0.	0.45509291

Table IV. Continued

Molecular Orbitals		9	10	11	12
Eigenvalues (e.v.)		−18.16906476	−14.61495626	−13.68024182	−12.84739494
		Eigenvectors			
Atom	*Quant. No. nlm*				
N_1	200	0.00109344	−0.41313259	−0.	0.12068905
N_1	210	0.	−0.	0.62751883	−0.
N_1	211	0.04737499	0.29995311	−0.	−0.50464226
N_1	211	−0.05862913	−0.38340110	−0.	0.38250598
N_2	200	−0.00109490	0.41313235	−0.	0.12068955
N_2	210	0.	−0.	0.62751895	−0.
N_2	211	0.04737571	0.29995219	−0.	0.50464258
N_2	211	0.05862644	0.38340084	0.	0.38250654
F_1N_1	200	0.00487876	0.08278017	−0.	0.02786175
F_1N_1	210	0.	−0.	−0.21516281	−0.
F_1N_1	211	0.67736866	0.02782384	0.	0.19886496
F_1N_1	211	−0.18952994	0.39280178	−0.	−0.05122792
F_2N_2	200	−0.00487915	−0.08278007	0.	0.02786167
F_2N_2	210	0.	−0.	−0.21516284	−0.
F_2N_2	211	0.67736178	0.02782413	−0.	−0.19886486
F_2N_2	211	0.18953306	−0.39280167	0.	−0.05122846

Publication Date: January 1, 1966 | doi: 10.1021/ba-1966-0054.ch002

Table IV. Continued

Molecular Orbitals		13	14	15	16
Eigenvalues (e.v.)		−9.24108136	−4.56146294	−1.27464172	18.63658595
		Eigenvectors			
Atom	*Quant No. nlm*				
N_1	200	−0.	−0.32054184	−0.19255363	0.98805027
N_1	210	0.80001870	0.	−0.	0.
N_1	211	−0.	0.37239958	0.31555633	0.99999903
N_1	211	−0.	0.51135442	0.75915721	−0.08966558
N_2	200	−0.	−0.32054111	0.19255503	−0.98805043
N_2	210	−0.80001863	0.	−0.	0.
N_2	211	−0.	−0.37239893	0.31555779	0.99999889
N_2	211	0.	0.51135146	−0.75915925	0.08966579
F_1N_1	200	−0.	0.30620152	0.30093171	−0.06878960
F_1N_1	210	−0.14713922	0.	−0.	0.
F_1N_1	211	0.	0.17864935	0.15486168	−0.10365552
F_1N_1	211	−0.	0.40197942	0.35851841	−0.06608787
F_2N_2	200	0.	0.30620050	−0.30093304	0.06878974
F_2N_2	210	0.14713921	0.	−0.	0.
F_2N_2	211	−0.	−0.17864884	0.15486250	−0.10365571
F_2N_2	211	0.	0.40197839	−0.35852019	0.06608824

Total Energy = −526.10111237 e.v.

Table V. Extended Hückel Eigenvalues and Eigenvectors of *trans*-N_2F_2

Molecular Orbitals		1	2	3	4
Eigenvalues (e.v.)		−40.73158979	−40.09752464	−27.82545686	−21.01187634
		Eigenvectors			
Atom	*Quant. No. nlm*				
N_1	200	0.18592550	−0.12530264	0.52526784	−0.38613354
N_1	210	0.	0.	0.	0.
N_1	211	−0.03127841	0.02114829	0.05575034	0.16302907
N_1	211	−0.02349646	0.03410017	0.07626627	−0.02478273
N_2	200	0.18592811	0.12529874	0.52526829	0.38613298
N_2	210	0.	0.	0.	0.
N_2	211	0.03127888	0.02114762	−0.05575008	0.16302957
N_2	211	0.02349711	0.03409962	−0.07626633	−0.02478249
F_1N_1	200	0.62710784	−0.66516065	−0.29156953	0.15729888
F_1N_1	210	0.	0.	0.	0.
F_1N_1	211	0.00126001	0.00234050	0.08925012	−0.14354626
F_1N_1	211	−0.00481083	0.00608575	0.13746469	−0.48508459
F_2N_2	200	0.62712174	0.66514783	−0.29156965	−0.15729869
F_2N_2	210	0.	0.	0.	0.
F_2N_2	211	−0.00125995	0.00234042	−0.08925031	−0.14354594
F_2N_2	211	0.00481093	0.00608556	−0.13746499	−0.48508541

Publication Date: January 1, 1966 | doi: 10.1021/ba-1966-0054.ch002

Table V. Continued

Molecular Orbitals		5	6	7	8
Eigenvalues (e.v.)		−18.59368253	−18.55727744	−18.53702331	−18.42626333
		Eigenvectors			
Atom	*Quant. No. nlm*				
N_1	200	0.01642434	−0.04670138	0.	0.
N_1	210	−0.	0.	0.13874203	0.09074432
N_1	211	0.15266256	0.07536162	0.	0.
N_1	211	0.04495608	−0.13341236	−0.	−0.
N_2	200	0.01642261	0.04670263	0.	0.
N_2	210	−0.	0.	0.13874197	−0.09074439
N_2	211	−0.15266582	0.07535401	0.	0.
N_2	211	−0.04494987	−0.13341504	0.	0.
F_1N_1	200	0.02109279	−0.01602264	−0.	−0.
F_1N_1	210	−0.	0.	0.67627994	0.69503304
F_1N_1	211	0.41186046	0.65724068	0.	0.
F_1N_1	211	−0.51864295	−0.12676843	−0.	−0.
F_2N_2	200	0.02109184	0.01602359	−0.	−0.
F_2N_2	210	−0.	0.	0.67627978	−0.69503316
F_2N_2	211	−0.41189143	0.65722326	0.	0.
F_2N_2	211	0.51864817	−0.12674312	0.	0.

Table V. Continued

Molecular Orbitals		9	10	11	12
Eigenvalues (e.v.)		−17.78113723	−15.83514202	−13.67695832	−11.74634004
		Eigenvectors			
Atom	*Quant. No. nlm*				
N_1	200	−0.13729162	−0.35995527	0.	0.20590325
N_1	210	0.	−0.	0.62727210	−0.
N_1	211	−0.12788840	0.23694726	0.	−0.55691156
N_1	211	−0.17790501	−0.38934629	−0.	0.36357281
N_2	200	−0.13729091	0.35995544	0.	0.20590322
N_2	210	0.	−0.	0.62727214	−0.
N_2	211	0.12788890	0.23694685	0.	0.55691167
N_2	211	0.17790387	−0.38934667	0.	−0.36357294
F_1N_1	200	−0.00214982	0.02303940	−0.	−0.03981328
F_1N_1	210	0.	−0.	−0.21660596	−0.
F_1N_1	211	0.55050948	−0.12836153	0.	0.08828261
F_1N_1	211	0.32618017	0.36837237	−0.	−0.16220003
F_2N_2	200	−0.00214980	−0.02303932	−0.	−0.03981322
F_2N_2	210	0.	−0.	−0.21660598	−0.
F_2N_2	211	−0.55050757	−0.12836045	0.	−0.08828255
F_2N_2	211	−0.32617949	0.36837307	0.	0.16220015

Publication Date: January 1, 1966 | doi: 10.1021/ba-1966-0054.ch002

Table V. Continued

Molecular Orbitals		13	14	15	16
Eigenvalues (e.v.)		−9.24289465	−5.06398100	−0.95323669	18.58283734
		Eigenvectors			
Atom	*Quant. No. nlm*				
N_1	200	0.	−0.27883912	−0.27058879	0.98576278
N_1	210	0.80007741	−0.	0.	0.
N_1	211	0.	0.34554380	0.27284800	1.00470398
N_1	211	−0.	0.54038424	0.75066002	−0.05988377
N_2	200	0.	0.27883924	−0.27058858	−0.98576291
N_2	210	−0.80007737	−0.	0.	0.
N_2	211	0.	0.34554390	−0.27284832	1.00470388
N_2	211	0.	0.54038423	−0.75065992	−0.05988403
F_1N_1	200	−0.	0.31135264	0.30405644	−0.06229587
F_1N_1	210	−0.14648370	−0.	0.	0.
F_1N_1	211	0.	0.19311186	0.15764681	−0.10124260
F_1N_1	211	−0.	0.40026405	0.36885121	−0.05971462
F_2N_2	200	−0.	−0.31135265	0.30405637	0.06229594
F_2N_2	210	0.14648364	−0.	0.	0.
F_2N_2	211	0.	0.19311190	−0.15764677	−0.10124278
F_2N_2	211	0.	0.40026415	−0.36885123	−0.05971508

Total Energy = −525.64051819 e.v.

Table VI. Hückel π-Orbital Eigenvalues and Eigenvectors of NF_2

Molecular Orbitals	1	2	3
Eigenvalues	3.0755	3.0000	0.9246
	Eigenvectors		
Atomic Orbitals			
1	0.6946	−0.7071	0.1325
2	0.1874	0.0000	−0.9823
3	0.6946	0.7071	0.1325

Table VII. Pople-SCF π-Orbital Eigenvalues and Eigenvectors of NF_2

Molecular Orbitals	1	2	3
Eigenvalues (e.v.)	−18.3315	−18.1511	−13.8843
	Eigenvectors		
Atomic Orbitals			
1	0.7005	0.7071	0.0966
2	0.1367	0.0000	−0.9906
3	0.7005	−0.7071	0.0966

Publication Date: January 1, 1966 | doi: 10.1021/ba-1966-0054.ch002

Table VIII. Hückel π-Orbital Eigenvalues and Eigenvectors of N_2F_2

Molecular Orbitals	1	2	3	4
Eigenvalues	3.0631	3.0275	1.7569	0.1525
	Eigenvectors			
Atomic Orbitals				
1	0.6898	−0.7037	0.1554	−0.0692
2	0.1554	−0.0692	−0.6898	0.7037
3	0.1554	0.0692	−0.6898	−0.7037
4	0.6898	0.7037	0.1554	0.0692

Table IX. Pople-SCF π-Orbital Eigenvalues and Eigenvectors of *cis*-N_2F_2

Molecular Orbitals	1	2	5	4
Eigenvalues (e.v.)	−18.3074	−18.2217	−13.9489	−1.7122
	Eigenvectors			
Atomic Orbitals				
1	0.6948	0.7048	0.1316	0.0566
2	0.1316	0.0566	−0.6947	−0.7048
3	0.1316	−0.0566	−0.6947	0.7048
4	0.6948	−0.7048	0.1316	−0.0566

Table X. Pople-SCF π-Orbital Eigenvalues and Eigenvectors of *trans*-N_2F_2

Molecular Orbitals	1	2	3	4
Eigenvalues (e.v.)	−18.2868	−18.2147	−13.9481	−1.7121
	Eigenvectors			
Atomic Orbitals				
1	0.6946	0.7048	0.1322	0.0567
2	0.1322	0.0567	−0.6946	−0.7048
3	0.1322	−0.0567	−0.6946	0.7048
4	0.6946	−0.7048	0.1322	−0.0567

Publication Date: January 1, 1966 | doi: 10.1021/ba-1966-0054.ch002

The Lattice Energy of Nitrogen Pentoxide

R. M. CURTIS and J. N. WILSON

Shell Development Co., Emeryville, Calif.

A revised value for the heat of formation of nitrate ion has been obtained by re-evaluating the lattice energy of cesium nitrate with consideration of charge distribution in the anion. With the revised value for $\Delta H_f(NO_3^-)$ the Born-Haber cycle yields a lattice energy of —157 kcal./mole for nitrogen pentoxide. The electrostatic (Madelung) energy of N_2O_5 has been found to depend significantly on the charge distribution within the two ions. Charge distribution estimated by means of a Hückel molecular orbital treatment leads to a Madelung energy very nearly equal to the lattice enthalpy given above.

Publication Date: January 1, 1966 | doi: 10.1021/ba-1966-0054.ch003

As an ionic crystal, N_2O_5 is unusual in several respects. It possesses a layer structure in which each ion is surrounded by only three nearest neighbors of opposite charge rather than the more usual coordination sphere of six or eight neighbors. The heat of formation is quite small, the vapor pressure is high (50 mm. at 0° C.), and the gaseous molecule is covalent rather than ionic. These factors plus the possible effects of charge distribution within both cation and anion indicate N_2O_5 to be a particularly interesting example for applying the ionic model of lattice energy.

Heat of Formation of NO_3^-

In applying the Born-Haber cycle to N_2O_5 to determine the lattice energy it is found that the heat of formation of the nitrate ion is the only major thermodynamic quantity for which an experimental value is not available. This quantity is obtained from calculated lattice energies of the alkali metal nitrates. Values ranging from —78 (*19*) to —85 (*14*) have been reported of which the average of —84 kcal./mole from Ladd and Lee (*14*) is probably the most reliable. In all these evaluations of the nitrate ion heat of formation, a simplified crystal structure is implied in which the nitrate group is treated as a point charge ion. The location of

In Advanced Propellant Chemistry; Holzmann, R.;
Advances in Chemistry; American Chemical Society: Washington, DC, 1966.

the entire unit negative charge of this ion at the position of the central nitrogen atom is unrealistic. A more reasonable assumption involves a charge distribution with nonintegral charges on all four atoms such that the algebraic sum of these charges is equal to the ion charge. Some time ago Topping and Chapman (*26*) calculated the electrostatic energy of sodium nitrate based on the charge assignment $N^{+5}O_3^{-2}$, but we have felt it desirable to consider a variable charge distribution in at least one case, $CsNO_3$, where more recent data are available.

Since the nitrate ion is not spherically symmetric, the value calculated for the heat of formation of nitrate ion from a lattice energy will depend in general on the charge distribution assigned within the ion. If the charge distribution on the ion in the crystal differs from that in the free ion, then the calculated heat of formation is likely also to be different in some degree from the true heat of formation of the free ion. Nevertheless, if the charge distribution does not change appreciably from one nitrate crystal to another, a lattice energy calculated for N_2O_5 or some other nitrate from the Born-Haber cycle should still be meaningful.

Cesium nitrate crystallizes at room temperature in a hexagonal (*29*) lattice, but the structure has not been determined. Above 160° C. it exists in a cubic modification containing eight molecules per unit cell. The structure of this form is known (*30*), having been determined at 167° C., and is the basis for calculation, later correcting to 25° C. The electrostatic energy of $CsNO_3$ was computed (*10*) for several assumed nitrate ion charge distributions and after correcting for the electrostatic self-energy of the ion the results were fittted with a second degree equation in x, the nitrogen atom charge, giving the Coulomb energy.

$$E_c = -150.40 + 0.534x - 0.979x^2 \text{ kcal./mole} \quad (1)$$

In this method of calculation the energy of electrostatic interaction among all of the charges in the structure is determined. The calculated energy thus includes a contribution from the interaction within each polyatomic ion among the charges assigned to its constituent atoms. This "self-energy" must be subtracted from the total calculated energy to obtain the Coulomb contribution to the lattice energy—i.e., the interaction energy of the ions in the crystal with each other. It is of course an approximation to represent the charge distribution in a polyatomic ion as a collection of discrete charges centered on each atom; this is equivalent to assuming that the electron distribution in the ion can be represented by a set of overlapping spherically symmetric distributions, each centered on one of the atomic nuclei. Since covalent bonding between the atoms making up the ion is caused by some concentration of electronic charge density in the region between bonded atoms, this representation cannot be precisely valid. In the absence of detailed information about the actual charge distribution, however, the procedure used here appears to be a

Publication Date: January 1, 1966 | doi: 10.1021/ba-1966-0054.ch003

useful approximation. Computationally, it appears to be simpler and faster than the alternative method of representing the charge distribution by superposing a point charge and a series of multipoles.

Equation 1 is relatively flat between the limits $x = +1$ and $x = 0$ which correspond, respectively, to a simple resonance hybrid for the nitrate ion and to unit negative charge distributed over the oxygen atoms with the nitrogen neutral. The exact value assumed for the charge distribution is thus unimportant. We shall assume $x = 0.17$ based on a Hückel molecular orbital treatment (*20*) which leads to $E_c = -150.3$ kcal./mole. This is almost exactly the value $E_c = -150.5$ kcal./mole obtained by assuming a simple monomolecular unit cell of the CsCl type with interatomic distance $r = 3.89$A.

The nonelectrostatic terms include van der Waals, polarization, repulsive, and zero-point energies. The van der Waals energy has been calculated in several ways with results ranging from 5 to 15 kcal./mole. Examples of these results are indicated in Table I. In the first two entries polarizabilities were taken from Böttcher (*3*), and the nitrate group was treated as a single entity with an ionization potential of 99 kcal./mole for the London equation (*23*) and an effective electron number of 24 for the Slater-Kirkwood equation (*23*). A simple CsCl type of lattice was assumed.

Table I. Van der Waals Energy in $CsNO_3$

$Cs^+NO_3^-$	London equation	4.5 kcal./mole
	Slater-Kirkwood	15.3
$Cs^+N^{+.17}O_3^{-.39}$	London equation	9.0
	Slater-Kirkwood	13.3

For the second two entries the nitrate group was treated in terms of individual atoms with effective charges as indicated above of +.17 on the nitrogen and −0.39 on each oxygen atom. Effective ionization energies of 190 kcal./mole for oxygen and 390 kcal./mole for nitrogen were obtained from curves connecting known ionization potentials with ionization state. Similarly, using various calculated and experimental polarizabilities (*1, 6, 12, 15, 17, 21, 22*), effective polarizabilities of 0.8 A.^{3} for oxygen and 1.0 A.^{3} for nitrogen were obtained. For cesium ion the Pauling (*22*) value was used. The sum of these atom polarizabilities in the nitrate group is 3.4 A.^{3}, rather close to the nitrate polarizabilities reported by Tessman, Kahn, and Shockley (*25*) (3.4–4.0 A.^{3}) and Böttcher (*3*) (3.7–3.8 A.^{3}). For the Slater-Kirkwood equation, we have used as electron numbers Cs = 8, N = 6, O = 6. In summing the van der Waals energy over all atom pairs, the lattice sum coefficients for the CsCl structure can no longer be used. Instead the sum has been made over all atom pairs out to 5 A., and this figure was increased by 10% to allow for more distant

neighbors. Of the values in Table I, we prefer the Slater-Kirkwood individual atom treatment giving 13.3 kcal./mole.

Our extrapolation of Bridgman's (*4*) data leads to a compressibility $\beta = 5.0 \pm 0.2 \times 10^{-12}$ sq. cm./dyne. This applies to the low temperature (hexagonal) form at room temperature. To apply this to the high temperature form at 167° C. we have assumed a temperature coefficient $\frac{1}{\beta}\frac{d\beta}{dt} = 6 \times 10^{-4}$ deg.$^{-1}$ similar to that for the alkali halides and a difference in β at the transition of 1.7×10^{-12} sq. cm./dyne from an earlier paper by Bridgman (*5*). The result at 167° C. is $\beta = 7.3 \pm 0.5 \times 10^{-12}$ sq. cm./dyne, a compressibility considerably larger than that used by Ladd and Lee (*14*).

Using the convenient expressions given by Ladd and Lee (*13*) and assuming 1.0 kcal./mole for the zero-point energy and 13.3 kcal./mole for the van der Waals energy, the repulsive energy is 15.7 kcal./mole and the lattice energy —146.9 kcal./mole.

It is necessary to correct the lattice energy to 25° C. and introduce the vibrational energy in order to obtain ΔH for the reaction at 298° K.:

$$Cs^+(g) + NO_3^-(g) = CsNO_3(c) \qquad (2)$$

From available heat capacity data (*18*) and a comparison with related compounds ($KBrO_3$, $CsClO_4$) the incremental enthalpy, $(H_o^T - H_o^0)$, was estimated at 25° C. (4.4 kcal.) and 167° C. (9.3 kcal.). Cesium nitrate does not appear to fit a simple Debye-type expression, but the vibrational energy has been estimated by difference from integrating C_p-$C_v = \alpha^2VT/\beta$ in which the expansion coefficient, α, was taken from density data (*8*). At 167° C. we thus estimate $(E_o^T - E_o^0) = 7.4$ kcal./mole. Adding the vibrational energy to the lattice energy and subtracting the difference $H_{167}° - H_{25}°$ as well as $5RT$ for the free ions gives, for Equation 2, $\Delta H = -147.4$ kcal./mole. From the Born-Haber cycle using as standard heats of formation $\Delta H_f(Cs^+) = 110.1$ kcal. (*24*), $\Delta H_f(CsNO_3) = -121.5$ kcal./mole (*24*), and the above heat of reaction, it follows that $\Delta H_f(NO_3^-) = -84.2$ kcal./mole with an estimated uncertainty of $\pm$ 2 kcal. If the heats of formation of $RbNO_3$ and $CsNO_3$ are revised (*16*) by —0.5 and —3.4 kcal., respectively, Ladd and Lee's determinations of $\Delta H_f(NO_3^-)$ become —86.5 and —85.4 kcal./mole.

The Lattice Energy of N_2O_5

Applying the Born-Haber cycle to N_2O_5 with $\Delta H_f(NO_2^+) = 233.5$ kcal./mole (*28*), $\Delta H_f(N_2O_5)_c = 10.0$ kcal./mole (*28*), and $\Delta H_f(NO_3^-) = -84.2$ kcal./mole (all at 298° K.) from above gives as the heat of formation from the gas ions at room temperature a value $\Delta H = -159 \pm 2$ kcal./mole. The corresponding lattice energy, obtained by subtracting an estimated 5 kcal. for vibrational energy and adding 3 kcal. = 5 RT

Publication Date: January 1, 1966 | doi: 10.1021/ba-1966-0054.ch003

for the translational energy and $P\Delta V$ term associated with the ions, is -157 kcal./mole.

Based on the known structure (*7*) the Coulomb energy for N_2O_5 was calculated, as with $CsNO_3$, by assuming specific charge distributions in the ions NO_2^+ and NO_3^-, correcting for the self-energy and fitting the results with a quadratic equation in X, the nitrate N atom charge and Y, the nitronium N atom charge: Thus:

$$E_c = -150.65 - 5.20X - 10.63Y + 2.278X^2 + 1.694XY - 1.520Y^2 \quad (3)$$

In Equation 3 there is a far greater dependence on charge distribution than in Equation 1. Examples of the Coulomb energy for several conceivable charge distributions are given in Table II.

Table II. Coulomb Energy of N_2O_5

Configuration	*N Atom Charge in* NO_3^- (X)	*N Atom Charge in* NO_2^+ (Y)	*Coulomb Energy* E_c
Minimum value of $-E_c$	2.02	2.37	-143.3
Point charges	-1	1	-157.0
Neutral nitrogen	0	0	-150.7
Resonance bond	1	1.67	-172.7
Molecular orbital (*20*)	0.17	0.58	-158.0

The minimum value of $-E_c$, while having no apparent physical significance, indicates the least energy that can be associated with this particular hexagonal structure. The most reliable result is probably that from quantum mechanics, the last entry in Table I. This energy is surprisingly close to that for the point charge configuration.

In deriving Equation 3 it was assumed that the self-energy of each ion, and hence the charge distribution and interatomic distance, are the same in the free state and in the crystal. It is quite possible that a real difference exists for the ions in these two states. There is evidence (*9*), for example, of a charge shift in the nitrate ions of molten alkali metal nitrates depending on the cation polarizability, and an even greater shift is expected in going to the isolated ion. Unfortunately, no quantitative estimate of this effect is available, but it should be noted that the results leading to Equation 2 indicate that a difference of only .01 unit in charge between gas and crystal ions can lead to 10 kcal. difference in E_c.

Errors arising from such effects are probably small for the nitrate ion since its heat of formation was obtained from a lattice energy. The heat of formation of NO_2^+, however, is obtained from the ionization potential and heat of formation of $NO_2(g)$; in this case no error cancellation occurs. The agreement between calculated and observed heats of formation suggests that the error from this effect is probably small for both ions.

The complexity of N_2O_5 and the absence of compressibility or elastic constant data preclude any reliable calculation of the nonelectrostatic

Publication Date: January 1, 1966 | doi: 10.1021/ba-1966-0054.ch003

terms in the lattice energy. It would be desirable to sum the repulsive energy over near pairs of atoms, but repulsive parameters for N and O atoms are not well established and doubtless depend on the charge density at each atom. Consequently, only an approximation is possible. In the simple Born-Mayer expression (*27*) for lattice energy the repulsive energy is given by $\rho E_c/R$ in which ρ is the exponential repulsive parameter and R is the interionic distance. Typically (*11*) ρ is taken equal to 0.345 A. With R equal to the shortest nitrogen-nitrogen distance between ions, 3.12 A., the repulsive energy is then 17 kcal./mole. While this value for R is close to the sum of the ion radii, 1.3 A. from Grison *et al.* (*7*) for NO_2^+ and 1.9 A. from Waddington (*27*) for NO_3^-, it probably results in too large an estimated energy. There are only three ion neighbors in the crystal at this distance while the next coordination sphere at 4.53 A. has six neighbors. A mean R for these nine neighboring ions given by $9/R = 3/3.12 + 6/4.53$ yields a repulsive energy of 13 kcal./mole. Our preferred estimate for the repulsive energy is the average, 15 ± 4 kcal./mole. The estimated uncertainty arises not only from R but from the rather large variations that have been observed (*2*) in ρ.

For the van der Waals energy in N_2O_5 we have again adopted the Slater-Kirkwood equation to individual atom pairs. The nitrate group was used with the electron numbers and polarizabilities noted previously. For NO_2^+, estimated polarizabilities of 0.7 A.^{3} for N and 0.5 A.^{3} for O were based on the charges (*20*) N = +.58 and O = +.21. Since NO_2^+ contains a total of only 16 outer electrons we have arbitrarily chosen electron numbers of 6 and 5, respectively, for N and O. The resulting van der Waals energy is 13.2 kcal./mole.

The combination of Coulomb, repulsive, van der Waals, and zero-point (estimated at 1 kcal.) energies yields a lattice energy of $-158 + 15 - 12 + 1 = -154 \pm 5$ kcal./mole. The discrepancy between this and the "experimental" lattice energy above of -157 ± 2 kcal./mole is well within the expected uncertainty. Incidentally, the alkali halides show a gradual compensation of repulsive and van der Waals energies with increasing ion size until with CsI these terms nearly cancel. In the case of $CsNO_3$ this sum is only 2.4 kcal. so that in N_2O_5 it may well be that the sum is appreciably less than the admittedly rough estimate of 3 kcal. obtained here. In addition, the theoretical charge distributions used for the Coulomb energy may be in error. Raising the N atom charge in NO_2^+ from 0.58 to 1.0 results in a 5 kcal. change. Together these two factors can account easily for the difference between "experimental" and theoretical lattice energies. In view of the possibly significant internal energy difference associated with free and lattice bound ions it appears that the ionic model fits N_2O_5 extremely well.

Publication Date: January 1, 1966 | doi: 10.1021/ba-1966-0054.ch003

Acknowledgment

Research in this paper was supported by the Advanced Research Projects Agency under Contract No. DA-31-124-ARO(D)-54, monitored by the U.S. Army Research Office, Durham, N. C.

Literature Cited

(1) Alpher, R. A., White, D. R., *Phys. Fluids* **2**, 153 (1959).
(2) Baughan, E. C., *Trans. Faraday Soc.* **55**, 736 (1959).
(3) Böttcher, C. J. F., *Rec. Trav. Chim.* **65**, 19 (1946).
(4) Bridgman, P. W., *Proc. Am. Acad. Arts Sci.* **76**, 1,9 (1945).
(5) Bridgman, P. W., *Proc. Am. Acad. Arts Sci.* **51**, 579 (1916).
(6) Dalgarno, A., *Advan. Phys.* **11**, 281 (1962).
(7) Grison, E., Eriks, K., de Vries, V. L., *Acta Cryst.* **3**, 290 (1950).
(8) "International Critical Tables," Vol. 3, p. 44, McGraw-Hill, New York, 1928.
(9) Janz, G. J., James, D. W., *J. Chem. Phys.* **35**, 739 (1961).
(10) Johnson, Q., Lawrence Radiation Laboratory, Livermore, Calif. The IBM 7090 Madelung constant program kindly provided by Dr. Johnson was adapted for 7040 operation by J. H. Schachtschneider.
(11) Kapustinskii, A. F., *Quart. Rev. (London)* **10**, 283 (1956).
(12) Ketelaar, J. A. A., "Chemical Constitution," Elsevier, Amsterdam, 1958.
(13) Ladd, M. F. C., Lee, W. H., *Trans. Faraday Soc.* **54**, 34 (1958).
(14) Ladd, M. F. C., Lee, W. H., *J. Inorg. Nucl. Chem.* **13**, 218 (1960).
(15) Landolt-Börnstein, "Physikalische-Chemische Tabellen," 6th Aufl., 1,3 Teil, Springer-Verlag, Berlin, 1950, 1951.
(16) Lewis, G. N., Randall, M., Pitzer, K. S., Brewer, L., "Thermodynamics," p. 678, McGraw-Hill, New York, 1961.
(17) Matossi, F., *J. Chem. Phys.* **19**, 1007 (1951).
(18) "Mellor's Comprehensive Treatise on Inorganic and Theoretical Chemistry," Vol. II, Suppl. III, Part 2, p. 2407, John Wiley and Sons, New York, 1963.
(19) Morris, D. F. C., *J. Inorg. Nucl. Chem.* **6**, 295 (1958).
(20) Mortimer, F. S., Shell Development Co., Emeryville, Calif., private communications.
(21) Parkinson, D., *Proc. Phys. Soc. (London)*, **75**, 169 (1960).
(22) Pauling, L., *Proc. Roy. Soc.* **A114**, 181 (1927).
(23) Pitzer, K. S. *Advan. Chem. Phys.* **2**, 59 (1959).
(24) Rossini, F. D., *Nat. Bur. Std. (U.S.) Circ.* **500** (1950).
(25) Tessman, J. R., Kahn, A. H., Shockley, W., *Phys. Rev.* **92**, 890 (1953).
(26) Topping, J, Chapman, S., *Proc. Roy. Soc.* **A113**, 658 (1927).
(27) Waddington, T. C., *Advan. Inorg. Chem. Radiochem.* **1**, 158 (1959).
(28) Wagman, D. D., *Nat. Bur. Std. (U.S.), Rept. No.* **7437** (1962).
(29) Waldbauer, L., McCann, D. C., *J. Chem. Phys.* **2**, 615 (1934).
(30) Wyckoff, R. W. G., "Crystal Structures," Vol. 2, John Wiley and Sons, New York, 1964.

RECEIVED April 27, 1965.

4

Estimated Stability of Perfluoroammonium Ion and Its Salts

J. NORTON WILSON

Shell Development Co., Emeryville, Calif.

Publication Date: January 1, 1966 | doi: 10.1021/ba-1966-0054.ch004

The heat of formation of NF_4^+ ion is estimated at 245 ± 20 kcal./mole from thermochemical correlations and from failure to detect NF_4^+ as product of an ion-molecule reaction between NF_3^+ and NF_3 in a mass spectrometer. The ion NF_3H^+ was detected as a product of a related reaction under similar conditions; its heat of formation appears to be less than 225 kcal./mole. Estimates of the heat of formation of some salts of NF_4^+ have been made by means of the Kapustinskii approximation for lattice energies. For this purpose a correlation was developed between known "thermochemical radii" of tetrahedral ions and their van der Waals radii. It is concluded that the perchlorate, sulfate, and fluoride salts will be unstable relative to likely decomposition products.

The hypothetical salt, NF_4ClO_4, would clearly be an excellent oxidizing agent if it could be made. This paper presents some estimates concerning the stability of the ion, NF_4^+, and of its salts. Our first concern is to estimate the heat of formation of the perfluoroammonium ion in the gas phase.

A rough but simple estimate can be made on the assumption that the dissociation energy of a fluorine atom from NF_4^+ is about the same as the average bond energy in either NF_3^+ or NF_3. From the known heats of formation and ionization potentials of NF_3 and N, and the heat of formation of F, we obtain for the dissociation $NF_3^+ = N^+ + 3F$ an average bond energy of 76.3 ± 2 kcal./mole; the corresponding bond energy in NF_3 is 66.5 ± 0.6. The first of these values leads to a heat of formation for NF_4^+ of 216.9 ± 8.5 and the second to 226.4 ± 7 kcal./mole. The thermochemical data used in this and subsequent computations are listed in the Appendix together with their sources.

A more realistic estimate can be made by examining trends in the dissociation energy of a fluorine atom from the series of molecules CF_2,

In Advanced Propellant Chemistry; Holzmann, R.;
Advances in Chemistry; American Chemical Society: Washington, DC, 1966.

CF_3, CF_4 and the isoelectronic series NF_2^+, NF_3^+, (NF_4^+). The relevant data are assembled in the Appendix; the trends are illustrated in Figure 1. The drop in dissociation energy between CF_2 and CF_3 is equal to that between NF_2^+ and NF_3^+ within the relatively broad limits of experimental error; a line parallel to that connecting the experimental points for CF_2 and CF_3 is shown intersecting the line connecting the points for NF_2^+ and NF_3^+. From Figure 1, the most likely value for the dissociation energy of F from NF_4^+ is estimated to lie in the range 50–55 kcal./mole. A substantial range of uncertainty is indicated by lines extending to the right from the upper and lower limits of error at the NF_3^+ point; these are drawn with the maximum and minimum slopes, respectively, of

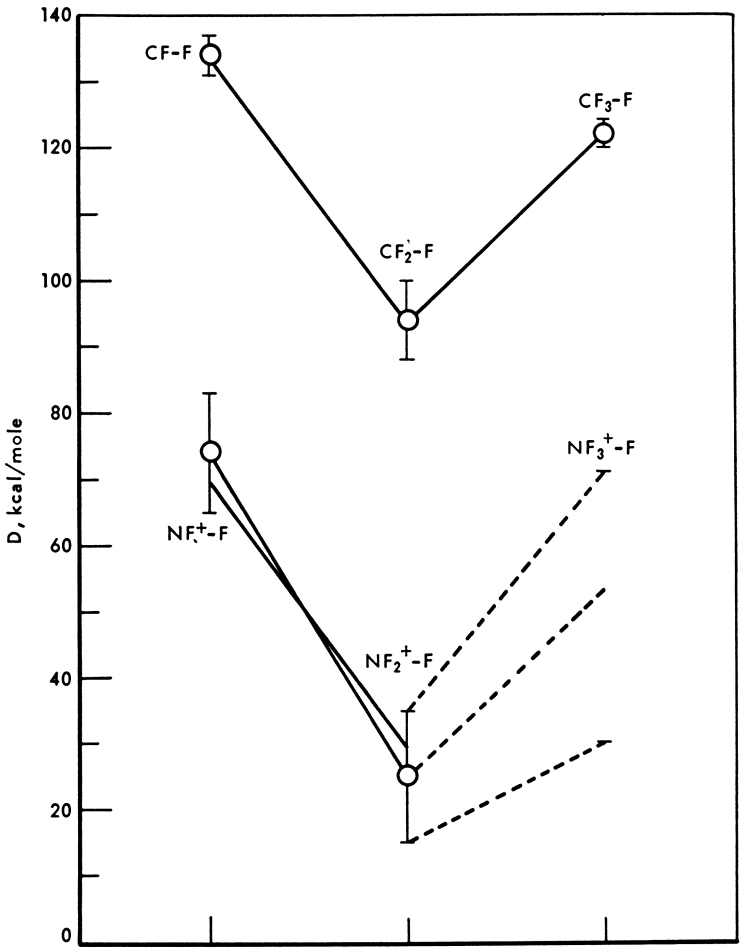

Figure 1. Dissociation energies of F from isoelectronic series CF_2, CF_3, CF_4; NF_2^+, NF_3^+, NF_4^+

the lines that can be drawn to connect the CF_3 and CF_4 points within their ranges of error. The dissociation energy $D(NF_3^+-F)$ is thus estimated as 50 ± 20 kcal./mole and the heat of formation of NF_4^+ as 244 ± 26 kcal./mole.

If $\Delta H_f(NF_4^+)$ were 236 ± 10 kcal./mole, then from the known heats of formation of NF_3, NF_2, and NF_3^+ the following ion-molecule reaction would be athermal:

$$NF_3^+ + NF_3 = NF_4^+ + NF_2$$

A search has therefore been made for this reaction in a mass spectrometer (Consolidated model 21-103A). Observations were made at the partial pressure of 200 microns Hg of NF_3 in the sample reservoir, with the ionization chamber operating at 260° C. and with 70 volt ionizing electrons. No formation of NF_4^+ was observed, though in an experiment with CD_4 under similar conditions, the ion CD_5^+ was clearly detected. In a similar experiment with CD_4 and NF_3 each at 200 microns partial pressure, CD_5^+ and NF_3D^+ were clearly observed, but no trace of NF_4^+ was found. If failure to find NF_4^+ is caused by the endothermicity of the reaction written above, then $\Delta H_f(NF_4^+)$ is greater than 225 kcal./mole.

Observation of the ion NF_3D^+ suggests, on the other hand, that either or both of the following ion-molecule reactions is exothermic

$$CH_4 + NF_3^+ = CH_3 + NF_3H^+$$

$$CH_4^+ + NF_3 = CH_3 + NF_3H^+$$

The first of these would be athermal if $\Delta H_f(NF_3H^+) = 225 \pm 6$ kcal./mole; the second, if the value were 220 ± 3. The heat of formation of NF_3H^+ is thus very likely less than 230 kcal./mole; this implies a dissociation energy $D(NF_3^+-H) > 97$ kcal./mole. The dissociation energy of H from the ions NH^+ to NH_4^+ is known to fall in the range 120–135 kcal./mole.

It seems reasonable then to conclude that the heat of formation of NF_4^+ is greater than 225 kcal./mole and probably less than 260 kcal./mole; a value around 240 kcal./mole seems not unlikely. This implies that dissociation of NF_4^+ to NF_3^+ and F should be endothermic by 50 ± 25 kcal./mole, and dissociation to $NF_2^+ + F_2$ endothermic by 38 ± 24 kcal./mole. The increase of standard entropy in the latter dissociation is estimated about 45 e.u.; this will contribute −13.5 kcal./mole to the standard free energy of dissociation at 300°K. It is thus not unlikely that the ion NF_4^+ can be prepared and observed in the gas phase by a suitable ion-molecule reaction.

Let us turn now to the question of the lattice energy of salts of NF_4^+. For tetrahedral ions such as this one, the simplest approach, though an approximate one, is that proposed many years ago by Kapustinskii (*10*).

He assumed that for salts made up of combinations of spherical or tetrahedral ions the lattice energy could be well approximated by assigning to the crystal structure (usually unknown) a Madelung constant equal to that of sodium chloride and estimating the repulsive contribution to the lattice energy by a Born-Mayer expression similar to that which holds approximately for the alkali halides. These assumptions lead to the following expressions for the lattice energy U:

$$U = Ne^2\mu \frac{n}{2} \frac{\nu_+\nu_-}{R_+ + R_-} \left(1 - \frac{\rho}{R_+ + R_-}\right) \tag{1}$$

$$= 290.2\, n \frac{\nu_+\nu_-}{R_+ + R_-} \left(1 - \frac{0.345}{R_+ + R_-}\right) \text{ kcal./formula wt.}$$

μ = Madelung constant = 1.7475 for NaCl
n = Number of ions per formula
ν = Ionic charge in units of electronic charge
R = Effective ionic radius ("thermochemical radius")
ρ = Born-Mayer repulsion parameter (exponential repulsive potential).

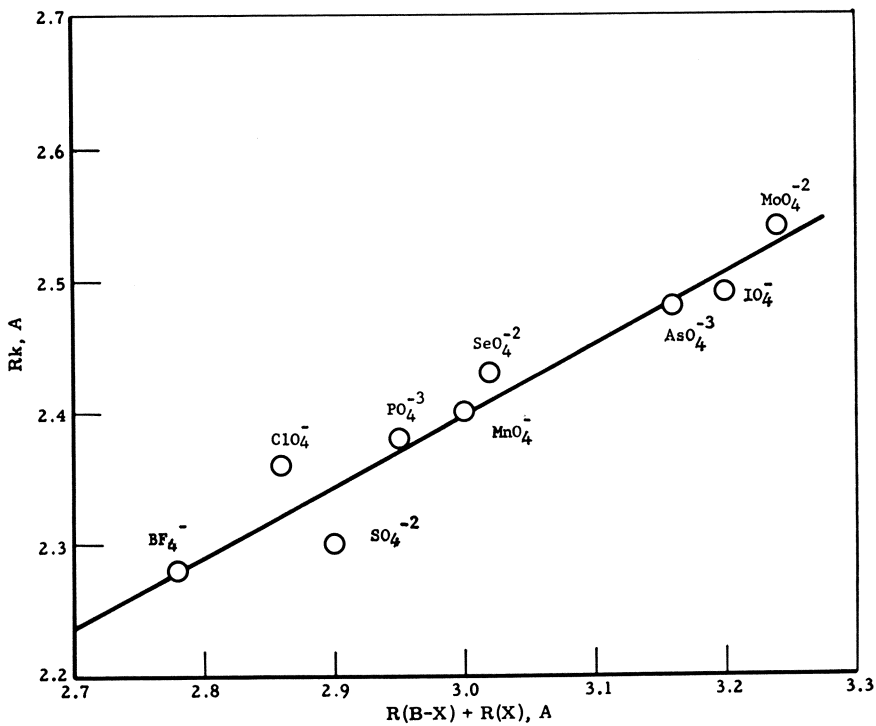

Figure 2. Correlation of thermochemical radius R_k with sum of bond distance R(B—X) and van der Waals radius R(X) in tetrahedral ions

Publication Date: January 1, 1966 | doi: 10.1021/ba-1966-0054.ch004

This expression has turned out to be remarkably useful in correlating the heats of formation of the salts of tetrahedral ions, provided suitable values are assumed for the "ionic radii" R_+ and R_-. Kapustinskii and his coworkers recognized that these quantities are not necessarily equal to the packing radii of the ions in the actual structure of the crystal; consequently, they have come to be known as thermochemical radii. The thermochemical radius and heat of formation for a tetrahedral ion are normally determined from Equation 1 and the known heats of formation of two of its salts.

In order to apply Equation 1 to the hypothetical salts of NF_4^+ it is necessary to estimate a thermochemical radius for that ion. We have found that a fairly good correlation exists for a number of symmetrical tetrahedral ions BX_4 between the thermochemical radius R_k and the sum of (a) the internuclear distance R(B–X) between the central atom of the ion and one of its ligands and (b) the van der Waals radius, R_w(X) of the ligand. This correlation, shown in Figure 2, is described approximately by:

$$R_k(BX_4^{-n}) = (0.75 \pm 0.07)\ \text{A.} + (0.55 \mp 0.024)\,(R(BX) + R_w(X)) \qquad (2)$$

with van der Waals radii 1.35 and 1.41 A. assigned to F and O, respectively. The form of this correlation testifies to the artificial character of the thermochemical radii R_k.

The N–F distance in NF_3 is reported to be 1.37 A (*23*); the N–C distance in the approximately tetrahedral complex $(CH_3)_3N{:}BF_3$ is reported as 1.50 A., about 0.03 A. larger than in trimethylamine, (*23*). A recent x-ray crystallographic study of $(CH_3)_4N^+Br^-$ gave 1.50 ± 0.02 A. also as the N–C distance in the tetramethylammonium ion (*8*). We therefore take the N–F distance in NF_4^+ as 1.40 A. From this and Equation 2 we obtain a thermochemical radius of 2.26 A. for perfluoroammonium ion.

Table I. Stability of Hypothetical

Energy Units, kcal./gm. mole

Anion		*Lattice Energy*	*Salt*	*Probable Decomposition Products*
Symbol	$\Delta H_f(g)$	*(Kapustinskii)*	$\Delta H_f(c)$	
F^-	60.7[a]	147	37 ± 20	$NF_3 + F_2$
	65		33 ± 20	
ClO_4^-	88	116	41 ± 20	$NF_3 + FClO_4$
SO_4^{-2}	151	352	−13 ± 20	$2NF_3 + F_2O + SO_3$
BF_4^-	426	118	−299 ± 20	$NF_3 + F_2 + BF_3$
	407[b]	118	−280 ± 20	

[a] From ΔH_f(F) and electron affinity (Appendix, Tables A,B).
[b] From detailed lattice energy calculations by Altschuller (*1*).

Publication Date: January 1, 1966 | doi: 10.1021/ba-1966-0054.ch004

Stability of Some Perfluoroammonium Salts

The results obtained by using Equation 1 are summarized in Table I. The heats of formation given for the isolated anions were computed from the standard heat of formation of the corresponding potassium salt by means of the Kapustinskii approximation. The value thus derived from F^- (using a radius of 1.33 A.) falls within 5 kcal./mole of that from the heat of formation and measured electron affinity of F. The value for BF_4^- differs by 19 kcal./mole from that obtained in a detailed lattice-energy calculation by Altschuller (*1*); his value is very close to that derived by Kapustinskii and Yatsimirskii (*11*) by modifying the Kapustinskii equation.

The heats of formation given for the hypothetical salts of NF_4^+ in Table I were obtained by adding the heat of formation computed for the anion to the value 245 ± 20 for the heat of formation of NF_4^+ and subtracting the lattice energy of the salt as obtained from the Kapustinskii approximation. The heat of decomposition was obtained by comparing this heat of formation with the sum of the heats of formation of the likely decomposition products. For the fluoride, perchlorate, and sulfate salts decomposition is predicted to be exothermic by a much larger margin than the estimated uncertainty of the prediction; these salts should be unstable at one atmosphere and any temperature. For the fluoroborate the conclusion is less clear. For this salt, the most reasonable estimate of the heat of decomposition probably lies between the two estimates given, and closer to the second estimate than to the first since the Kapustinskii approximation in the simple form used here tends to underestimate the lattice energy (*24*). We therefore conclude that the fluoroborate also may well be unstable at one atmosphere and any temperature.

Even if the heat of decomposition of the fluoroborate is positive by as much as 10 kcal./mole, which seems unlikely, stability of the crystal would be limited to low temperatures by the high entropy of dissociation. The sum of the standard entropies of the likely products, $NF_3 + F_2 + BF_3$, is

Publication Date: January 1, 1966 | doi: 10.1021/ba-1966-0054.ch004

Perfluoroammonium Salts

ΔH_f	*Decomposition* ΔH	*Conclusion*
−29.7	−67 ± 20	Unstable
	−63 ± 20	
<(−30)[c]	<(−70 ± 20)	Unstable
−146	−133 ± 40	Unstable
−301	−2 ± 20	Probably
	−21 ± 20	Unstable

[c] Assuming heat of formation of $FClO_4$ is slightly negative.

171.4 e.u. at 298°K. (7); the entropy of mixing will increase this to 177.9 e.u. The entropy of the hypothetical salt, NF_4BF_4, has been estimated as follows, using entropy data taken from the JANAF Tables (7). At 298°K. S° for $KClO_4(c)$ is 36.1 e.u. while the value for KCl(c) is 19.75 e.u.; an entropy increase of 16.3 e.u. accompanies the replacement of the monoatomic ion Cl^- by the tetrahedral ion ClO_4^- in the crystal lattice. Similarly S° for $KBF_4(c)$ has been estimated as 32.0 e.u. while that of KF(c) is 15.92 e.u.; again the increase is 16 e.u. Thus the entropy of $NF_4BF_4(c)$ should be about 16 e.u. greater than that of KBF_4 or $KClO_4$, and we arrive at a value around 50 e.u. at 300°K.

Decomposition of NF_4BF_4 should therefore be accompanied by an increase in entropy of about 128 e.u. Even if decomposition is endothermic by as much as 10 kcal./mole, the standard free energy change on decomposition will be about —28 kcal./mole, and the calculated decomposition pressure will be of the order of 10^7 atm. at room temperature. Under these circumstances the decomposition pressure would reach one atmosphere only at a temperature below 100°K.

Conclusion

Despite the uncertainties inherent in the Kapustinskii approximation and in the estimated heat of formation of $NF_4^+(g)$, it seems safe to conclude that the hypothetical salts NF_4^+F, NF_4ClO_4 and $(NF_4)_2SO_4$ are unstable relative to their possible decomposition products. The compound NF_4BF_4 is also likely to be unstable at one atmosphere and all temperatures, but may possibly be capable of existence at low temperatures.

Acknowledgment

The work reported here was supported by the Advanced Research Projects Agency, Department of Defense, under Contract No. DA-31-124-ARO(D)-54, monitored by the Chemistry Division, U. S. Army Research Office, Durham, N. C.

We also are grateful to D. O. Schissler and P. A. Wadsworth, of these laboratories, who carried out the experiments.

Literature Cited

(1) Altshuller, A. P., *J. Am. Chem. Soc.* **77**, 6187 (1955).
(2) Berry, R. S., Reimann, C. W., *J. Chem. Phys.* **38**, 1540 (1963).
(3) Bisbee, W. R., Hamilton, J. V., Rushworth, R., Houser, T. J., Gerhauser, J. M., ADVAN. CHEM. SER. **54**, 215 (1966).
(4) Edwards, J. W., Small, P. A., *Nature* **202**, 1329 (1964).

(5) Evans, W. H., *Nat. Bur. Std. (U.S.), Rept. No.* **8504**, 164 (1964).
(6) Herron, J. T., Dibeler, V. H., *J. Chem. Phys.* **35**, 747 (1961).
(7) "JANAF Interim Thermochemical Tables," Dow Chemical Co., Midland, Mich., 1965.
(8) Johnson, Q. C., *U.S. At. Energy Comm.* **UCRL-9350** (1960).
(9) Johnson, F. A., Colburn, C. B., *J. Am. Chem. Soc.* **83**, 3043 (1961).
(10) Kapustinskii, A. F., *Z. Physik. Chem.* **B22**, 257 (1933); *Quart. Rev.* **10**, 284 (1956).
(11) Kapustinskii, A. F., Yatsimirskii, K. B., *Z. Obshch. Khim.* **19**, 2191 (1949).
(12) Kennedy, A., Colburn, C. B., *J. Chem. Phys.* **35**, 1892 (1961).
(13) Loughran, E. D., Mader, C., *J. Chem. Phys.* **32**, 1578 (1960).
(14) Moore, C. E., *Nat. Bur. Std. (U.S.), Circ.* **467** (1949).
(15) *Nat. Bur. Std. (U.S.), Circ.* **500** (1952).
(16) Patrick, C. R., *Adv. Fluorine Chem.* **2**, 1 (1962).
(17) Patrick, C. R., Gozzo, F., *Nature*, **202**, 80 (1964).
(18) Pottie, R. F., *J. Chem. Phys.* **42**, 2607 (1965).
(19) Pritchard, G. O., Thommarson, R. L., *J. Phys. Chem.* **68**, 568 (1964).
(20) Reese, R. M., Dibeler, V. H., *J. Chem. Phys.* **24**, 1175 (1956).
(21) Skuratov, S. M., Vorob'ev, A. F., Privalova, N. M., *Russ. J. Inorg. Chem.* **7**, 343 (1962); *Zh. Neorg. Khim.* **7**, 677 (1962).
(22) Steele, W. C., *J. Phys. Chem.* **68**, 2359 (1964).
(23) Sutton, L. E., "Interatomic Distances," The Chemical Society, London, 1958.
(24) Waddington, T. C., *Advan. Inorg. Chem. Radiochem.* **1**, 158 (1959).
(25) Watanabe, K., *J. Chem. Phys.* **26**, 542 (1957).
(26) Wise, S. S., *et al.*, *J. Phys. Chem.* **65**, 2157 (1961).

RECEIVED April 27, 1965.

Publication Date: January 1, 1966 | doi: 10.1021/ba-1966-0054.ch004

Appendix

The thermochemical data used in the text are listed in the following tables. The standard heats of formation given in Table A have, for the most part, been taken from established compilations; references to the original literature have been given for recent determinations or where some discordance exists among reported values. The value cited for CF_4 conforms to the recent revision in the heat of formation of HF.

The dissociation energies given in Table C were obtained by subtracting 0.6 kcal./mole (RT) from the heats of dissociation. For the charged NF_n^+ species the mass spectrometric appearance potentials, A, listed in Table B were also used as follows—e.g.,

$$NF_3 + e^- = NF_2^+ + F + 2e^- \qquad \Delta E_1 = A_1 - T_1$$

$$NF_3 + e^- = NF^+ + 2F + 2e^- \qquad \Delta E_2 = A_2 - T_2$$

$$D(NF^+—F) = \Delta E_2 - \Delta E_1 = A_2 - A_1 + T_1 - T_2 \simeq A_2 - A_1$$

where T_1 is the kinetic energy of the fragments formed in Reaction 1.

Table A. Standard Enthalpies of Formation, ΔH_f, kcal./gm. mole at 298°K.

Substance	ΔH_f	*Reference*
H	52.095	*5*
C	171.29	*5*
N	112.98	*5*
F	18.88	*5*
NF_3	−29.8 ± 1.8	*5*
NF_2	10.3 ± 2	*5*
	8.9 ± 1.7	*12*
	9.8 ± 2.1	*6*
CF_4	−220.5 ± 1	*7*
CF_3	−115.7 ± 3	*7, 16, 19*
CF_2	−40 (+3, −5)	*4, 17, 18, 22*
CF	74.7	*7*
CH_4	−17.90 ± 0.08	*7*
CH_3	31.94 ± 2	*7*
F_2O	−4.40 ± 0.82	*3*
BF_3	−270.1 ± 0.5	*7, 26*
K(g)	21.31 ± 0.20	*7*
SO_3(g)	−94.58	*5*
KF(c)	−134.46	*7*
KBF_4(c)	−454.2 ± 1.3	*7*
$KClO_4$(c)	−103.45 ± 0.15	*5*
	−101.9 ± 0.2	*21*
K_2SO_4(c)	−342.66	*15*

Table B. Ionization Potentials, I_z, and Appearance Potentials A, e.v.

Substance	I_z	*Reference*
K	4.339	*14*
NF_3	13.20 ± 0.2	*20*
NF_2	11.8 ± 0.1	*9, 13*
F^-	3.448 ± 0.005	*2*
N	14.54	*14*
CH_4	12.99 ± 0.05	*25*
Reaction	*A*	
$NF_3 = NF_2^+ + F + e^-$	14.2 ± 0.3	*20*
$NF_3 = NF^+ + 2F + e^-$	17.9 ± 0.3	*20*
$NF_2 = NF^+ + F + e^-$	15.0 ± 0.2	*9, 13*

Table C. Dissociation Energies, D, kcal./mole at 300°K.

Dissociation	*D*	*Reference*
CF_3—F	124 ± 4[a]	Table A
	122 ± 2	*16*
CF_2—F	95 ± 6	Table A
CF—F	134, −3, +5	Table A
NF_2^+—F	27 ± 11	Tables A and B
	25 ± 10[a]	*20*
NF^+—F	85 ± 14	*20*
	74 ± 9[a]	*9, 13*

[a] Preferred Value

Publication Date: January 1, 1966 | doi: 10.1021/ba-1966-0054.ch004

5

Energies of Atomization from Population Analysis on Hückel Wave Functions

FORREST S. MORTIMER

Shell Development Co., Emeryville, Calif.

Publication Date: January 1, 1966 | doi: 10.1021/ba-1966-0054.ch005

Three-dimensional Hückel molecular orbital calculations have been performed on a series of molecules made from the atoms H, C, N, O, F, and Cl. It has been found that the sum of the Mulliken overlap populations is closely related to the energy of atomization. For 40 compounds not containing carbon, the observed energies of atomization can be reproduced with a mean deviation of 11.1 kcal./mole by a simple empirical equation which includes a term to account for the extra stability of polar molecules. A slightly more complicated expression is needed for compounds of carbon, and the fit to the observed data is not as good.

This study was initiated to determine to what extent empirical molecular orbital (MO) theories of the Hückel type can provide information on the thermodynamic stability of a hypothetical unknown compound. The test, of course, has to be made on known compounds. Our interests have centered on compounds involving atoms such as N, O, F, and Cl, but compounds with C and H have also been included. The results thus far have been encouraging.

From the papers of Lipscomb, Lohr, Hoffmann, *et al.* (*7, 8, 9, 10, 11, 12*) we first learned of their work on an "extended" Hückel theory for polyatomic molecules. We also benefited from a visit to Harvard to discuss this work before their computer program became generally available. Our computer program is based on what we learned from them at that time and on our experience since then in applying it to our particular types of molecules.

The other major influence in the work has come from the papers of Mulliken and his co-workers, in particular the series (*14*) on population analysis of LCAO-MO wave functions and their relation to energies of atomization. As Mulliken suggested (*14*), we have attempted to relate

In Advanced Propellant Chemistry; Holzmann, R.;
Advances in Chemistry; American Chemical Society: Washington, DC, 1966.

the calculated overlap populations to the energy of atomization for the molecule with corrections for the polarity of the bonds.

Three-Dimensional Hückel Theory

The theory (*7, 8, 9, 10, 11, 12*) will be outlined for molecules having n atoms with a total of P valence shell electrons. We seek a set of molecular orbitals (LCAO-MO's), ψ, that are linear combinations of atomic orbitals centered on the atoms in the molecule. Since we shall not ignore overlap, the geometry of the molecule must be known, or one must guess it. The molecule is placed in an arbitrary Cartesian coordinate system, and the coordinates of each atom are determined. Orbitals of the s and p Slater-type (STO) make up the basis orbitals, and as indicated above we restrict ourselves to the valence-shell electrons for each of the atoms in the molecule. The STO's have the following form for the radial part of the function (*13, 18*):

$$R(r) = Nr^m \exp(-\zeta r/a_H) \tag{1}$$

where N is a normalization factor, $m = 0$ for 1 s electrons, 1 for 2 s or 2 p electrons and 2 for 3 s or 3 p electrons, ζ = orbital exponent, and α_H = Bohr radius = 0.529175 A.

The mathematical representation of the basis is needed only for calculating the overlap matrix, which is assumed to give a good representation of the tendency to form a bond.

If Φ is a row vector of the atomic orbitals that make up the basis: $\Phi_1, \Phi_2 \ldots \Phi_N$, then the molecular orbitals are given by an $N \times N$ matrix, ψ.

$$\psi = \Phi C \tag{2}$$

C is a transformation matrix that satisfies the equations:

$$HC = SC\epsilon \tag{3}$$

and

$$C'SC = 1 \qquad (C'_{ij} = C_{ji}) \tag{4}$$

In Equation 3 ϵ is a diagonal matrix of the orbital energies, and S is the overlap matrix of the atomic orbitals (*13*),

$$S_{ij} = \int \varphi_i \varphi_j d\tau \tag{5}$$

It reflects the known or assumed geometry of the molecule.

The Hamiltonian matrix, H, is approximated in the following way. The diagonal elements are effective valence-state ionization potentials

Publication Date: January 1, 1966 | doi: 10.1021/ba-1966-0054.ch005

for the s and p electrons of the atom in question. The off-diagonal elements are calculated according to one of the following options (*15*):

$$H_{ij} = -K_1(H_{ii}H_{jj})^{1/2}\, S_{ij} \tag{6}$$

$$H_{ij} = K_2\, \frac{(H_{ii} + H_{jj})}{2}\, S_{ij} \tag{7}$$

K_1 and K_2 are adjustable parameters having an empirical value of *ca.* 2.0.

A population analysis (*14*) is performed, and a "charge-density-overlap-population" matrix is calculated. The latter is an $n \times n$ matrix whose diagonal elements are "gross atomic populations" (its trace is P). The off-diagonal elements are "overlap populations." It is convenient to define a matrix, R, of dimensions $N \times N$ whose elements are

$$R_{ij} = \sum_k n(k) C_{ik} C'_{kj}$$

where $n(k)$ is the occupation number of the kth MO—i.e., 2, 1, or 0. The elements of the charge-density-overlap-population matrix, ρ, can then be written (*14*):

$$\rho_{\mu\mu} = \sum\nolimits^{\mu} (SR)_{ii} \tag{8}$$

$$\rho_{\mu\nu} = 2 \sum_{j>i}^{\mu\nu} S_{ij} R_{ij} \tag{9}$$

The Σ^{μ} means that the sum goes over the atomic orbitals associated with the μth atom. Similarly, $\Sigma^{\mu\nu}$ means that the sum includes all terms where orbital i is on the μth atom and orbital j is on the νth atom. As indicated above, it can be shown that: trace $(SR) = P$.

The individual diagonal elements of ρ can be associated with the atomic charges, q_{μ}:

$$q_{\mu} = p_{\mu} - \rho_{\mu\mu} \tag{10}$$

where p_{μ} is the number of valence-shell electrons contributed by the μth atom.

If the molecule has a π-system that is completely separated by symmetry from the σ-system a separate π-electron ρ-matrix is also calculated from the π-MO's.

The H_{ii}'s are actually a function of the appropriate q_{μ}, and when these are different from zero it is possible to make $H(q)$ consistent with the calculated q_{μ}'s by an iterative procedure. The S matrix is also a function of q through the dependence of the orbital exponents on q, and these are also altered periodically during the course of the perturbation.

It is to be noted that the Hamiltonian matrix when constructed as described above will not transform properly if the orbitals are first hybridized by the usual procedure. This means that the calculated energies depend on whether the orbitals are hybridized or not. This situation arises for the following reason. A hybridized set of basis orbitals, η,

Publication Date: January 1, 1966 | doi: 10.1021/ba-1966-0054.ch005

would be written as $\eta = \Phi T$ where T is an orthogonal transformation. Thus, the S matrix in the hybridized basis is $T'ST$. However, if the original valence-state ionization potentials are given by the diagonal matrix h, the transformed values are *not* $T'hT$ but only the diagonal elements of this matrix. Thus, H in the Φ basis does *not* become $T'HT$ in the η basis if it is constructed according to the options given by Equations 6 or 7.

One can adopt one of two viewpoints: either to form the Hamiltonian in another way so that it will transform in the same way as S or to consider that the Hamiltonian matrices (as formed by Equations 6 or 7) are good approximations to the true Hartree-Fock matrix for the unhybridized basis, Φ; in this case, in the transformed basis it must be $T'HT$. We have chosen the latter viewpoint in these calculations. (J. A. Pople (*17*) has proposed that the off-diagonal elements be constructed as $H_{ij} = {}^1/_2(\beta_\mu + \beta_\nu)S_{ij}$ where the β's are empirical energies depending only on the atom and not on the state of hybridization.)

Parameters for the Calculations

The values for the valence-state ionization potentials, I_v, and their dependence on charge were obtained from the work of Hinze and Jaffé (*3, 4, 5, 6*). The values that have given the best overall results are those for ionization from s^2 or p^2 configurations. From the original tables of Hinze, Whitehead, and Jaffé (*6*) values of I_v were calculated for the neutral atom A, and for A^+ and A^-. These values never quite lie on a straight line, so a simple parabola was used to interpolate for any intermediate value of the charge. Table I gives the values used for the atoms of interest and the equations as a function of charge.

Table I. Orbital Exponents, ζ, and Equations for H_{ii}

$$H_{ii} = -I_v - A_{qi} - B_{qi}^2$$

Atom	*Orbital*	ζ	I_v	A	B
H	$1s$	1.20[a]	13.20[a]	12.85	—
C	$2s$	1.6083	19.52	11.75	1.15
	$2p$	1.5679	9.75	10.86	1.55
N	$2s$	1.9237	25.58	13.31	1.78
	$2p$	1.9170	12.38	13.09	1.54
O	$2s$	2.2458	32.30	15.35	1.49
	$2p$	2.2266	14.61	14.77	2.17
F	$2s$	2.5638	39.42	17.27	2.21
	$2p$	2.5500	18.31	16.62	1.85
Cl	$3s$	2.3561	25.23	11.48	0.70
	$3p$	2.0387	13.92	10.44	0.24

[a] I_v is altered so that the ionization potential of H_2 is moderately well reproduced, and ζ is altered to agree with values used in the best simple LCAO treatments of H_2.

Orbital exponents for the calculation (Table I) have been taken from Clementi and Raimondi (*1*). Their dependence on charge has been assumed to be that given by Slater's formulas for orbital exponents (*18*).

Publication Date: January 1, 1966 | doi: 10.1021/ba-1966-0054.ch005

Various values of K and the option of the arithmetic or geometric mean (Equations 6 and 7) have been tried, and the results cited here are all for the geometric mean (Equation 6) and for $K_1 = 2.0$.

Results

The total electronic energy at this level of approximation can be written as the sum of two terms, one involving single atoms and a second one involving pairs of atoms.

$$E = \sum_{\mu} E_{\mu} + \sum_{\mu>\nu} E_{\mu\nu} \tag{11}$$

where

$$E_{\mu} = \sum{}^{\mu} H_{ii} R_{ii} \tag{12}$$

and

$$E_{\mu\nu} = 2\sum{}^{\mu\nu} H_{ij} R_{ij} \tag{13}$$

Since H_{ij} is proportional to S_{ij}, one expects $E_{\mu\nu}$, which is an MO approximation to the bond energy, to depend directly on the Mulliken overlap population as given in Equation 9. It should not be expected to include effects caused by the bond polarity, however.

Consequently, we have sought the best empirical relationship we could find between the molecular energies of atomization and sums of the calculated overlap populations. We allowed for the possibility that π-electrons might be different from σ-electrons, and we included various possible terms expressing the polarity of the bonds.

A set of 62 molecules made up of H, C, N, O, F, and Cl have been used to test various relationships between these calculated quantities and the observed energies of atomization, E_{atom}. Of these molecules, 40 contain no carbon atoms, and 22 contain carbon. Multiple regression techniques were used to test the significance of various relationships of the form:

$$E_{\text{atom}} = \text{A}.\sum_{\mu<\nu} \rho_{\mu\nu} + \text{B}\cdot\sum_{\mu<\nu}{}^{+} \rho^{\pi}_{\mu\nu} + C\cdot f(\Delta X_{\mu\nu}) \tag{14}$$

In the early tests, total net positive and net negative overlap populations were considered separately, and the net positive π-electron overlap populations were then the third term. No advantage was found in considering the small negative term separately and thus Equation 14 became the form used. The last term introduces some function of the polarity of the molecule, $f(\Delta X_{\mu\nu})$. Approximate Coulomb energies were calculated for each molecule from the gross atomic charges, q_{μ}. These were tried as a

polarity function but they were only moderately successful. Much more successful was a term of the Pauling (*16*) type:

$$f^P(X_{\mu\nu}) = \sum_{\text{bonds}} \Delta X_{\mu\nu}^2 \tag{15}$$

where $\Delta X_{\mu\nu}$ is the difference between the electronegativities of the bonded atoms, μ and ν. A scale of electronegativities similar to Pauling's was determined so as to give a best fit to the data. This scale is given in Table II; Pauling's values (*16*) are also given for comparison. The optimum value of C in Equation 14, however, was always less than half the value of 30 kcal./mole that was used by Pauling in deriving his electronegativity scale (*16*).

Table II. Effective Atomic Electronegativities

Atom	*Electronegativity*		*Pauling Scale (16)*
H	1.70[a]	1.7[b]	2.1
C	—	2.3	2.5
N	3.10	2.85	3.0
O	3.45	3.45	3.5
F	4.08	3.95	4.0
Cl	2.90	3.0	3.0

[a] Determined for compounds not containing carbon. They are indicated as being significant to ±0.05 to 0.1 unit.
[b] For carbon compounds. Significance is *ca.* 0.1 unit.

Table III. Constants in Equations for E_{atom} and Standard Deviations in kcal./mole[a]

Calculation Type[b]	*Number of Molecules*	*Standard Deviation*	*Maximum Deviation*	*A*	*B*	*C*
I	62	25.2	69.2	132.7 ± 1.9	−48.5 ± 6.3	10.35 ± 0.95
II		22.7	51.8	132.6 ± 1.6	−56.9 ± 5.5	15.2 ± 1.2
I[c]	40[d]	11.1	22.3	116.0 ± 1.1	—	11.63 ± .94
II		13.7	40.4	116.4 ± 1.4	—	17.3 ± 1.9
I	22[e]	24.4	63.8	138.2 ± 2.0	−57.8 ± 6.5	9.8 ± 1.0
		20.0	49.2	137.6 ± 1.7	−65.2 ± 5.2	14.2 ± 1.2
II[c]	[f]	17.3	38.8	136.6 ± 1.5	−61.5 ± 4.5	16.8 ± 1.2

[a] *See* Equation 14.
[b] Calculation I uses f^P; calculation II uses f^C. All but one use the first set of electronegativities from Table II.
[c] Preferred formula for extrapolation.
[d] All molecules without carbon.
[e] Compounds of carbon; in each case maximum deviation is for CO_2.
[f] Using second set of electronegativities from Table II.

A second, closely related polarity function has some advantages for carbon compounds:

$$f^C = f^P\,(1/b\sum_{\mu<\nu}^{+}\rho_{\mu\nu}) \tag{16}$$

where b is the number of bonds in the molecule, and the sum is over net positive values of overlap population. Then, f^C is the Pauling function, f^P, weighted by the average bond overlap population. This was found to be important for strong covalent bonds such as occur in CO_2, but its use

for weakly covalent bonds such as those in ClF_3 leads to underestimating their stability. An advantage to an altered set of electronegativities was also found. This set of electronegativities is also given in Table II.

Table III gives a summary of the results of using Equation 14 as a representation of the energies of atomization for the 62 test molecules. Results are quoted for both polarity functions, f^P and f^C. When the entire set of molecules is tested, f^C seems to be the preferred function; however, f^P is definitely superior for the compounds without carbon, and f^C and the alternate electronegativities are superior for the carbon compounds. For extrapolations to other molecules it would seem desirable to use f^P for compounds without carbon and f^C and the alternate electronegativities

Table IV. Calculated and Observed Energies of Atomization (E_{atom}) for Compounds without Carbon[a]

Compound	Sum Overlap Populations: All Values	Sum Overlap Populations: Only $+\pi$	Sum Bond $(\Delta X)^2$	E_{atom} (Obs.) kcal./mole	E_{atom} (Calc.) kcal./mole
H_2	0.794	0	0	110.5	92.1
N_2	1.791	0.905	0	229.3	207.7
O_2	0.854	0.170	0	121.4	99.1
F_2	0.281	0	0	39.0	32.6
Cl_2	0.484	0	0	59.7	56.1
NH_3	2.105	0	5.880	300.8	312.6
OH	0.685	0	3.062	107.4	115.1
H_2O	1.303	0	0.125	234.3	222.4
HF	0.612	0	5.664	141.5	136.9
HCl	0.717	0	1.440	107.3	99.9
NO	1.205	0.417	0.122	153.4	141.2
N_2O	2.482	0.918	0.122	272.6	289.3
NO_2	1.951	0.420	0.245	229.0	229.1
N_2O_3	3.303	0.750	0.367	394.5	387.4
N_2O_4	4.110	0.765	0.490	472.0	482.4
N_2O_5	4.634	0.728	0.735	536.2	546.0
FNO	1.528	0.376	1.083	211.6	189.8
ClNO	1.505	0.373	0.162	192.8	176.5
FNO_2	2.277	0.330	1.205	278.1	278.1
$ClNO_2$	2.268	0.375	0.285	262.9	266.4
$FONO_2$	2.681	0.344	0.764	316.6	319.9
NF	0.543	0.077	0.960	71.0	74.2
NF_2	1.046	0.074	1.921	155.0	143.7
t—N_2F_2	2.060	0.402	1.921	215.4	261.3
c—N_2F_2	2.054	0.403	1.921	254.8	260.6
t—N_2F_4	2.438	0	3.842	316.5	327.5
g—N_2F_4	2.438	0	3.842	316.5	327.5
NF_3	1.489	0	2.881	206.0	206.2
O_3	1.336	0.249	0	149.7	155.0
OF	0.392	0	0.397	53.0	50.1
F_2O	0.739	0	0.794	95.0	94.9
F_2O_2	1.227	0	0.794	156.5	151.6
F_2O_3	1.680	0	0.794	219.0	204.1
OCl	0.573	0	0.302	65.0	70.0
Cl_2O	0.812	0	0.605	103.0	101.2
ClO_2	1.140	0	0.605	126.6	139.3
ClO_3	1.527	0	0.907	177.0	187.7
Cl_2O_7	3.347	0	2.420	437.0	416.4
ClF	0.368	0	1.392	62.3	58.9
ClF_3	0.622	0	4.177	128.8	120.7

[a] Mean deviation: 11.1 kcal./mole. Electronegativities: H = 1.70, C = 2.30, N = 3.10, O = 3.45, F = 4.08, Cl = 2.90.

Publication Date: January 1, 1966 | doi: 10.1021/ba-1966-0054.ch005

Table V. Calculated and Observed Energies of Atomization (E_{atom}) for Compounds of Carbon[a]

Compound	Sum Overlap Populations: All Values	Sum Overlap Populations: $+\pi$ Only	Sum wt. Bond $(\Delta X)^2$	E_{atom} (Obs.) kcal./mole	E_{atom} (Calc.) kcal./mole
C_2	1.738	0.934	0	145.0	180.0
CH_4	2.991	0	1.164	420.0	428.1
C_2H_6	5.025	0	1.740	710.7	715.5
C_2H_8	7.056	0	2.319	1005.3	1002.7
C_4H_{10}	9.087	0	2.899	1300.7	1289.8
C_3	2.978	1.272	0	329.5	328.6
CN	1.741	0.916	0.527	178.0	190.3
$(CN)_2$	4.451	1.970	0.926	504.0	502.4
C_4N_2	7.197	3.132	0.913	801.7	805.8
FCN	2.434	0.997	3.737	310.5	333.9
ClCN	2.495	1.022	1.015	285.3	295.0
CO	1.554	0.790	2.055	206.0	198.2
CO_2	2.619	1.053	3.527	391.0	352.2
C_3O_2	5.149	2.087	3.560	654.0	634.7
F_2CO	2.489	0.459	5.885	429.4	410.5
Cl_2CO	2.485	0.470	2.067	346.8	345.2
CF	0.729	0.201	1.985	117.0	120.5
CF_4	2.550	0	7.397	476.1	472.3
C_2F_4	3.605	0.500	8.398	582.0	602.5
C_2F_6	4.325	0	10.998	775.0	775.2
$CClF_3$	2.475	0	5.805	424.0	435.4
CCl_4	2.338	0	1.336	318.5	341.8

[a] Mean deviation: 17.3 kcal./mole. Electronegativities: H = 1.70, C = 2.30, N = 2.85, C = 3.45, F = 3.95, Cl = 3.00.

Table VI. Estimated Energies of Atomization and Energies of Formation for Some Molecules

Molecule	E_a (calc.) kcal./mole	$\Delta E_{formation}$ kcal./mole	Known Stability
NCl_3	205	+34	unstable
CH_3NCl_2	513	−2	stable
$(CH_3)_2NCl$	824	−6	stable
NHF_2	227	− 18	stable
N_6[a]	579	+109	unknown

[a] Assumed to be the aromatic analog of benzene with bond lengths equal to 1.29 A.

for those with carbon. It is interesting that the A-value is considerably larger for carbon compounds than for others. This, plus the need for a relatively large negative value for B, must reflect the particular stability of the tetrahedral hybrid orbitals used by carbon. Table IV and V give the results for the 62 compounds, each calculated according to the preferred formula.

Only a few calculations have thus far been performed on unknown compounds or on compounds whose energy of formation has not been reported. Our estimates for these are given in Table VI. For NCl_3, which is known to be unstable, we estimate a positive energy of formation of +34 kcal./mole while NF_3, which is stable, is known to have a negative value of −31.9. CH_3NCl_2 and $(CH_3)_2NCl$, both of which are relatively stable, have calculated energies of formation of −2 kcal./mole and −6 kcal./mole, respectively. The hypothetical molecule N_6, assumed to be

Publication Date: January 1, 1966 | doi: 10.1021/ba-1966-0054.ch005

an analog of benzene, is predicted to have a positive energy of formation of +109 kcal./mole. It would thus be quite unstable relative to 3 moles of N_2, which probably explains why the compound has not been made. It would appear that were it not for repulsions between the lone pairs, the molecule might be stable.

Acknowledgment

The author wishes to acknowledge J. H. Schachtschneider for his contributions to this work. He wrote the first version of the computer program and has provided valuable guidance at many points during the writing of the program now being used. He also wrote the program for determining the Cartesian coordinates of the atoms in a molecule from the known or assumed geometry.

The work reported here was supported by the Advanced Research Projects Agency, Department of Defense, under Contract No. DA-31-124-ARO(D)-54, monitored by the U. S. Army Research Office, Durham, N. C.

Literature Cited

(1) Clementi, E., Raimondi, D. L., *J. Chem. Phys.* **38**, 2686 (1963).
(2) Coulson, C. A., "Valence," p. 40, University Press, Oxford, 1953.
(3) Hinze, J., Jaffé, H. H., *J. Am. Chem. Soc.* **84**, 540 (1962).
(4) Hinze, J., Whitehead, M. A., Jaffé, H. H., *Ibid.* **85**, 148 (1963).
(5) Hinze, J., Jaffé, H. H., *Can. J. Chem.* **41**, 1315 (1963).
(6) Hinze, J., Jaffé, H. H., private communication.
(7) Hoffmann, R., Lipscomb, W. N., *J. Chem. Phys.* **36**, 2179 (1962).
(8) Hoffmann, R., Lipscomb, W. N., *J. Chem. Phys.* **37**, 2872 (1962).
(9) Hoffmann, R., *J. Chem. Phys.* **39**, 1397 (1963).
(10) Jordon, T., Smith, H. W., Lohr, L. L., Jr., Lipscomb, W. N., *J. Am. Chem. Soc.* **85**, 846 (1963).
(11) Lohr, L. L., Jr., Lipscomb, W. N., *J. Am. Chem. Soc.* **85**, 240 (1963).
(12) Lohr, L. L., Jr., Lipscomb, W. N., *J. Chem. Phys.* **38**, 1607 (1963).
(13) Mulliken, R. S., Rieke, C. A., Orloff, D., Orloff, H., *J. Chem. Phys.* **17**, 1248 (1949).
(14) Mulliken, R. S., *J. Chem. Phys.* **23**, 1833, 1841, 2338, 2343 (1955).
(15) Mulliken, R. S., *J. Phys. Chem.* **56**, 295 (1952).
(16) Pauling, L., "Nature of the Chemical Bond," 3rd ed., pp. 88-95, Cornell University Press, Ithaca, 1960.
(17) Pople, J. A., *et al.*, *J. Chem. Phys.* **43**, S129 (1965).
(18) Slater, J. C., *Phys. Rev.* **36**, 57 (1930).

RECEIVED April 19, 1965.

6

Synthetic Applications of Nitronium Tetrafluoroborate

ROBERT E. OLSEN, DUANE W. FISH, and EDWARD E. HAMEL
Aerojet-General Corp., Sacramento, Calif.

Publication Date: January 1, 1966 | doi: 10.1021/ba-1966-0054.ch006

Nitronium tetrafluoroborate has been shown to be a versatile nitrating agent for nitrogen compounds, giving the corresponding N-*nitro derivative when it reacts with secondary aliphatic amines, an acyl aliphatic amine, a carbamate ester, a diacyl amine, and primary amides. Reaction of secondary alkane nitronate salts with nitronium tetrafluoroborate gives mixtures of the* gem-*dinitroalkane and pseudonitrole while treating the same salts with nitrosonium tetrafluoroborate yields only the corresponding pseudonitrole.*

Oláh and Kuhn showed that nitronium salts are effective nitrating agents for alcohols (*15*) and aromatics (*10*). In a recent summary of their work (*14*) they state that such salts can also nitrate amines; however, they refer to unpublished work, and no experimental details are provided. This paper describes the use of nitronium tetrafluoroborate to nitrate several amines, amine derivatives, and salts of nitroalkanes.

Since no differences in product yield have been reported as being caused by an effect of different anions in nitronium salts (*10*) and considering its ease of preparation and stability, nitronium tetrafluoroborate was chosen as the nitronium salt during our investigations. To use nitronium salts, one must rigorously exclude moisture (which hydrolyzes the salt to nitric acid) and select a suitably inert solvent. We have found that acetonitrile and methylene chloride offer a major advantage over solvents previously employed for nitronium salts since they permit the use of low (−40 to −30° C.) reaction temperatures, thus minimizing oxidative side reactions. Acetonitrile reacted slowly with nitronium salts at room temperature, but this did not lead to complications since the reactions were carried out at low temperatures and were complete usually in one hour or less. In most of the reactions investigated, we did not attempt to find optimum conditions; hence, the reported yields may not represent maximum values.

In Advanced Propellant Chemistry; Holzmann, R.;
Advances in Chemistry; American Chemical Society: Washington, DC, 1966.

Nitration of Primary Amides

There appears to be no general procedure available for preparing primary nitramides. *N*-nitroacetamide (*7*) (described as quite unstable in the free state), methyl *N*-nitrosuccinamidate, and ethyl *N*-nitrophthalamidate (*9*) (prepared by the alcoholysis of the corresponding *N*-nitrimides) are the only reported primary nitramides. Commenting on their rarity, Lamberton (*11*) has speculated that they decompose under normal nitration conditions. However, using nitronium tetrafluoroborate with acetonitrile or methylene chloride solvent in the presence of one equivalent of potassium acetate (to react with the hydrofluoroboric acid formed during the reaction), aliphatic and aromatic primary amides were converted to their *N*-nitro derivatives in good yields. With the exception of *N*-nitroacetamide, the primary nitramides prepared were relatively stable solids which decomposed above their melting points. *N*-Nitroacetamide was obtained only in low yields and decomposed during attempted purification. As expected, the primary nitramides were acidic and could be converted to their alkali metal salts by treatment with an acetate salt in a nonaqueous solvent. Infrared spectra were consistent with the proposed structure, and the following characteristic (*13*) absorption bands were observed: a sharp single NH band at 3374–3390 cm.$^{-1}$, two strong *N*-nitro bands at 1620–1610 cm.$^{-1}$ and 1307–1302 cm.$^{-1}$, and a carbonyl band shifted to 1751–1739 cm.$^{-1}$. Table I shows the primary nitramides which were prepared, along with their yields and melting points.

Table I. Nitration of Primary Amides with Nitronium Tetrafluoroborate

$$RCONH_2 + NO_2BF_4 \rightarrow RCON(NO_2)H + HBF_4$$

Primary Amide	*Yield of N-nitro derivative, %*	*m.p., °C.*	*Analysis*					
			Calculated			*Found*		
			C	*H*	*N*	*C*	*H*	*N*
Acetamide	12.5[a]	65–72[a]						
2-Chloroacetamide	54.5	80–82	17.4	1.4	20.2	17.4	2.2	20.1
2,2,2-Trichloroacetamide	61.7	72–73	11.6	0.5	13.5	11.9	1.0	13.1
Benzamide	52.5	91–93	50.6	3.7	16.9	50.6	3.7	16.9
p-Chlorobenzamide	50.0	152–154	41.8	2.5	14.0	41.6	2.7	14.0
p-Nitrobenzamide	52.5	178–180	38.0	2.3	19.0	40.8	2.9	18.3

[a] Crude reaction product. The material was identified as *N*-nitroacetamide by infrared analysis but decomposed during attempted purification.

Nitration of Amines and Amine Derivatives

At present there are four good methods for preparing secondary nitramines. They are: the oxidation of nitrosamines by peroxytrifluoroacetic acid (*5*), the chloride-ion catalyzed direct nitration of amines (*3*), the nitrolysis of dialkylamides with nitric acid (*16*), and the alkaline nitration of amines with acetone cyanohydrin nitrate (*6*). We have found that treating two equivalents of several secondary aliphatic amines

with nitronium tetrafluoroborate in methylene chloride solvent gave, along with a quantitative yield of the ammonium fluoroborate salts, the corresponding secondary nitramines in yields similar to the most general previously reported method, chloride-ion catalyzed nitration. However, preparing secondary nitramines via nitronium tetrafluoroborate offers a simplified work-up procedure since the difficult-to-separate nitrosamine derivatives were not produced by this method. Essentially pure nitramines were obtained by removing the ammonium salt by filtration and evaporating the methylene chloride solvent. The role of solvent is not clear since, under widely varying conditions, treating the same secondary amines with nitronium tetrafluoroborate in acetonitrile gave a quantitative yield of the ammonium fluoroborate and little if any secondary nitramine. Similarily, Wright (*2*) has reported that treating a secondary aliphatic amine with nitronium perchlorate in acetic anhydride gave none of the desired secondary nitramine.

Reaction of a primary aliphatic amine, *n*-butylamine, with nitronium tetrafluoroborate in methylene chloride or acetonitrile produced not *n*-butylnitramine, but *n*-butyl nitrate in about 20% yield. However, treating an electronegatively substituted primary aromatic amine, picramide, with nitronium tetrafluoroborate did give the primary nitramine, *N*,2,4,6-tetranitroaniline, in 85% yield. Oláh (*16*) had reported previously that aniline was oxidized vigorously by nitronium salts.

Table II. Nitration of Amines and Amine Derivatives with Nitronium Tetrafluoroborate

$$R_1R_2NH + NO_2BF_4 \rightarrow R_1R_2NNO_2 + HBF_4$$

Amine or Derivative	*Yield of N-nitro Derivative, %*	*b.p. (m.p.), °C.*	*Ref.*
Di-*n*-butylamine	54[a]	127–129 at 10 mm.	*12*
Morpholine	72[a]	(51.0–52.0)	*12*
β,β'-bis(Cyanoethyl)amine	62[a]	(55.5–57.0)	*2*
Ethyl *n*-butylcarbamate	91	75–77 at 0.8 mm.	*17*
n-Butylacetamide	40	45–47 at 0.5 mm.	*18*
Succinimide	43	(92.0–93.0)	*9*
Picramide	85	(78.0[b] (def.))	*1*

[a] Methylene chloride solvent; all others used acetonitrile.
[b] Caution should be exercised during recrystallization since *N*-2,4,6-tetranitroaniline has been found to deflagrate at temperatures near 50°C. while in an impure state. An analytical sample was obtained by recrystallization from chloroform.

Aliphatic and alicyclic carbamates are nitrated smoothly and in excellent yields by a nitric acid-acetic anhydride mixture (*4*). Similarily, we have found that treating an acyl aliphatic amine and a urethane with one equivalent of nitronium tetrafluoroborate in acetonitrile at —30° C. gave the corresponding *N*-nitro derivatives in good to excellent yields. However, diacylamines are more difficult to nitrate, and Kauffman and Burger (*9*) have reported that nitrating succinimide required 13 hours

Publication Date: January 1, 1966 | doi: 10.1021/ba-1966-0054.ch006

reaction time with a nitric acid-acetic anhydride mixture. Employing nitronium tetrafluoroborate as the nitrating agent, *N*-nitrosuccinimide was formed after 30 minutes reaction time in acetonitrile at —30° C. although the yields were somewhat lower than previously reported (43 *vs.* 63%).

The amines and amine derivatives which were nitrated with nitronium tetrafluoroborate are summarized in Table II.

Nitration of Salts of Secondary Nitroalkanes

The oxidative nitration reaction of Kaplan and Shechter (*8*) is the only general method for preparing secondary *gem*-dinitroalkanes. We have found that treating salts of secondary nitroalkanes with nitronium tetrafluoroborate in acetonitrile at —40°C. also gives secondary *gem*-dinitroalkanes although the yields are much lower than those obtained by the Shechter technique and the reaction is characterized by the formation of pseudonitrole byproduct. The cation of the nitroalkane salt considerably influences the reaction since treating the potassium, sodium, and lithium salts of 2-nitropropane or nitrocyclohexane with nitronium tetrafluoroborate gave 0, 25, and 35% yields, respectively, of the *gem*-dinitro product and 5, 25, and 25% yields, respectively, of the corresponding pseudonitrole. Using reaction temperatures higher than —40°C. in acetonitrile resulted in diminished yields of both products while using methylene chloride as solvent afforded no reaction, probably owing to the insolubility of both reactants in this solvent. The reaction of nitronium tetrafluoroborate with salts of nitroalkanes is summarized in Table III.

Table III. Nitration of Alkyl Nitronate Salts with Nitronium Tetrafluoroborate

$$R_1R_2C{=}NO_2M + NO_2BF_4 \rightarrow R_1R_2C(NO_2)_2 + R_1R_2C(NO)NO_2 + MBF_4$$

		% Yield			% Yield	
Cation	*Alkyl*	*Dinitro*	*Pseudonitrole*	*Alkyl*	*Dinitro*	*Pseudonitrole*
Li	isopropyl	35	25	cyclohexyl	35	25
Na	isopropyl	25	25	cyclohexyl	25	25
K	isopropyl	0	5	cyclohexyl	0	5

Table IV. Nitrosation of Alkyl Nitronate Salts with Nitrosonium Tetrafluoroborate

$$R_1R_2C{=}NO_2M + NOBF_4 \rightarrow R_1R_2C(NO)NO_2 + MBF_4$$

Cation	*Alkyl*	% Yield, *Pseudonitrole*	*Alkyl*	% Yield, *Pseudonitrole*
Li	isopropyl	95	cyclohexyl	95
Na	isopropyl	80	cyclohexyl	80
K	isopropyl	60	cyclohexyl	60

The formation of pseudonitrole byproducts during the reactions of nitronium tetrafluoroborate led us to investigate the reactions of salts of

Publication Date: January 1, 1966 | doi: 10.1021/ba-1966-0054.ch006

secondary nitroalkanes with nitrosonium tetrafluoroborate. It was found that pseudonitroles were produced in excellent yields, with the cation of the nitroalkane salt again showing a strong influence on the reaction. Treating the potassium, sodium, and lithium salts of 2-nitropropane or nitrocyclohexane with nitrosonium tetrafluoroborate gave 60, 80, and 95% yields, respectively, of 2-nitro-2-nitrosopropane and 1-nitro-1-nitrosocyclohexane. The results are tabulated in Table IV.

Experimental

Melting and boiling points are uncorrected. Reactions involving nitronium tetrafluoroborate were carried out in a dry box under a nitrogen atmosphere. Elemental analyses were conducted at the Analytical Laboratories of Aerojet-General Corp., Sacramento, Calif.

Nitronium Tetrafluoroborate. We followed the procedure of Oláh and Kuhn (*10*) in which nitric acid, hydrogen fluoride, and boron trifluoride were allowed to react in a suitable solvent. The previously reported solvent was nitromethane; however, in view of the reported mineral acid sensitization of nitromethane toward detonation, we decided to use 2-nitropropane as solvent. With this modified procedure it was necessary to wash the nitronium tetrafluoroborate with Freon 113 (1,1,2-trichloro-1,2,2-trifluoroethane) and dry the nitronium salt for 4 hours at 60°C. under reduced pressure (1 mm.) to ensure complete removal of solvent.

It should be mentioned that occasional batches of nitronium tetrafluoroborate have exhibited poor nitration ability. The poor reactivity has usually been associated with the sample of nitronium tetrafluoroborate adsorbing moisture.

Preparation of Secondary Aliphatic Nitramines. A solution of β,β'-bis(cyanoethyl)amine (10.0 grams, 0.08 mole) in 60 ml. of methylene chloride was cooled to −30°C., and 5.3 grams (0.04 mole) of nitronium tetrafluoroborate was added over a 10-minute period. The mixture was stirred for 1 hour at 0°C., then 4 hours at room temperature. The hydrofluoroboric acid salt of β,β'-bis(cyanoethyl)amine, 8.3 grams, 99% yield, m.p. 159°–160°C.) was removed by filtration.

Elemental analysis showed the following values. Calculated for $C_6H_{10}N_3BF_4$: C, 34.2; H, 4.8; N, 19.9. Found: C, 34.8; H, 4.9; N, 21.2.

The filtrate was concentrated under reduced pressure to leave crude β,β'-bis(cyanoethyl)nitramine, which after one recrystallization from methanol gave a product (3.3 grams, 62% yield) which melted at 55.5°–57.0°C. (literature value (*2*) 55.5°–56.8°C.). The other secondary aliphatic nitramines prepared, along with their yields and melting or boiling points are given in Table II.

Preparation of Acyl *N*-Nitramine Compounds. Ethyl *n*-butylcarbamate (4.0 grams, 0.03 mole) was dissolved in 50 ml. of acetonitrile, cooled to −30°C., and treated with 4.0 grams (0.03 mole) of nitronium tetrafluoroborate. The solution was allowed to warm, with stirring, to 0°C. and quenched into 200 ml. of ice water. A yellow oil separated, which was dissolved in methylene chloride and dried over anhydrous magnesium sulfate. After removing the solvent 5.0 grams (91% yield) of ethyl

Publication Date: January 1, 1966 | doi: 10.1021/ba-1966-0054.ch006

N-nitro-*n*-butylcarbamate (b.p. 75°–77°C. at 0.8 mm., n_D^{24} 1.4476, literature value (*17*) n_D^{21} 1.4488) was obtained by fractional distillation under reduced pressure. Other acyl *N*-nitramine derivatives, with their yields and melting or boiling points are shown in Table II.

Preparation of *gem*-Dinitroalkanes. A methanolic solution of alkali metal hydroxide (Li, Na, or K) was treated with 10% excess nitroalkane and stirred for 30 minutes. The solution was evaporated to dryness in vacuo, and the alkali metal alkyl nitronate was dried over phosphorus pentoxide at reduced pressure (0.1 mm.) for 24 hours. (Caution: nitronate salts may be shock sensitive and have been known to explode after prolonged storage.) A slurry of 3.3 grams (0.02 mole) of lithium 1-nitrocyclohexane in 50 ml. of acetonitrile was cooled to —40°C., and 2.7 grams (0.02 mole) of nitronium tetrafluoroborate were slowly added. The reaction was not exothermic, and the reaction mixture turned brilliant blue upon adding nitronium tetrafluoroborate. The reaction mixture was stirred for 2 hours at —30° to —40°C., then filtered to give a quantitative yield of lithium tetrafluoroborate. The filtrate was quenched into 100 ml. of ice water to yield an insoluble oil, which was dissolved in methylene chloride and dried over anhydrous magnesium sulfate. Removal of solvent under reduced pressure left a semisolid, which was extracted with hexane. The hexane-insoluble residue (0.8 grams 25% yield) was a white powder identified as 1-nitroso-1-nitrocyclohexane, m.p. 78.0°–79.0°C. (blue melt).

Elemental analysis showed the following values. Calculated for $C_6H_{10}N_2O_3$: C, 46.6; H, 6.4; N, 17.7. Found: C, 46.4; H, 6.4; N, 18.0.

Evaporating the hexane extract under reduced pressure followed by fractional distillation gave 1.2 grams (35% yield) of 1,1-dinitrocyclohexane (b.p. 62°–63°C. at 0.5 mm., literature value (*8*) b.p. 67°C. at 0.7 mm.). The yields of *gem*-dinitro and pseudonitrole derivatives obtained from the reaction of other salts of alkyl nitronates are shown in the Table III.

Preparation of Pseudonitroles. The procedure used to prepare pseudonitroles was identical to that described for preparing *gem*-dinitroalkanes except that nitrosonium tetrafluoroborate was used in place of nitronium tetrafluoroborate. The yields of pseudonitrole obtained from the various nitronate salts are presented in Table IV.

Publication Date: January 1, 1966 | doi: 10.1021/ba-1966-0054.ch006

Acknowledgment

A portion of this work was supported by the Advanced Research Projects Agency and monitored by the Air Force Flight Test Center, Edwards Air Force Base, Calif., Contract AF 04(611)-9891.

Literature Cited

(1) Blatt, A. H., **OSRD-2014** (1944).
(2) Chute, W. J., Dunn, G. E., MacKenzie, J. C., Myers, G. S., Smart, G. N. R., Suggitt, J. W., Wright, G. F., *Can. J. Res.* **26B**, 114 (1948).
(3) Chute, W. J., Herring, K. G., Toombs, L. E., Wright, G. F., *Can. J. Res.* **26B**, 89 (1948).
(4) Curry, H. M., Mason, J. P., *J. Am. Chem. Soc.* **73**, 5043 (1951).

(5) Emmons, W. D., *J. Am. Chem. Soc.* **76**, 3468 (1954).
(6) Emmons, W. D., Freeman, J. P., *J. Am. Chem. Soc.* **77**, 4387 (1955).
(7) Hinsberg, V., *Ber.* **25**, 1092 (1892).
(8) Kaplan, R. B., Shechter, H., *J. Am. Chem. Soc.* **83**, 3535 (1961).
(9) Kauffman, H. F., Burger, A., *J. Org. Chem.* **19**, 1662 (1954).
(10) Kuhn, S. J., Oláh, G. A., *J. Am. Chem. Soc.* **83**, 4564 (1961).
(11) Lamberton, A. H., *Quart. Rev.* **5**, 75 (1951).
(12) Myers, G. S., Wright, G. F., *Can. J. Res.* **26B**, 257 (1948).
(13) Nakanishi, K., "Infrared Absorption Spectroscopy, Practical," Holden Day Inc., San Francisco, 1962.
(14) Oláh, G. A., Kuhn, S. J., "Friedel-Crafts and Related Reactions," Vol. III, pp. 1393–1491, G. A. Oláh, Ed., Interscience Publishers, New York, 1964.
(15) Oláh, G. A., Kuhn, S. J., *Chem. Ber.* **89**, 2374 (1956).
(16) Oláh, G. A., Kuhn, S. J., *Chem. Ind.* **1956**, 98.
(17) Robson, J. H., Reinhart, J., *J. Am. Chem. Soc.* **77**, 2453 (1955).
(18) White, E. H., *J. Am. Chem. Soc.* **77**, 6008 (1955).

RECEIVED April 23, 1965.

7

The Deflagration of Hydrazine Perchlorate

J. B. LEVY, G. VON ELBE, R. FRIEDMAN,
T. WALLIN, and S. J. ADAMS

Atlantic Research Corp., Alexandria, Va.

Publication Date: January 1, 1966 | doi: 10.1021/ba-1966-0054.ch007

The deflagration of hydrazine perchlorate, both pure and with fuel and catalyst additives, has been investigated. Hydrazine perchlorate will deflagrate reproducibly if a few percent fuel is present. The deflagration process is catalyzed by copper chromite, potassium dichromate, and magnesium oxide. Deflagration rates have been measured photographically from 0.26 to 7.7 atm. A liquid layer was observed at the surface in these experiments. Vaporization rate measurements from 180°–235° C. have yielded the expression $\log_{10} P_{(mm.)} = 10.2 - \frac{6400}{T}$ *for the vapor pressure of hydrazine perchlorate. Temperature profiles of the deflagration wave have been measured, and spectroscopic measurements of the flame temperature above a deflagrating strand have been made. The results are discussed in terms of the mechanism of deflagration of hydrazine perchlorate.*

We are engaged in a general program of research to understand the factors that govern the nature of the deflagration of composite solid propellants. Our efforts have been devoted to studies of the oxidizer alone ever since early observations that ammonium perchlorate deflagrated as a monopropellant at rates comparable to those found for propellant formulations containing it (*1, 9*). Earlier work in this laboratory dealt with the self-deflagration of ammonium perchlorate (*16*). We report here on studies with the related but more energetic material—hydrazine perchlorate.

Hydrazine perchlorate is a white crystalline solid melting at 140°–142° C. and having a density of 1.939 grams/cc. (*5*). It forms a hemihydrate which can be dehydrated readily at 64.5° C. under vacuum. It has been reported (*5*) that dry hydrazine perchlorate can be detonated by shock or friction and that it has a shock sensitivity comparable to that of initiating explosives. We have observed the usual precautions in

In Advanced Propellant Chemistry; Holzmann, R.;
Advances in Chemistry; American Chemical Society: Washington, DC, 1966.

handling this material and have experienced explosions with it only under extreme conditions—i.e., in certain deflagration experiments. However, it is a very energetic material and must be handled with great care.

The thermal decomposition of hydrazine perchlorate has been investigated, and ammonium perchlorate was found to be a major product (*13*). We know of no studies of the self-deflagration of hydrazine perchlorate. The results reported here are concerned with studies of pure hydrazine perchlorate and hydrazine perchlorate containing small amounts of additives.

Experimental

Preparation of Hydrazine Perchlorate. Hydrazine perchlorate was prepared by titrating a solution of 85% hydrazine hydrate to a pH of 3.2 with 48% perchloric acid. This yielded a stock solution which could be stored indefinitely. Hydrazine perchlorate was precipitated by pouring a volume of this solution into 5 volumes of 2-propanol at 0° C. The hydrazine perchlorate was filtered, washed with cold 2-propanol, and vacuum dried at 80° C.

The material was analyzed iodometrically (*3*). Purities > 99%, as indicated by the analysis, were obtained. The melting point was 142°–143° C.

Processing Hydrazine Perchlorate. The hydrazine perchlorate used for the deflagration measurements was prepared in the form of small spherical particles of fairly uniform size distribution by means of a melt-shot apparatus. In this apparatus solid hydrazine perchlorate is fed into a spinning aluminum dish maintained at a temperature above the melting point of hydrazine perchlorate and fitted with a small lateral hole in the side, which permitted the ejection of the molten spheres which cool as they fly through the air. It was found that 160° C. was a satisfactory temperature for the dish. With the dish spinning at 2400 r.p.m. the particle sizes of the spheres obtained, as determined by microscopic examination of a random selection, varied from 50–300μ. Analysis of material prepared in this way indicated that no decomposition occurred during the shotting process.

Strand Preparation. Strands were either tamped or pressed. Tamped strands were prepared by pouring small increments of material

Table I. Vaporization Rates

Temp. ° K.	*Area sq. cm.*	*Duration sec.*	*Weight, grams* charged	*Weight, grams* sublimed
453	4.90	18,900	1.56	0.22
463	0.50	21,240	0.244	0.073
473	4.90	18,900	1.70	0.54
492	0.50	2,220	0.239	0.036
508	4.90	2,400	1.65	08.3

Publication Date: January 1, 1966 | doi: 10.1021/ba-1966-0054.ch007

into a tube and tamping each increment gently with a Teflon rod. Pressed strands were prepared in a steel mold by means of a hydraulic press. Pressures of ~40,000 p.s.i.g. gave strands of 95–98% of crystal density, which was considered adequate. Pressing operations were performed remotely.

The mixtures of hydrazine perchlorate and the fuels or catalysts were prepared by mixing the hydrazine perchlorate shot with the finely ground other ingredients in an ordinary vee mixer for several hours. The uniform deflagration rates observed with the various mixtures attest to the homogeneity of strands prepared in this way.

Sublimation Experiments. The sublimation experiments were performed with a conventional cold-finger vacuum sublimation apparatus with a removable cold finger. The apparatus was evacuated by an oil pump to about 5 microns, lowered into a thermostat, and the timer started.

Two sublimation apparatuses were used. At first a fairly small one with a cross-sectional area of 0.5 sq. cm. was used to keep the amount of hydrazine perchlorate required down to about 0.5 grams. Subsequently a larger apparatus having a cross-sectional area of 4.90 sq. cm. was used with amounts of hydrazine perchlorate of the order of 1.5–2.0 grams.

At the conclusion of the experiment the sublimate was carefully removed from the cold finger and weighed. The weight of the residue was found by weighing the outer tube, washing out the residue, and reweighing the tube. The analyses were performed by iodometry.

Flame Temperature Measurements. A tungsten ribbon filament lamp, calibrated by the National Bureau of Standards for the temperature range 1100°–2300° C., was used for these measurements which were performed in the conventional manner (*17*).

Results

The experiments performed in this program are grouped into: (a) experiments in which vaporization rates of pure hydrazine perchlorate were measured; (b) deflagration rate measurements; (c) temperature profile measurements; (d) flame temperature measurements.

Vaporization Rate Measurements. These experiments were performed in the glass sublimation apparatuses described under Experimental. The surface area of the liquid was quite undisturbed by bubbles

of Hydrazine Perchlorate

residue	% *recov.*	% *Hydrazine Perchlorate in* *Sublimate*	% *Hydrazine Perchlorate in* *Residue*	$10^6 \times$ *Rate of Vaporation grams/sq. cm.-sec.*
1.32	99	99.8	99.4	2.38
0.163	97			6.85
1.14	99	95.0	99.0	5.84
0.200	99			32.4
0.79	98	99.0	100.0	70.5

Publication Date: January 1, 1966 | doi: 10.1021/ba-1966-0054.ch007

during these experiments, and its magnitude was constant during an experiment. The temperature of the liquid was assumed to be that of the bath in which the apparatus was immersed. The results are given in Table I.

The relation between vaporization rate and vapor pressure is given by (*7*):

$$g = \alpha P \frac{M}{2\pi RT}$$

g = vaporization rate in grams cm.$^{-2}$sec.$^{-1}$
α = evaporation coefficent
P = vapor pressure in dynes cm.$^{-2}$
M = molecular weight o vaporizing species
T = absolute temperature
R = gas constant in ergs mole^{-1} deg.$^{-1}$

It can be seen that, once an assumption is made for the value of M, the only quantity still unknown in the above equation is α, the evaporation coefficient, which must have a finite value equal to or less than 1. If it is assumed that α is constant but unknown, then the vapor pressure at any given temperature is proportional to the vaporization rate, and the enthalpy of vaporization may be found from the Clausius-Clapeyron type treatment. If a value is assigned to α, then vapor pressure values and the entropy of vaporization can be calculated as well. If the entropy of vaporization found in this way is a reasonable value, then the assumed value of α receives support. The latter procedure has been adopted here, and a value of unity has been taken for α. The reasons for choosing this value are:

(a) Values for α for a wide variety of substances have been reported (*18*), and for the majority of cases values close to unity (i.e., within a factor of 2 or 3) have been reported;

(b) The cases (*15, 21*) where $\alpha \ll 1$ are restricted to solids, and the explanation offered has been that an adsorbed layer at the surface interferes with the vaporization process. Since hydrazine perchlorate in this experiment was molten, this condition does not apply. (Values of 0.02 to > 0.25 have been reported for liquid water (*18*).)

The vapor pressure values obtained from the data of Table I by letting $\alpha = 1$ and $M = 66$ (the average for hydrazine and perchloric acid-(*vide infra*) are tabulated in Table II and plotted as the Clausius-Clapeyron expression in Figure 1.

The data in Figure 1 are fairly linear, and the line which has been drawn visually through them yields the equation:

$$\log_{10} P_{(\mathrm{mm})}. = 10.2 - \frac{6400}{T}$$

The heat of vaporization, ΔH_v, from the above slope, is 29.2 kcal./mole.

Publication Date: January 1, 1966 | doi: 10.1021/ba-1966-0054.ch007

Table II. Vapor Pressue of Hydrazine Perchlorate

Temp., ° K.	*Vapor Pressure, mm.*
453	1.16×10^{-4}
463	3.08×10^{-4}
473	2.66×10^{-4}
492	15.1×10^{-4}
508	33.4×10^{-4}

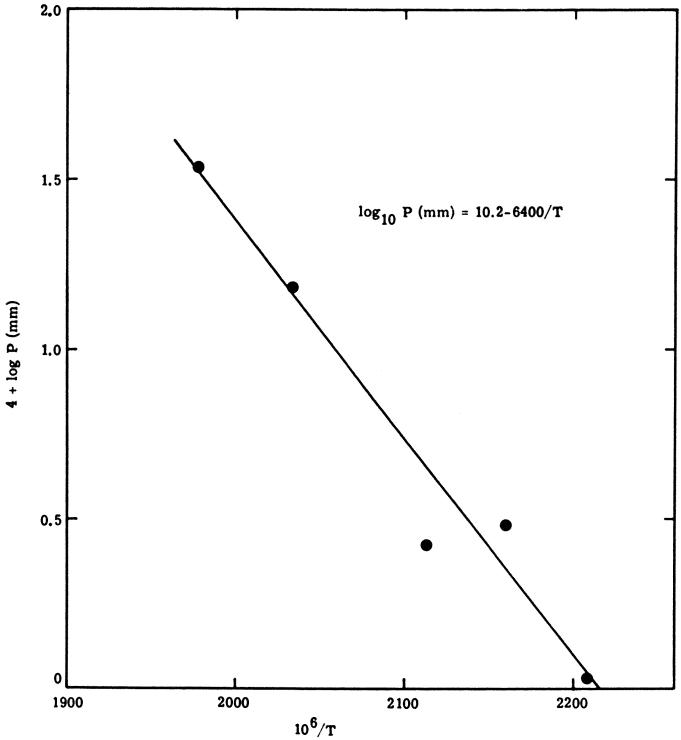

Figure 1. Rate of vaporization of hydrazine perchlorate

It is of interest to consider this value in terms of an assumed vaporization process where vaporization occurs with dissociation as is believed to be the case for ammonium perchlorate. The equilibrium is

$$N_2H_5ClO_4(l) \rightleftarrows N_2H_4(g) + HClO_4(g)$$

The heat of formation of crystalline hydrazine perchlorate is —42.5 kcal./-mole. This was estimated from the heats of formation of the ions in solution, the heat of hydration of anhydrous hydrazine perchlorate to the hemihydrate, and the heat of solution of the hemihydrate (*11*). A value of 3.84 kcal./mole has been reported for the heat of fusion (*19*) yielding —38.7 kcal./mole for the heat of formation of the liquid. The heats of formation of gaseous perchloric acid and gaseous hydrazine are —1.1 (*6*)

and 22.75 (*22*) kcal./mole, respectively. These values lead to an enthalpy change of 60.4 kcal./mole for the above equilibrium. The heat of vaporization of 29.2 kcal./mole would correspond to an enthalpy change for the above equilibrium of 58.4 kcal./mole. The agreement supports the belief that the vaporization rates are proportional to the pressures, and that the vaporization process is dissociative.

The standard entropy of vaporization for liquid hydrazine perchlorate calculated from the vapor pressure expression is 64 cal./deg. mole. Although values for the standard entropies of gaseous hydrazine and perchloric acid are known, the value for hydrazine perchlorate is not, and hence it is not possible to compare the above experimental figure with a calculated figure. It is possible to compare it with another case where the entropy of vaporization is known and would be expected to have a comparable value. Ammonium perchlorate has been selected for this purpose.

The standard entropy of vaporization of crystalline ammonium perchlorate can be calculated from the standard entropies of crystalline ammonium perchlorate and gaseous ammonia and perchloric acid. The values, in cal./deg. mole are 44.02, 45.967 (*14*), and 70.7 (*10*), respectively, yielding a value of 72.7 cal./deg. mole for the entropy change for:

$$NH_4ClO_4(c) \rightarrow NH_3(g) + HClO_4(g)$$

(The experimental value (*12*) determined from vapor pressure measurements is 71.0 cal./deg. mole.) The entropy of fusion of hydrazine perchlorate may be calculated from the cited heat of fusion and the melting point and is found to be 9 cal./deg. mole. Thus the entropy change for the process

$$N_2H_5ClO_4(c) \rightarrow N_2H_4(g) + HClO_4(g)$$

is found to be 73 cal./deg. mole. This is in reasonable agreement with the value for ammonium perchlorate and supports the belief that $\alpha = 1$ for hydrazine perchlorate is a reasonable assumption. (Had it been assumed that α for hydrazine perchlorate were of the same order as ammonium chloride,—i.e., $\sim 10^{-3}$ (*18*), the data would have yielded an entropy of vaporization of 100 cal./deg./mole.)

A final point is worth noting in comparing ammonium perchlorate and hydrazine perchlorate. The experimentally determined vapor pressure expression for the former (*12*) is

$$\log_{10} P_{(mm.)} = 10.56 - \frac{6283.7}{T}$$

which is very similar to that for hydrazine perchlorate. Despite the closeness of the vaporization curves, it would be expected that hydrazine per-

Publication Date: January 1, 1966 | doi: 10.1021/ba-1966-0054.ch007

chlorate would vaporize much more rapidly than ammonium perchlorate in experiments of the type performed here. This is because the evaporation coefficient of ammonium perchlorate appears to be much less than 1 (*20, 21*), and this circumstance is directly connected with the fact that ammonium perchlorate does not liquify and hence vaporization occurs from a solid phase, presumably via an adsorbed layer.

Deflagration Rate Measurements. Deflagration rates were measured from motion picture records of the deflagration experiments. The lengths of strands used were in the range of 1.5–2.0 cm. In all cases the linear deflagration rate was determined from the slope of the curve of length deflagrated *vs.* time. These curves were all linear—i.e., the deflagration rates were constant over the length of the strand. In all the deflagration experiments a molten layer could be seen at the surface of the deflagrating strand. Gas evolution within the layer was so vigorous that the liquid layer never appeared transparent but rather like a foam. The liquid-solid interface was distinct however, and the rate measurements were made by measuring the regression rate of this interface.

Deflagration of Pure Hydrazine Perchlorate. The behavior of pure hydrazine perchlorate—i.e., material containing no additives, was unreproducible. Smooth deflagration of tamped (ρ = 1.1–1.3 grams/cc.) and pressed (ρ = 1.8–1.9 grams/cc.) strands of hydrazine perchlorate was attained for pressures from 0.24 to 4.3 atm., but later, strands prepared and ignited in the same way did not propagate deflagration. When this was observed, experiments were performed with strands preheated to 50° C. Smooth deflagration was attained at 2, 4, and 6 atm., but these results also were not reproducible at a later date.

Deflagration of Hydrazine Perchlorate-Additive Mixtures. FUEL ADDITIVES. In the case of ammonium perchlorate, it has been found (*2*) that at pressures below that at which pure ammonium perchlorate will sustain deflagration, ammonium perchlorate-fuel mixtures containing of the order of 5% fuel do deflagrate smoothly. Paraformaldehyde was the most effective fuel additive in promoting deflagration, and for that reason experiments were performed with mixtures of hydrazine perchlorate and various formaldehyde polymers.

Experiments with paraformaldehyde were unsuccessful because it was found that when these additives were mixed with hydrazine perchlorate the mixture became yellow, and the consistency changed from that of the original powders to that of a dough. S-trioxane, a more stable formaldehyde polymer than paraformaldehyde, gave a less reactive mixture than paraformaldehyde, but the results were still unsatisfactory. Delrin, a stabilized formaldehyde polymer, proved even less reactive than S-trioxane. Magnesium oxide was added to hydrazine perchlorate-Delrin mixtures on the theory that acidity in the hydrazine perchlorate might be

Publication Date: January 1, 1966 | doi: 10.1021/ba-1966-0054.ch007

responsible for the reaction's occurring. It was found that mixtures of 94.5% hydrazine perchlorate-0.5% MgO-5% Delrin were stable, and a series of experiments was performed with this mixture.

Other fuel-type additives were effective in promoting the deflagration of hydrazine perchlorate. Experiments have been performed with thiourea and naphthalene. The results of the deflagration experiments for preheated pure hydrazine perchlorate and for the hydrazine perchlorate-fuel mixtures are summarized in Table III and Figure 2. The strands used were all pressed to about 95% of the crystal density—i.e., to a density of about 1.85 grams/cc.

Deflagration rates are given for pressures ranging from 0.26 to 7.7 atm. The experiment at 0.26 atm. yielded a curve of length-deflagrated *vs.* time that was somewhat concave upward. The rate cited is thus a rather crude value but is of interest because of the low pressure. All the other rates were constant. Attempts to measure rates at pressures higher than 7.7 atm. resulted either in a complete lack of ignition or in a deflagration that proceeded down the sides of the strands leaving a central unburned core.

Figure 2 shows that all the data fall fairly well around a single line, $\dot{r} = 0.22\,P$, where $\dot{r}$ is in cm./sec. and P is in atmospheres.

Effects of Catalysts. It has been found that copper chromite, potassium dichromate, and magnesium oxide promote the deflagration of hydrazine perchlorate. Since none of these additives has any fuel content, they must be considered to be catalysts. The results of experiments with these additives are shown in Table IV. Experiments were performed both with pressed ($\rho \sim 1.9$ grams/cc.) and tamped ($\rho \approx 1.1$. grams/cc.) strands.

It may be noted that for copper chromite and potassium dichromate a minimum of about 5% catalyst was necessary in order to attain steady deflagration; however when deflagration did occur, the rate was high compared to the case for fuel-promoted deflagration. It may be noted too (entries 2 and 3 in Table IV), that for strands containing 5% copper chromite but having different densities, the mass deflagration rates agree well while the linear rates do not. It thus seems satisfactory to compare mass rates for strands of different densities. A comparison of this type shows that potassium dichromate is a powerful catalyst but not as powerful as copper chromite.

Magnesium oxide exerts quite a different effect than do the above catalysts. Thus, less of it, 2%, is required to promote steady deflagration, but it is not capable of producing as spectacular a rate as copper chromite or potassium dichromate even in amounts as great as 10%.

The effect of calcium oxide was briefly examined since it is chemically similar to magnesium oxide. A tamped strand deflagrated at 1

Table III. Deflagration Rates for Hydrazine Perchlorate

No.	Composition	ρ grams/cc.	P atm.	$\dot{r}$ cm./sec.	$\dot{m}$ grams/sq. cm.-sec.
1	5% Delrin–0.5% MgO	1.87	0.26	0.01–0.02	0.02–0.04
2	5% Delrin–0.5% MgO	1.85	0.52	0.11	0.21
3	Pure HP preheated to 69° C.	1.87	1.0	0.24	0.45
4	5% Delrin–0.5% MgO	1.85	1.0	0.22	0.41
5	5% Delrin–0.5% MgO	1.85	1.0	0.22	0.41
6	2% Thiourea	1.86	1.0	0.17	0.32
7	5% Naphthalene	1.83	1.0	0.21	0.38
8	20% Thiourea	1.79	1.0	0.18	0.32
9	Preheated to 50° C.	1.91	2.0	0.52	0.98
10	5% Delrin–0.5% MgO	1.85	3.0	0.56	1.0
11	5% Delrin–0.5% MgO	1.85	4.3	0.90	1.67
12	Preheated to 50° C.	1.91	6.0	1.29	2.48
13	5% Delrin–0.5% MgO	1.85	7.0	1.39	2.5
14	5% Thiourea	1.82	7.7	1.73	3.18
15	10% Thiourea	1.81	7.7	1.71	3.1

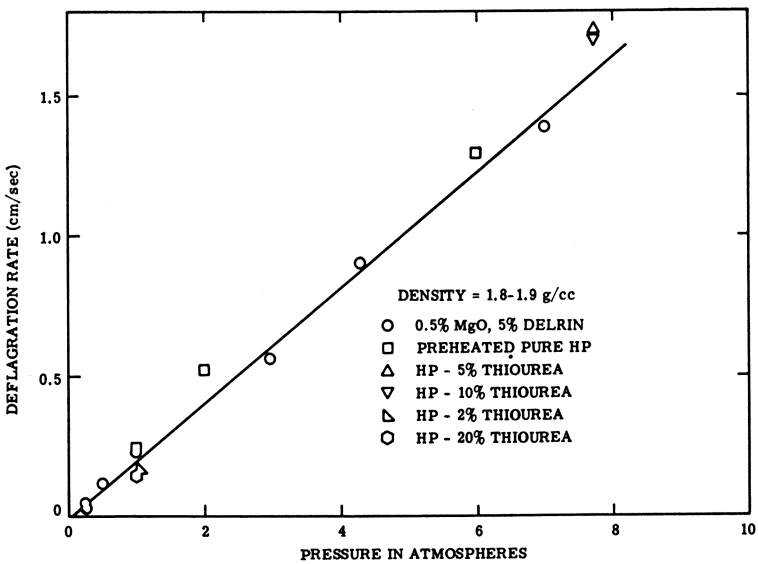

Figure 2. Rate of deflagration of hydrazine perchlorate with a small amount of fuel

atm. to give a somewhat lower rate—i.e., as compared with the curve of Figure 2. Calcium oxide is quite hygroscopic, and there were indications in this experiment of some moisture absorption.

In a side experiment to see if the effect of magnesium oxide was general, a tamped strand of hydrazine nitrate containing 2% magnesium oxide was found to deflagrate steadily at 0.04 cm./sec. (ρ = 0.93 grams/cc., $\dot{m}$ = 0.037 grams/cc.-sec.) while pure hydrazine nitrate would not propagate deflagration.

Table IV. Effect of Catalysts on the Deflagration of Hydrazine Perchlorate

No.	*Composition (% of additives)*	*ρ grams/cc.*	*P atm.*	*ṙ cm./sec.*	*ṁ grams/sq. cm.-sec.*
1	2.5% $CuCrO_2$	1.13	1	did not deflagrate	
2	5% $CuCrO_2$	1.10	1	1.20	1.32
3	5% $CuCrO_2$	1.93	1	0.71	1.37
4	5% $CuCrO_2$	1.95	0.52	0.36	0.69
4a	5% $CuCrO_2$	1.93	2	exploded	
5	2.5% $K_2Cr_2O_7$	1.17	1	did not deflagrate	
6	5% $K_2Cr_2O_7$	1.19	1	0.75	0.89
7	2% MgO	1.90	1	0.26	0.50
8	5% MgO	1.91	1	0.31	0.59
9	10% MgO	1.89	1	0.35	0.66
10	20% MgO	1.86	1	partial deflagration	
11	2% CaO	1.31	1	0.12	0.16

Publication Date: January 1, 1966 | doi: 10.1021/ba-1966-0054.ch007

The Temperature Profile Measurements. Temperature profiles of the deflagration wave have been made using thermocouples of 0.0005-inch Pt-Pt, 10% Rh wires joined in a fused bead of approximately 0.001-inch diameter. The voltage changes were recorded by a Visicorder which registers voltage changes by deflecting a light point on a moving film. The deflagration rates were measured simultaneously so that it was possible to convert temperature-time records to temperature-distance records. The turbulence of the liquid layer as observed in the deflagration rate measurements indicated that one could not expect a smooth temperature-time record. Figures 3 and 4 illustrate the type of record obtained. There are some irregularities in the curves, but the data are not too erratic for analysis.

Figure 3 shows tracings of the records obtained at 0.5 atm. with a pressed strand of 94.5% hydrazine perchlorate, 5% Delrin, 0.5% magnesium oxide, $\rho = 1.85$ grams/cc., and Figure 4 shows the tracing of the record obtained for a tamped strand of the same composition, $\rho = 1.24$ grams/cc. at 1 atm. Figures 5 and 6 show the experimental data converted to a temperature-distance function by means of the measured deflagration rates.

The solid curves in Figures 5 and 6 are the theoretical curves obtained for indicated values of thermal diffusivity of the solid. The following treatment has been applied. The temperature gradient within the zone bounded by the deflagrating surface on the one hand and ambient temperature on the other can be written:

$$k \frac{d^2T}{dx^2} - c\rho r \frac{dT}{dx} + q_e = 0$$

k = coefficient of heat conduction
c = specific heat
ρ = density
q_e = heat produced within the zone
T = temperature at point x
r = deflagration rate

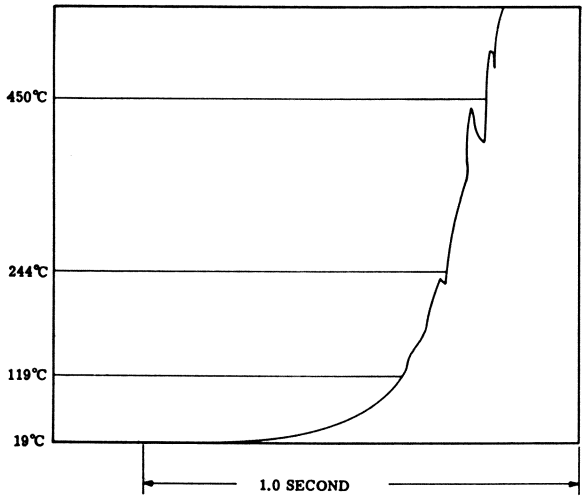

Figure 3. Tracing of thermocouple record of hydrazine perchlorate deflagration wave. Strand composition: 94.5% hydrazine perchlorate, 5% Delrin, 0.5% magnesium oxide; density: 1.85 grams/cc.; pressure: 0.5 atm.; deflagration rate: 0.09 cm./sec.

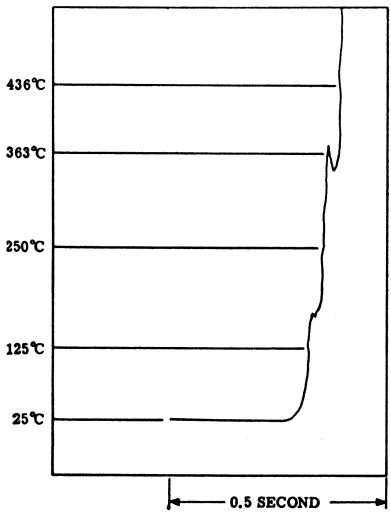

Figure 4. Tracing of thermocouple record of hydrazine perchlorate deflagration wave. Strand composition: 94.5% hydrazine perchlorate, 5% Delrin, 0.5% magnesium oxide; density: 1.24 grams/cc.; pressure: 1 atm.; deflagration rate: 0.30 cm./sec.

Publication Date: January 1, 1966 | doi: 10.1021/ba-1966-0054.ch007

If $q_c = 0$, the above on integration yields:

$$\ln \frac{T_2 - T_u}{T_1 - T_u} = \frac{r}{K}(x_2 - x_1)$$

where $K = \frac{k}{p}$ = thermal diffusivity, T_2 and T_1 are the temperatures at point x_2 and x_1, and T_u is the ambient temperature.

It is possible to evaluate K for the particular experimental data and to fit a T-x curve to the points. As Figures 5 and 6 show, the values for K that give the best fits are 0.0012 sq. cm./sec. for the pressed ($\rho = 1.86$ grams/cc.) strand and 0.0018 sq. cm./sec. for the tamped ($\rho = 1.24$ grams/cc.) strand. These values can be compared with the value of 0.00285 sq. cm./sec. which can be calculated for ammonium perchlorate of

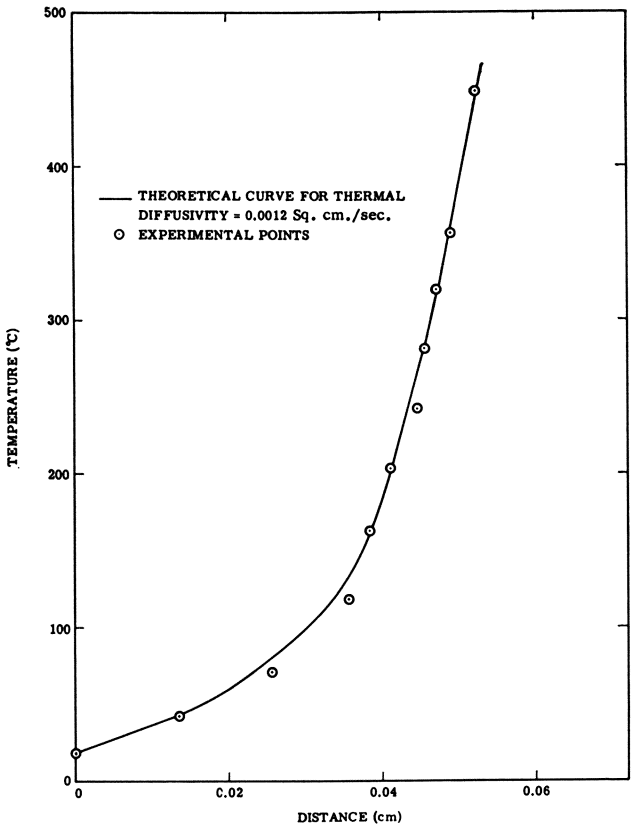

Figure 5. Temperature profile of a hydrazine perchlorate deflagration wave. Strand composition: 94.5% hydrazine perchlorate, 5% Delrin, 0.5% magnesium oxide; density: 1.85 grams/cc.; pressure: 0.5 atm.; deflagration rate: 0.09 cm./sec.

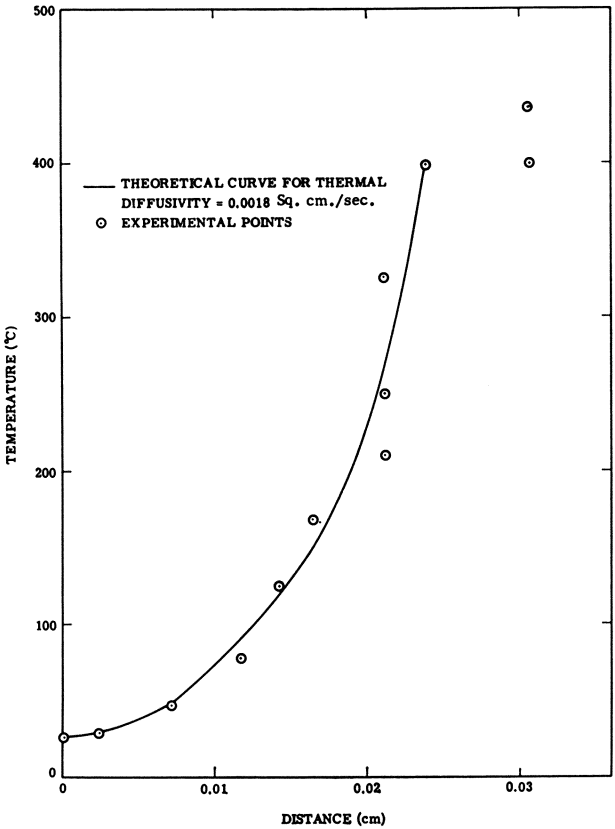

Figure 6. Temperature profile of a hydrazine perchlorate deflagration wave. Strand composition: 94.5% hydrazine perchlorate, 5% Delrin, 0.5% magnesium oxide; density: 1.24 grams/cc.; pressure: 1 atm.; deflagration rate: 0.3 cm./sec.

Publication Date: January 1, 1966 | doi: 10.1021/ba-1966-0054.ch007

crystal density, from reported values (*4*) of heat capacity and thermal conductivity. The values found here thus appear to be of the right order of magnitude.

The curves of Figures 5 and 6 fit the data fairly well. Thus, Figure 5 gives no indication of heat release in the condensed phase below 450° C. Figure 6 shows the same result at least to 400° C. It may be further noted that at 0.5 atm., for the pressed strand (Figure 5) the condensed phase reaction zone was about 0.5 mm. thick while at 1 atm., for the tamped strand it was about 0.3 mm. thick.

Flame Temperature Measurements. Thermodynamic calculations of the nature of the products of hydrazine perchlorate self-deflagration at a series of processes were performed by an IBM-7090 computer program. The results are shown in Table V. The calculations were made assuming

constant-pressure adiabatic combustion to give equilibrium products. As Table V shows the flame temperature at 1 atm. is 2245.5° K.; this is about 800° K. higher than that for ammonium perchlorate (9).

Table V. Hyrazine Perchlorate Self-Daflagration[a]

ΔH_f = 42.5 kcal./mole

P, atm. →	*1 atm.*	*10*	*68.05*	*100*
T, ° K.	2245.5°K.	2291.6	23.187	2323.2
Total moles per 100 grams	3.815 moles	3.798	3.787	3.784
Species moles per 100 grams ↓				
H	1.008×10^{-3}	2.606×10^{-4}	0.766×10^{-4}	5.949×10^{-5}
O	5.871×10^{-3}	2.456×10^{-3}	1.103×10^{-3}	9.341×10^{-4}
N	0	0	0	0
Cl	0.940×10^{-1}	6.146×10^{-2}	4.112×10^{-2}	3.774×10^{-2}
H_2	5.369×10^{-3}	2.204×10^{-3}	0.982×10^{-3}	8.313×10^{-4}
H_2O	1.526	1.523	1.524	1.525
HCl	0.659	0.688	0.699	0.700
O_2	0.705	0.715	0.719	0.720
OH	4.872×10^{-2}	3.262×10^{-2}	2.231×10^{-2}	2.060×10^{-2}
N_2	0.741	0.740	0.739	0.739
NO	2.606×10^{-2}	2.889×10^{-2}	3.062×10^{-2}	3.090×10^{-2}
NO_2	2.698×10^{-5}	0.898×10^{-4}	2.410×10^{-4}	2.933×10^{-4}
N_2O	0	2.354×10^{-6}	6.512×10^{-6}	0.796×10^{-5}
Cl_2	7.932×10^{-4}	2.588×10^{-3}	6.764×10^{-3}	0.816×10^{-2}

[a] Constant-pressure adiabatic combustion. Initial temperature 25°C.

The stoichiometry corresponds closely to:

$$N_2H_5ClO_4 \rightarrow N_2 + HCl + 2H_2O + O_2$$

Since it has been found that the self-deflagration of ammonium perchlorate does not lead to the products calculated on the basis of thermodynamic equilibrium, we felt it desirable to measure the flame temperature for hydrazine perchlorate. A flame temperature appreciably different from that calculated would indicate a nonequilibrium distribution of products which would require investigation.

Preliminary experiments were performed in which lengths of 1-mil platinum wire were stretched through the center of tamped strands of hydrazine perchlorate. Examination of the wire after deflagration showed that the passage of the flame had melted it. The melting point of platinum is 2042° K. and the heat loss by radiation was estimated at about 40° K. This placed the flame temperature as somewhere above 2082° K.

Flame temperature measurements by the sodium line reversal method were made with hydrazine perchlorate strands containing 2% thiourea and 2% sodium chloride. This amount of sodium chloride was necessary to achieve a sufficient intensity of emission of the sodium D-line for these experiments. It may be pointed out that in oxygen-rich, chlorine-containing flames such as this, the concentration of sodium atoms is decreased

Publication Date: January 1, 1966 | doi: 10.1021/ba-1966-0054.ch007

because the equilibrium, $H + NaCl \rightleftarrows HCl + Na$, is shifted to the left since the hydrogen atom concentration is so low.

Thermodynamic calculations for the composition containing 2% thiourea and 2% sodium chloride were made, and the theoretical flame temperature was found to be 2224° K. A series of measurements by the sodium line reversal method gave 2275 ± 50° K. for the flame temperature. This is close enough agreement so that we feel that thermodynamic equilibrium is achieved in the flame, and the reaction products are as written above. This differs markedly from the results with ammonium perchlorate where a substantial fraction of the nitrogen was present as oxides of nitrogen even at elevated pressures (*16*).

Publication Date: January 1, 1966 | doi: 10.1021/ba-1966-0054.ch007

Discussion

A General Description of the Hydrazine Perchlorate Deflagration Process. Let us first describe the deflagration process for hydrazine perchlorate from the above results. It is a process characterized by the formation of a molten zone which is quite turbulent and foamy; it is a very erratic process, particularly for the pure material, and it is subject to very potent catalysis by copper chromite and potassium dichromate and to moderate catalysis by magnesium oxide. The process is comparatively reproducible in the presence of small amounts of fuel, and the rate obtained apparently does not depend on the nature of the fuel but only on the ambient pressure. It can be expressed by $\dot{r} = 0.22P$ where $\dot{r}$ is in cm./sec. and P in atmospheres. This corresponds to a rate, at 1 atm., some 15 times greater than that calculated by extrapolation for ammonium perchlorate (*16*). However the process is unstable at pressures above about 7 atm. and steady deflagration cannot be attained above this pressure.

The temperature profile in uncatalyzed strands is such as to indicate little heat production in the condensed phase, and a liquid layer thickness of 0.3 mm. at 1 atm. and 0.56 mm. at 0.5 atm.

Finally, from the measured flame temperature, we conclude that thermodynamic equilibrium is attained in the deflagration products.

Mechanism of Deflagration of Hydrazine Perchlorate. One approach to the mechanism of hydrazine perchlorate deflagration is to consider whether it fits the classification of a vaporization-type process like ammonium perchlorate where the material vaporizes without decomposition, and exothermic gas phase reactions occur with resultant heat transfer to the condensed phase. The alternative to a process of this type is one wherein heat production occurs in the molten zone as a result of condensed phase reactions.

Here it is of interest to consider the vaporization rate measurements. From the expression given earlier for the vapor pressure of hydrazine

perchlorate, the following expression for the vaporization rate can be derived,

$$\log_{10} g \sqrt{T} = 9.9 - \frac{6400}{T}$$

In the temperature profiles of the deflagration experiments both at 1 atm. (Figure 6) and 0.5 atm. (Figure 5), temperatures of the order of 450° C. were attained. Inserting this temperature in the above expression yields a vaporization rate of ~0.4 gram/sq. cm.-sec. The deflagration rate found at 1 atm. was 0.36 gram/sq. cm.-sec. while that at 0.5 atm. was 0.18 gram/sq. cm.-sec. The vaporization rate measurements are thus not inconsistent with a vaporization-type mechanism for hydrazine perchlorate deflagration.

If this is considered as one point in favor of a vaporization-type mechanism, a second point in its favor is the observation that the shape of the temperature profile in the condensed phase was that expected for the case where there is no heat release in the condensed phase. A third point consistent with this picture is the increase of deflagration rate with pressure, a relation that can be explained on the basis that as the pressure is increased, the exothermic gas phase reactions occur ever closer to the condensed phase resulting in a higher rate of heat transfer.

The main features of our results which are inconsistent with the above picture are the very erratic nature of the deflagration of pure hydrazine perchlorate and the turbulent behavior of the molten zone. It is difficult to see how, for example, small amounts of impurities could affect the vaporization process from the turbulent molten layer. In other words, if the deflagration depends on vaporization it appears that it should be more reproducible. Contrariwise, if condensed phase reactions are important, then the presence of small amounts of impurities which could catalyze these reactions could easily be important in deciding whether deflagration occurred or not. The turbulent, foaming appearance of the molten zone also suggests that gas evolution—i.e., reaction, is occurring within the body of the molten liquid.

The most plausible description of the process is one in which the mechanism is predominantly a vaporization process but where there is a small (because the temperature profile does not show it) but necessary contribution from condensed phase reaction.

We feel that the erratic deflagration behavior of pure hydrazine perchlorate is attributable to the presence or absence of small amounts of impurities that catalyzed the condensed phase process, which implies that when the condensed phase process did not occur, deflagration would not propagate. The function of the fuels then would be to allow exothermic oxidation-reduction reactions to occur in the condensed phase

Publication Date: January 1, 1966 | doi: 10.1021/ba-1966-0054.ch007

that would likewise promote deflagration. The fact that the deflagration rates observed depended only on ambient pressure, irrespective of whether the strand was pure hydrazine perchlorate, whether it was preheated, or what the nature of the fuel was, suggests that although a condensed phase reaction is a *sine qua non* for stable deflagration, the actual rate is determined by the ambient pressure.

We attribute the effects of copper chromite, potassium dichromate, and magnesium oxide to catalysis of condensed phase reactions in view of the catalysis of the pyrolysis reaction by species of this type (*11*).

Finally we consider that the apparent upper pressure limit of deflagration occurs at about 7 atm. A similar phenomenon was observed for ammonium perchlorate at pressures near 2000 p.s.i.g. This was found to be caused by convective cooling and was eliminated by altering the strand geometry or by wrapping the strand with asbestos. It does not appear that convective cooling is occurring here since deflagration ceases even when the material is contained with a glass tube, which should minimize convective effects. At present we can only conclude that at pressures of the order of 7 atm., the liquid layer becomes too thin to support the contribution of condensed phase reaction necessary for stable deflagration, and it is for this reason that the upper limit is observed.

Publication Date: January 1, 1966 | doi: 10.1021/ba-1966-0054.ch007

Acknowledgments

This research was supported by the Advanced Research Projects Agency through the Propulsion Research Division of the Air Force Office of Scientific Research under Contract No. AF49(638)-1169, ARPA Order No. 332-62.

Literature Cited

(1) Adams, G. K., Newman, B. H., Robins, A. B., "Selected Combustion Problems: Fundamentals and Aeronautical Applications," p. 387, Butterworth, Inc., London, 1954.
(2) Arden, E. A., Powling, J., Smith, W. A. W., *Combust. Flame* **6**, 21 (1962).
(3) Audrieth, L. F., Ogg, B. A., "The Chemistry of Hydrazine," John Wiley and Sons, Inc., New York, 1951.
(4) Baer, A. D., Ryan, N. W., Salt, D. L., **AFOSR-TN-59-516** (1959).
(5) Barlot, J., Marsaule, S., *Compt. Rend.* **228**, 1947 (1949).
(6) Cummings, G. A. McD., Pearson, G. S., *RPE Tech. Note No.* **244**, (1963).
(7) Dushman, S., Lafferty, J. M., "Scientific Foundations of Vacuum Technique," 2nd ed., p. 14, John Wiley and Sons, Inc., New York, 1962.
(8) *Ibid.*, p. 18.
(9) Friedman, R., Nugent, R. G., Rumbel, K. E., Scurlock, A. C., *Symp. Combust, 6th, Yale Univ., 1956*, 612 (1957).
(10) Giguere, P. A., Savoie, R., *Can. J. Chem.* **40**, 495 (1962).
(11) Gilbert, E. C., Cobb, A. W., *J. Am. Chem. Soc.* **57**, 39 (1935).
(12) Inami, S. H., Rosser, W. A., Wise, H., *J. Phys. Chem.* **67**, 1077 (1963).

(13) Jacobs, P. W. M., Imperial College of Science and Technology, University of London, private communication.
(14) "JANAF Thermochemical Tables," Dow Chemical Co., Midland, Mich. (1963).
(15) Jepsen, D. W., Somorjai, G. A., *J. Chem. Phys.* **39**, 1965 (1963).
(16) Levy, J. B., Friedman, R., *Symp. Combust., 8th, Pasadena, Calif., 1960*, 663 (1962).
(17) Lewis, B., von Elbe, G., "Combustion, Flames, and Explosives in Gases," 2nd ed., pp. 620-8, Academic Press, New York, 1961.
(18) Paul, B., *ARS J.*, **32**, 1321 (1962).
(19) Rathmann, G. B., Minnesota Mining and Mfg. Co., private communication.
(20) Schultz, R. D., Dekker, A. O., *J. Phys. Chem.*, **60**, 1095 (1956).
(21) Schultz, R. D., Dekker, A. O., *Symp. Combust., 6th, Yale Univ., 1956*, 618 (1957).
(22) Scott, D. W., *et al.*, *J. Am. Chem. Soc.* **71**, 2293 (1949).

RECEIVED April 21, 1965.

Thermal Decomposition of Hydrazinium Monoperchlorate and Hydrazinium Diperchlorate

CHESTER J. GRELECKI and WILLIAM CRUICE

Thiokol Chemical Corp., Reaction Motors Division, Denville, N. J.

Publication Date: January 1, 1966 | doi: 10.1021/ba-1966-0054.ch008

A manometric technique was used to measure the rate of pressure rise which in turn is a measure of the rate of formation of volatile products produced during the thermal decomposition of hydrazinium monoperchlorate and hydrazinium diperchlorate. Kinetic expressions were developed, temperature coefficients were determined, and an attempt was made to interpret these in terms of current theories of reaction kinetics. The common rate-controlling step in each case appears to be the decomposition of perchloric acid into active oxidizing species. The reaction rate is proportional to the amount of free perchloric acid or its decomposition products which are present. In addition the temperature coefficients are similar for each oxidizer and are equivalent to that of anhydrous perchloric acid.

The perchlorates of hydrazine—namely, hydrazinium monoperchlorate ($N_2H_5ClO_4$) and hydrazinium diperchlorate ($N_2H_6(ClO_4)_2$) are receiving increasing attention as high energy solid propellant ingredients. While both of these compounds have been known for some time, very little has appeared concerning their thermal reactions.

The monoperchlorate was first reported by Salvadori in 1907 (*3*). He reported decomposition after prolonged heating at 131°–132°C., a rapid increase in rate with increased temperature, and explosion at 240°C. Barlot and Marsule (*1*) reported decomposition beginning at 145°C. The most recent information was reported by Shidlovskii, Semishin, and Shmagin (*4*) who studied weight loss at temperatures from 160° to 250°C. The dihydrate of hydrazinium diperchlorate was reported by Turrentine in 1915 (*5*). However, there is no information reported on the properties of the anhydrous material.

In Advanced Propellant Chemistry; Holzmann, R.;
Advances in Chemistry; American Chemical Society: Washington, DC, 1966.

Because of the lack of definite information, we have examined their thermal reactions as the first step toward elucidating the chemistry of these important materials.

Experimental

Materials. HYDRAZINIUM DIPERCHLORATE (HP-2). The HP-2 used in this study consisted of uniform small crystals (0.3–0.8 mm.). Its purity was determined by a potentiometric titration with a standard base. The major impurities were hydrazine (mono-) perchlorate or free perchloric acid. A precise balance was difficult to obtain during preparation, and their presence thus depended upon the extent of drying. Examples of the purity of various batches used are shown in Table I.

Table I. Analysis of Various HP-2 Samples

Batch No.	*%HP-2*	*% Impurity*
1	99.86	0.42—HP
2	99.89	0.26—HP
3	99.79	0.15—$HClO_4$
4	99.37	0.15—HP
5	99.58	0.04—$HClO_4$

HYDRAZINIUM MONOPERCHLORATE (HP). High purity HP was prepared by neutralizing 60% $HClO_4$ with 75% N_2H_4 at temperatures from 0°–25°C. The salt precipitates from water at 0°C. and was filtered cold in sintered glass funnels. The fine white crystals were gently removed from the filter with a Teflon spatula and placed in a drying tube at 70°C. for 2 hours at a constant vacuum of 0.05 mm. Hg to break down the hemihydrate. Samples were titrated either potentiometrically or to a phenolphthalein end point with 0.1000*N* NaOH. Characteristic purity factors range from 99.83–99.94%.

Apparatus and Procedure. The decompositions were followed manometrically by monitoring pressure rise at constant temperature in a constant volume reactor. The apparatus was made completely of glass and contained a thin glass membrane which was used for sensing pressure. A diagram of the apparatus is shown in Figure 1. A glass pointer was fused to the diaphragm, and the apparatus was used as a null device. The sensitivity of the gage varied from one diaphragm to another; however, all gave perceptible deflections of the pointer for pressure differentials of 1 mm.

At the completion of the reaction, gas samples were collected through the break-off seal and analyzed on the mass spectrometer. Condensed phase residues were analyzed by conventional wet analytical techniques.

Results and Discussion

General Nature of the Decomposition Reaction. In a sealed system the decomposition reaction of HP-2 is characterized by an induction

Publication Date: January 1, 1966 | doi: 10.1021/ba-1966-0054.ch008

period, during which time a gradual pressure rise is observed. At the end of the induction period, the reaction accelerates very sharply, and complete decomposition results. A typical pressure *vs.* time curve is shown in Figure 2. The initial phase of the HP reaction is also acceleratory. However, there is no sign of acceleration of the type characteristic of HP-2. A typical pressure *vs.* time curve for HP is shown in Figure 3.

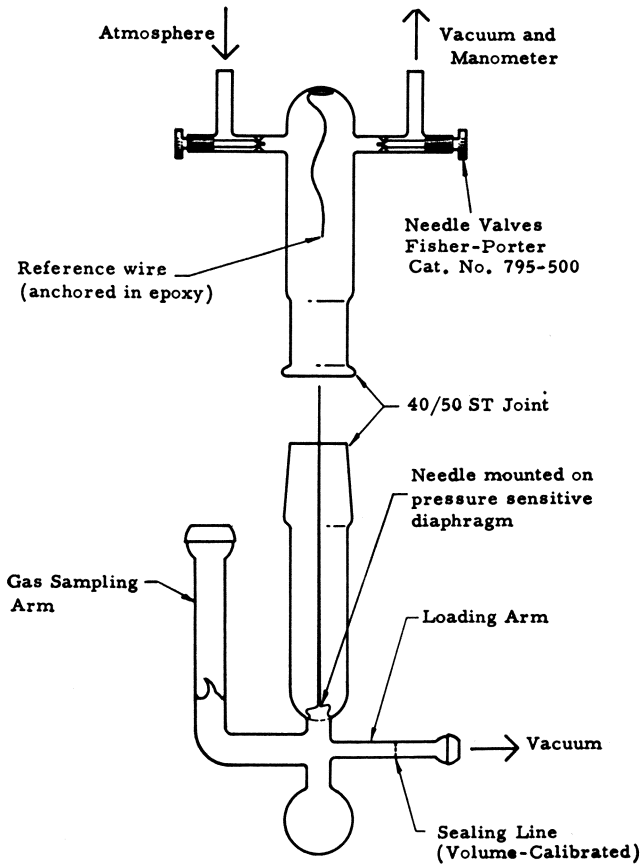

Figure 1. Sickle gage apparatus

Stoichiometry. Analysis of the vapor and condensed products of the overall HP-2 reaction indicate the following stoichiometry.

$$12N_2H_6(ClO_4)_2 \rightarrow 4NH_4ClO_4 + 22H_2O + 10N_2 + 5O_2 + 4Cl_2$$

The overall stoichiometry of the HP reaction is:

$$8N_2H_5ClO_4 \rightarrow 7NH_4ClO_4 + NH_4Cl + 4N_2 + 4H_2O$$

Rate Measurements. HYDRAZINIUM DIPERCHLORATE. For the case of HP-2 there is a very sharp transition at the initiation of the accelerated

Publication Date: January 1, 1966 | doi: 10.1021/ba-1966-0054.ch008

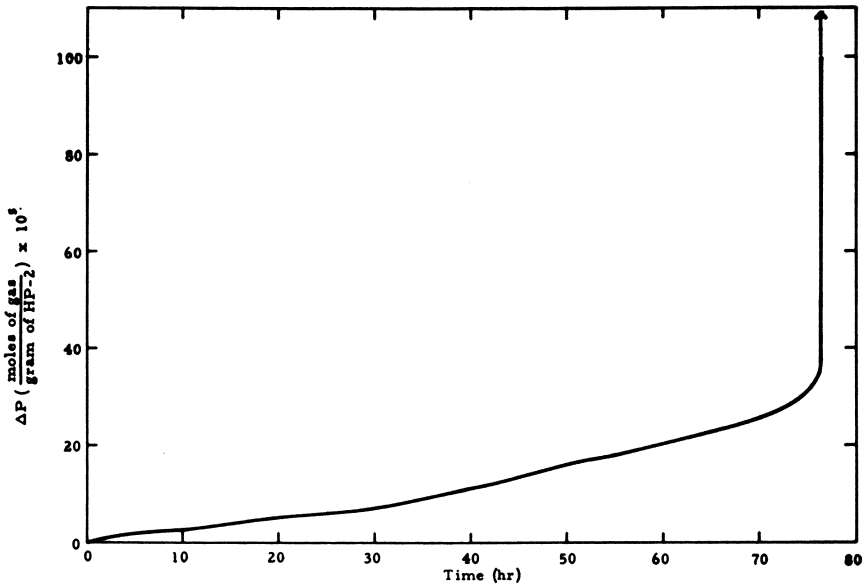

Figure 2. Pressure vs. time curve for hydrazinium diperchlorate at 120°C.

phase. The assumption was made that when the reaction goes into the accelerated phase, the concentrations of all reaction species are the same from one experiment to another. Thus, the expression for the rate of disappearance of HP-2 may be written as follows:

$$\frac{-d[\text{HP-2}]}{dt} = kf(C) \tag{1}$$

where k is the specific rate constant and $f(C)$ is some function of the concentration of reactants.

Integration, (Equation 1) gives:

$$kt_i = f'(C_i) \tag{2}$$

the subscript i represents the initiation of the accelerated phase of decomposition.

The assumption is made that at t_i, the concentrations of all reactants, are the same in any series of experiments; thus $f'(c_i)$ is constant, and the time to acceleration is inversely proportional to the specific rate constant.

$$1/t_i = k_0k \tag{3}$$

where $1/k_0$ is $f'(C_i)$.

In any series of experiments the rates of reaction were compared on the basis of k_0k or $1/t_i$.

HYDRAZINIUM MONOPERCHLORATE. The decomposition reaction of HP is not characterized by the same type of rapid acceleration as is found for

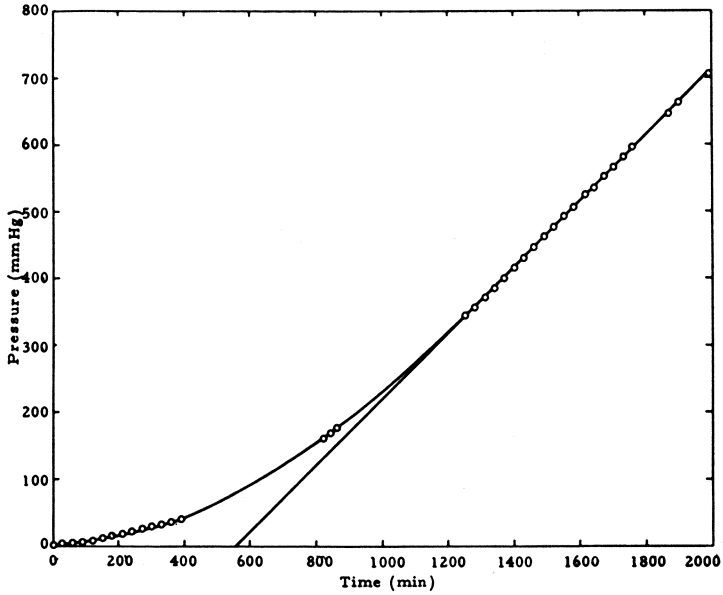

Figure 3. Pressure vs. time curve for hydrazinium perchlorate at 140°C.

Table II. Time to Acceleration as a Function of Temperature

Temperature, °C.	*Induction Period, hrs.*
120	77
130	32
140	22
150	9

HP-2. Rather the first 10% of reaction is acceleratory following the expression

$$\eta/No = At^2$$

where η = number of moles of gaseous products, No = number of moles of HP originally present, and t = time in minutes.

The rate of reaction remains constant from approximately 10–70% decomposition and is given by the following expression:

$$\eta/No = C(t - D)$$

For comparison of rates at various temperatures the linear portion of the curve was used.

Effect of Temperature. The time to acceleration (t_i) for HP-2 is shown as a function of temperature in Table II.

Publication Date: January 1, 1966 | doi: 10.1021/ba-1966-0054.ch008

The dependence of reaction rate on temperature is given by the Arrhenius relationship

$$k = Ae^{-E/RT} \tag{4}$$

Substituting for the specific rate constant from Equation 3 gives:

$$1/t_i = k_0Ae^{-E/RT} \tag{5}$$

$$\ln(1/t_i) = \ln(k_0A)^{-E/RT} \tag{6}$$

For HP-2 between 100° and 150°C. the relationship between $1/t_i$ and temperature is:

$$\log 1/t_i = 11.203 - \frac{5143}{T(°K.)}$$

and the activation energy, E, is 23.5 kcal./mole.

The effect of temperature on the decomposition rate of HP is shown in Table III. The table gives the values of A, C, and D which are the parameters of the power expression:

$$\eta/No = At^2 \qquad 0 > \eta/No > 0.1$$

and the linear expression:

$$\eta/No = C(t - D) \qquad 0.1 > \eta/No > 0.7$$

Values of t_i (time of transition from the power law to the linear law) and values of η/No at t_i are also given.

A plot of values of log C *vs.* $1/T$°K. gives an activation energy for the linear portion of the curve of 23.8 kcal./mole from 140° to 200°C.

Effect of Reaction Products. The reaction of HP-2 is self-accelerating and suggests autocatalysis by reaction products. The effect of two of the reaction products are given below.

Perchloric Acid Dihydrate. Adding perchloric acid dihydrate accelerates the decomposition of HP-2. The exact effect in terms of the time to acceleration $1/t_i$ is given by the following expression.

$$1/t_i = k_0k_1 + k_0k_2\,[HClO_4 \cdot 2H_2O]$$

At 140°C., $k_0k_1 = 0.04$ hr.$^{-1}$, which is the rate of the reaction in the absence of additive, and $k_0k_2 = 0.04$ hr.$^{-1}$ (wt. %)$^{-1}$.

Table III. Temperature Effect of HP Decomposition

T, °C.	$A \times 10^8$	$C \times 10^4$	D	T_i[a]	η/No at t_i[a]
140	6.25	1.31	552	1200	0.090
150	22.9	3.25	320	480	0.080
158	107	6.9	166	300	0.090
170	260	10.9	104	170	0.070
181	1070	21.0	53	95	0.090
200	18,000	86.0	10	27	0.140

[a] Approximate values; time in minutes.

Publication Date: January 1, 1966 | doi: 10.1021/ba-1966-0054.ch008

Thus the reaction rate is doubled when 1% of the acid dihydrate is added.

ANHYDROUS PERCHLORIC ACID. Adding anhydrous perchloric acid accelerates the reaction of HP-2 to such an extent that it exceeds the capacity of the experimental technique at 140°C. Using the above convention, however, it was possible to determine a lower limit on the value of the rate constant k_0k_2. At 140°C. the value of k_0k_2 is greater than 2.5 hr.$^{-1}$ (wt. %)$^{-1}$. Thus, the rate of HP-2 decomposition is increased by a factor of at least 60 when 1% anhydrous $HClO_4$ is present.

Reaction Mechanism. The initial step in the decomposition of HP-2 is the dissociation to HP and perchloric acid:

$$N_2H_5ClO_4 \cdot HClO_4 \rightleftarrows N_2H_5ClO_4 + HClO_4$$

This step was verified by isolating anhydrous $HClO_4$ as the only vapor phase species during the early phases of the reaction. The equilibrium constants in terms of the pressure of $HClO_4$ were determined as a function of temperature and are given by the following expression.

$$\log P_{(\text{mm.})} = 22.86 - \frac{8650}{T, {}^\circ\text{K.}} \qquad (100°–140°\text{C.})$$

The heat of dissociation is 37 kcal./mole.

The initial step of the HP decomposition is a proton transfer to produce free hydrazine and anhydrous perchloric acid:

$$N_2H_5ClO_4 \rightleftarrows N_2H_4 + HClO_4$$

The dissociation pressures for this reaction could not be measured directly in the Sickle gage apparatus. No dissociation pressure could be detected to 150°C. At higher temperatures the decomposition was too rapid to attain equilibrium.

The initial dissociation in both cases is followed by decomposition of $HClO_4$ since it is considerably less stable than HP-2 or HP.

The reaction of anhydrous $HClO_4$ has been studied by Levy (*2*). At high temperatures (above 300°C.) the vapor phase reaction is homogeneous. Below approximately 300°C. the reaction is heterogeneous, whose rate depends on the nature of the surface with which it is in contact. Zinov'ev and Tsentsiper (*6*) report an activation energy of 22.2 kcal./mole for the low temperature reaction. The similarity of the temperature coefficient of the HP, HP-2, and $HClO_4$ reactions suggest that the decomposition of $HClO_4$ may be the controlling step in each case.

Since the decomposition of $HClO_4$ is mainly heterogeneous in the temperature range of interest, tests were performed to determine the effect of surface on the HP-2 reaction. The borosilicate glass surface was increased by adding known quantities of borosilicate glass micro spheres. These were intimately mixed with the reactant, and the presence of the

glass surface increased the rate. The overall rate of the heterogeneous reaction is given by the following expression:

$$1/t_i = k_0k_1 + \Sigma k_0k_j[S_j]$$

where k_0k_1 is the rate in the absence of added surface; k_j is the specific rate constant on surface j and S_j is the surface area of the jth surface.

At 140° C. on borosilicate glass (bg) the value of k_0k_{bg} is 0.005 hr.$^{-1}$ sq.cm.$^{-1}$. Thus the heterogeneous nature of the reaction is important, and this further suggests that the decomposition of $HClO_4$ is a controlling step in the reaction.

At 140° C. the perchloric acid decomposes on a surface to form active oxidizing species. Since the weakest bond in the anhydrous perchloric acid molecule is the Cl—OH bond, a possible initial reaction is the following:

$$HClO_4 \rightarrow HO\cdot + \cdot ClO_3$$

Many other active oxidizing species such as ClO_2, ClO_4, Cl_2O_6, and Cl_2O_7 are also possible, and some undoubtedly form. The oxidizing species formed can oxidize the hydrazine moiety of HP-2 to ammonia, thereby releasing a mole of perchloric acid. The reaction is illustrated below for the $HO\cdot$ and ClO_3 radicals.

$$HO\cdot + N_2H_5ClO_4\cdot HClO_4 \rightarrow H_2O + \tfrac{1}{2}N_2 + NH_4ClO_4 + HClO_4$$

$$ClO_3\cdot + 6N_2H_5ClO_4\cdot HClO_4 \rightarrow 3H_2O + 3N_2 + 6NH_4ClO_4 + \tfrac{1}{2}Cl_2 + 6HClO_4$$

The same overall results would be obtained with other oxidizing intermediates. The significant point is that each mole of perchloric acid has the capacity to oxidize seven moles of hydrazine, and in doing so, releases seven additional moles of perchloric acid. Such a rapid chain-branching step can account for the rapid transition from the slow preacceleration phase of the reaction to the rapid acceleration.

The suggested reactions are also consistent with the fact that the decomposition of HP does not accelerate rapidly. Oxidizing intermediates formed by the decomposition of $HClO_4$ react with HP as follows.

$$N_2H_5ClO_4 + \cdot OH \rightarrow H_2O + NH_4ClO_4 + \tfrac{1}{2}N_2$$

$$7N_2H_5ClO_4 + \cdot ClO_3 \rightarrow 3H_2O + 6NH_4ClO_4 + 3\tfrac{1}{2}N_2 + NH_4Cl + HClO_4$$

An approximate kinetic expression based on the above consideration in which all oxidizing species are included, reduces to:

$$\frac{dn}{dt} = [HP](k_1[OH] + k_2[ClO_3] + \ldots\ldots k_1[O_i])$$

Publication Date: January 1, 1966 | doi: 10.1021/ba-1966-0054.ch008

This expression shows that the rate of gas evolution should increase until steady state concentrations of all oxidizing species are reached. After this time, t_i, the concentrations of oxidizing intermediates remain constant and depend on the equilibrium dissociation pressure of HP at the experimental temperature. The rate then remains constant until the HP becomes depleted.

Summary and Conclusions

The initial step in the thermal decomposition of HP-2 and HP is the dissociation of the acid-base complex to give free perchloric acid. The subsequent decomposition of perchloric acid controls the rate of the overall reaction.

In the case of HP-2 the reaction is autocatalytic. The general form of the reaction sequence is as follows:

$$\mathrm{A} \xrightarrow{k_1} 7\mathrm{B} + \text{Products}$$

$$\mathrm{A} + \mathrm{B} \xrightarrow{k_3} 7\mathrm{B} + \text{Products}$$

where B is equal to one oxidizing equivalent.

The large branching coefficient, 7, and the fact that $k_3 > k_1$ leads to a very sharp transition from a slow preacceleration reaction to a rapid accelerated phase.

The HP reaction differs from that of HP-2 in that no autocatalysis is involved. The initial rate of the HP reaction does increase as active oxidizing intermediates are built up, but after a steady state concentration is reached, the rate remains constant until the concentration of HP becomes depleted.

Acknowledgment

This report is based on work performed under Air Force Contract No. AF 04(694)334 and Navy Contract No. NOnr 4364(00) under the sponsorship of the Advanced Research Projects Agency.

Literature Cited

(1) Barlot, J., Marsaule, S., *Compt. Rend.* **228**, 1479 (1949).
(2) Levy, J. B., *J. Phys. Chem.* **66**, 1092 (1962).
(3) Salvadori, R., *J. Soc. Chem. Ind.* **26**, 1066 (1908).
(4) Shidlovskii, A. A., Semishin, V. I., Shmagin, L. F., *Zh. Prikl. Khim.* **35**, 756 (1962).
(5) Turrentine, J. W., Gill, A. C., *J. Am. Chem. Soc.* **37**, 1122 (1915).
(6) Zinov'ev, A. A., Tsentsiper, A. B., *Zh. Neorgan. Khim.* **4**, 724 (1959).

RECEIVED April 28, 1965.

9

Decomposition of Nitronium Perchlorate

M. D. MARSHALL and L. L. LEWIS

Callery Chemical Co., Callery, Pa.

Publication Date: January 1, 1966 | doi: 10.1021/ba-1966-0054.ch009

The decomposition reaction for nitronium perchlorate is believed to involve the formation of nitrosonium perchlorate and oxygen. The other products (NO_2, Cl_2, ClO_2) observed during the decomposition appear to be the result of the subsequent decomposition of nitrosonium perchlorate. This mechanism is clearly demonstrated in vacuo by a preponderance of oxygen in the volatiles during the early stages of the decomposition of nitronium perchlorate in vacuo and by the products of the latter stages which describe the decomposition of nitrosonium perchlorate. In sealed tubes, the reaction of dinitrogen tetroxide with nitronium perchlorate ultimately predominates, giving nitrosonium perchlorate and oxygen as products. This reaction is catalyzed by dinitrogen tetroxide.

Nitronium perchlorate begins to decompose slowly at approximately 50° C., producing gaseous products. There is some evidence that the stability of the sample is related to the purity. Despite efforts by several investigators to obtain high purity samples, however, decomposition is significant when a temperature of 60° C. is reached.

By establishing the mechanism of decomposition, we hoped to obtain information that would allow us to prevent or suppress the decomposition.

The decomposition of nitronium perchlorate between 70° and 112° C. has been reported by Cordes (*2*) to proceed to the gaseous products NO_2, Cl_2, ClO_2, NO_3Cl, and O_2. As a result of some screening experiments we were aware that at 65° C. in sealed tubes, nitrosonium perchlorate was a major decomposition product. We were also aware that dinitrogen tetroxide, at least in the liquid phase, would quantitatively convert nitronium perchlorate to nitrosonium perchlorate. Thus, a mechanism involving only gaseous products appeared unlikely.

To avoid any such back reaction of dinitrogen tetroxide with nitronium perchlorate, we decided to carry out our study under vacuum, with

In Advanced Propellant Chemistry; Holzmann, R.;
Advances in Chemistry; American Chemical Society: Washington, DC, 1966.

continuous removal of products. We chose a temperature of 65° C. which would give a significant decomposition rate but at which the gaseous products could be handled by the pumping system.

Experimental

The decompositions were carried out in glass reactors of 50–100 cc. volume equipped with a 12-mm. charging tube and a stockcock. Since nitronium perchlorate is extremely moisture reactive, all transfers were conducted in a dry atmosphere, and the charging tube was sealed off under dry nitrogen. Even with utmost care, however, a small amount of hydrolysis occurs. Consequently, after completing the sample transfer to the reactor, the hydrolysis products (HNO_3 and $HClO_4$) were removed at room temperature by subjecting the sample to a high vacuum until a constant weight was obtained. (The effectiveness of this procedure was demonstrated by adding a measured amount of water to a sample of nitronium perchlorate, and after pumping according to the procedure described, the weight loss was measured for the sample and the nitric and perchloric acids titrated in the recovered volatiles. All values were theoretical within limits of the analyses.)

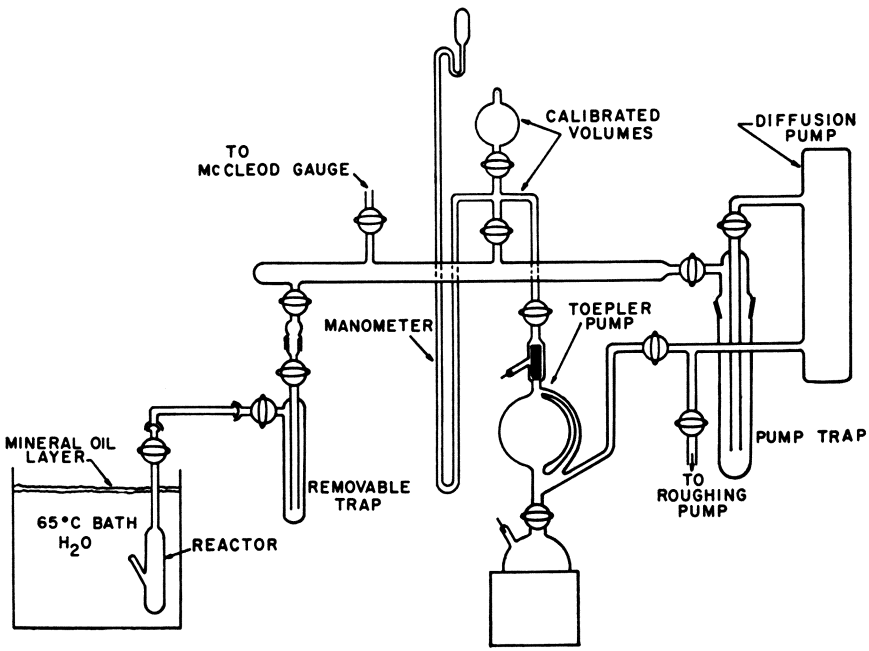

Figure 1. Apparatus

The reactor was connected to a small glass vacuum system through a short glass coupling, and immersed in the constant temperature bath controlled to 65.0° ± 0.1° C. The vacuum system (Figure 1) was equipped with a McLeod gage for measuring pressure, a Toepler pump for handling

Publication Date: January 1, 1966 | doi: 10.1021/ba-1966-0054.ch009

noncondensables, and a removable trap for entraining condensable products for later analyses. The Toepler pump was placed after the diffusion pump so that the latter could aid in collecting the small quantity of noncondensables. Fluorolube grease was used throughout the system.

The nitronium perchlorate initially charged was standard production grade material of better than 97% purity. The $NOClO_4$ content was measured by the procedure outlined by Vogel (*13*) and was below 0.05%, the limits of the analysis. The sample was further purified by subjecting it to a high vacuum, as described previously. The sample used for experimentation had a purity in excess of 99%.

The decomposition was monitored at 65° C. while continuously subjecting the sample to pumping. The volatile decomposition products were passed through a −196° C. trap, where condensables were removed and periodically analyzed. Noncondensables, consisting entirely of oxygen, were measured either continuously or periodically to check their rate of removal. The weight loss of the sample was checked against volatiles recovered or measured, and appropriate analyses were carried out on the residue. Sublimed nitronium perchlorate was weighed with the residue. In most runs, the sublimed solids were measured and analyzed.

Results and Discussion

The decomposition experiments all followed the same pattern. This consisted of: (1) an immediate deposition of sublimed materials on the cooled reactor walls within 1 minute after placing the sample in the 65° C. bath; (2) an induction period of 24–40 hours during which no visible evidence of volatiles was observed; (3) an initially slow, but rapidly accelerating production of oxygen which maximized at approximately 100 hours with concurrent appearance of yellow condensable in the −196° C. trap; finally, (4) a noticeable decrease in the rate of oxygen evolution, which diminished slowly throughout the remainder of the run.

Oxygen Evolution. A plot of the total oxygen evolved *vs.* time gave the typical sigmoid curve characteristic of solid decomposition (Figure 2). The induction and acceleration periods are clearly evident along with the subsequent lower rate of total oxygen evolution during the decay stage.

A plot of the rate of oxygen evolution for one experiment is also shown in Figure 2. The peak rate of oxygen release occurred at approximately 100 hours at about a 10% weight loss and with more than 80% of the nitronium perchlorate still intact in the sample (80% value obtained from a similar run stopped at this point and the solids analyzed).

The amount of oxygen released per gram of weight loss incurred also varied throughout the run. Table I summarizes these data for two experiments.

The change from 15.5 to 6.5 for the mmoles of O_2 per gram weight loss is significant in that it denotes a mechanism change or the increasing importance of a secondary reaction. The 15.5 and 6.5 values are also

Publication Date: January 1, 1966 | doi: 10.1021/ba-1966-0054.ch009

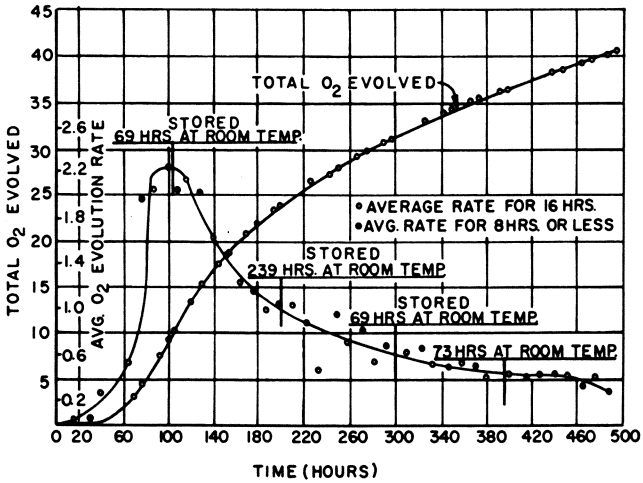

Figure 2. Oxygen evolution of NO_2ClO_2 at 65°C.

Table I. Summary of Condensables Produced

Total Time hrs.	*Wt. Loss gram*	*O_2 Produced mmoles*	*mmoles O_2 per gram wt. loss*	*NO_2 Produced mmoles*	*mmoles NO_2 per gram wt. loss*
Run No. 1					
73	0.160	2.46	15.5	0.90	5.6
92	0.140	2.01	14.3	0.77	5.5
112	0.161	2.13	13.3	0.93	5.8
132	0.154	1.93	12.6	0.99	6.4
154	0.163	1.80	11.1	1.07	6.6
174	0.150	1.47	9.8	1.02	6.8
Run No. 2					
198	0.341	3.98	11.7		
298	0.177	1.32	7.3		
397	0.129	0.88	6.8	4.32[a]	6.7[a]
492	0.103	0.66	6.5	0.78	7.6

[a] Value for period 0–397 hours.

significant since they cannot be obtained from nitronium perchlorate decomposition reactions giving only gaseous products, but they must arise from a combination of reactions in which the production and decomposition of $NOClO_4$ is involved. The highest and lowest possible values obtainable from NO_2ClO_4 for this ratio are shown by the equations:

	(mmoles O_2/gram wt. loss)
$NO_2ClO_4 \rightarrow NO_2 + \frac{1}{2}Cl_2 + 2O_2$	13.8
$NO_2ClO_4 \rightarrow NO_2 + ClO_2 + \frac{1}{2}O_2$	6.9

On the other hand, values of 31.3 and 3.9 are possible from the production and decomposition, respectively, of nitrosonium perchlorate.

	(mmoles O_2/gram wt. loss)
$NO_2ClO_4 \rightarrow NOClO_4 + \frac{1}{2}O_2$	31.3
$NOClO_4 \rightarrow NO_2 + ClO_2 + \frac{1}{2}O_2$	3.9

Volatiles Condensable at −196° C. The condensed materials were identified as NO_2, Cl_2, and ClO_2 by means of infrared and mass spectrometry. The sample was hydrolyzed and analyzed for chlorine and nitrogen content. The combined gram atoms of chlorine ($Cl_2 + ClO_2$) invariably equaled the gram atoms of nitrogen found within the limits of the analyses.

The nitrogen dioxide produced (measured as nitrogen in the hydrolysate) per gram of weight loss of sample slowly increased as the decomposition progressed. The values for two runs are shown in Table I.

It is again significant that the value of 7.6 mmoles of NO_2 per gram of weight loss of sample obtained over the last period from 397 to 492 hours of decomposition for run No. 2 cannot be obtained from any decomposition reaction one may write for NO_2ClO_4. It is, however, nearly theoretical for the decomposition of $NOClO_4$ to volatiles:

	mmoles NO_2/gram wt. loss
$NOClO_4 \rightarrow NO_2 + ClO_2\,(Cl_2 + O_2) + \frac{1}{2}O_2$	7.7

and in a separate experiment, a value of 7.6 mmoles of NO_2 per gram of weight loss was observed for the decomposition of $NOClO_4$ under similar conditions.

Analysis of Solids. In our original hypothesis, we believed the formation of $NOClO_4$ in the residue would be avoided by carrying out the decomposition under vacuum. By doing so, we hoped to prevent the back reaction of the NO_2 produced in the decomposition with NO_2ClO_4. Nevertheless, $NOClO_4$ was observed in the residue in substantial quantities, possibly suggesting its formation by a different mechanism. Its presence was confirmed by x-ray (*6*), Raman (*1*), and wet analysis (*13*) techniques.

Figure 3 shows the $NOClO_4$ found in the residue and the NO_2ClO_4 decomposed as a function of time. With the limited data available, the peak production of $NOClO_4$ is observed to coincide with the peak rate of NO_2ClO_4 decomposition. The $NOClO_4$ also appears to decompose at a faster rate than the nitronium perchlorate as indicated by the slopes of the curves. This would most certainly be true if, as we suspect, nitrosonium perchlorate is also being continuously produced from the decomposition of nitronium perchlorate during this period.

A study of the decomposition of $NOClO_4$ under conditions identical to this study gave the following results: (1) nitrosonium perchlorate decomposes with no noticeable induction period, giving only the gaseous products, NO_2, ClO_2, Cl_2 and O_2; nitronium perchlorate is reported as a

major product of this decomposition at 99° C. (*11*), but only trace quantities were observed in our study; (2) the decomposition of $NOClO_4$ proceeds at a faster rate than that of NO_2ClO_4, even after the acceleratory period of the latter compound. This observation is consistent with conclusions of Rosolovskii (*11*).

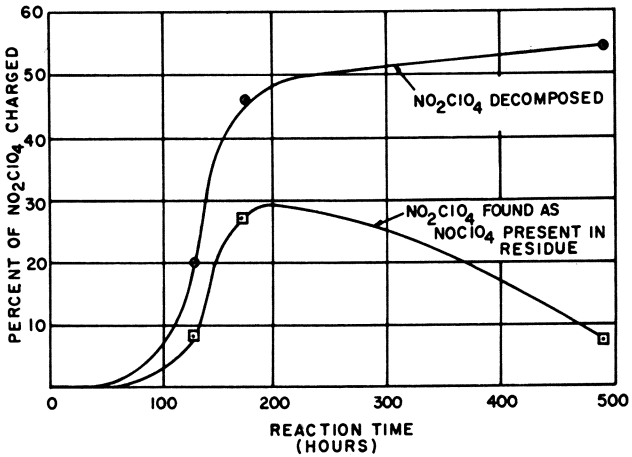

Figure 3. Decomposition of NO_2ClO_4 at 65°C.

Several interesting facts concerning the sublimed solids should be noted: (1) sublimation occurred immediately upon heating the sample to 65° C.; (2) the sublimed solids were shown to be NO_2ClO_4, both by x-ray and elemental analyses; (3) analyses did not detect the presence of $NOClO_4$; (4) the rate of sublimation appeared to be comparatively constant over the decomposition period; sublimation usually occurred at about one-half to one-third the rate of decomposition. These facts are significant in that they indicate that the sublimation is entirely independent of the decomposition.

The Decomposition Mechanism. The vacuum decomposition of NO_2ClO_4 at 65° C. proceeds by a mechanism which must take into account a decreasing amount of oxygen evolved per unit weight loss of samples, an increasing amount of NO_2 produced per unit weight loss of sample, the production of $NOClO_4$ as a product and its subsequent decomposition, and the decomposition of $NOClO_4$ as the predominant reaction in the latter stages. The observations are best explained by the following two-step mechanism:

$$NO_2ClO_4 \rightarrow NOClO_4 + \tfrac{1}{2}O_2 \quad (1)$$

$$NOClO_4 \rightarrow NO_2 + ClO_2(Cl_2 + O_2) + \tfrac{1}{2}O_2 \quad (2)$$

Assuming the mechanism described, the mmoles of O_2 and NO_2 produced per gram of weight loss of sample that would be expected at various ratios of Reactions 1 and 2 can be calculated. These are shown in Table II.

Table II. Calculated Quantities of O_2 and NO_2 Produced per Weight Loss of NO_2ClO_4

	Mmoles produced/gram wt. loss		
Ratio of Reactions 1:2	*NO_2*	*O_2, Assuming All Cl as ClO_2*	*O_2, Assuming All Cl as Cl_2*
10:0	none	31.2	31.2
10:1	3.5	19.0	22.5
10:2	4.8	14.4	19.1
10:3	5.5	11.8	17.3
10:4	5.8	10.3	16.2
10:6	6.4	8.5	14.9
10:8	6.7	7.5	14.2
10:10	6.9	6.9	13.8
8:10	7.0	6.3	13.4
6:10	7.2	5.8	12.9
4:10	7.4	5.2	12.5
2:10	7.5	4.5	12.1
0:10	7.7	3.9	11.6

In the early stages of the decomposition when Reaction 1 is predominant, the oxygen-to-weight loss ratio would be at its highest and diminish as the concentration of $NOClO_4$ increases and Reaction 2 becomes significant. A reverse trend would be expected for the NO_2-to-weight loss ratio.

The experimental values for these same ratios for the two experiments previously cited in Table I follow these general trends. That Reaction 1 predominates in the early stages is supported by the initially high experimental values obtained for the ratio of O_2 evolution per unit weight loss of sample. A theoretical value of 31.3 would be expected if only Reaction 1 occurred since oxygen is the only volatile. This would be true only momentarily, since $NOClO_4$ decomposes rapidly at 65° C. without any induction period by Reaction 2 which would immediately become operative. Any contribution by Reaction 2 would lower the oxygen-to-weight loss ratio since at its highest possible rate of oxygen production (giving NO_2, Cl_2, and O_2 as decomposition products), a theoretical value of 11.6 for the ratio of mmoles of oxygen to weight loss would be observed. The initial value of 15.5 observed after 73 hours is therefore a "net" figure for Reactions 1 and 2 during this initial interval and represents a substantial contribution from Reaction 1.

A quantitative correlation of Reactions 1 and 2 with the oxygen ratio is not possible because of the uncertainty in the quantity of ClO_2 decomposed to Cl_2 and O_2. On the other hand, the amount of NO_2 produced per weight loss can be directly correlated. The initial ratio of 5.6 for NO_2, for example, indicates that during the first 73 hours the ratio of moles of

Publication Date: January 1, 1966 | doi: 10.1021/ba-1966-0054.ch009

NO_2ClO_4 decomposed to $NOClO_4$ decomposed averaged 10:3, or stated otherwise, approximately 30% of the $NOClO_4$ that was produced during this period by Reaction 1 subsequently decomposed.

At the conclusion of run No. 1, during the interval of 154–174 hours, Reactions 1 and 2 were operating at an approximate 10:9 ratio. Thus, $NOClO_4$ decomposed at nearly the same rate as it was produced from NO_2ClO_4.

The 7.6 value for the NO_2 ratio, obtained over the period of 397–492 hours of run No. 2 indicates that the decomposition of $NOClO_4$ (Reaction 2) was occurring 10 times faster than the rate of $NOClO_4$ production by Reaction 1, and rapidly diminishing the excess produced during the accelerated period of the NO_2ClO_4 decomposition.

The 7.6 value for NO_2 production and the 6.5 value for the oxygen evolution obtained in the latter stages of the decomposition of NO_2ClO_4 are almost identical to corresponding values obtained from the decomposition of $NOClO_4$ under similar conditions. The respective values for $NOClO_4$ were 7.6 and 6.9 mmoles per gram of weight loss, indicating the predominance of this reaction in the latter stages of NO_2ClO_4 decomposition.

As a further check on this mechanism the decomposition of NO_2ClO_4 was monitored by Raman spectroscopy, employing the Raman cell as the reactor. The sample was analyzed by Raman periodically throughout the course of the decomposition at 65° C. A plot of the absorptions for NO_2^+ (1400 cm.$^{-1}$) and NO^+ (2300 cm.$^{-1}$) is shown in Figure 4. As would be expected from the proposed mechanism, the rapid drop in the NO_2^+ absorption coincides with the appearance and increase in the NO^+ absorption. Figure 5 shows the oxygen production for the sample over the

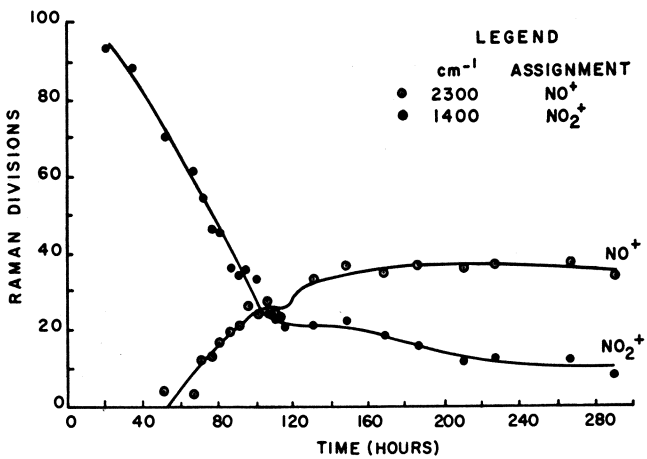

Figure 4. Raman analysis of decomposition of NO_2ClO_4 at 65°C.

corresponding interval. As noted in previous experiments the peak rate of oxygen production occurred at approximately 100 hours.

It is significant that the Raman data also indicate a break at about 100 hours in the absorption curves for NO_2^+ which was decreasing, and NO^+, which was increasing. Since a Raman spectrum of solids is predominantly a surface phenomenon, this agreement suggests an initially rapid surface reaction converting the surface NO_2ClO_4 to $NOClO_4$ which then controls continued decomposition.

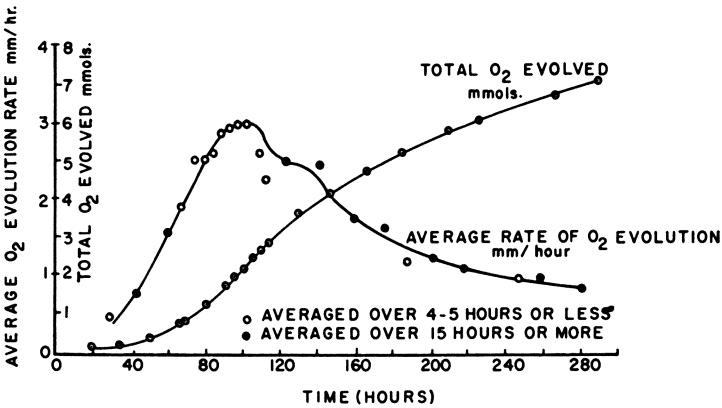

Figure 5. Oxygen evolution of Raman sample

A mechanism for the decomposition of NO_2ClO_4 in the presence of its decomposition products, as in a sealed tube, would include the dinitrogen tetroxide-catalyzed conversion of NO_2ClO_4 to $NOClO_4$ in addition to Reactions 1 and 2.

$$NO_2ClO_4 + N_2O_4 \rightarrow NOClO_4 + N_2O_5$$

$$N_2O_5 \rightarrow N_2O_4 + \tfrac{1}{2}O_2$$

When a critical concentration of NO_2 has been reached from the decomposition of nitrosonium perchlorate, this catalytic conversion rapidly becomes the predominating reaction in the mechanism. Previous work had shown this reaction to be quantitative in the presence of liquid N_2O_4 (*9*). In the course of this investigation, gaseous N_2O_4 at ambient temperature in less than equimolar quantities was also shown to effect the quantitative conversion, presumably by the above mechanism (*9*).

Discussion of Thermal Stability. The foregoing discussion does not explain the instability of NO_2ClO_4, but with this information a reasonable picture of the decomposition process can be presented.

The classical concept is that decompositions of solids probably initiate at defect sites on the crystal surface where circumstances offer a lowered

energy of activation (*4*). In the case of NO_2ClO_4 it appears most probable that the decomposition initiates with $NOClO_4$ formation. Therefore, ion interactions are involved.

It can be stated with confidence that the instability of NO_2ClO_4 is not inherent in the nitronium ion. More stable nitronium species are known; NO_2BF_4 is reportedly stable at 170° C. (*7*), and $(NO_2)_3Al(ClO_4)_6$ and $NO_2Zn(ClO_4)_3$ are quantitatively prepared at 125° C. (*8*), a temperature at which NO_2ClO_4 rapidly decomposes. We are also well aware of stable perchlorate salts. Obviously, then the instability of NO_2ClO_4 is peculiar to the NO_2^+ and ClO_4^- combination.

The following mechanism is suggested as occurring at the crystal surface.

$$NO_2^+ + ClO_4^- \rightleftharpoons [NO_2ClO_4] \begin{cases} \nearrow NO_2ClO_4 \text{ (sublimed)} \\ \searrow NOClO_4 + \tfrac{1}{2}O_2 \end{cases}$$

Nitronium perchlorate, as an ion complex may exist as a transitory intermediate, which may either revert to ions, sublime, or decompose. A similar mechanism has been proposed for the decomposition of ammonium perchlorate (*3*).

Evidence for interaction between the NO_2^+ and ClO_4^- has been observed in the NO_2ClO_4 crystal lattice. Distortions from linearity in the NO_2^+, and from the tetrahedral angle for the Cl—O bonds of the ClO_4^-, as observed in single crystal x-ray data, have been interpreted by Truter *et al.* as being caused by interaction between cation and anion (*12*). In addition, both Raman and infrared spectra of nitronium perchlorate have shown the splitting of the perchlorate Cl—O bands which, according to Hathaway (*5*), is characteristic of bidentate coordination for the perchlorate group. The appearance of the Raman frequency at 571 cm.$^{-1}$ for NO_2ClO_4 has also been reported as direct evidence for distortion of the NO_2^+ in the crystal lattice. Nebgen concludes (*10*) that a band for the NO_2^+ would not appear in the Raman spectrum at this frequency if the NO_2^+ were linear. Thus, something less than a truly ionic crystal lattice is present in NO_2ClO_4, and decomposition may therefore be facilitated by this interaction.

Acknowledgments

This research was supported by the Advanced Research Projects Agency under the U.S. Army Research Office, Contract No. DA-31-124-ARO(D)-12, Durham, N.C.

Literature Cited

(1) Angus, W. R., Leckie, A. H., *Proc. Roy. Soc.* (*London*) **A150,** 615 (1935).
(2) Cordes, H. F., *J. Phys. Chem.* **67,** 1693 (1963).
(3) Galwey, A. K., Jacobs, P. W. M., *Proc. Roy. Soc.* (*London*) **A254,** 455 (1960).
(4) Garner, W. E., ed., "Chemistry of the Solid State," Chap. 7, Academic Press, New York, 1955.
(5) Hathaway, B. M., Underhill, A. E., *J. Chem. Soc.* **1961,** 3091.
(6) Klinkenberg, L. J., *Rec. Trav. Chim.* **56,** 749 (1937).
(7) Kuhn, S. J., and Oláh, G. A., *J. Am. Chem. Soc.* **83,** 4564 (1961).
(8) McElroy, A. D., Guibert, C. R., Bellissimo, J. S., Hashman, J. S., *Inorg. Chem.* to be published.
(9) McElroy, A. D., Marshall, M. D., to be published.
(10) Nebgen, J. W., McElroy, A. D., Klodowski, H. F., *Inorg. Chem.* **4,** 1796 (1965).
(11) Rosolovskii, V. Ya., Rumyantsev, E. S., *Russ. J. Inorg. Chem.* **8,** 689 (1963).
(12) Truter, M. R., Cruikshank, D. W. J., Jeffrey, G. A., *Acta Cryst.* **13,** 855 (1960).
(13) Vogel, A. I., "Quantitative Inorganic Analysis," 2nd ed., p. 285, Longmans, Green, and Co., London, 1951.

RECEIVED June 23, 1965.

10

Advanced Binders for Solid Propellants—A Review

MURRAY S. COHEN

Thiokol Chemical Corp., Reaction Motors Division, Denville, N. J.

Publication Date: January 1, 1966 | doi: 10.1021/ba-1966-0054.ch010

Binder development began with the early asphalt systems, proceeded to polymeric systems with random cure sites and to polymeric systems with end group cure sites. Attempts to introduce oxidants into the binder structure in the form of nitrato, nitro, perchlorate, and difluoramine groups were explored. Fluorocarbon polymers were investigated because of their high density, compatibility with reactive oxidants, and low fuel value. Paralleling these developments was the work on fuel binders where the high heat of formation acetylenic group was incorporated into the binder. This was followed by work on decaborane, carborane, and aluminum hydride-derived polymers. Many of the approaches studied were successful from a scientific viewpoint; however, cost, preparative complexity, physical properties, and energetics in combustion have restricted the application of the advanced systems to limited tasks.

This paper discusses new polymer chemistry associated with a large and heterogeneous body of work embracing what is commonly termed "solid propellant technology." For the sake of brevity and clarity only those solid propellant developments not directly tied to polymer research which have influenced the direction of binder synthesis will be introduced. As a result, the significant advances in formulation techniques, grain design, effect of additives and catalysts on interior ballistics and other important areas of solid propellant technology will not be covered. However, the reader should realize that these neglected portions of solid propellant technology are of far greater practical importance than much of the data covered here.

The earliest known use of solid propellants dates from reports of Chinese military rockets in the 11th Century (*14*). From then until relatively recent times the composition of solid propellants remained essen-

In Advanced Propellant Chemistry; Holzmann, R.;
Advances in Chemistry; American Chemical Society: Washington, DC, 1966.

tially constant—i.e., a mixture of loose powder containing sulfur, nitrate salts, and carbon (charcoal) (*1*). A composition of this type could never be developed for a major role in propulsion because by its very nature it could not give reliable ballistic properties nor could it be used in large diameter (high thrust) motors. With the advent of World War I, smokeless powder or double base gunpowder was adapted to propel rockets. Here again loose powder mixtures were first used with many of the previously mentioned limitations. Consolidating the loose powders into homogeneous forms or grains was a major development in double base technology. The colloidal solution of the polymer, nitrocellulose, in the plasticizer, nitroglycerin, gave a solid mass or grain which could be molded to conform to a wide range of motor geometries and used to deliver long duration thrust in a programmed manner (*22*).

Another variety of compression molded propellants was developed when it was found that rubber could be mixed with an oxidant and the mass formed under heat and pressure into a strong, well-consolidated grain (*6*). These molding techniques, however, limited the size of the charge which could be formed because the total force exerted over the grain surface was limited to the size of the mold and the force capacity of the compression molding apparatus. The use of physically cured systems or colloidal solutions of a solid polymer in a liquid plasticizer has been extended to the polyvinyl chloride hydrocarbon ester plasticizers by the Atlantic Research Corp. By varying this technique, high thrust, complex geometry motors were constructed and satisfactorily fired (*2*). Large diameter solid grains suitable for first-stage ballistic missiles or space boosters could not be fabricated until new processing techniques were discovered. This was accomplished with the development of cast, composite-propellant compositions (*20*). The cast composite procedure called for a liquid fuel to be mixed with a solid oxidizer. When the solids were thoroughly dispersed, the semisolid, pourable "batter" could then be cast into a rocket motor cavity. By cooling, or by controlled chemical reactions within the fuel the mixture would set up or cure to a solid. The liquid fuel thus became a binder—i.e., a component which performed two functions—imparted good mechanical properties to the propellant and burned as fuel. In practice, the mechanical properties of a solid propellant improves as the ratio of binder to oxidizer increases. However, in most systems, peak energetics occur at the 9–11% by weight binder level whereas minimum acceptable physical properties are first achieved at the 14–16% level. The importance of reliable mechanical properties can be illustrated by showing that most operational systems accept the sacrifice in energy and operate at the 14–16% binder level (*21*). The effect of binder level on energetics is shown in Figure 1, a plot of energy (as specific impulse) *vs.* binder level.

Publication Date: January 1, 1966 | doi: 10.1021/ba-1966-0054.ch010

A major advance in propellant technology occurred when it was discovered that metallic fuels could be incorporated into the binder-oxidizer mixture to give higher energy as well as higher density propellants without affecting the mechanical properties of the system (i.e., without lowering

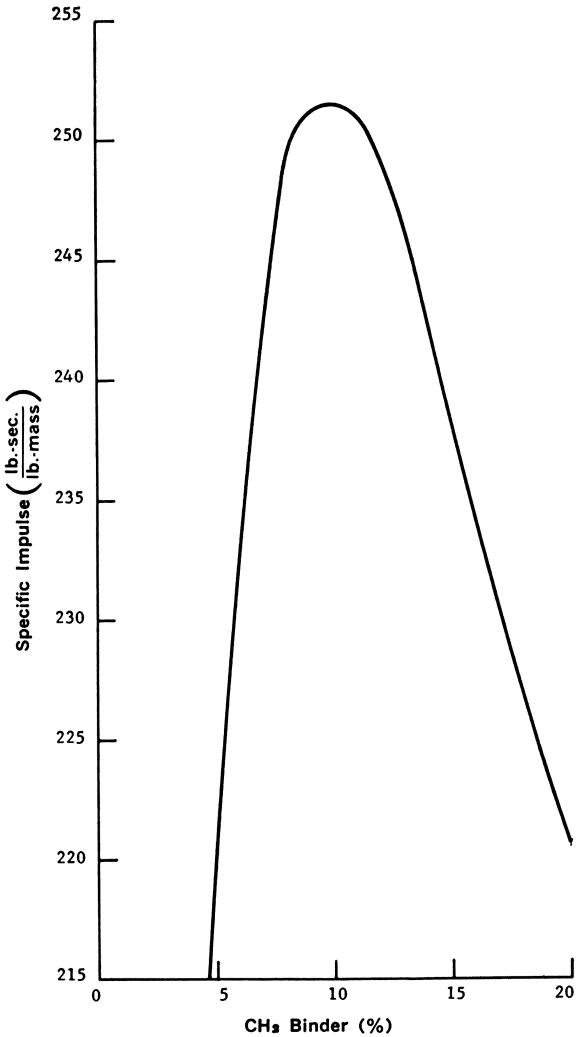

Figure 1. I_{sp} vs. percent binder for a $\text{-}(CH_2)\text{-}_x$/AP propellant

the allowable binder level). This paradoxical situation can be understood if it is realized that a hydrocarbon-oxidizer system is balanced to give carbon monoxide, carbon dioxide, and steam as combustion products. The metallic additive can be considered to be oxidized by the steam, and

therefore it does not require additional oxidant. In the case where aluminum is added to a hydrocarbon-ammonium perchlorate system, the combustion proceeds as follows:

$$NH_4ClO_4 + (CH_2)_n + 2Al \longrightarrow {}^1/_2N_2 + CO + {}^5/_2\,H_2 + Al_2O_3 + HCl$$

The performance or energetics of a propellant system has been shown to be proportional to the factor:

$$\sqrt{\frac{T_c}{\bar{M}}}$$

where T_c is the flame temperature and $\bar{M}$ is the mean molecular weight of the combustion products. Although introducing aluminum into the fuel results in the formation of a high molecular weight combustion product, Al_2O_3, this is offset by two factors. First, a large percent of low molecular weight hydrogen gas is formed in the combustion process, and second, the combustion of a metal gives rise to extremely high flame temperatures.

Figure 2 illustrates a number of significant points associated with metallized propellant systems. It shows: (1) performance improves as the percent by weight of metal increases to an optimum at about 22% aluminum; (2) peak performance does not require lower binder levels although the percent by weight of total fuel has increased as a result of increasing the aluminum level; (3) the peak performance now occurs over a flatter region of binder content. This last factor is important because it means that improved mechanical properties can be obtained (by increasing binder content) without an appreciable fall-off in theoretical performance. In actual practice peak energetics are not realized when propellants containing the theoretically optimum percentage of aluminum are burned in a rocket engine. This is caused by failure to achieve complete combustion as well as the lag which occurs in transferring energy from the metal oxide particles to the gas stream during the expansion process in the nozzle.

With this background it is possible to discuss the directions that research has taken to develop new and improved binder systems. Two major efforts can be categorized. The first was motivated by attempts to improve the physical properties of propellants while maintaining their energetics. The second was a straightforward attempt to increase energetics while maintaining acceptable mechanical properties.

For a treatment of binder developments leading to improved physical properties one must recognize that all hydrocarbon binders are equal in energetics. Nevertheless, the binding capability of a hydrocarbon polymer will vary with small changes in its geometrical structure. Although there was enough scientific information available early in the developments of solid propellants to aid in selecting the best polymeric structures, the actual developments followed a typical evolutionary route.

Publication Date: January 1, 1966 | doi: 10.1021/ba-1966-0054.ch010

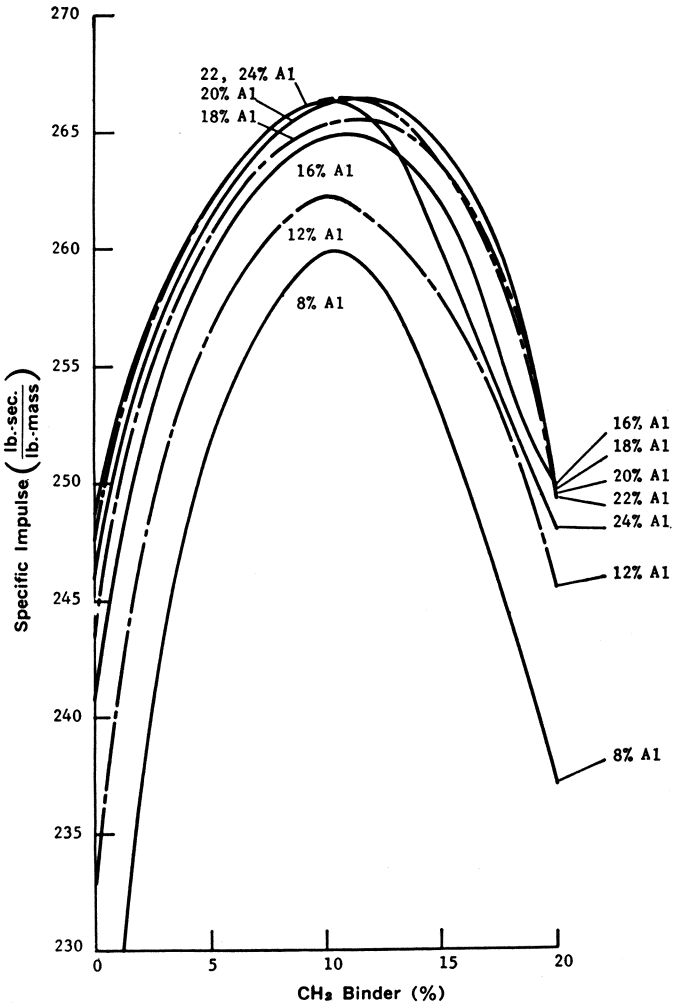

Figure 2. I_{sp} vs. percent binder at various Al levels for a $\text{-}(CH_2)\text{-}_x$/Al/AP propellant

The earliest cast, composite binder was studied by Jet Propulsion Laboratories (JPL) and made use of molten asphalt (*7*). This material was heated until it formed a fluid melt, was mixed with oxidant, and the heated mixture cast into a motor cavity and allowed to cool. This system was poor because of the limited temperature range, the low solids content which could be formulated, and the poor mechanical properties of highly loaded asphalt. A chemically cured system was then introduced when acrylate monomers were mixed with oxidizer and curative (*8*). The mixture could be cast, heated to cure temperature, and the acrylate polymerized to give a well consolidated grain. The basic deficiencies encountered

Publication Date: January 1, 1966 | doi: 10.1021/ba-1966-0054.ch010

in this type of system were the exotherm, at times uncontrollable, during cure and the shrinkage of the solid owing to the fact that the polymer had an appreciably higher density than the monomer. Furthermore, the acrylates used were not particularly rubbery so that their mechanical properties were suitable only for small grains. When a polyfunctional unsaturate, such as divinylbenzene, was added to the acrylate, it acted as a cross-linking agent in this system.

The next advance in solid propellant binders came from using partially polymerized liquids which retained functionality for subsequent curing. The first system of this type was the Thiokol polysulfide polymer (*5*). This was followed by other types of castable, case-bondable systems such as one developed by Thiokol which possessed a controlled molecular weight and was obtained from the copolymerization of butadiene and acrylic acid (*13*). This is still a liquid of 200–300 poise viscosity at 25° C. at 2000–3000 molecular weight. It is sufficiently fluid at processing temperatures (50°–60° C.) to allow formulation with 80–85% by weight of solids and still give a castable mix. Curatives of the epoxy or imine type are added to the mix, and the system is allowed to cure over a period of 3–24 hours to a resilient solid. The system can be represented in the following manner:

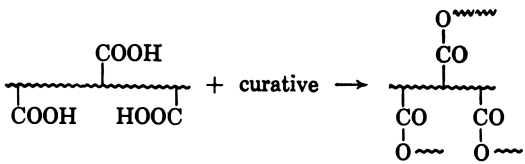

From a theoretical viewpoint the mechanical properties of a polymeric system can be optimized if the cross-links are introduced regularly and not at random as shown above. A desirable development occurred when controlled molecular weight systems, such as the Thiokol HC binder, were made available, having their functional groups only at the ends of chains. These systems were cured with tri- and polyfunctional curing agents of the trisimine type. The following equation illustrates the curing reaction of a carboxy terminated hydrocarbon polymer.

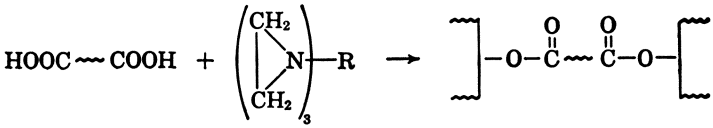

R is $>P{=}O$ or aromatic or heterocyclic nucleus.

The foregoing developments outlined more conventional improvements which were directed primarily at achieving a better binder to impart superior physical properties to a formulated propellant without ap-

preciably upsetting the ratio of oxidizer and metallic fuel ingredients. Two additional routes of investigation, however, were undertaken to incorporate the traditional "bound" ingredients—i.e., the oxidizer and the metallic fuel—as part of the binder structure. The impetus behind this work was a desire to reduce the bound solids and to introduce more energetic sources of oxygen and fuel. These studies are categorized into efforts to develop (1) oxidizing binders and (2) fuel binders.

Incorporating oxygen into the binder structure began with introducing nitrato groups into the polymeric system. The earliest example of nitrocellulose-nitroglycerin mixtures in rockets used gunpowder or explosives technology. Nitrocellulose-nitroglycerin systems were used as powders for World War II bazooka missiles and were later modified so that homogeneous grains could be prepared by compression molding or by "plastisol" techniques (22). In the latter system the liquid (nitroglycerin) was brought into contact with the nitrocellulose powder which loosely filled the rocket motor cavity. By physical solution the system "cured" to a solid gel. These systems showed poor thermal stability characteristics, and their sensitivity to shock increased as the number of nitrato groups increased. Alternate nitrate ester systems were therefore studied to seek additional improvements in properties.

The Naval Powder Factory investigated the preparation of polyvinyl nitrate by nitration of polyvinyl acetate using epichlorohydrin as a cross-linking site.

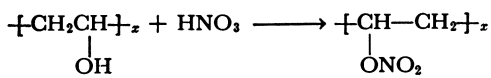

The U. S. Naval Ordnance Test Station and JPL studied the preparation and polymerization of glycidyl nitrate:

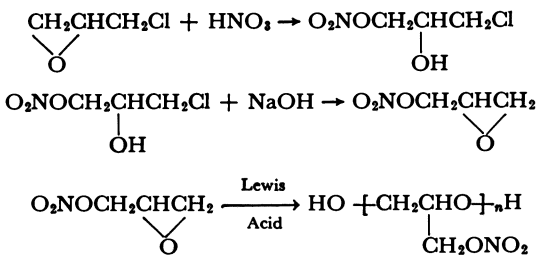

where n was 20–50, and the hydroxy-terminated polymer could be cured with mixtures of diol, triol, and diisocyanates.

The Rohm and Haas Co. used their extensive background in acrylate polymer technology to develop the "petrin acrylate" system.

Publication Date: January 1, 1966 | doi: 10.1021/ba-1966-0054.ch010

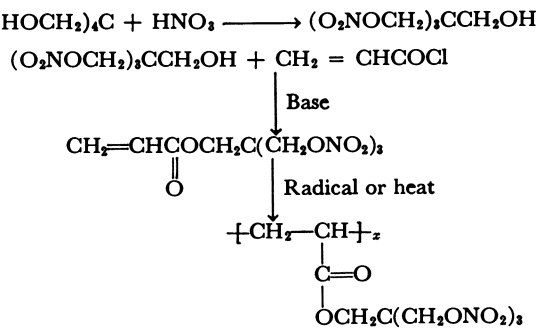

These polymers were of high molecular weight and when plasticized, possessed rubbery characteristics suitable for binders (*19*).

Some attempts were made to prepare nitrate esters of condensation polymers, but in most cases these gave low molecular weight solid products. Typical of this work was the study carried out by the Naval Powder Factory on hydroxylated polyamides.

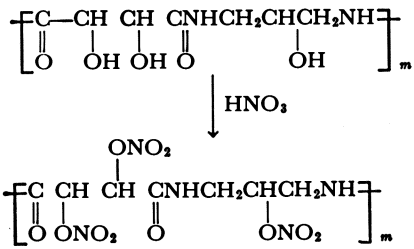

The propellants derived from nitrate ester-based binders possessed the undesirable characteristics associated with nitrate ester groups such as thermal instability, hydrolytic instability, and impact instability (especially for highly nitrated compositions). For this reason a study was undertaken to prepare polymeric binders in which oxygen is carried in the form of the more thermally and hydrolytically stable nitro group. Aerojet General Corp., working with both the Purdue and the Ohio Research Foundations, carried out the bulk of these studies. The following are typical of the condensation monomers synthesized by Aerojet:

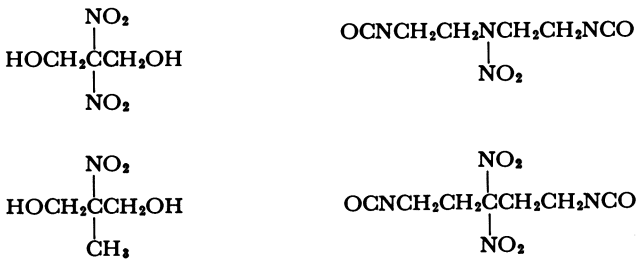

The vinyl monomers are:

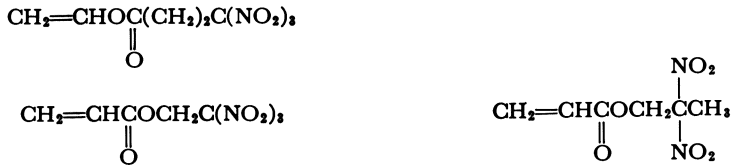

A polyurethane derived from one combination of these condensation monomers is:

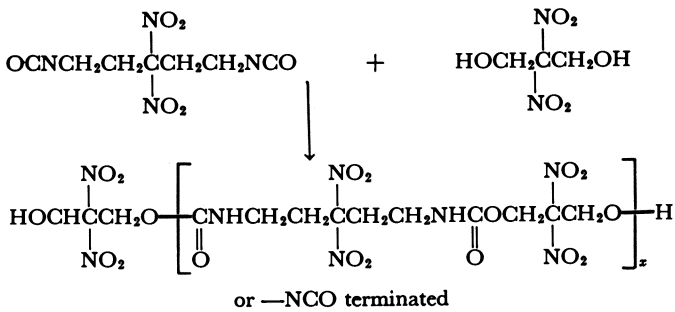

Of the vinyl polymers, only those monomers of very specific structure gave high molecular weight polymer.

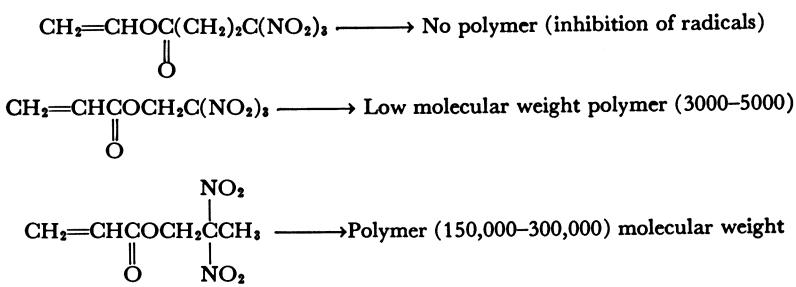

In evaluating the energetics of oxidizers, it is apparent that the perchlorate salts are more desirable than nitrate salts. Therefore one would expect that attempts would be made to incorporate the perchlorate group into binder structures. The study of perchlorate esters was not pursued when it was found that simple model compounds obtained from alcohols and perchloric acid were excessively shock sensitive. However, when the ClO_4 group existed in ionic or salt-like form, these materials were found to be far less sensitive. Bell Aerosystems Corp., in conjunction with the Food Machinery Corp. prepared the polyethylene hydrazine perchlorates.

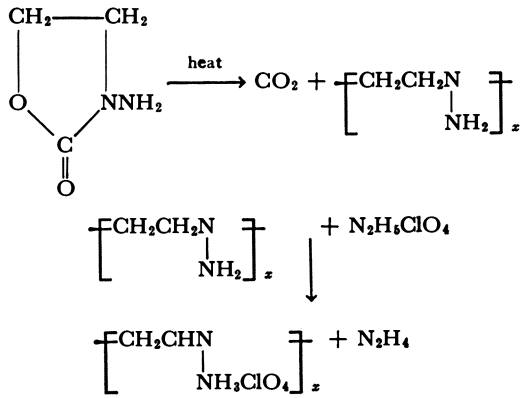

A typical example of polymeric structures containing the difluoramine group is the poly (bis-difluoraminobutylene) shown here. Many other variations of this basic structure have been pioneered by the Rohm and Haas Corp.

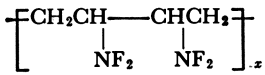

The lower energy fluorocarbon polymers have been studied because of their excellent compatibility with oxidizers and fuels and their high density. The Hughes Tool Co. developed the fluoroalkyl-acrylate polymer by preparing binders through the following route.

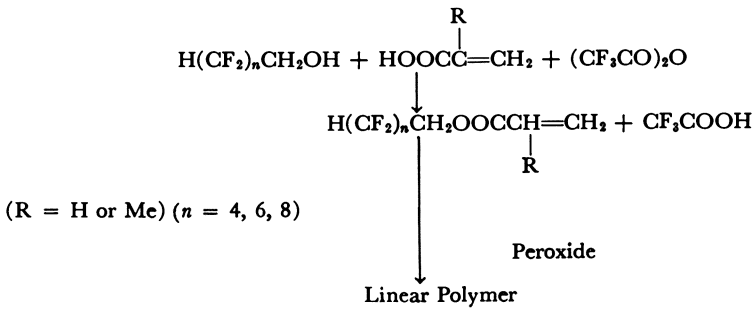

Condensation polymers of the polyester type were studied by Thiokol by using monomers originally developed by the Hooker Chemical Co.

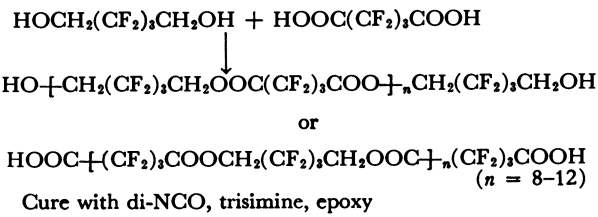

Publication Date: January 1, 1966 | doi: 10.1021/ba-1966-0054.ch010

Paralleling the oxidizing binder developments, work was carried out on incorporating energetic fuel atoms or groups into a binder structure. The motivation was an attempt to use the binder for its energetic contribution to the propellant as well as for its normal role—that of conferring usable mechanical properties to the propellant. An early example of such a study was work done by Thiokol to utilize carbon and hydrogen in more energetic combinations—i.e., to incorporate the high heat of formation acetylenic group into the polymer structure. A castable system was prepared based upon the available acetylenic monomer butynediol and its reaction with formaldehyde (*15, 16, 17, 18*).

$$HOCH_2C{\equiv}CCH_2OH + (CH_2O)_3 \text{ or } (CH_2(OR)_2 \longrightarrow HO[CH_2C{\equiv}CCH_2OCH_2O]_x{-}CH_2C{\equiv}CCH_2OH + ROH$$

Where R = Me or Et
x = 19–30
Cure through $OCN(CH_2)_6NCO$ + triol

Vinyl polymers were also studied in the in situ polymerization of methyldivinylacetylene and dimethyldivinylacetylene. Both monomers could be made to give high molecular weight polymer, but they were excessively cross-linked and therefore far too brittle to use as binders.

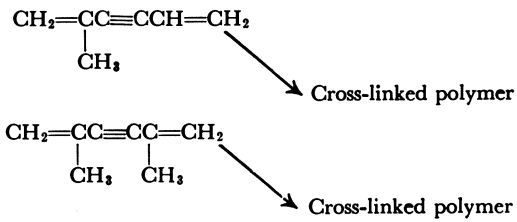

Boron hydrides could be incorporated successfully into polymeric structures through various routes. Early studies by Thiokol had established the difunctionality of decaborane to Lewis bases (*9*).

$$L + B_{10}H_{14} \longrightarrow L{:}B_{10}H_{12}{:}L + H_2$$
L = Organic base ($RC{\equiv}N$, R_2S, R_3N, R_3P, etc)

This work was extended to difunctional reagents, such as adiponitrile, to give a linear polymer:

$$N{\equiv}C(CH_2)_4C{\equiv}N + B_{10}H_{14} \longrightarrow \left[N{\equiv}C(CH_2)_4C{\equiv}N{:}B_{10}H_{12}{:}N{\equiv}C(CH_2)_4C{\equiv}N{:}B_{10}H_{12}\right]_x + H_2 \qquad (x = 10\text{–}12)$$

Borane polymers were prepared by the Rohm and Haas Corp. by using the Friedel-Crafts addition to an olefinic linkage followed by a typical silicone hydrolytic polymerization.

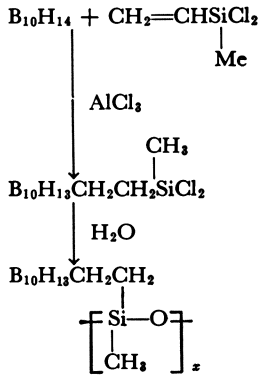

The borane polymers discussed were never fully developed because of several basic drawbacks. They were resinous and acted like strong reducing agents; consequently, they could not be safely formulated with oxidants. A major development took place when the dicarbaclovododecaborane (carborane) compounds were discovered because these materials were extremely stable and organophilic in character. (The formula —C—C—(O, $B_{10}H_{10}$) is used for carborane to symbolize the delocalized bonding that exists in all of the atoms which make up this icosahedral structure.) The basic reaction for carborane formation is illustrated in the following equation (*4*):

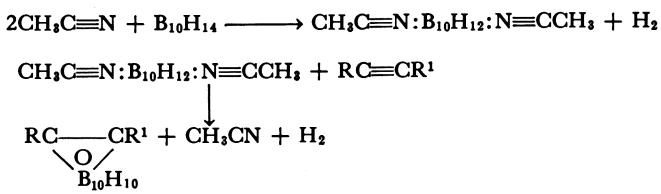

R, R^1 = H, alkyl, aryl, acetoxymethyl, halomethyl, vinyl, allyl, etc.

A wide range of monomers, such as the condensation monomers shown here, were synthesized by Thiokol, Olin-Mathieson, and Rohm and Haas (*10, 11*).

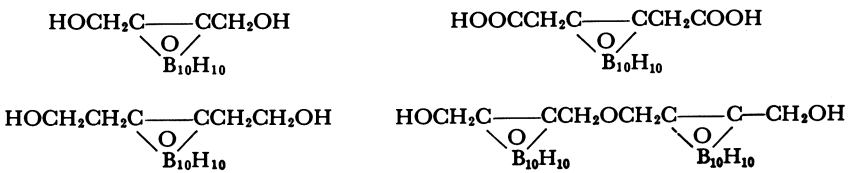

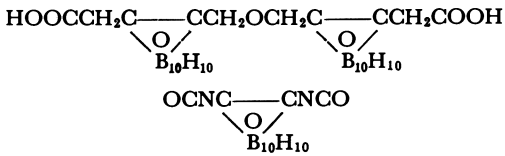

Vinyl carborane monomers were also studied (*12*). Some of the typical structures prepared were:

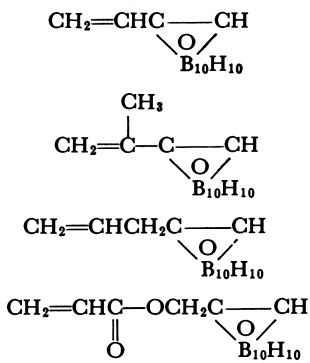

An example of the type of condensation polymers which could be synthesized is the polyester condensation polymer of controlled molecular weight and terminal functionality illustrated in the following equation (*10*):

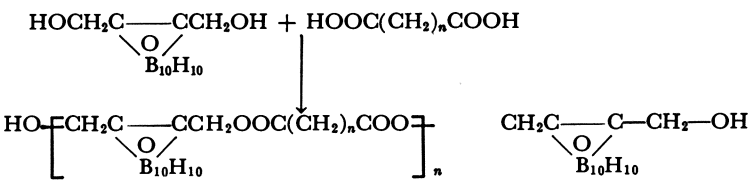

(*n* = 15–25)

Cure with toluene diisocyanate and castor oil

Rubber when 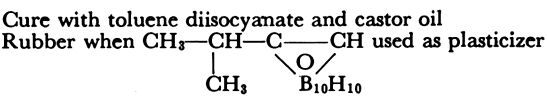 used as plasticizer

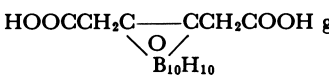 gave a useful polymer when used in place of organic acid

Vinyl polymers could be prepared, but the molecular weight and physical properties depended strongly upon structure (*12*).

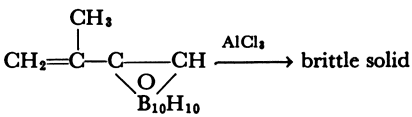

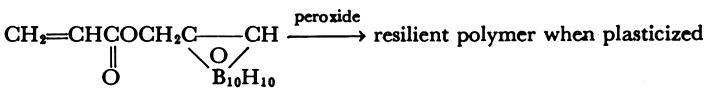

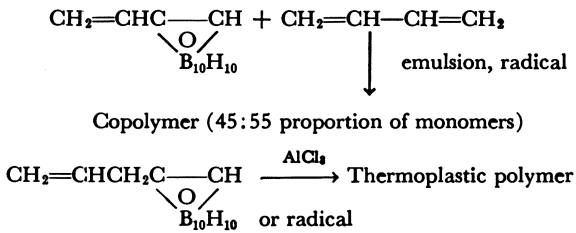

Studies aimed at incorporating other metals into the polymeric structure were not as intensively pursued as the borane studies. The aluminum-based polymers synthesized by Thiokol possessed the Al–H bond as part of a linear structure (3).

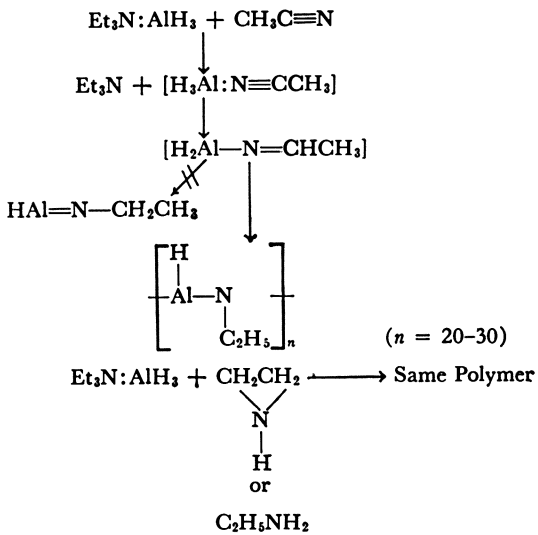

It can be seen from a review of the synthetic chemistry associated with binder research that significant scientific contributions came from this work. Most of the advanced systems developed, however, have found very limited application in solid propulsion owing to such factors as thermal and shock sensitivity, lower energy than originally calculated, high cost and lack of availability of chemicals, and deficiencies in the physical properties of the polymers prepared.

Literature Cited

(1) Davis, T. L., "Chemistry of Powder and Explosives," pp. 73-8, John Wiley and Sons, New York, 1943.
(2) De Fries, M. G., Godrey, J. N., *SPE J.* **19**, 637 (1963).
(3) Ehrlich, R. *et al.*, *Inorg. Chem.* **3**, 628 (1964).
(4) Fein, M. M. *et al.*, *Inorg. Chem.* **2**, 1111 (1963).

(5) Fettes, E. M., "Organic Sulfur Compounds," p. 266, Pergamon Press, New York, 1961.
(6) Geckler, R. D., Klager, K., "Handbook of Astronautical Engineering," Keinz H. Koelle, ed., p. 19-5, McGraw-Hill Book Co., Inc., New York, 1961.
(7) *Ibid.*, p. 19-4.
(8) *Ibid.*, p. 19-6.
(9) Green, J. *et al.*, *J. Polymer Sci.* Pt. B, **2**, 987 (1964).
(10) Green, J. *et al.*, *J. Polymer Sci.* Pt. A, **2**, 3113 (1964).
(11) Green, J. *et al.*, *J. Polymer Sci.* Pt. B, **2**, 109 (1964).
(12) Green, J., *et al.*, *J. Polymer Sci.* **3A**, 3275 (1965).
(13) Klager, K., Wrightson, J. M., *Intern. Conf. Mech. Chem. Solid Propellants*, Lafayette, Ind., **1965**.
(14) Ley, W., "Rockets, Missiles, and Space Travel," p. 5, Viking Press, New York, 1945.
(15) Mann, D. J. *et al.*, U. S. Patent **2,941,010** (June 14, 1960).
(16) Mann, D. J. *et al.*, U. S. Patent **3,083,235** (March 26, 1963).
(17) Perry, D., Dudak, R., U. S. Patent **3,145,192** (Aug. 18, 1964).
(18) Perry, D. *et al.*, ADVAN. CHEM. SER. **54**, 118 (1966).
(19) Preckel, R. F., U. S. Patent **3,116,597** (Jan. 7, 1964).
(20) Ritchy, H. W., McDermott, J., "Advances in Space Science and Technology," Vol. 5, Academic Press, New York, 1962.
(21) Smith, T. L., *Ind. Eng. Chem.* **52**, 776 (1960).
(22) Steinberger, R., "The Chemistry of Propellants," p. 246, Pergamon Press, New York, 1960.

RECEIVED April 28, 1965.

11

Synthesis and Thermochemistry of Tricyanomethyl and Other Polycyano Compounds

MILTON B. FRANKEL,[1] ADOLPH B. AMSTER, EDGAR R. WILSON, MARY McCORMICK,[2] and MARVIN McEACHERN, JR.

Stanford Research Institute, Menlo Park, Calif.

Publication Date: January 1, 1966 | doi: 10.1021/ba-1966-0054.ch011

A series of tricyanomethyl compounds were prepared in refluxing acetonitrile by alkylating potassium tricyanomethanide with alkyl iodides, allyl, propargyl, and benzyl bromides. Yields of 20–57% were obtained for mono- and difunctional halides with a reflux time of 72 hours. The heats of combustion of these tricyanomethyl compounds as well as of two polycyano compounds were measured using a Dickenson-type calorimeter, and heats of formation were calculated with a precision of approximately ±1.0%. From Pitzer's values for C—C and C—H bond energies, that of the tricyanomethyl moiety is calculated to be about 810 kcal./mole, and the tricyanomethyl group is less stable than expected from comparison with ΔH^0_f of propylcyanide.

As a result of synthesizing tetracyanoethylene (*6*), a large class of organic molecules, heavily substituted with cyano groups, has become available. Many of these have interesting physical and chemical properties. Tricyanomethane exists in the free state only as the dicyanoketenimine (*25*) although aquoethereal solutions of tricyanomethane have been used for synthetic reactions (*16*). Other known tricyanomethyl compounds are the salts of tricyanomethane (*3, 7, 10, 15, 16, 21, 24*), bromotricyanomethane (*4*), 1,1,1-tricyanoethane (*10*), 2,2,2-tricyanoethylbenzene (*10*), hexacyanoethane (*23*), tricyanoarenes (*26*), and compounds of the type α,α-dimethylbenzylcyanoform (*14*). This paper describes the synthesis and thermochemistry of a new series of tricyanomethyl compounds.

[1] Present address: Rocketdyne, Canoga Park, Calif.
[2] Present address: Chemical Propulsion Information Agency, Johns Hopkins Applied Physics Laboratory, Silver Spring, Md.

In Advanced Propellant Chemistry; Holzmann, R.;
Advances in Chemistry; American Chemical Society: Washington, DC, 1966.

Synthesis

Hantzsch and Oswald (*10*) prepared 1,1,1-tricyanoethane and 2,2,2-tricyanoethylbenzene in very low yields from a heterogenous mixture of silver tricyanomethanide with methyl and benzyl iodides, respectively. Since the silver salt of tricyanomethane was unsuitable for alkylation reactions because of its virtual insolubility in organic solvents, a search was made to find a salt of tricyanomethane which was partially soluble in organic solvents. Since a ready preparation of potassium tricyanomethanide was now available (*24*), we studied the solubility characteristics of this salt. We found that potassium tricyanomethanide was soluble to the extent of 19% in refluxing acetonitrile and that it could be alkylated in this medium with alkyl iodides, allyl, propargyl, and benzyl bromides. Optimum yields of 20–57% were obtained for mono- and difunctional halides with a reflux time of 72 hours. The importance of the reactivity of the organic halide was demonstrated by the fact that 1,4-dibromobutyne-2 was converted to 1,1,1,6,6,6-hexacyanobutyne-3 in 43% yield while diiodomethane gave only a 2% yield of the monoalkylated product, 1,1,1-tricyanoethyl iodide, and none of the dialkylated product.

As an alternative method of introducing the tricyanomethyl group into organic compounds, the Michael reaction of cyanoform and α,β-unsaturated compounds was studied. Cyanoform was generated in situ by adding a stoichiometric amount of 100% sulfuric acid to an acetonitrile solution of potassium tricyanomethanide and the α,β-unsaturated compound. Under these conditions, addition of cyanoform to acrylonitrile, acrylic acid, methyl acrylate, acrylamide, and acrolein did not occur for only the red polymer of cyanoform was isolated. However, methyl vinyl ketone did react in the expected manner to give 1,1,1-tricyano-4-pentanone.

The tricyanomethyl compounds are a stable class of organic compounds whose solid products can be purified by sublimation. Their exceptional thermal stability is evidenced by the fact that 1,1,1,6,6,6-hexacyanobutyne-3 was sublimed at 170° C./0.05 mm. The infrared spectra of these compounds show a weak absorption for cyano at 4.4 μ. The properties of these compounds are summarized in Table I.

In addition to the above tricyanomethyl compounds, 1,4-dicyanobutyne-2 (*8*) and 1,1,2,2-tetracyanocyclopropane (*22*) were prepared for the thermochemical studies.

Experimental. All analyses were made by Stanford University, Stanford, Calif. Melting points are uncorrected.

ALKYLATION OF ORGANIC HALIDES WITH POTASSIUM TRICYANOMETHANIDE. The preparation of 1,1,1-tricyanobutene-3 is given as a typical example of the experimental procedures used in the reaction of organic halides with potassium tricyanomethanide.

Table I. Properties of

Compound	*m.p.* ° *C.*	*Recryst. Solvent*
$(NC)_3CCH_3$	94–95	*a*
$(NC)_3CCH_2I$	102–103	*b*
$(NC)_3CCH_2CH_2\overset{O}{\overset{\|}{C}}CH_3$	50–51	Ethanol
$(NC)_3CCH_2C_6H_5$	140–141	*c*
$(NC)_3CCH_2CH{=}CH_2$	30[d]	*e*
$(NC)_3CCH_2CH{=}CHCO_2C_2H_5$	60–61	2-Propanol
$(NC)_3CCH_2C{\equiv}CH$	61–62	2-Propanol
$(NC_3)CCH_2CH{=}CHCH_2C(CN)_3$	258–259	Acetonitrile
$(NC)_3CCH_2C{\equiv}CCH_2C(CN)_3$	219–220	*f*
$(NC)_3CCH_2C{\equiv}C{-}C{\equiv}CCH_2C(CN)_3$	177–178	Chloroform

[a] Sublimed at 40° C./0.10 mm., (Lit. (*21*), m.p. 93.5° C.)
[b] Sublimed at 70° C./0.2 mm.
[c] Sublimed at 100° C./0.05 mm., (Lit. (*21*), m.p. 138° C.)

A mixture of 29.0 grams (0.225 mole) of potassium tricyanomethanide (*24*), 26.6 grams (0.32 mole) of allyl bromide, and 500 ml. of acetonitrile was refluxed with stirring for 72 hours. The mixture was cooled and filtered to give 21.8 grams (83.5%) of precipitated potassium bromide. The filtrate was concentrated and diluted with ether to precipitate the residual potassium salts. After filtering, the filtrate was concentrated and distilled to give 16.7 ml. (57.8%) of colorless liquid, b.p. 95° C./26 mm. n_D^{30} 1.4419.

Δ1,1,1-Tricyano-D-pentanone. To a stirred solution of 200 ml. of acetonitrile containing 14.4 grams (0.11 mole) of potassium tricyanomethanide was added 7.74 gram (0.11 mole) of methyl vinyl ketone. Then 5.84 grams (0.055 mole) of sulfuric acid were added dropwise at ambient temperature. There was an immediate precipitation of potassium sulfate. The reaction mixture was stirred for 2 hours and filtered to remove 8.86 grams (92.6%) of potassium sulfate. The filtrate was concentrated to give 15.3 grams of semisolid product which was treated with 2-propanol to give 11.4 grams (64.5%) of white crystals, m.p. 49°–50° C. Recrystallization from ethanol raised the melting point to 50°–51° C.

Δ1,4-Dicyanobutyne-2 (*8*). A mixture of 55.0 grams (0.615 mole) of dry cuprous cyanide, 55.0 grams (0.26 mole) of 1,4-dibromobutyne-2, and 175 ml. of acetonitrile was heated under reflux with good mechanical stirring. After 2 hours, a clear brown solution was attained which was refluxed for an additional 1.5 hours, cooled, and treated with 500 ml. of ether. The precipitated cuprous bromide was separated, and the filtrate was treated four times with charcoal. The light yellow ether solution was then concentrated to give 12.4 grams of yellow crystals. The product was recrystallized from 36 ml. of benzene-hexane (80/20) to give 3.6 grams (13.3%) of colorless needles, m.p. 91°–92° C.

Analyses showed the following: calculated for $C_6H_4N_2$: C, 69.2; H, 3.9; N, 26.9; found: C, 68.96; H, 3.73; N, 26.68.

The infrared spectrum showed a strong absorption for C≡N at 2280 cm^{-1}.

Tricyanomethyl Compounds

Yield %	Formula	Analyses: Calculated C	Calculated H	Calculated N	Found C	Found H	Found N
53.0	$C_5H_3N_3$	57.14	2.88	39.99	57.10	2.88	39.60
2.2	$C_5H_2N_3I$	26.00	0.87	18.20	26.25	0.85	18.73
64.5	$C_8H_4N_3O$	59.62	4.38	26.07	59.58	4.50	26.23
55.3	$C_{11}H_7N_3$	72.91	3.89	23.19	72.89	3.99	23.40
57.8	$C_7H_5N_3$	64.11	3.84	32.04	64.00	3.85	32.30
56.4	$C_{10}H_9N_3O_2$	59.11	4.47	20.68	59.35	4.82	20.86
47.3	$C_7H_3N_3$	65.11	2.34	32.55	64.87	2.51	32.74
22.4	$C_{12}H_6N_6$	61.52	2.58	35.88	61.40	2.83	36.11
43.4	$C_{12}H_4N_6$	62.07	1.74	36.20	62.11	1.83	36.30
27.2	$C_{14}H_4N_6$	65.62	1.57	32.80	64.95	1.47	32.22

[d] b.p. 95° C./26 mm., n_D^{20} 1.4419.
[e] Sublimed at 50° C./1 mm.
[f] Sublimed at 170° C./0.05 mm.

Thermochemistry

Experimental. A Parr model 1221 oxygen bomb calorimeter was modified for isothermal operation and to ensure solution of nitrogen oxides (2). The space between the water jacket and the case was filled with vermiculite (exploded mica) to improve insulation. A flexible 1000-watt heater (Cenco No. 16565-3) was bent in the form of a circle to fit just within the jacket about 1 cm. above the bottom. Heater ends were soldered through the orifices left by removing the hot and cold water valves. A copper-constantan thermocouple and a precision platinum resistance thermometer (Minco model S37-2) were calibrated by comparison with a National Bureau of Standards-calibrated Leeds and Northrup model 8164 platinum resistance thermometer. The thermometer was used to sense the temperature within the calorimeter bucket; the thermocouple sensed the jacket temperature. A mercury-in-glass thermoregulator (Philadelphia Scientific Glass model CE-712) was used to control the jacket temperature.

Jacket temperature was controlled by connecting the thermoregulator and the heater to an American Instrument Co. relay model No. 4-5300. Power to the heater was supplied by a 60-cycle variable transformer normally operated at about 10 volts. Jacket temperature was recorded by feeding the thermocouple output through a Leeds and Northrup d.c. amplifier (No. 9835-B) to a Speedomax H Azar strip chart recorder.

Calorimeter temperature was measured with a Leeds and Northrup G-1 Mueller bridge used in conjunction with a d.c. Null Detector (No. 9834) or with a moving coil galvanometer (No. 2284-D) and lamp and scale.

Time was measured with a 60-cycle synchronous motor clock. Sample weight was determined using an analytical balance and a set of class S stainless steel weights.

Procedure. GENERAL. The samples were burned in the Parr bomb (360 ml. capacity), containing, initially, 3 ml. of water in the cup over the combustion crucible and 99.99% pure oxygen at 450 p.s.i.g. at about

Table II. Energies

Compound	*State*	*Mass of Addend, grams*	*Ms grams*
Benzoic Acid	solid		1.0494
			0.9843
			1.0006
			1.0426
			0.9934
Nujol	liquid		0.9379
			0.9541
			0.9647
1,4-Dicyanobutyne-2	solid	1.1348	0.3300
		1.1315	0.3325
Tetracyanoethylene	solid	0.5902	0.9302
		0.0964	1.0929
1,1,2,2-Tetracyanocyclopropane	solid	0.6351	0.6678
		0.7467	0.7313
1,1,1-Tricyanoethane	solid	0.7063	0.7560
		0.6812	0.6957
1,1,1-Tricyanobutene-3[c]	liquid	1.0932	0.3191
		1.0902	0.3222
1,1,1-Tricyanobutyne-3	solid	1.0402	0.4275
		1.0373	0.4230
1,1,1,6,6,6-Hexacyanohexene-3	solid	1.0315	0.4490
		0.9573	0.4983
1,1,1,6,6,6-Hexacyanohexyne-3	solid	0.7415	0.7839
		1.1114	0.3212
1,1,1,8,8,8-Hexacyanooctadiyne-3,5	solid	1.1165	0.3362
		1.1254	0.3309

[a] Notation is that of Jessup (*11*).
[b] Unburned carbon correction: 4.7 cal.

23° C. The air was flushed out by filling several times with oxygen to 450 p.s.i.g. The weight of the water for the calorimeter, 2000 grams, was measured to 0.1 gram on a high capacity balance.

Sample pellets were weighed in the combustion crucible to 0.05 mg. after overnight storage in a desiccator over anhydrous calcium sulfate. To our knowledge none of the compounds was hygroscopic. The sample was ignited using the usual iron wire supplied by Parr.

For all samples, except one, the jacket temperature during a run was maintained constant within ±0.01° C. at about 29° C., and the calorimeter temperature at the start of a run was generally of the order of 25° C. 1,1,1-tricyanobutene-3 was treated specially because of its melting point ~30° C. (*see* below).

The temperature of the calorimeter was obtained by using the detector as a null instrument or the galvanometer in a more conventional way. During the fore and after periods, resistance was measured each minute. During the heating period, the time was noted at which several predetermined values of resistance were attained. Resistance could be measured to within 3×10^{-4} ohms or about 0.0015° C.

Publication Date: January 1, 1966 | doi: 10.1021/ba-1966-0054.ch011

of Combustion[a]

E_s cal./gram	E cal./°C.	Cz Cal.	Q_v 25° C. cal./gram	Q_p 25° C. cal./gram	ΔH^0_f 25° C. kcal./mole in vacuo	ΔH^0_f average 25° C. in vacuo
2434.1	2434.5	1.8				
2435.7	2436.1	1.7				
2434.0	2434.4	1.8				
2434.1	2434.6	1.9				
2438.3	2438.7	1.8				
2439.8	2440.4	3.3	10976.8			
2439.8	2440.4	3.2	10962.1			
2439.8	2440.4	3.2	10982.0			
2434.9	2435.7	17.1	7590.2	7590.2	88.7	
2434.9	2435.7	17.1	7558.0	7558.0	85.3	87.0 ± 1.7
2438.4	2439.1	33.4	5585.0	5594.3	151.8	
2438.4	2438.9	32.4	5577.9	5587.2	150.9	151.4 ± 0.5
2434.9	2435.5	26.6	6131.9[b]	6138.2	145.0	
2434.9	2435.6	28.2	6096.6	6102.9	140.0	142.5 ± 2.5
2435.5	2436.2	30.3	6263.4	6267.7	85.6	
2435.5	2436.2	27.6	6240.7	6245.0	83.2	84.4 ± 1.2
2445.5	2446.1	14.5	7148.5	7149.6	108.0	
2445.5	2446.1	14.0	7187.0	7188.1	112.9	110.3 ± 2.5
2434.9	2435.7	21.7	7002.9	7006.4	143.3	
2434.9	2435.7	21.3	7030.9	7034.4	146.9	145.1 ± 1.8
2434.9	2435.7	22.0	6578.2	6582.0	207.1	
2434.9	2435.7	23.2	6525.3	6529.1	194.5	200.8 ± 6.3
2435.5	2436.2	28.9	6494.5	6499.6	242.8	
2434.9	2435.7	19.2	6483.0	6488.1	240.5	241.7 ± 1.2
2434.9	2435.7	18.3	6825.0[d]	6829.7	295.0	
2434.9	2435.7	17.6	6801.6	6806.3	289.0	292.0 ± 3.0

[a] A separate calibration, not given, was performed with benzoic acid, because of the high temperature used. Benzoic acid was used as the addend.
[d] Unburned carbon correction: 4.7 cal.

The nitric acid produced in the combustion was determined by titrating with standardized alkali using a methyl orange indicator. The thermal correction was calculated on the basis 14.0 kcal./mole evolved for each mole of aqueous acid formed. A correction was made for the average firing energy, 12.2 cal.

CALIBRATION. The calorimeter was calibrated by burning standardized benzoic acid obtained from the Parr Instrument Co. ($\Delta H_c = 197.72$ kcal./mole). Measurements were made under conditions paralleling as closely as possible those used during a run. For reasons explained below it was also necessary to determine the heat of combustion of Nujol brand mineral oil. For this purpose the contents of two 1-pint bottles of Nujol were mixed thoroughly and stored in a 1-liter bottle. Runs were made on aliquots withdrawn from this new mixture. Table II includes the results obtained both for the benzoic acid and the Nujol and indicates the precision of the experiment.

SAMPLE PREPARATION. Samples were purified by recrystallization; we believe each substance to be of better than 99% purity.

The 1,1,1-tricyanobutene-3 formed a glassy solid below 29° C. with a smooth transition. It was run as a liquid with the calorimeter jacket maintained at about 35° C. A small, weighed pellet of benzoic acid was heated to above 30° C., and the pellet was wetted with the liquid by dropwise addition. The weight of liquid added was determined by difference. The wet pellet was maintained above 29° C. until ignition. Thus, uncertainty as to the physical state of the liquid was avoided. No attempt was made to correct results for the heat of wetting.

All other samples were prepared by pressing solid pellets which were then wet with the calibrated Nujol to obtain complete combustion.

Results. All computations were made according to the method described by Jessup (*11*). The unit of energy used is the defined calorie equal to 4.183 international joules. The unit of mass is the gram true mass derived from the weight in air against stainless steel weights; buoyancy corrections were made. Molecular weights were calculated using 1959 values of the Commission on Atomic Weights. Heats of formation were calculated from heats of combustion. The results of individual combustions and corrected values of the heats of formation are presented in Table II.

Discussion. It is now possible to compare the measured heats of formation with those predicted on the basis of bond or group additivity. We use the same method as that discussed by Boyd (*5*). Assume ΔH for the following reaction is 0:

$$m\text{R—CN} + C_lH_{m+n} \rightarrow m\text{R—H} + C_l(CN)_mH_n$$

R–CN is taken to be propylcyanide (gas) for which $\Delta H^0_f = 7.45$ kcal./mole (*9*). The heats of formation used for the compounds C_lH_{m+n} are given in Table III. The heats of sublimation for all the solids were estimated to be 20.0 kcal./mole; for the one liquid we used an estimated value for the heat of vaporization of 5.0 kcal./mole.

Table III

Compound	ΔH^0_f, *kcal./mole gas*	*Reference*
Ethane	−20.236	*19*
Propane	−24.826	*20*
Ethylene	12.496	*19*
Cyclopropane	12.74	*12*
Butyne-1	39.70	*20*
Hexyne-3	25.84	*1*
Hexyne-1	29.55	*20*
Hexane	−39.96	*20*
Butyne-2	35.37	*20*
cis-Hexene-3	−11.56	*20*
trans-Hexene-3	−12.56	*20*
Average (*cis*, *trans*)	−12.06	
Butene-1	0.28	*20*
Octadiyne-3,5	93.8[a]	

[a] Calculated from ΔH^0_f octane = −49.82 kcal./mole (*19*).
ΔH hydrogenation (octa-1,7 diyne) = 139.7 (Ref. *17*, p. 53) and ΔH hydrogenation (dodeca-1,7-diyne) minus ΔH hydrogenation 3,9 isomer = −3.9 kcal./mole (Ref. *17*, p. 54)

The results of the comparison are shown in Table IV where the last column, Δ, represents the excess of the measured heat of formation over that calculated. Accordingly, the positive values are evidence of the decreased stability of the polysubstituted cyanocarbons.

Table IV

Compound	ΔH^0_f *kcal./mole, gas* *Measured*	*Calculated*	Δ
1,4-Dicyanobutyne-2	107.0	99.9	7.1
Tetracyanoethylene	171.4	141.6	29.8[a]
1,1,2,2-Tetracyanocyclopropane	162.5	141.8	20.7
1,1,1-Tricyanoethane	104.4	76.6	27.8
1,1,1-Tricyanobutene-3	115.3	97.1	18.2
1,1,1-Tricyanobutyne-3	165.1	136.5	28.6
1,1,1,6,6,6-Hexacyanohexene-3	220.8	181.6	39.2
1,1,1,6,6,6-Hexacyanohexyne-3	261.7	219.5	42.2
1,1,1,8,8,8-Hexacyanooctadiyne-3,5	312.0	287.4	24.6

[a] *See* R. H. Boyd (*5*) for comparison.

Table V

Compound	$E(-C(CN)_3)$ *kcal.*
1,1,1-Tricyanoethane	800
1,1,1-Tricyanobutene-3	816
1,1,1-Tricyanobutyne-3	819
1,1,1,6,6,6-Hexacyanohexene-3	814
1,1,1,6,6,6-Hexacyanohexyne-3	814
1,1,1,8,8,8-Hexacyanooctadiyne-3,5	822

It is also possible to calculate the bond energy of the tricyanomethyl moiety in each of the molecules. To do this we calculate standard heats of formation at 0° K. from the values given in Table III for 298° C. In the absence of reliable data we note the following reported (*13*) specific heats, C_p:

Acetonitrile: 0.54 cal./gram
Propionitrile: 0.538 cal./gram
Butyronitrile: 0.547 cal./gram

Taking an average value of $C_p = 0.54$ cal./gram, for each compound we can calculate $H^0_{298} - H^0_0 = 298\ Mc$ where M = molecular weight. The bond energy of the $-C(CN)_3$ group is then calculated using values for other bond energies as given by Pitzer (*18*) and values for the heats of formation of H, N, and C atoms as given in reference (*2*). The results of these calculations are listed in Table V.

The following are our conservative estimates, of the uncertainties in the calculated values of the stabilization energies:

Combustion process: 1.0 kcal.
Heat of vaporization: 1.0 kcal.
Heat of sublimation: 10.0 kcal.

Publication Date: January 1, 1966 | doi: 10.1021/ba-1966-0054.ch011

In addition, the bond energy calculations are erroneous because of the uncertainty in the enthalpy calculation. For, not only is C_p estimated at 25° C. but the further assumption is made that C_p is temperature-independent. This may introduce an error as large as 2 or 3 kcal. Consequently, neither the scatter in the stabilization energies nor the apparently increasing trend in the bond energy with increasing unsaturation is significant. Nevertheless, assigning a bond energy to the tricyanomethyl group is reasonable. To calculate the heat of formation of linear or cyclic hydrocarbons with the group substituted in one or more locations, an average value of 810 kcal. for the $-C(CN)_3$ bond energy would appear to introduce an error of about 10 kcal. We are in the process of determining the latent heats and heat capacities necessary to improve the significance of the data.

Publication Date: January 1, 1966 | doi: 10.1021/ba-1966-0054.ch011

Acknowledgment

Research reported in this publication was supported by the Advanced Research Projects Agency through the U.S. Army Research Office, Durham, N. C. The authors wish to thank Harry S. Mosher for his interest and helpful suggestions throughout the course of this work.

Literature Cited

(1) API Project 44, "Selected Values of Properties of Hydrocarbons and Related Compounds," A & M College of Texas, College Station, Tex., 1955.
(2) Armstrong, G. T., Marantz, S., *J. Phys. Chem.*, **64**, 1776 (1960).
(3) Birckenbach, L., Huttner, K., *Ber.* **62A**, 153 (1929).
(4) Birckenbach, L., Huttner, K., *Ibid.* **62B**, 2065 (1929).
(5) Boyd, R. H., *J. Chem. Phys.* **38**, 2529 (1963).
(6) Cairns, T. L., *et al.*, *J. Am. Chem. Soc.* **80**, 2775 (1958).
(7) Cox, E., Fontaine, A., *Bull. Soc. Chim. France* **21**, 948 (1954).
(8) Elvidge, J. A., University of London, private communication.
(9) Evans, F. W., Skinner, H. A., *Trans. Faraday Soc.* **55**, 255 (1959).
(10) Hantzsch, A., Oswald, G., *Ber.* **32**, 641 (1899).
(11) Jessup, R. S., *Nat. Bur. Std.* (*U.S.*), *Monograph* **7**, (1960).
(12) Knowlton, J. W., Rossini, Jr., F. D., *J. Res. Nat. Bur. Std., A*, **43**, 113 (1949).
(13) Lange, N. A., "Handbook of Chemistry," 10th ed., McGraw-Hill, New York, 1961.
(14) Martin, E. L., Williams, J. K., U. S. Patent **3,166,583** (Jan. 19, 1965).
(15) Middleton, W. J., Engelhardt, V. A., *J. Am Chem. Soc.* **80**, 2788 (1958).
(16) Middleton, W. J., *et al. J. Am. Chem. Soc.* **80**, 2795 (1958).
(17) Mortimer, C. T., "Reaction Heats and Bond Strengths," Pergamon Press, New York, 1962.
(18) Pitzer, K. S., *J. Am. Chem. Soc.*, **70**, 2140 (1948).
(19) Rossini, F. D., *et al.*, *Nat. Bur. Std. (U.S.), Circ.* **500**.
(20) Rossini, F. D., *et al.*, *Nat. Bur. Std. (U.S.), Circ.* **C461**.
(21) Schmidtmann, H., *Ber.* **29**, 1168 (1896).
(22) Scribner, R. M., Sausen, G. N., Prichard, W. W., *J. Org. Chem.* **25**, 1440 (1960).

(23) Trofimenko, S., McKusick, B. C., *J. Am. Chem. Soc.* **84**, 3677 (1962).
(24) Trofimenko, S., Little, E. L. Jr., Mower, H. F., *J. Org. Chem.* **27**, 433 (1962).
(25) Trofimenko, S., *J. Org. Chem.* **28**, 217 (1963).
(26) Williams, J. K., U. S. Patent **2,995,597** (Aug. 8, 1961).

RECEIVED July 21, 1965.

12

Acetylenic Propellant Binders

DONALD D. PERRY, GERALD GOLUB, RITA D. DWYER, and PAUL F. SCHAEFFER

Thiokol Chemical Corp., Reaction Motors Division, Denville, N. J.

Publication Date: January 1, 1966 | doi: 10.1021/ba-1966-0054.ch012

*Hydroxy-terminated polyacetals can be prepared by the reaction of acetylenic glycols with aldehydes and acetals. The polymer from 2-butyne-1,4-diol and paraformaldehyde (I.) [$HO\text{-}CH_2C{\equiv}CCH_2OCH_2O\text{-}_nH$] is a waxy solid, m.p. 55°–60° C., molecular weight 1000–2500. Reaction of I with diisocyanates gives rubbery polyurethanes. A binder having optimum physical properties uses I, hexamethylene diisocyanate, castor oil as a cross-linking agent, and butylcyclohexyl phthalate as a plasticizer. Propellant compositions containing the acetylenic binder and ammonium perchlorate oxidizer exhibit plateau burning behavior in the 700–2000 p.s.i.g. region. Small motor firings confirm the calculated performance improvement resulting from the presence of the acetylenic groups. A solid polyacetal can also be obtained from 2,4-hexadiyne-1,6-diol and paraformaldehyde, and liquid polymers can be formed from 2-butyne-1,4-diol and both 2-ethylbutyraldehyde and di-*n*-propyl acetal.*

A solid propellant binder actually performs two functions. In addition to acting as a matrix that physically holds the propellant ingredients together, it must also provide fuel energy. Modern solid propellant technology employs casting techniques which introduces an additional requirement—namely that the binder be a liquid polymer, curable to a rubber-like solid.

This paper is concerned with the problem of increasing the propellant specific impulse by introducing endothermic groups into the binder structure. Since the acetylenic bond is one of the most energetic organofunctional groups, a program was undertaken to synthesize polymers containing carbon-carbon triple bonds and to evaluate these polymers as binders in castable propellant systems. The studies conducted included the synthesis of prepolymers, curing the prepolymers to elastomeric binders with

In Advanced Propellant Chemistry; Holzmann, R.;
Advances in Chemistry; American Chemical Society: Washington, DC, 1966.

diisocyanates, laboratory propellant evaluation, and small rocket motor tests.

Prepolymer Preparation

The formation of acetals by the reaction of aldehydes with alcohols (Equation 1) is a well-known and useful preparative method in organic

$$2ROH + R'CHO \overset{H^+}{\rightleftharpoons} (RO)_2CHR' + H_2O \qquad (1)$$

chemistry (*1*). As Equation 1 shows, it is an equilibrium reaction which is catalyzed by strong acids and favored by the removal of water. A modification of this method is the acetal interchange reaction shown in Equation 2. The success of this method depends on the ability to remove

$$2ROH + (R''O)_2CHR' \overset{H^+}{\rightleftharpoons} (RO)_2CHR' + 2R''OH \qquad (2)$$

R″OH preferentially and thereby shift the equilibrium to the right. This is generally accomplished by distillation, and the conversion therefore requires that R″OH be significantly more volatile than ROH. The acetal interchange reaction has found application in preparing acetals where direct reaction of an alcohol and an aldehyde is difficult or inconvenient or where the acetal of a low boiling alcohol is more readily available. Both reactions have been used frequently to protect carbonyl groups during other synthetic operations since regeneration of the free aldehyde or ketone can usually be accomplished readily.

In attempting to extend this reaction to polymer preparation, Hill and Hibbert (*3*) carried out the reaction of acetylene or acetaldehyde with various glycols (Equation 3). They found that when n was 2 or 3, cyclic products (route A) were obtained, while for $n = 8$–10 the products were

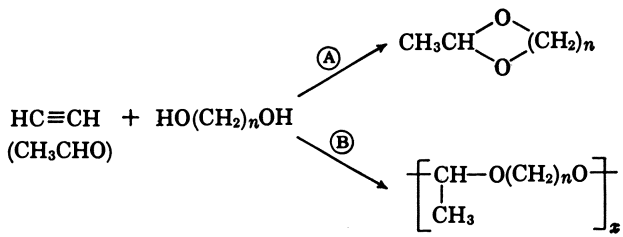

(3)

sirupy, polymer-like materials. When n was 4, a mixture of a volatile compound—apparently the seven-membered cyclic acetal—and a sirupy polymer was obtained.

Hill and Carothers (*4*) investigated the acetal interchange reaction with di-*n*-butyl formal and glycols (Equation 4). When n was 3 or 4, cyclic formals were the principal products. Pentamethylene glycol ($n = 5$) gave a sirupy liquid polymer. The reaction with decamethylene gly-

$$m\mathrm{HO(CH_2)_nOH} + m\mathrm{BuOCH_2OBu} \xrightarrow{150^\circ\ \mathrm{C.},\ \mathrm{H}^+} \left[\mathrm{CH_2O(CH_2)_nO}\right]_m + 2m\mathrm{BuOH} \quad (4)$$

col, where cyclic structures are not favored, was studied most extensively. Initially, a waxy polymer (m.p. 56.5°–57° C.) of molecular weight 2190, was formed. On heating this product in vacuo at 230°–250° C. polymers of 10,000–20,000 molecular weight, capable of being drawn into fibers, were obtained.

The objectives of this study were to extend these synthetic methods to the preparation of low molecular weight, hydroxy-terminated polymers containing acetylenic bonds and evaluating these prepolymers in castable solid propellant formulations. Since 2-butyne-1,4-diol was commercially available, the formation of polyacetals from this glycol seemed to be an attractive route to the desired polymers. It was believed that the rigid triple bond would inhibit the cyclic acetal formation observed by the earlier workers with the lower members of the saturated glycol series. Thus, in an acetal interchange reaction a linear polymer (I) should be favored over the cyclic acetal (II):

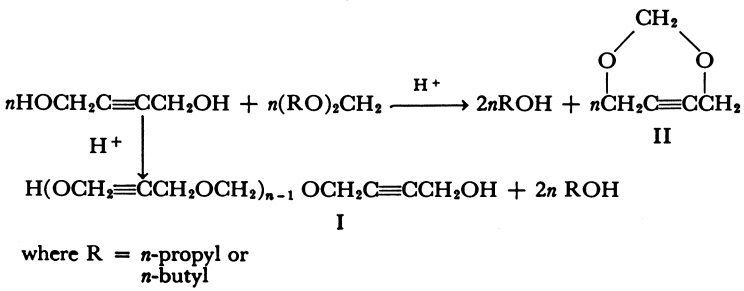

Initial studies used the reaction of butynediol with di-*n*-butyl formal and di-*n*-propyl formal. The reaction with the former required relatively high temperatures (*ca.* 190° C.) in order to remove the byproduct, *n*-butyl alcohol (b.p. 117.7° C.), and this apparently caused some polymer degradation. As a result, only a semisolid polymer (I) of molecular weight 475 was obtained. The reaction with di-*n*-propyl formal, however, gave polymers with molecular weights of 680 and 1020 in two experiments. The higher molecular weight material was obtained by heating an equimolar mixture of the reactants at 130°–180° C. for 9 hours in the presence of polyphosphoric acid and continuously removing *n*-propyl alcohol by distillation into a Dean-Stark trap. The product was a waxy material, m.p. 55° C., which was shown by chemical and infrared analysis to have the structure I.

Similar acetal interchange reactions were carried out between butynediol and di-*n*-propyl acetal (IIIa) and butynediol and diethylpropional (IIIb), to give low molecular weight, liquid polyacetals (IVa and IVb):

$$(n+1)HOCH_2C{\equiv}CCH_2OH + n(R'O)_2CHR \xrightarrow{H^+}$$

IIIa = R = CH_3, R′ = C_3H_7
IIIb = R = C_2H_5, R′ = C_2H_5

$$HO(CH_2C{\equiv}CCH_2O\underset{\underset{R}{|}}{CH}O)_nCH_2C{\equiv}CCH_2OH + 2nR'OH \quad (6)$$

IVa R = CH_3
IVb R = C_2H_5

Despite the success achieved in preparing low molecular weight acetylenic ether polymers by the acetal interchange reaction, an improved method was desired since it was difficult to obtain molecular weights above 1000, and the reactions were slow. It was found at this point that direct reaction of butynediol with paraformaldehyde (Equation 7) proceeded rapidly in refluxing benzene or toluene to yield polymers having molecular weights in the 1500–2500 range. These were hard, brownish-colored

$$nHOCH_2C{\equiv}CCH_2OH + \frac{n}{x}(CH_2O)_x \xrightarrow{H^+}$$

$$HO\text{-}(CH_2C{\equiv}CCH_2OCH_2O)\text{-}_nH + (n-1)H_2O \quad (7)$$

I

waxes, quite similar to the products obtained in the acetal exchange reactions, except for their molecular weights. The reaction proceeded approximately twice as fast in toluene as in benzene owing to the higher temperature attainable. The generality of the method was shown by the fact that it could also be successfully used with 2,4-hexadiyne-1,6-diol and paraformaldehyde, and with butynediol and 2-ethylbutyraldehyde, although in these cases only low molecular weight (600–800) products were obtained.

The polyformal (I) was characterized by wet chemical and infrared analyses, and by cryoscopic molecular weight determinations. For the latter, the preferred method was the freezing point depression of an ethylene bromide solution. The other polyacetals were characterized primarily by infrared analysis and molecular weight determinations.

Infrared and functional group analyses showed the presence of hydroxyl end groups in the products. In addition, the results of chain extension and cross-linking reactions with diisocyanates (*vide infra*) confirmed the presence of two terminal hydroxyl groups.

Calorimetry

Calorimetric studies were undertaken to determine whether the acetylenic linkage had remained intact during the polymerization. If the linkage were affected, heats of combustion determined experimentally should agree with the theoretical values calculated for acetylenic polymers. The heats of combustion of the acetylenic polymers were measured in a

Publication Date: January 1, 1966 | doi: 10.1021/ba-1966-0054.ch012

Table I. Physical Properties of

Sample No.	*Prepolymer Mol. Wt.*	*Diisocyanate*	*Cross-linking Agent*	*Plasticizer*	(%)
1	1915	TDI[b]	TMP	...	...
2	1915	HDI	TMP	...	...
3	1180	HDI	TMP	...	...
4	1180	HDI	TMP	BCPH	14
5	1915	HDI	CO	BCPH	14

[a] Cure conditions: 20 hours at 80° C., sample 5 cured for 44 hours.

Table II. Physical Properties of

Formulation No.	*Isocyanate*	*% Oxidizer*[a]	*Max. Tensile Strength p.s.i.g.*	*Elongation at Max. Tensile, %*
12[b]	TDI	69.7	176	15.5
57[c]	TDI	77.8	90	16
66[c]	HDI	75	108	14
73[c]	TDI	75	110	25

[a] Oxidizer used was bimodal JAN A-192 blend, 80 wt. % ground at 2600 r.p.m. and 20 wt. % ground at 16,000 r.p.m.
[b] Cross-linked with TMP.

Publication Date: January 1, 1966 | doi: 10.1021/ba-1966-0054.ch012

Parr adiabatic calorimeter containing a Parr double-valve oxygen combustion bomb. The water equivalent of the calorimeter was determined from the combustion of a weighed sample of benzoic acid standardized by the National Bureau of Standards (NBS). The agreement between results of any two acceptable runs was better than 0.10%.

Stoichiometric reaction with oxygen to give carbon dioxide and water in their standard states was assumed. The data are summarized in the Experimental section. It can be seen that the experimental results agree well with calculated values showing that the triple bond was retained during polymerization.

Curing Studies

Curing of the acetylenic polyacetals to rubbery polyurethanes could be achieved with any of a number of commercially available diisocyanates, including 2,4-toluene diisocyanate (TDI), hexamethylene diisocyanate (HDI), dianisidine diisocyanate (DADI), and 4,4′-diisocyanatodiphenylmethane (MDI). The first two diisocyanates were studied most extensively. The reactions were carried out in solution in benzene, toluene, and ethylene bromide, and in bulk. The bulk reaction, which is the only

Typical Acetylenic Polyurethane Binders[a]

Catalyst	*Ultimate Tensile Strength p.s.i.g.*	*Ultimate Elongation %*	*Permanent Deformation %*	*Shore A-2 Hardness*
...	913	73	31	97
...	773	63	37	...
...	681	64	28	96
FeAA, DPPD	257	412	137	64
FeAA, DPPD	1300	506	187	...

[b] Abbreviations: TDI = 2,4-Toluene diisocyanate; HDI = Hexamethylene diisocyanate; TMP = Trimethylolpropane; CO = Castor oil; BCPH = Butylcyclohexyl phthalate; FeAA = Ferric acetonylacetonate; DPPD = Diphenyl-*p*-phenylenediamine.

Acetylenic Polyurethane Propellants

Modulus of Elasticity p.s.i.g.	*Density lbs./cu. in.*	*Impact Sensitivity in.*	*Auto-ignition Temp. ° F.*
1000	...	...	665
...	0.0625	9–10	670
...	0.061	8	660
...	0.061	9–10	685

[c] Contained 5% BCPH plasticizer; cross-linked with castor oil; Triton X-100 and DPPD used as processing aids.

Publication Date: January 1, 1966 | doi: 10.1021/ba-1966-0054.ch012

suitable method for practical solid propellant processing, generally gave products with superior properties.

In addition to the diisocyanate, cross-linking agents, catalysts, and plasticizers were used to accelerate the cure reaction and to improve the physical properties of the ultimate binder composition. The cross-linking agents consisted of trifunctional alcohols (castor oil and trimethylolpropane), aminoalcohols, and aliphatic or aromatic diamines. Best results were obtained with castor oil and trimethylolpropane. Castor oil was preferred because of its lower rate of reaction with the isocyanate, which resulted in a longer pot life for the propellant mix. Catalysts for the polyurethane formation reaction included tertiary amines and ferric acetonylacetonate. A variety of typical ester-type plasticizers were investigated to give improved physical properties. The best of these was butylcyclohexyl phthalate (BCPH). Compositions containing this plasticizer were unique in combining good tensile strength with high elongations. Finally, a study of reaction stoichiometry *vs.* physical properties showed that a molar ratio of polyformal:diisocyanate:cross-linking agent of 1:1.5:0.2 gave the best results. Cure was essentially complete in 20 hours at 80° C.

Table I lists the physical properties of some typical binder compositions both with and without plasticizer. All of these used the stoichiom-

etry and cure conditions given above, except for sample 5 for which a 44 hour cure time was used.

Laboratory Propellant Formulation and Evaluation

Propellant compositions containing the acetylenic fuel binder and ammonium perchlorate oxidizer were prepared and cured, and their physical and ballistic properties determined. Formulations containing up to 83% by weight of ammonium perchlorate oxidizer have been prepared. This represents the optimum level of oxidizer for this fuel binder. Processing characteristics and propellant physical properties were good. Preparation of a typical propellant batch is given in the Experimental section, and Table II summarizes the principal physical properties of characteristic batches of cured propellant at ambient temperature. The tensile properties were measured on 4–6-inch dumbell specimens, having a 1-inch gage length, $^3/_{32}$-inch thick, and ends of $^1/_4$-inch thickness.

Among the most interesting features of the acetylenic polyurethane propellants were their ballistic properties. Burning rates of propellant strands were determined in a Crawford bomb apparatus. The burning rates measured at 1000 p.s.i.g. were somewhat higher than normally encountered in ammonium perchlorate type composite propellants, ranging from 0.5 to 0.8 in./sec. for uncatalyzed compositions. The occurrence of a plateau in the burning rate *vs.* pressure curves in the 700–2000 p.s.i.g. region was unusual. The exact position and extent of the plateau region varied somewhat from batch to batch, but it was a constant feature of all the compositions containing the acetylenic polyurethane binder. The value of such a region of relative lack of pressure dependence of burning rate in providing controlled burning despite pressure fluctuations is obvious. By using a catalyst, it was possible to increase the propellant burning rate up to 2.2 in./sec. Curves of burning rate *vs.* pressure for catalyzed and uncatalyzed propellant compositions are shown in Figure 1.

Safety tests were carried out in order to determine the handling characteristics of the propellant system. These results are also summarized in Table II. The impact sensitivity of the propellant was approximately the same as that of pure ammonium perchlorate (9–12 inches) when tested with a 2-kg. weight in the Picatinny Arsenal impact dropweight tester (5). Detonation tests made with a No. 8 blasting cap and 20 grams of tetryl indicated that the propellant is not sensitive to detonation. The autoignition temperature of these propellants is in the range of 315°–370° C. (600°–700° F.), as measured by the Picatinny Arsenal test method (5). Propellant samples have been stored at 80° C. (175° F.) for periods up to 30 days without any signs of degradation or change in their physical properties.

Publication Date: January 1, 1966 | doi: 10.1021/ba-1966-0054.ch012

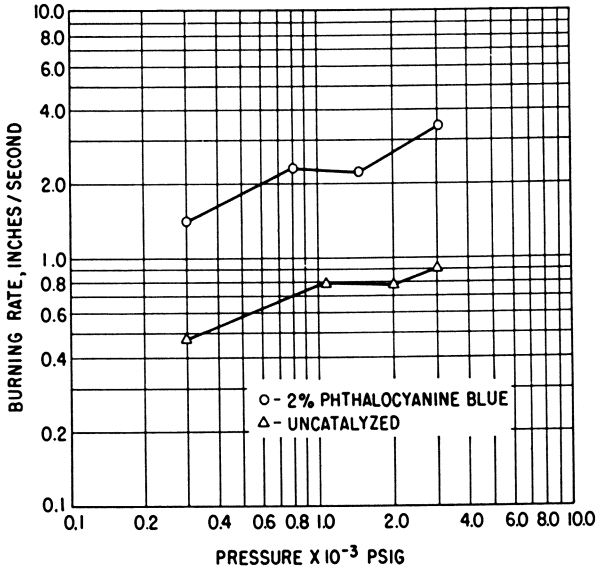

Figure 1. Burning rate of acetylenic polyurethane propellant compositions containing 80% ammonium perchlorate

Small Motor Firings

Although the program was primarily concerned with the synthesis and laboratory evaluation of these new propellant compositions, some practical confirmation of their theoretical performance was also desired. Consequently, a limited number of small motor firings were carried out.

Theoretical performance calculations were first made on propellant compositions containing the acetylenic polyurethane binder and ammonium perchlorate as the oxidant. These calculations assumed a shifting equilibrium in the rocket exhaust. The calculations demonstrated two of the principal advantages of the acetylenic binders—namely the increased performance provided by the energetic triple bond and the fact that optimum performance is achieved at relatively low levels of oxidizer. Specific impulse values of 251–253 lbf.-sec./lbm. were calculated at 1000 p.s.i.a. chamber pressure for optimum oxidizer loadings. Furthermore, peak performance was achieved at 83% oxidizer, and even at an 80% loading a theoretical I_{sp} of 250 seconds was obtained.

For the actual compositions tested, the theoretical values were somewhat lower than optimum. In all, 18 acetylenic polyurethane propellant grains were test fired in small motors. These ranged in weight from 0.40 to 6 lb. and included both 3-inch and 6-inch diameter end-burning grains. Motor firings are reported in Table III for a 77.8% oxidizer-loaded composition having a theoretical I_{sp} of 249 seconds. These can be compared

Table III. Summary of

Test No.	Oxidizer Loading Wt. %	Grain Configuration	Grain Weight lb.	Motor diameter in.	Burning Time sec.
A. OGK Propellant[a]					
8AX166	OGK	double end	0.5	3	3.69
3611	OGK	double end	0.5	3	4.03
3619	OGK	double end	0.5	3	3.61
3608	OGK	internal-external	8.0	6	3.62
B. Polypropylene Glycol Propellant					
157	77.5	single end	0.8	3	7.8
158	77.5	single end	0.7	3	6.62
158a	77.5	single end	0.7	3	6.62
159	77.5	single end	0.7	3	6.6
160	80.0	single end	0.7	3	5.45
161	80.0	single end	0.7	3	5.28
164	80.0	single end	0.7	3	5.50
162	82.5	single end	0.8	3	4.39
165	82.5	single end	0.7	3	3.67
C. Acetylenic Polyurethane Propellant					
3636	77.8	single end	0.6	3	3.05
3637	77.8	single end	0.7	3	2.52
3638	77.8	single end	0.8	3	3.22
3640	77.8	internal-external	3.9	6	1.97

[a] Allegany Ballistics Laboratory, Propellant Powder Manual, M-2. Chemical Propulsion Information Agency, The Johns Hopkins Applied Physics Laboratory, Silver Spring, Md., Unit No. 131 (1955).

with data from calibration runs carried out on two standard propellants, an OGK (double base) composition, and a polypropylene glycol (PPG) composite propellant. The efficiencies obtained with the acetylenic polyurethane propellant were reasonable for motors of this size, and averaged about half-way between those for the two standard propellants, demonstrating that the performance improvement indicated by the theoretical calculations could be achieved. No motor tests were performed on aluminized systems.

Experimental

Molecular weights were determined cryoscopically in ethylene bromide or benzene.

Poly(2-butyne-1,4-dioxymethylene). FROM DI-*n*-PROPYL FORMAL. A three-necked, round-bottomed flask, fitted with a gas inlet tube, a mechanical stirrer, and a graduated Dean-Stark moisture trap with a condenser attached, was charged with 66 grams of di-*n*-propyl formal, 45

Publication Date: January 1, 1966 | doi: 10.1021/ba-1966-0054.ch012

Propellant Motor Test Data

Average Chamber Pressure p.s.i.g.	*Average Thrust lb.*	I_{sp} *sec.* (q = 0; p = 1000 *p.s.i.a*(*S.L.*))	I_{sp} (*Theory*)	*Efficiency %*	C^a *ft./sec.* (p = 1000 (q = 0) *p.s.i.a.*(*S.L.*))	
941	18.3	183	205	89.3	3900	1.51
917	12.7	190	205	92.7	4223	1.45
900	16.8	183	205	89.3	4017	1.46
968	311	185.5	205	90.5	4164	1.43
			Av.	90.5		
683	17.6	207.8	227	91.5	4844	1.33
736	16.5	202.6	227	89.4	4374	1.45
736	16.5	202.6	227	89.4	4655	1.36
948	19.3	215.6	227	95.2	4954	1.40
			Av.	91.2		
1110	23.2	220.3	237	92.8	4991	1.43
1132	24.0	223.9	237	94.4	5037	1.44
1114	23.4	221.7	237	93.5	5113	1.38
			Av.	93.5		
1229	30.8	226	241.5	93.7	5253	1.38
1025	28.3	221.8	241.5	91.8	5009	1.4
			Av.	92.7		
840	33.6	229	249	92.0	5009	1.47
1053	13.1	225	249	90.4	4951	1.46
851	34.9	226	249	90.8	4853	1.50
750	100	229	249	92.8	5109	1.44
			Av.	91.5		

grams of 2-butyne-1,4-diol, and 0.5 grams of *p*-toluenesulfonic acid. A slow stream of nitrogen was passed through the system via the gas inlet tube to aid in entraining the byproduct, *n*-propyl alcohol, and the mixture was heated in an oil bath. When it became sufficiently fluid, the mixture was stirred mechanically and was heated for 2–3 hours at 125°–150° C. During this time 70–75 ml. of *n*-propyl alcohol were distilled into the Dean-Stark trap. The mixture then was heated for another 3 hours under reduced pressure (1–3 mm.). Traps cooled with dry ice-acetone were placed in the system to collect any additional alcohol formed in the reaction. An additional 5–15 ml. of *n*-propyl alcohol were isolated during this heating cycle. The reaction mixture then was allowed to cool. The product, a waxy solid weighing 46 grams, melted at 60° C. and represented a 90% yield. Its molecular weight, based on the freezing point depression in ethylene bromide, was 680. Analysis showed: calculated for $C_5H_6O_2$: C, 61.26; H, 6.75. Found: C, 60.76; H, 6.75.

The reaction described above was repeated, except that polyphosphoric acid was used as the catalyst, and a longer reaction time (9 hours)

Publication Date: January 1, 1966 | doi: 10.1021/ba-1966-0054.ch012

and higher temperature (130°–180° C.) were employed. A quantitative yield of a polymer in the form of a dark brown, waxy solid, m.p. 55° C., with a molecular weight of 1020 (determined cryoscopically), was obtained. Found: C, 60.44; H, 6.58.

FROM DI-*n*-BUTYL FORMAL. When 2-butyne-1,4-diol and di-*n*-butyl formal were allowed to react as described above, in the presence of a catalytic amount of *p*-toluenesulfonic acid at temperatures up to 190° C., nearly two equivalents of *n*-butyl alcohol distilled off. The product was a mushy, light brown solid of molecular weight 475, as determined cryoscopically in benzene.

FROM PARAFORMALDEHYDE. A three-necked, 300-ml. flask was equipped with a thermometer, mechanical stirrer, and Dean-Stark trap with a condenser attached. The flask was charged with 130 grams of toluene and 43 grams of 2-butyne-1,4-diol. Paraformaldehyde (15 grams) and 0.5 grams of *p*-toluenesulfonic acid were added portionwise to the mixture, over a 3.5-hour period. After adding the first portion of paraformaldehyde and catalyst, the mixture was heated to reflux temperature (100°–110° C.). During the reaction, nearly 9 ml. of water were collected in the Dean-Stark trap. The reaction mixture was allowed to cool, and the toluene was decanted from the solid polymer, which had separated from the solution. The polymer then was heated at 80°–115° C. for 4 hours under a vacuum of 1–2 mm. A yield of 46 grams (94%) of a hard, waxy polymer, of molecular weight 2300, was obtained.

Poly(2-butyne-1,4-dioxyethylidene). A 250-ml., three-necked flask equipped as in the first example, was charged with 130 grams of benzene, 22 grams of 2,4-hexadiyne-1,6-diol, and 6.1 grams of paraformaldehyde. *p*-Toluenesulfonic acid (0.2 gram) was added, and the mixture was heated at reflux temperature for 3 hours. Approximately 3.0 ml. of water distilled into the Dean-Stark trap during this time. The mixture was allowed to cool, and the benzene was decanted from the solid polymer. The polymer then was heated for 3 hours at 90°–100° C. under a vacuum (2–3 mm.). The product was a dark-colored, waxy solid, melting at 70°–75° C. and had a molecular weight of 810.

Poly(2-butyne-1,4-dioxyethylidene). A 250-ml., three-necked flask equipped as in the first example, was charged with 43 grams of 2-butyne-1,4-diol, 73 grams of di-*n*-propyl acetal, and 0.5 gram of *p*-toluenesulfonic acid. The mixture was heated at 125°–150° C. for 3 hours at atmospheric pressure under a slow stream of nitrogen, during which time 65 ml. of *n*-propyl alcohol were collected. The reaction mixture then was heated for an additional 4 hours at 1–3 mm. pressure, and an additional 10 ml. of *n*-propyl alcohol were isolated. The product, obtained in quantitative yield, was a viscous, dark-brown liquid. Its molecular weight was 920 as determined cryoscopically in ethylene bromide.

Publication Date: January 1, 1966 | doi: 10.1021/ba-1966-0054.ch012

Poly(2-butyne-1,4-dioxy-2′-ethylbutylidene). A 500-ml., three-necked, round-bottomed flask, equipped as in the first example, was charged with 43.0 grams of crude 2-butyne-1,4-diol, 0.5 gram of *p*-toluenesulfonic acid, and 250 ml. of benzene. The mixture was heated to 60° C., and 50.1 grams of 2-ethylbutyraldehyde were added. The theoretical amount of water was collected by azeotropic distillation during an 8-hour heating period at 75°–82° C. To remove the acid catalyst, a mildly basic ion exchange resin, Amberlite IR-45 (10 grams) was added, and the mixture was stirred at room temperature for 2–3 hours. The resin and other insoluble impurities then were filtered off, and benzene was distilled from the remaining product during a 5-hour heating period at 80°–90° C./2–15 mm. A dark, viscous liquid, having a molecular weight of 620, was obtained.

Calorimetry. Polymer samples were ground in a Wiley mill, screened through a 100-mesh sieve, and vacuum dried at 35° C. for 15–20 hours. The samples were then pressed into cylindrical $^1/_2 \times {}^3/_8$-inch pellets at 40,000 p.s.i.g. The pellets were then placed in a tared porcelain crucible and weighed. The crucible containing the sample was placed in the bomb of a Parr adiabatic calorimeter, and the sample was burned at an oxygen pressure of 450 p.s.i.g. at 25° C. The heats of combustion of the polymer samples were obtained by applying the following corrections to the experimental values:

Bomb Pressure Correction. Any change in the operating pressure of the combustion bomb results in a change in the water equivalent (heat capacity) of the calorimeter. However, the difference is less than 1 cal./° C. when operating in the 15–450 p.s.i.g. range of pressure and is therefore negligible.

Thermometer Scale Correction. An NBS thermometer was used for the adiabatic jacket and a Beckmann differential thermometer for the calorimeter water. The Beckmann thermometer was calibrated against the NBS thermometer. Corrections were made to the initial and final temperatures recorded on the Beckmann thermometer.

Radiation Corrections. Since the calorimeter was adiabatic, radiation losses were considered to be negligible and no corrections were required.

Fuse Wire Correction. This correction is made by measuring the length (in cm.) of wire burned and multiplying it by the known heat of combustion per centimeter of the wire (2.8 cal./cm).

Conversion of ΔE to ΔH. Since the actual thermochemical measurements were made in a closed bomb at constant volume, it was necessary to convert the increase in the energy content at constant volume, ΔE, to that at constant pressure, ΔH, where ΔH represents the heat of reaction to the products at standard conditions. The difference between these two

quantities is equal to $P\Delta V$, which is the work of expansion when the process is carried out at constant pressure. $P\Delta V$ is equal to $RT\Delta n$, where Δn is the difference between the number of moles of carbon dioxide formed and the number of moles of oxygen required for combustion of the fuel.

The corrected experimental and the theoretical heat of combustion data are tabulated below. Theoretical heats of combustion were calculated by conventional methods using heats of formation for the acetylenic polymers which were calculated by the method of group contributions (*2, 6*).

Polymer Structure	*Mol. Wt.*	*Heat of Combustion (kcal./gram)* *Exp.*	*Theor.*	*% of Theory*
$H(OCH_2OCH_2C{\equiv}CCH_2O)_{10}OH$	1074	6.512	6.504	100.13
$H(OCH_2OCH_2C{\equiv}CCH_2O)_{20}OH$	2370	6.417	6.540	98.04

Polyurethanes from Poly(2-butyne-1,4-dioxymethylene). REACTION WITH 2,4-TOLUENE DIISOCYANATE. A sample of polyformal of molecular weight 1915 (95.7 grams, 0.05 mole) was melted in a 500-ml. beaker, and 1.34 grams (0.01 mole) of trimethylolpropane (TMP) were added. The mixture was heated to 80° C., agitated thoroughly, and then degassed at 80° C./5 mm. in a vacuum oven. After cooling to 50° C., 13.05 grams (0.075 mole) of 2,4-toluene diisocyanate (TDI) were added and the mixture was again heated to 80° C. and thoroughly mixed. It was then cast into a Teflon-coated mold, degassed at 80° C./5 mm. again for 1 hour, and cured at 80° C. for 20 hours. The physical properties of the resulting polyurethane are given in Table I (sample 1).

REACTION WITH HEXAMETHYLENE DIISOCYANATE. The above procedure was repeated using 12.60 grams (0.075 mole) of hexamethylene diisocyanate (HDI) instead of TDI. The physical properties of the product are listed in Table I (sample 2).

When the same procedure was repeated with 60 grams (0.05 mole) of polyformal prepolymer of molecular weight 1180, a polyurethane with similar physical properties was obtained (sample 3, Table I).

PREPARATION OF PLASTICIZED POLYURETHANE COMPOSITIONS. The procedure given immediately above was repeated, except that 10.5 grams of butylcyclohexyl phthalate (BCPH) were added to the original mixture as a plasticizer, and 0.5 gram of di-*p*-phenylphenylenediamine and 0.05 gram of ferric acetonylacetonate were used as catalysts. The properties of the resulting cured polymer are given in Table I (sample 4).

The above procedure was repeated using 95.7 grams (0.05 mole) of the 1915-molecular weight prepolymer and 9.18 grams (0.01 mole) of castor oil as the cross-linking agent. Physical properties are listed under sample 5 in Table I.

Publication Date: January 1, 1966 | doi: 10.1021/ba-1966-0054.ch012

Propellant Processing. Propellant compositions were mixed in a sigma blade mixer at a temperature sufficient to maintain a fluid mix (70°–80° C.). The order of adding the ingredients had little effect on the properties of the final propellant. Consequently, for safety reasons, all fuel ingredients except for the diisocyanate were blended first, and the ammonium perchlorate was added to this mix. The diisocyanate was then added portionwise to the remainder of the propellant mix. This procedure resulted in increased pot life. The most important factors in the propellant mixing were the mixing temperature and the mixing time. The mixing temperature was governed primarily by the temperature-viscosity relationships of the particular prepolymer batch.

Propellants containing up to 77.8% oxidizer were cast through a "bayonet" with $^1/_{16}$-in.–$^1/_8$-in. wide slits into an evacuated, vibrated mold. Propellant containing 80% oxidizer was cast by applying 20 p.s.i.g. nitrogen pressure to the casting feed can. The propellant and casting equipment were maintained at 70°–75° C. during casting. The measured densities of the propellants were 0.063, 0.061, and 0.058 lb./cu. in. for 80, 77.8, and 75 wt.% ammonium perchlorate, respectively. These densities represent 98.5, 97, and 95% of the theoretical densities. Grains were cured at 75°–80° C. for 16–44 hours. A satisfactory cure was generally obtained in 20 hours at 80° C.

Publication Date: January 1, 1966 | doi: 10.1021/ba-1966-0054.ch012

Acknowledgments

This work was supported by the U. S. Navy under Contracts NOrd 16575 and 17851. The authors wish to thank David J. Mann of these laboratories for his guidance and encouragement. The assistance of Edward Schonfeld in some phases of the synthetic work is also acknowledged.

Literature Cited

(1) Fieser, L. F., Fieser, M., "Organic Chemistry," 3rd. ed., p. 215, D. C. Heath and Co., Boston, 1956.
(2) Franklin, J. L., *Ind. Eng. Chem.* **41**, 1070 (1949).
(3) Hill, H. S., Hibbert, H., *J. Am. Chem. Soc.* **45**, 3117, 3124 (1923).
(4) Hill, J. W., Carothers, W. H., *J. Am. Chem. Soc.* **57**, 925 (1935).
(5) Picatinny Arsenal Technical Report No. 1401, Rev. 1 ,Feb. 28, 1950.
(6) Souders, M., Jr., Matthews, C. S., Hurd, C. O., *Ind. Eng. Chem.* **41**, 1048 (1949).

RECEIVED April 29, 1965.

13

Isotopic Exchange Reactions of Difluoramine with Deuterium Oxide and Trifluoroacetic Acid

WARREN E. BECKER and FRED J. IMPASTATO

Ethyl Corp., Baton Rouge, La.

Publication Date: January 1, 1966 | doi: 10.1021/ba-1966-0054.ch013

The isotopic exchange reactions of HNF_2 with D_2O and with CF_3COOD have been investigated in tetrahydrofuran-d_8 solution at low temperatures using NMR techniques. The former exchange is first order with respect to HNF_2 and zero order with respect to D_2O. The latter exchange proceeds by this same path plus a second-order path. Both exchange reactions were studied at several temperatures, and the activation energies were determined.

While investigating the mode of ionization of HNF_2, we had occasion to study the isotopic exchange of hydrogen between HNF_2 and D_2O. Although the literature contains two references (*2*, *9*) to this exchange reaction, no attempt to determine the mechanism of exchange was made in either of these investigations. When we learned that the exchange is acid catalyzed, our study was extended to include the exchange of hydrogen between HNF_2 and CF_3COOD. Tetrahydrofuran-d_8 was used as solvent in both of these studies. In addition, the ionic behavior of HNF_2 in H_2SO_4 was investigated by cryoscopic techniques. This paper reports the results of these investigations.

Experimental

Reagents. Difluoramine was prepared from tetrafluorohydrazine (Air Products, Inc.) and thiophenol by the method of Freeman, Kennedy, and Colburn (*3*). It was purified by fractional condensation in a high vacuum system and was stored in a borosilicate glass bulb attached to the vacuum line.

Deuterated trifluoroacetic acid was prepared by hydrolyzing a slight excess of trifluoroacetic anhydride with D_2O. The product was purified by distillation and stored under vacuum in sealed glass ampoules until needed. The isotopic purity was estimated from NMR measurements to be at least 95%.

In Advanced Propellant Chemistry; Holzmann, R.;
Advances in Chemistry; American Chemical Society: Washington, DC, 1966.

Deuterium chloride was prepared by hydrolyzing acetyl chloride with excess deuterium oxide. The product was purified by fractional condensation in a high vacuum system and was stored in a borosilicate glass bulb attached to the vacuum manifold.

Tetrahydrofuran-d_8 and D_2O, both of 98% isotopic purity, were purchased from Merck, Sharp, and Dohme of Montreal. The tetrahydrofuran-d_8 was dried by distillation over $NaAlH_4$ and was stored in sealed glass ampoules until used.

Cryoscopic Studies. In general, the techniques developed by Gillespie (5) were used. The apparatus was modified in order that adding HNF_2 as well as measuring the freezing point could be carried out under vacuum. Acetone was used to check the apparatus and the procedure. The average of four determinations was 29.0 ± 1.3. Since acetone accepts a proton from H_2SO_4 to form $CH_3COHCH_3^+$ and HSO_4^-, the experimentally determined molecular weight should be one-half the theoretical value, or 29.0.

The following procedure was used. Fuming sulfuric acid was weighed into the apparatus and titrated with water until the maximum freezing point, measured with a Beckmann thermometer, was just passed. The apparatus was allowed to stand overnight to allow desorption of water from the walls. The apparatus was evacuated and degassed, and the freezing point was determined. Increments of HNF_2 were measured out in a calibrated portion of the vacuum system and allowed to diffuse into the apparatus. The freezing point was determined after each addition.

Kinetic Experiments. Kinetic data were obtained by NMR techniques. In general the intensity of the H_2O (or CF_3COOH) peak was followed as a function of time with a Varian A-60 NMR analytical spectrometer. The instrument was equipped with a variable temperature probe and a V-6040 temperature controller capable of maintaining temperatures as low as −60° C. with a precision of ±1° C.

A ground-glass joint was sealed onto the open end of an NMR tube so that the tube could be attached to the vacuum line. A small bulb of about 1 ml. volume was blown at the point where the glass joint was sealed to the NMR tube to facilitate mixing. The tube was dried overnight in an oven at 150° C., then evacuated, cooled, filled with nitrogen, stoppered, and weighed on an analytical balance. Deuterium oxide was placed in the tube with a syringe, and the tube was reweighed. The solvent, tetrahydrofuran-d_8, was added in the same manner, and the tube was weighed again.

The tube was then attached to the vacuum line, frozen, and degassed. Difluoramine was measured out in a calibrated portion of the vacuum system and was condensed into the tube at −128° C. (methylcyclohexane slush), and the tube was then sealed off with a torch just above the small bulb. Trifluoroacetic acid, when used, was measured out as a gas in the vacuum system and condensed into the tube just before the HNF_2 was added.

The contents of the tube were thoroughly mixed; the tube was then inserted into the precooled probe of the NMR spectrometer, and a stop watch was started.

At preselected time intervals the proton spectrum was scanned. By using a sweep time of 50 sec. and scanning only that spectrum portion of

Publication Date: January 1, 1966 | doi: 10.1021/ba-1966-0054.ch013

interest, points could be obtained at 30-sec. intervals. The exchange at infinite time, t_∞, was obtained by removing the tube from the probe and allowing it to stand at room temperature for 5–10 minutes. It was then put back into the probe, and the spectrum was run 10 times in order to assure a good t_∞ value. The temperature was determined before and after a run by calibrating with methanol and was found to be constant to within ±1° C.

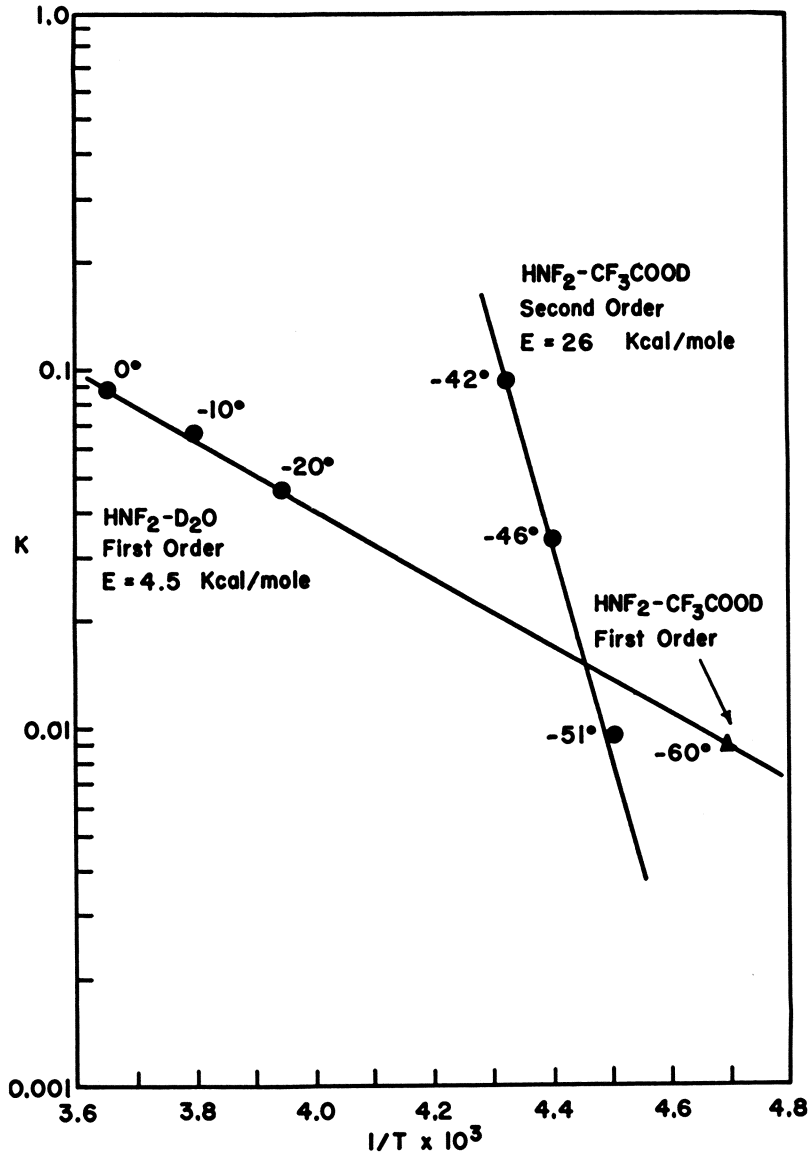

Figure 1. Plot of log (1-F) vs. t for HNF_2-D_2O exchange

Publication Date: January 1, 1966 | doi: 10.1021/ba-1966-0054.ch013

Calculations

The areas of the H_2O, CF_3COOH, and tetrahydrofuran peaks were measured by the method of triangulation (peak height times width at half-peak height). One of the tetrahydrofuran peaks (the deuterated tetrahydrofuran contains about 2% of the protonated material) was used as an internal standard. All peak areas were corrected to a standard peak area for tetrahydrofuran. In this way instrument errors owing primarily to changes in the field were compensated.

The fraction exchange F at time t was calculated by dividing the area of the H_2O (or CF_3COOH) peak at time t by the value at infinite time t_∞. A plot of log (1-F) *vs.* t is linear as shown in Figure 1. Since the plot is linear, we may use the rate expression derived by McKay (*10, 11*) and ignore isotope effects. These effects are fully discussed by Harris (*6*) and by Bunton, Craig, and Halevi (*1*). The best straight line was determined by the method of least squares, and the half-time of exchange, $t_{1/2}$, was calculated from the slope.

The rate of exchange (*4*) R was calculated from

$$R = \frac{ab}{a+b}\,\frac{\ln 2}{t_{1/2}}$$

where a and b are the total molar concentrations of HNF_2 and H_2O (or CF_3COOH). In the case of H_2O the molar concentrations must be multiplied by 2 since there are two hydrogen atoms per molecule. (For a discussion of the definition of R, its determination, the relationship be-

Table I. Summary of HNF_2-D_2O Exchange Runs

Conc., moles/liter		$t_{1/2}$, min.	R, moles liter^{-1} min.$^{-1}$	K, min.$^{-1}$	T, ° C.
$[D_2O]$	$[HNF_2]$				
1.27	1.28	9.2	0.064	0.050	−20
1.40	0.69	11.3	0.034	0.049	−20
1.91	1.16	9.8	0.063	0.054	−20
1.38	2.08	10.3	0.080	0.038	−20
1.31	1.87	10.3	0.073	0.039	−20
1.04	0.28	14.1	0.012	0.043	−20
2.64	1.73	15.2	0.046	0.036	−20
0.50	2.73	3.5	0.146	0.053	−20
0.25	2.79	2.9	0.102	0.037	−20
			Av.	0.044 ± 0.006	
1.97	1.02	11.8	0.048	0.047	−10
1.97	2.02	6.2	0.150	0.075	−10
2.80	2.03	6.7	0.157	0.076	−10
			Av.	0.066 ± 0.013	
2.82	1.38	5.3	0.144	0.105	0
1.36	1.52	6.3	0.107	0.070	0
			Av.	0.088 ± 0.017	

Publication Date: January 1, 1966 | doi: 10.1021/ba-1966-0054.ch013

tween R, the rate constant K, and the order of reaction with respect to the reactants, *see* Friedlander and Kennedy (*4*).)

The activation energy was calculated from the Arrhenius equation while the entropy of activation was obtained from the Eyring equation.

Results and Discussion

Difluoramine-Deuterium Oxide Exchange. Table I summarizes the results of this investigation. The exchange is first order with respect to HNF_2 and zero order with respect to water. The mechanism proposed for this exchange is:

$$HNF_2 = H^+ + NF_2^- \quad \text{Slow}$$

$$H^+ + D_2O = D^+ + HDO \quad \text{Fast}$$

$$D^+ + NF_2^- = DNF_2 \quad \text{Fast}$$

where the rate-determining step is ionization of HNF_2.

Figure 2 shows the dependence of the rate constant on temperature. The activation energy is 4.5 ± 0.2 kcal./mole as calculated from the Arrhenius equation while the entropy of activation is —55e.u. as calculated from the Eyring equation. This large decrease in entropy is typical of ionic equilibria in nonaqueous systems. It has been suggested (*12*) that this entropy loss includes the change in entropy of the solvent molecules which surround the ions and which can be considered to be "frozen."

Finally, the experimental data are represented by the rate law:

$$R = 3.37 \times 10^2 e^{-(4500/RT)}(HNF_2)$$

where R is in units of gram atoms liter^{-1} min.$^{-1}$.

In order to test for acid catalysis, the exchange was run in the presence of CF_3COOH. At —20° C. the rate was too fast to measure, showing that the exchange is acid catalyzed.

Difluoramine-Trifluoroacetic Acid Exchange. Since the mechanism discussed above—namely the ionization of HNF_2, will also lead to exchange between HNF_2 and CF_3COOD, the total rate of exchange must include this path plus another path and would have the general form

$$R = K_1(HNF_2) + K_2(HNF_2)^a(CF_3COOD)^b$$

The contribution of this first-order path $K_1(HNF_2)$ can be subtracted from the total rate since K_1 has been evaluated separately for the HNF_2-D_2O exchange. Both a and b have a value of unity as shown in Table II, which summarizes the data.

At —60° C. the exchange is first order for all practical purposes. The first-order rate constant lies on the same line as the values calculated at —20°, —10°, and 0° C. for the HNF_2-D_2O exchange. This is shown

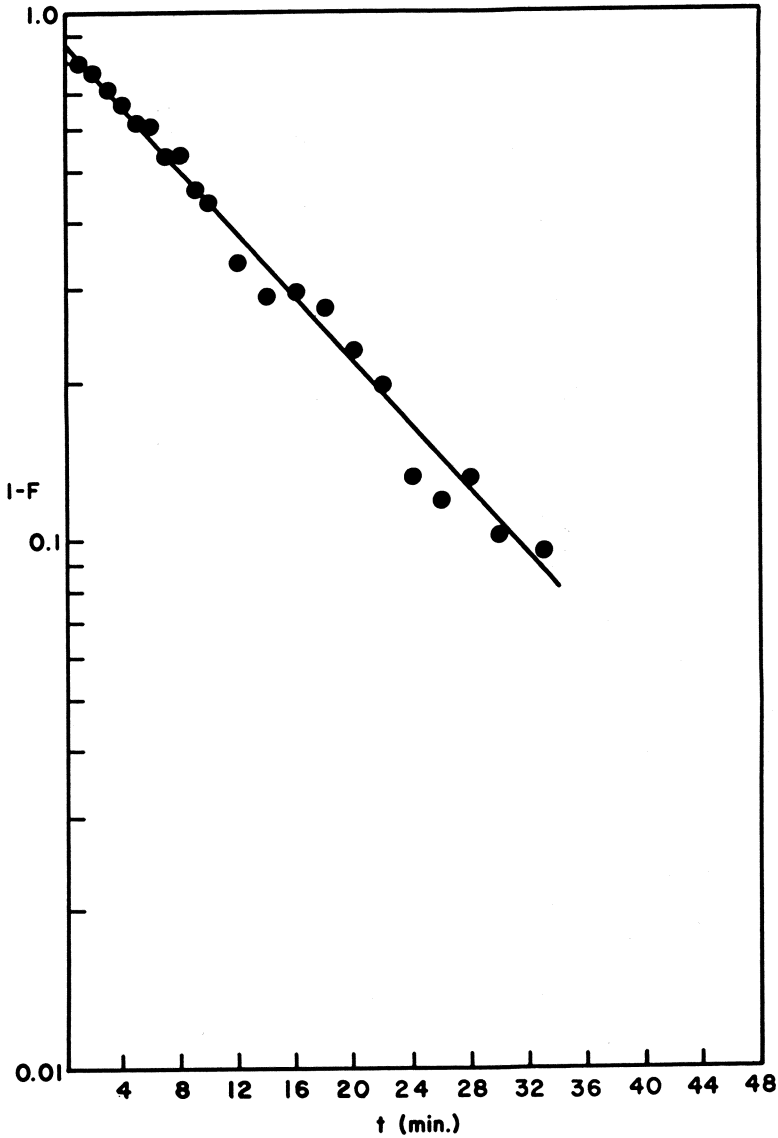

Figure 2. Temperature dependence of rate constants

in Figure 2 and further proves that the same mechanism is involved in both these exchange reactions.

At —42° C. the exchange proceeds predominantly by a second-order path while at the intermediate temperatures (—46° and —51° C.) both paths make appreciable contributions. The activation energy calculated

Table II. Summary of

Conc., moles/liter		$t_{1/2}$, min.	R moles liter^{-1} min.$^{-1}$	R from 1st-order path
$[HNF_2]$	$[CF_3COOD]$			
1.53	0.95	30.5	0.0133	
1.56	1.98	46.0	0.0131	
1.50	1.50	36.4	0.0143	
1.47	0.75	30.1	0.0114	
0.81	1.45	39.3	0.0092	
0.72	1.52	74.4	0.0046	
1.56	1.84	1.86	0.315	0.031
0.78	1.76	2.75	0.136	0.015
0.83	0.47	3.98	0.052	0.016
1.02	2.00	7.2	0.065	0.017
0.96	0.98	8.5	0.040	0.016
2.05	1.01	4.4	0.107	0.034
0.96	1.98	4.3	0.104	0.016
1.43	0.75	18.1	0.0188	0.0190
1.52	1.50	12.6	0.0415	0.0202
0.83	0.75	27.3	0.0100	0.0110

for the second-order reaction is 26 kcal./mole; however, owing to the short temperature range investigated and to the poor temperature control, this value has an uncertainty of several kcal.

There are two possible mechanisms for the second-order exchange—namely, the protonation of HNF_2 and complex formation. The protonation path can be represented by:

$$HNF_2 + CF_3COOD \rightleftharpoons HDNF_2^+ + CF_3COO^- \qquad \text{Slow}$$

$$HDNF_2^+ \rightleftharpoons H^+ + DNF_2 \qquad \text{Fast}$$

$$H^+ + CF_3COO^- \rightleftharpoons CF_3COOH \qquad \text{Fast}$$

and the complex formation path by:

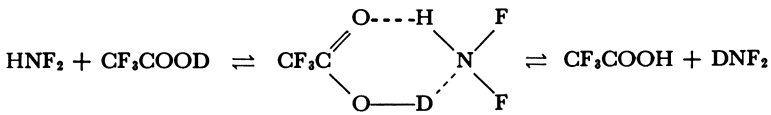

To obtain data supporting one or the other of these mechanisms, the exchange of hydrogen between HNF_2 and DCl was briefly investigated. If this exchange were second order as expected, the same two paths would be available as for the HNF_2-CF_3COOD exchange. However, if HNF_2 and DCl form a 1:1 complex, it would be a four-membered ring

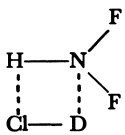

HNF_2-CF_3COOD Exchange Runs

R from 2nd-order path	*2nd order K, liter mole^{-1} min.$^{-1}$*	*1st Order K, min.$^{-1}$*	*T, °C.*
		0.0087	−60
		0.0084	−60
		0.0095	−60
		0.0078	−60
		0.0113	−60
		0.0063	−60
		Av. 0.0087 ± 0.012	
0.284	0.099		−42
0.121	0.088		−42
0.036	0.092		−42
	Av. 0.093 ± 0.004		
0.048	0.024		−46
0.024	0.026		−46
0.073	0.035		−46
0.088	0.046		−46
	Av. 0.033 ± 0.008		
...			−51
0.0213	0.0094		−51
...			−51

Table III. Molecular Weight Determination of HNF_2 in H_2SO_4

Run No.	*H_2SO_4 (g)*	*Mmoles HNF_2*	*Δt*	*M*	*Mmoles HNF_2 cumulative*	*Δt cumulative*	*M*
I		1.04	0.036	47.7			
	192.9	0.91	0.025	60.0	1.95	0.061	52.7
		1.30	0.040	53.6	3.25	0.101	53.1
				Av. 53.8			
II		1.75	0.055	50.4			
	201.4	2.15	0.070	48.7	3.90	0.125	49.4
		2.81	0.080	55.7	6.71	0.205	51.8
				Av. 51.6			

instead of a six-membered ring. Since the HNF_2-D_2O exchange does not proceed through the 1:1 complex which also contains a four-membered ring, we would expect exchange via this path to be slower than for the HNF_2-CF_3COOD case.

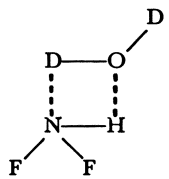

On the other hand, HCl (*7*) is a stronger acid than CF_3COOH (*8*), having a dissociation constant of 22 compared with 1.8, and should exchange faster than CF_3COOH via a protonation mechanism.

In a single run, we found that the HNF_2-DCl exchange is too fast to follow even at —60° C. The evidence, then, seems to favor the protonation mechanism.

In order to determine whether there is any gross protonation or ionization, the molecular weight of HNF_2 in H_2SO_4 was measured by cryoscopic techniques. The results are shown in Table III. Within experimental error, HNF_2 is monomeric in H_2SO_4, and the extent of ionization or protonation is too slight to measure. Both exchange reactions, HNF_2-D_2O and HNF_2-CF_3COOD, can proceed through only a small amount of ionization or protonation.

Acknowledgment

The support of the Advanced Research Projects Agency, Washington, D. C. 20330, and the Air Force Rocket Propulsion Laboratory, Research and Technology Division, Edwards Air Force Base, Calif., Air Force Systems Command, U.S. Air Force, under whose sponsorship this work was conducted, is gratefully acknowledged.

Literature Cited

(1) Bunton, C. A., Craig, D. P., Halevi, E. A., *Trans. Faraday Soc.* **51**, 196 (1955).
(2) Comeford, J. J., Mann, D. E., Schoen, L. J., Lide, D. R. Jr., *J. Chem. Phys.* **38**, 461 (1963)
(3) Freeman, J. P., Kennedy, A., Colburn, C. B., *J. Am. Chem. Soc.* **82**, 5304 (1960).
(4) Friedlander, G., Kennedy, J. W., "Nuclear and Radiochemistry," p. 315, John Wiley and Sons, New York, 1955.
(5) Gillespie, R. J., *J. Chem. Soc.* **1950**, 2493.
(6) Harris, G. M., *Trans. Faraday Soc.* **47**, 716 (1951).
(7) Hood, G. C., Redlich, O., Reilly, C. A., *J. Chem. Phys.* **22**, 2067 (1954).
(8) Hood, G. C., Redlich, O., Reilly, C. A., *J. Chem. Phys.* **23**, 2229 (1955).
(9) Lide, D. R. Jr., *J. Chem. Phys.* **38**, 456 (1963).
(10) McKay, H. A. C., *Nature* **142**, 997 (1938).
(11) McKay, H. A. C., *J. Am. Chem. Soc.* **65**, 702 (1943).
(12) Wynn-Jones, W. F. K., Eyring, H., *J. Chem. Phys.* **3**, 492 (1935).

RECEIVED April 19, 1965

14

Reactions of Difluoramine with Lewis Acids

J. N. KEITH, R. J. DOUTHART,[1] W. K. SUMIDA, and I. J. SOLOMON

IIT Research Institute, Chicago, Ill.

Publication Date: January 1, 1966 | doi: 10.1021/ba-1966-0054.ch014

The acid-base chemistry of difluoramine, HNF_2, and its methyl derivative is being studied to establish the existence of difluorammonium compounds and to obtain new oxidizers containing difluoramino groups. The protic acids, hydrogen chloride and trifluoroacetic acid, do not form compounds with difluoramine in the condensed state; methyldifluoramine, however, may form a weak complex with hydrogen chloride. Trimethylaluminum, a strong Lewis acid, reacts with difluoramine liberating methane. The postulated intermediate, has not yet been isolated. Although trimethylgallium and difluoramine do not form a compound at low temperatures, methane is slowly evolved. Both difluoramine and methyldifluoramine form 1:1 adducts with sulfur trioxide. NMR analysis of the difluoramine adduct indicates that the proton and fluorine atoms are no longer adjacent, possibly indicating that it is difluoramidosulfamic acid.

Craig (2) has recently reported the results of studying the reactions of several nitrogen-fluorine compounds with Lewis acids. As expected he found that all the compounds he studied were extremely weak bases, difluoramine and its methyl derivative being among the strongest. Here we report some of our data on the reactions of the latter compounds with other strong acids.

To obtain new nitrogen-fluorine type oxidizers, we have been studying the possibility of preparing difluorammonium salts and introducing difluoramino groups into compounds of light metals such as $Al(NF_2)_3$. To this end, the reactions of difluoramine and methyldifluoramine with certain acids have been studied.

[1] Present address: University of Illinois, Urbana, Ill.

In Advanced Propellant Chemistry; Holzmann, R.;
Advances in Chemistry; American Chemical Society: Washington, DC, 1966.

Experimental

Apparatus and Materials. A standard Stock-type high vacuum line was used, except for experiments with SO_3 or CH_3NF_2. In these cases stopcocks lubricated with Kel F-90 grease were used, and pressures were measured with a Bourdon gage.

The commercially available materials, HCl, $(CH_3)_3Al$, and CF_3CO_2H, were purified by trap-to-trap distillation in the vacuum line. SO_3 was generated as needed by passing the vapors from a sample of Sulfan B over a P_2O_5 column. Trimethylgallium was prepared by the reaction of gallium with dimethylmercury at 130° C. Difluoramine was prepared by the thiophenol reduction of tetrafluorohydrazine (*3*). Methyldifluoramine was obtained by fluorinating sodium *N*-methyl sulfamate.

Pressure Composition Studies. Pressure composition studies were performed in small, calibrated U-traps fitted with a manometer or Bourdon gage. A measured sample of the less volatile component was condensed in the trap, and successive small amounts of the more volatile component added. The trap was then brought to the appropriate temperature and allowed to equilibrate until the pressure became constant (usually 15–30 minutes were required). The data were plotted *vs.* the composition of the liquid phase. The results are summarized in Table I.

Table I. Pressure-Composition Studies

System	*Temperature ° C.*	*Result*
HNF_2–HCl	−112 to −138	Miscible, with positive deviations
CH_3NF_2–HCl	−95, −112	Miscible, with negative deviations
	−127	Slight plateau up to 0.5 more fraction HCl, P = 6 mm.
HNF_2–CF_3CO_2H	−45.2	Solid, slightly soluble in HNF_2
	−63.5	Components readily separated by distillation
HNF_2–SO_3	0	Minimum 14 mm. at 0.4 mole fraction HNF_2, inflection at 0.5, homogeneous liquid 0–0.6
CH_3NF_2–SO_3	−63.5	Slight solubility
	−45.2	1:1 adduct v.p., 30 mm. m.p., −10° C.
HNF_2–$(CH_3)_3Al$	−80	1:1 adduct slowly loses CH_4
	25	2 moles HNF_2 consumed, yielding 2 CH_4
CH_3NF_2–$(CH_3)_3Al$	−80	1 mole HNF_2 + 1 $(CH_3)_3Al$ gave 2 CH_4 + HCN
HNF_2–$(CH_3)_3Ga$	−78.5, −45.2	Solution positive deviation, CH_4 at room temperature

The HNF_2–SO_3 System. Because of the corrosive nature of sulfur trioxide and the tendency of the low melting form to undergo transition to more highly polymerized forms, it is a rather difficult material to use in an equilibrium process. It was not possible to obtain reproducible saturation pressures for this system by adding HNF_2 to SO_3 at low temperatures. However, at 0° C. a liquid was obtained over the whole composition range studied (up to $x = 0.6$ mole fraction), and equilibrium could be obtained, although slowly. The pressure-composition diagram (Figure 1) shows a minimum at $X_{HNF_2} = 0.4$, and an inflection at about 0.5, with a sharp increase in pressure beyond that. Possibly, a 2:1 as well as a 1:1 compound is formed.

The proton and F^{19} NMR spectra of the 1:1 mixture without solvent at 0° C. indicated only single frequencies for hydrogen and fluorine,

Publication Date: January 1, 1966 | doi: 10.1021/ba-1966-0054.ch014

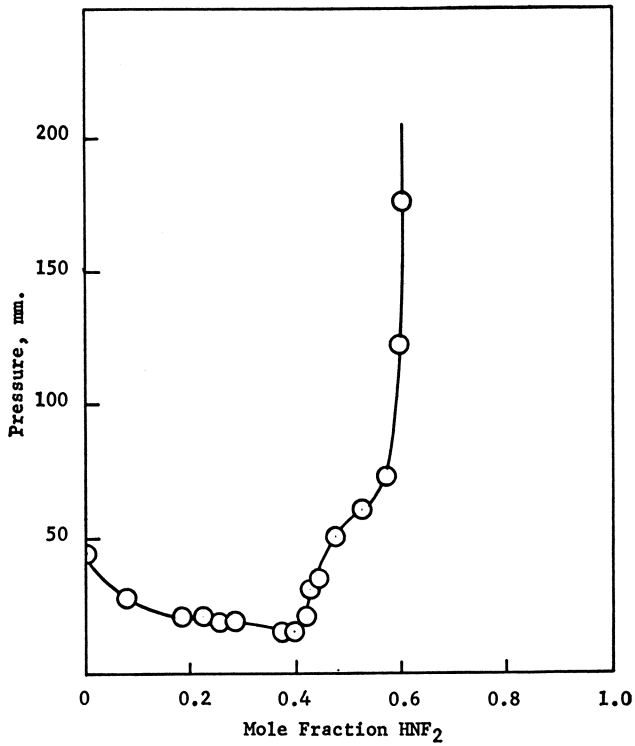

Figure 1. The HNF_2–SO_3 system at 0°C.

neither of which was split, indicating that the hydrogen is no longer on the nitrogen atom. These observations are consistent with the structure F_2NSO_2OH but not with the coordination compound, $HNF_2{:}SO_3$.

Slow decomposition of the product occurs at room temperature, the volatile products being N_2F_4 and SO_2. The reaction is probably the following:

$$2\ NF_2SO_2OH \rightarrow N_2F_4 + SO_2 + H_2SO_4 \qquad (5)$$

The HNF_2–$(CH_3)_3Al$ System. When attempts were made to study the pressure-composition curve of this system at —80° C. explosions occurred whenever liquid HNF_2 was present. However, no explosions occurred with gaseous difluoramine at low pressures. Several attempts were made to obtain a pressure-composition curve by adding very small amounts of HNF_2, but even under these conditions methane was slowly evolved. The following procedure was used to determine the stoichiometry of the reaction: 19.3 cc. HNF_2 were condensed in the tip of a small reactor, and 7.7 cc. of $(CH_3)_3Al$ (calculated as monomer) were condensed in a ring above it. The mixture was thawed to —80° C. for 30 min. during which the pressure rose to 45 mm. (v.p. of HNF_2 = 25 mm.); 2.3 cc. of methane (v.p., 10 mm. at —196° C.) and 14.2 of difluoramine (v.p., 1 mm. at —127° C.) were obtained by distillation from the reactor at —80° C. An additional 2.5 cc. of methane were obtained on thawing the

Publication Date: January 1, 1966 | doi: 10.1021/ba-1966-0054.ch014

reactor. Additional treatment with the recovered difluoramine produced further evolution of methane, as tabulated below:

$$HNF_2 + (CH_3)_3Al \rightarrow CH_4 + (Me_2AlNF_2)$$

19.3 cc.	7.7 cc.	
	30 min. −80° C.	2.3 cc.
−14.2 cc.	thawed	2.5 cc.
5.1 cc.		4.8 cc.
	overnight −80° C.	0.7 cc.
	thawed residue	0.9 cc.
	with HNF_2, 25° C., 2 hr.	2.2 cc.
19.3 cc.	with HNF_2, 25° C., overnight	6.2 cc.
−3.9 cc.	with HNF_2, 25° C., 3 days	0.5 cc.
15.4 cc.		15.3 cc.

When the methane production had essentially ceased, only 3.9 cc. of condensable gas remained, consisting of HNF_2 contaminated with a small quantity of N_2F_4 as shown by its infrared spectrum. Assuming this impurity to be negligible, the agreement is rather good: 15.4 cc. HNF_2 was consumed, producing 15.3 cc. of methane. This corresponds to the replacement of two methyl groups per aluminum atom ($2 \times 7.7 = 15.4$).

The product first formed at −80° C. was a clear, colorless, viscous liquid, and remained so at room temperature. On prolonged standing, however, it gradually changed to a pale yellow powder.

In a similar experiment, a mixture of 6.0 cc. $(CH_3)_3Al$ and excess HNF_2 were allowed to stand for 1 hour at −80° C., then overnight at 25° C. 12.7 cc. HNF_2 were consumed, yielding 12.9 cc. methane. The hydrolysis of the nonvolatile products of these reactions in neutral or acidic iodide solution liberated only traces of iodine but was accompanied by evolution of methane.

The HNF_2–$(CH_3)_3Ga$ System. HNF_2 and $(CH_3)_3Ga$ were combined in a small reactor and thawed. The reaction to form methane was very slow, about $^2/_3$ mole being produced overnight at room temperature. No explosion occurs, even in the presence of large excess of HNF_2. A preliminary pressure-composition study did not reveal an adduct at −78.5° or −45.2° C. Distillation of the mixture through a −80° C. trap separated the components almost completely in one pass.

Results and Discussion

Difluoramine, HNF_2, and methyldifluoramine, CH_3NF_2, form isolable complexes with BF_3, BCl_3, and SO_2, and in some cases dissociation data could be obtained. It is evident from Craig's work that usable thermodynamic data will be available only for the strongest acids. The problem is further complicated by the tendency for irreversible decomposition to occur in most of these systems. The acids chosen for this study included the protic acids, hydrogen chloride and trifluoroacetic acid, the alkyl metals, trimethylaluminum and trimethylgallium, and sulfur trioxide, one of the strongest, gaseous Lewis acids known. Pressure-composition studies were made of these systems to detect adduct formation or other condensed phase interactions.

Publication Date: January 1, 1966 | doi: 10.1021/ba-1966-0054.ch014

The pressure-composition diagrams of the difluoramine-protic acid systems did not indicate compound formation. HNF_2 was miscible in all proportions with HCl, with large positive deviations from Raoult's Law while CF_3CO_2H was partially soluble in HCl, giving an ideal solution. The stronger base, methyldifluoramine, was also miscible with HCl in all proportions, with large negative deviations from Raoult's Law. At the lowest temperature, —127° C., a plateau was obtained, indicating the formation of a weak 1:1 adduct.

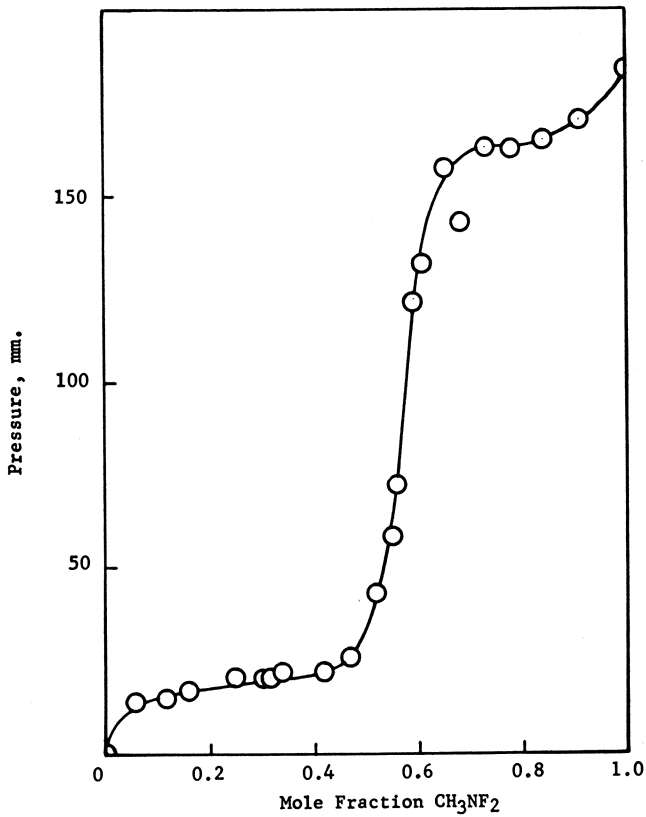

Figure 2. The CH_3NF_2–SO_3 system at —45.2°C.

The pressure-composition curves shown in Figures 1 and 2 indicate the formation of 1:1 adducts between SO_3 and the fluoramines. Contrary to what might be expected of the coordination compounds $HNF_2{\cdot}SO_3$ and $CH_3NF_2{\cdot}SO_3$, the HNF_2 adduct is much less volatile than the CH_3NF_2 adduct (although CH_3NF_2 is probably the stronger base). Furthermore, it was extremely difficult to obtain equilibrium pressures in the HNF_2 case, but no difficulty was experienced with CH_3NF_2. This fact suggests that something more than a simple addition reaction occurs in the former.

The proton and F^{19} NMR spectra of the HNF_2–SO_3 adduct at 0° C. showed only a single line with no evidence of the splitting which should occur if the fluorine and hydrogen atoms were both still bound to nitrogen. A possible explanation of this may be that the HNF_2 adduct is not the coordination compound, but *N,N*-difluorosulfamic acid, $HOSO_2NF_2$.

The reaction between $(CH_3)_3$ Al and HNF_2 appears to produce a 1:1 adduct at −80° C. which liberates CH_4 slowly at this temperature. This elimination reaction, typical of the behavior of $(CH_3)_3$ Al with secondary amines and related bases (*1*), probably occurs via the coordination compound, which, although not isolated, appears to be moderately stable at −80° C. The mass balance seems to indicate that only one mole of HNF_2 can react at this temperature. In fact even at room temperature only two moles of methane are displaced by HNF_2. The assumed reaction agrees well with the HNF_2–CH_4 balance:

$$(CH_3)_3Al + HNF_2 = (CH_3)_3Al{:}HNF_2 \quad (1)$$

$$(CH_3)_3Al{:}HNF_2 = (CH_3)_2AlNF_2 + CH_4 \quad (2)$$

$$(CH_3)_2AlNF_2 + HNF_2 = CH_3Al(NF_2)_2 + CH_4 \quad (3)$$

The reaction of equimolar amounts of methyldifluoramine and with trimethylaluminum produces two moles of methane and a small amount of HCN. The reaction is evidently the decomposition of the amine:

$$CH_3NF_2 = HCN + 2\ HF \quad (4)$$

followed by reaction of the HF with trimethylaluminum, liberating methane.

The difluoramine-trimethylgallium system was studied briefly in an attempt to isolate a coordination compound. No evidence was obtained for such a compound from the pressure-composition data, and the mixture obtained was easily resolved into its components by simple trap-to-trap distillation. At room temperature, however, one mole of methane was slowly evolved from one mole of $(CH_3)_3Ga$, producing a colorless, viscous liquid.

Work in progress on the IR and NMR data of the aluminum and gallium compounds will be reported elsewhere.

Acknowledgment

This research was supported by the Advanced Research Projects Agency under ARPA Order No. 350-62, Project Code No. 9100. Technical direction was provided by the Director of Engineering Sciences, SREP, Air Force Office of Scientific Research Contract No. AF 49(638)-1175.

Literature Cited

(1) Coates, G. E., "Organometallic Compounds," John Wiley and Sons, New York, 1956.
(2) Craig, A. D., *Inorg. Chem.* 3, 1628 (1964).
(3) Freeman, J. P., Kennedy, A., Colburn, C. B., *J. Am. Chem. Soc.* 82, 5304 (1960).

RECEIVED April 23, 1965.

15

The Chemistry of Difluoramines

A. D. CRAIG, G. A. WARD, C. M. WRIGHT, and J. C. W. CHIEN

Research Center, Hercules Powder Co., Wilmington, Del.

Publication Date: January 1, 1966 | doi: 10.1021/ba-1966-0054.ch015

The chemistry of difluoramines of the type X–NF_2 has been studied to gain an understanding of the nature of the N–F and N–X bonds, to obtain a picture of the relative electron distributions in X–NF_2 compounds, and to determine the existence and stabilities of N–F radicals and ions. These compounds have been studied using electrochemistry, complexation, infrared spectroscopy, and theoretical calculations. Oxidation-reduction reactions have been carried out, and the effects of various environments on the N–F and N–X bonds have been investigated. The results of these studies emphasize the chemistry of difluoramine and the existence and stability of NF_2^+, $\cdot NF_2$, NF_2^-, and $H_2NF_2^+$.

Compounds containing the NF_2 group are commonly referred to as difluoramines. The chemistry of these compounds has been studied more intensively during recent years than previously and has been the subject of three review articles (*3, 9, 14*). The aims of our work, part of which we describe here, are to obtain a picture of the relative electron distributions in X–NF_2 compounds, to gain an understanding of the nature of the N–F and N–X bonds, and to determine the existence and stabilities of N–F radicals and ions. We have concentrated on X–NF_2 compounds, where X = F, Cl, H, NF_2, CH_3, C_2H_5, and CF_3. The radical and ionic species which have held our attention are $\cdot NF$, $\cdot NF_2$, NF^+, NF^-, NF_2^+, NF_2^-, NF_3^+, and $H_2NF_2^+$. This paper emphasizes the chemistry of difluoramine, HNF_2, and the existence of NF_2-containing ions to illustrate our investigations in NF_2 chemistry.

Results and Discussion

Theoretical Considerations. One approach we have taken is calculating molecular parameters of various N–F species by using molecular orbital treatments (*2, 7*). The π-bond orders and atomic charges calcu-

In Advanced Propellant Chemistry; Holzmann, R.;
Advances in Chemistry; American Chemical Society: Washington, DC, 1966.

lated for NF_2 moieties (Table I) are particularly relevant to NF_2 chemistry.

Table I. Calculated Charges and Bond Orders of NF_2 Species

	Atomic Charges		*π-Bond Orders*
	Q_N	Q_F	
NF_2^+	+1.706	−0.353	0.3
NF_2	+0.86	−0.43	0.35
NF_2^-	0	−0.5	0

Kaufman and co-workers have made similar calculations and have shown that in covalent NF_2 compounds there are no orbitals available on the nitrogen having energies low enough for significant π-bonding with the unshared electrons on the fluorine atoms (*12*, *13*). In a series of X-NF_2 compounds, the relative electron distributions are thus a function of the inductive effects of the X group. The various situations are envisioned as follows:

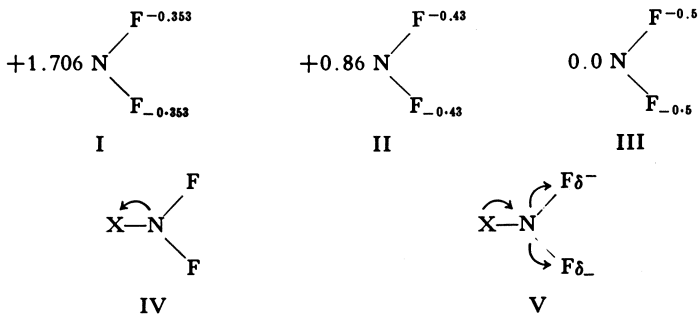

The relatively high negative charge on fluorines causes many NF_2 species to decompose readily by losing a fluoride ion. This work indicates that the NF_2-containing ions which have the greatest probability of long term existence are the cations because NF_2^+, of all the NF_2 species, has the lowest negative atomic charge on the fluorines. In all of the difluoramine derivatives studied, the nonbonding *L*-shell electrons of the nitrogen are more displaced toward the fluorines than strictly localized on the nitrogen. As a result, the nitrogen in many NF_2 species carries a relatively high positive charge. Any cationic NF_2 species would be expected to have a high electron affinity, probably higher than that of NO_2^+. In isolating an NF_2 cation, one must stabilize it with a large anion of low charge density so that polarization can occur or one must select a hypothetical NF_2 salt in which the lattice stabilization energy is very high. Candidates for the latter are moderately sized divalent anions. No NF_2-containing ions of any type have been observed except for NF_2^+ which has been observed in the mass spectrometer (*8*).

Experimental Observations. The nearest we have come to demonstrating the existence of N–F ions is in the electrochemical oxidation-reduction reactions of HNF_2. The oxidation has been carried out in water and in various polar organic solvents under acid conditions (*15*). The first step of this reaction is formation of the $\cdot NF_2$ radical. The $\cdot NF_2$ radical undergoes combination processes on the surface of the electrode rather than diffusing into the body of the solution before being involved in further reactions. The combination process on the electrode surface has been used to prepare various NF_2 compounds by simultaneously generating other radical species—e.g.,

$$HNF_2 \rightarrow H^+ + e^- + \cdot NF_2$$

$$CH_3COOH \rightarrow \cdot CH_3 + H^+ + CO_2 + e^-$$

$$\cdot NF_2 + \cdot CH_3 \rightarrow CH_3NF_2$$

The oxidation of HNF_2 involves the removal of an electron from the nitrogen in a solvated HNF_2 species rather than from NF_2^-. All of our work on the solution chemistry of HNF_2 show that under conditions favoring the formation of NF_2^- (proton removal), this species loses a fluoride ion to form difluorodiazine.

$$NF_2^- \rightarrow {}^1/_2N_2F_2 + F^-$$

The reduction of HNF_2 in aqueous media is a four-electron process in which HNF_2 is reduced to ammonia (*16*). In nonaqueous solvents the reduction depends on the availability of protons in the system, and the reduction potential is strongly influenced by the degree and type of solvation (Table II). Nitrogen trifluoride is electrolytically reduced in aqueous solution at —1.40 volts *vs.* S.C.E. Six electrons per molecule of NF_3 are involved in the reduction.

$$HNF_2 + 4e^- + 2H^+ \rightarrow NH_3 + 2F^-$$

$$NF_3 + 6e^- + 3H^+ \rightarrow NH_3 + 3F^-$$

NF_3 could not be electrolytically oxidized in systems similar to those used for the reduction.

Table II. Effect of Solvent on the Polarographic Reduction of HNF_2

Solvent	$E^{1/2}$ *HNF_2* (*volts vs. S.C.E.*)
H_2O	1.22
CH_3OH	1.55
CH_3CN	1.42
Dimethylformamide	1.61
Dimethyl sulfoxide	1.64

The solvation of HNF_2 in various solvents was studied by conventional and low temperature infrared techniques and by determining the dissociation pressure-temperature relationships of several HNF_2 solvent complexes (*16*). Total enthalpies of dissociation were determined where

Publication Date: January 1, 1966 | doi: 10.1021/ba-1966-0054.ch015

experimentally feasible. Shifts in the N–H and N–F stretching frequencies in the IR spectra of 1:1 complexes of HNF_2 with solvents and of 1*M*-solutions of HNF_2 were examined to determine the nature of bonding in the solvated species (Table III). In general these data indicate the order $H_2O < CH_3OH < CH_3CN < HCONH_2 < HOCN(CH_3)_2 \sim (CH_3)_2SO$ for the strength of solvation of HNF_2. It was found that 1:2 complexes of HNF_2 with DMF and DMSO exert very little vapor pressure at room temperature. Equimolar complexes of HNF_2 with formamide, dimethylformamide, and dimethyl sulfoxide exert relatively little vapor pressure at 0° C. HNF_2 is by far the least solvated by water.

Table III. Infrared Absorption Maxima of HNF_2 Complexes

		N—H		*N—F*	
Material	*N—H Stretch*	*Asym. Bend*	*Sym. Bend*	*Sym. Stretch*	*Asym. Stretch*
$CH_3CN \cdot HNF_2$ (solid)[a]	2710	1424	[c]	960	860
1*M* HNF_2 in CH_3OH (liquid)[b]	2725	[c]	1325[c]	955	855
$H_2O \cdot HNF_2$ (solid)[a]	2800 2975	1390	1320	973	875
$DMF \cdot HNF_2$ (solid)[a]	2725	[c]	[c]	952	850
1*M* HNF_2 in DMSO (liquid)[b]	2740	[c]	[c]	[c]	855
HNF_2 (solid)[a]	3110	1450	1350	972	880

[a] At −160° C.
[b] At 25° C.
[c] Solvent interference

In all of the solvents studied, the most important factor, determined from vibrational spectra, is the strength of the difluoramine hydrogen bond with the solvent. Thus, HNF_2 appears to be bonded to these solvents in structures of the type

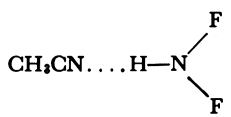

However, in some systems the infrared spectra indicate moderate bonding of the fluorines with the solvent—e.g.,

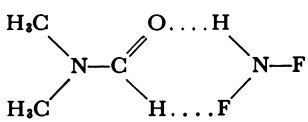

We attempted to protonate HNF_2 and CH_3NF_2 to determine if ammonium-type ions such as $H_2NF_2^+$ and $CH_3NF_2H^+$ could be formed (*5*). Three approaches were used. First, 1*M* amounts of H_2O and $HClO_4$ were added to 1*M* solutions of HNF_2 in acetonitrile or dimethylformamide. Conventional infrared spectroscopic techniques indicated that no interaction with the HNF_2 occurred. Second, the strengths of association of CH_3NF_2 and HNF_2 with anhydrous HCl, anhydrous HBr, and water were

measured. The techniques employed were similar to those described earlier (*4*). Little or no association of the difluoramines with any of the acids was observed. Third, infrared spectra of the solid equimolar mixtures HNF_2-H_2O, HNF_2-HCl, HNF_2-HBr, CH_3NF_2-H_2O, CH_3NF_2-HCl, and CH_3NF_2-HBr showed no evidence of protonation. The difluoramines did appear to be weakly associated with the acids through bonding of the acid hydrogen with the lone pair of electrons on the difluoramine nitrogen. Spectra were obtained at −160° C. Both HNF_2 and CH_3NF_2 were observed to oxidize HBr to bromine. No reaction was observed with HCl or H_2O.

A measure of the relative distribution of electrons in various NF_2 compounds was obtained by studying the interaction of the difluoramines with Lewis acids (*4*). The low temperature infrared spectra of complexes of difluoramines showed that bonding occurs through donation of electrons on the nitrogen to the Lewis acid. In no cases was evidence found for fluorine bridging or complete charge transfer. The strength of the complexes formed depended directly on the electron-withdrawing or electron-donating power of the attached group. A strongly electron-withdrawing group, such as CF_3, renders the X-NF_2 compound an essentially nonpolar species. An electron-donating group such as CH_3 increases the electron density on the nitrogen but also increases the apparent electron density on the fluorines so that compounds such as $CH_3CH_2NF_2$ or HNF_2 readily undergo fluoride abstraction reactions—e.g.,

$$CH_3CH_2NF_2 \rightarrow CH_3CN + 2HF$$

$$HNF_2 \rightarrow {}^1/_2N_2F_2 + HF$$

Studies of the proton resonance of CH_3NF_2 and $C_2H_5NF_2$ showed that the effective electronegativity of the NF_2 group is about 3.3. This value was obtained from the linear relationships

$$E = 0.01\,\Delta + 1.51$$

and

$$E = 0.0144\,\delta_{int} + 1.78$$

for the methyl and ethyl derivatives, respectively, where Δ is the absolute chemical shift of CH_3-X and δ_{int} is the difference between the CH_3 and CH_2 chemical shifts in CH_3CH_2X. The linear equations are taken from Dailey and Shoolery (*6*) and Cavanaugh and Dailey (*1*), who showed that the absolute chemical shift of the methyl protons in methyl derivatives and the internal chemical shift in ethyl derivatives are linearly proportional to the electronegativity of the substituent as determined by Huggins (*10*). Recently, the electronegativity was calculated to be between 3.6 and 3.7 (*11*). Thus, the NF_2 group is a strong electron-withdrawing moiety itself. The competition for nonbonded electrons may be pictured

Publication Date: January 1, 1966 | doi: 10.1021/ba-1966-0054.ch015

as in IV and V above. In V the N—F bond is weakened so that reactions of XNF_2 favor routes which involve loss of F^-. In IV the N—F bond is stronger so that XNF_2 reactions favor the loss of $\cdot NF_2$. We examined the mass spectral cracking patterns of CH_3NF_2 and CF_3NF_2 at low ionization potentials (11 e.v.) and found that the most abundant ions (99%) were $CH_3NF_2^+$ and CF_3^+, respectively (*7*). These data indicate that the C—N bond in CF_3NF_2 is weaker than that of CH_3NF_2. The N—F bond in CH_3NF_2, however, appears to be weaker than in CF_3NF_2. The thermal decompositions of these two difluoramines probably occur through different mechanisms. CF_3NF_2 will lose an NF_2 radical in the first step, whereas CH_3NF_2 will lose a fluorine:

$$CF_3NF_2 \rightarrow \cdot CF_3 + \cdot NF_2$$

$$CH_3NF_2 \rightarrow CH_3\dot{N}F + \cdot F$$

The $\cdot NF_2$ and $\cdot F$ will probably then undergo further reactions with the parent molecules:

$$\cdot NF_2 + CF_3NF_2 \rightarrow NF_3 + CF_3\dot{N}F \text{ or } N_2F_4 + \cdot CF_3$$

$$\cdot F + CH_3NF_2 \rightarrow HF + \cdot CH_2NF_2, \text{ etc.}$$

The CF_3NF_2 does not easily lose a fluoride ion to Lewis acids such as BF_3 (*4*).

Conclusion. These studies tend to substantiate the prediction of the theoretical calculations that if N—F anions are formed, the electron density on the fluorines will be so high that loss of a fluoride ion would be almost impossible to prevent. Further, the electron affinity of NF_2^+ appears to be extremely high, so that adding an electron to form $\cdot NF_2$ or adding an anion to form a covalent NF_2 compound is highly favored. In general, the reaction routes of NF_2 compounds appear to be favored where the reaction intermediate is an $\cdot NF_2$ radical. The $\cdot NF_2$ radical is a relatively stable species with a π-bond order of 0.35. The electron distribution in this species is much more symmetrical than those of the anion or cation. Reaction routes which involve an NF_2 anion intermediate are not very favorable because of the ease of fluoride loss. The NF_2 cation is equally as unfavorable since its oxidizing power will probably prevent it from existing in most systems.

Acknowledgment

Research reported in this publication was supported by the Advanced Research Projects Agency through the U. S. Army Research Office, Durham, N. C., Contract DA-31-124-ARO(D)-62.

Literature Cited

(1) Cavanaugh, J. R., Dailey, B. P., *J. Chem. Phys.* **34**, 1099 (1961).
(2) Chien, J. C. W., Hercules Powder Co., *Ann. Rept.* April 15, 1964, Contract No.DA-31-124-ARO(D)-62, ARPA Order No. 402.
(3) Colburn, C. B., *Advan. Fluorine Chem.* **3**, 92 (1963).
(4) Craig, A. D., *Inorg. Chem.* **3**, 1628 (1964).
(5) Craig, A. D., Hercules Powder Co., *Quart. Rept.* No. **7**, December 21, 1964, Contract No. DA-31-124-ARO(D)-62, ARPA Order No. 402.
(6) Dailey, B. P., Shoolery, J. N., *J. Am. Chem. Soc.* **77**, 3977 (1956).
(7) Hercules Powder Co., *Quart. Rept.* No. **6**, September 21, 1964, Contract No. DA-31-124-ARO(D)-62, ARPA Order No. 402.
(8) Herron, J. T., Dibeler, V. H., *J. Chem. Phys.* **33**, 1595 (1960).
(9) Hoffman, C. J., Neville, R. G., *Chem. Rev.* **62**, 1 (1962).
(10) Huggins, M. L., *J. Am. Chem. Soc.* **75**, 4123 (1953).
(11) Huheey, J. E., *J. Phys. Chem.* **68**, 3073 (1964).
(12) Kaufman, J. J., *J. Chem. Phys.* **37**, 759 (1962).
(13) Kaufman, J. J., Hamann, J. R., "Abstracts of Papers," 148th Meeting, ACS, Sept. 1964, p. 6K.
(14) Pankratov, A. V., *Russ. Chem. Rev.* **32**, 157 (1963).
(15) Ward, G. A., Wright, C. M., *J. Am. Chem. Soc.* **86**, 4333 (1964).
(16) Ward, G. A., Wright, C. M., Craig, A. D., *J. Am. Chem. Soc.*, **88**, 713 (1966).

RECEIVED April 26, 1965.

16

Some Reactions of Alkyl— and Arylalkyldifluoramines

HARRY F. SMITH, JOSEPH A. CASTELLANO, and DONALD D. PERRY

Reaction Motors Division, Thiokol Chemical Corp., Denville, N. J.

Publication Date: January 1, 1966 | doi: 10.1021/ba-1966-0054.ch016

The thermally initiated reaction between tert-*butyl iodide and tetrafluorohydrazine provides a convenient synthetic route to* tert-*butyldifluoramine. Tertiary alkyldifluoramines have been found to react with organolithium reagents and with concentrated nitric acid. The reaction of triphenylmethyldifluoramine with* n-*butyllithium produced benzophenone anil and* n-*octane.* tert-*Butyldifluoramine reacted with organolithium reagents to yield a mixture of azo compound, dialkyldifluorohydrazine, tertiary amine, and the hydrocarbon resulting from the coupling of two free radicals derived from the organometallic reagent. A mechanism involving two successive one-electron reduction steps, to give first nitrogen radicals and then nitrenes as intermediates, is compatible with all of the products observed.* tert-*Butyldifluoramine was attacked by concentrated nitric acid to yield a complex array of products, including alkyl nitrates and nitrites while triphenylmethyldifluoramine gave principally triphenylcarbinol.*

The continuing search for more energetic rocket propellant compositions has focused attention on several previously unexplored fields of chemistry. Compounds containing fluorine bound to nitrogen offer attractive prospects in such applications. Since effective utilization of any chemical system requires an understanding of the components involved, we have studied the reactions of some simple model compounds of this class.

Synthesis of tert-*Butyldifluoramine*

The first synthesis of an *N,N*-difluoroalkylamine (alkyldifluoramine) in 1936 (*14*) introduced a new family of organic compounds. The perfluoroalkyldifluoramines obtained by fluorinating various carbon-nitrogen

In Advanced Propellant Chemistry; Holzmann, R.;
Advances in Chemistry; American Chemical Society: Washington, DC, 1966.

compounds (*1, 2, 3, 7, 12*) have more recently been supplemented by a limited number of analogous compounds containing nonfluorinated alkyl groups (*5, 6, 13*). This paper is devoted to the study of the chemical properties of these interesting compounds.

A reported synthesis (*13*) of *tert*-butyldifluoramine capitalized on the equilibrium dissociation of tetrafluorohydrazine into NF_2 free radicals (*9*) by generating *tert*-butyl radicals via the decomposition of azoisobutane in the presence of tetrafluorohydrazine. Azoisobutane has been synthesized by two methods (*4, 16*). Using the more efficient of these methods (*16*), which gave us a 30% yield of the intermediate, the overall yield of *tert*-butyldifluoramine obtained in the two-step reaction sequence was only 6% of theoretical.

Ethyl- and methyldifluoramine have been prepared by reaction of the respective iodides with tetrafluorohydrazine excited by ultraviolet radiation (*5*). We therefore investigated the free radical reaction of *tert*-butyl iodide with tetrafluorohydrazine and found that it produced the desired *tert*-butyldifluoramine routinely in 40% yield. The reaction is believed to take place by the following steps:

$$2(CH_3)_3CI \rightarrow 2(CH_3)_3C\cdot + I_2 \quad (1)$$

$$N_2F_4 \rightarrow 2NF_2\cdot \quad (2)$$

$$(CH_3)_3C\cdot + NF_2\cdot \rightarrow (CH_3)_3CNF_2 \quad (3)$$

tert-Butyldifluoramine was obtained by exposing a mixture of the reactants to light or, more conveniently, by heating. The yield of product in the thermal reaction was not increased by a 50% increase in reaction time.

The product was identified by boiling point and elemental analysis. Its infrared spectrum and fragmentation pattern in the mass spectrometer were also consistent with the assigned structure.

The presence of small amounts of C_8 and C_{12} olefins (telomers of isobutene) among the reaction products attests to the occurrence of disproportionation between *tert*-butyl radicals (Equation 4). Coupling of *tert*-butyl radicals (Equation 5) also occurred to a minor extent, as evidenced by the appearance of traces of tetramethylbutane.

$$2(CH_3)_3C\cdot \rightarrow (CH_3)_3CH + (CH_3)_2C{=}CH_2 \quad (4)$$

$$2(CH_3)_3C\cdot \rightarrow (CH_3)_3CC(CH_3)_3 \quad (5)$$

Reactions with Organometallic Reagents

Triphenylmethyldifluoramine (I) reacts rapidly with *n*-butyllithium to yield *n*-octane and benzophenone anil (II). With equimolar quantities of the reactants the reaction was incomplete, and some I was recovered. Only 40% of the fluorine was converted to fluoride ion under these condi-

Publication Date: January 1, 1966 | doi: 10.1021/ba-1966-0054.ch016

tions. Increasing the amount of organometallic reagent to two molar equivalents resulted in complete disappearance of the difluoramine; 77% of the total fluorine was recovered as fluoride ion, and the yield of II was 70% of theory.

tert-Butyldifluoramine (III) reacted rapidly with either *n*-butyllithium or phenyllithium to produce *n*-octane and biphenyl, respectively. Recovery of fluoride ion was 20–27% in equimolar systems and increased to approximately 50% when more than one equivalent of *n*-butyllithium was used.

Two additional products, present in small quantity, were detected by infrared and mass spectral methods. The first was identified as azoisobutane (IV), and the second appeared, on the basis of mass spectral evidence, to be 1,2-difluoro-1,2-di-*tert*-butylhydrazine (V).

IV V

The reaction of III with two or four equivalents of *n*-butyllithium resulted in the formation of a new product, *N*, *N*-di-*n*-butyl-*tert*-butylamine (VI), in yields up to 16% of theory. This previously unknown tertiary amine was identified by infrared and mass spectrometric analyses. A comparison of the mass spectrum of VI with that of the known tri-*n*-butylamine (Table I) shows that the same major peaks appear but in quite

Table 1. Principal Mass Peaks of *N,N*-di-*n*-Butyl-*tert*-butylamine and Tri-*n*-Butylamine

		Relative Intensity	
m/e	*Ionic Species*	*(n-Bu)₂N-tert-Bu*	*(n-Bu)₃N*[a]
41	$C_3H_5^+$	90	21.4
42	$C_3H_6^+$	34	16.0
43	$C_3H_7^+$	85	7.8
57	$C_4H_9^+$	100	13.4
58	C_4H_{10} or $C_3H_3NH_2^+$ (Rearrangement)	75	5.0
72	$C_4H_9NH^+$ (Rearrangement)	91	1.16
86	$C_4H_9NHCH_2^+$ (Rearrangement)	92	4.26
99	$C_4H_9N(CH_2)_2^+$ (Rearrangement)	12	...
100	$C_4H_9NH(CH_2)_2^+$ (Rearrangement)	8	26.3
113	$C_4H_9N(CH_2)_3^+$	8	...
114	$C_9H_9NH(CH_2)_3^+$ (Rearrangement)	4	0.25
128	$(C_4H_9)_2N^+$	68	1.03
142	$(C_4H_9)_2NCH_2^+$	63	100.00
170	$(C_4H_9)_2NC_3H_6^+$	26	0.14
185	$(C_4H_9)_3N^+$	8	5.22

[a] Mass spectral data, A. P. I., Serial No. 1132

different relative intensities. The mass peaks caused by rearrangements were generally more intense, and two such peaks ($m/e = 86, 114$) which do not occur in tri-*n*-butylamine were observed.

The results of this series of experiments are summarized in Table II.

Table II. Reactions of *tert*-Alkyldifluoramines with Organolithium Reagents

Reactants		*Molar*	*Products*		
RNF_2	*R'Li*	*Ratio*	*% R'R'*	*% F^-*	*Others*
I	*n*-BuLi	1:1	...	40.1	I, II
I	*n*-BuLi	1:2	present	77.0	I, 42 + %II
I	*n*-BuLi	1:2	...	...	72% II
III	PhLi	1:1	present	21.1	III, IV, V
III	PhLi	1:1	50.8	19.5	III
III	*n*-BuLi	1:1	88.0	25.6	III
III	*n*-BuLi	1:1	present	25.6	III
III	*n*-BuLi	1:2	present	48.8	VI
III	*n*-BuLi	1:4	...	52.0	16.2%VI

Publication Date: January 1, 1966 | doi: 10.1021/ba-1966-0054.ch016

Proposed Mechanism of Organolithium Reactions

The various products obtained in the experiments described above can be explained on the assumption that the organometallic reagents reduced the tertiary alkyldifluoramines via a succession of one-electron transfer steps. A possible alternative for the step shown in Equation 7

$$R_3CNF_2 + R'Li \rightarrow \underset{\substack{\text{VII a, R = CH}_3 \\ \text{b, R = Ph}}}{R_3CNF} + R'\cdot + LiF \qquad (6)$$

$$R_3C\dot{N}F + R'Li \rightarrow \underset{\substack{\text{VIII a, R = CH}_3 \\ \text{b, R = Ph}}}{R_3C\dot{N}\cdot} + R'\cdot + LiF \qquad (7)$$

would be interaction of the R′ radical derived from the organometallic reagent with the fluoramino radical (VII). Such a process would also

$$R_3C\dot{N}F + R'\cdot \rightarrow R_3C\dot{N}\cdot + R'F \qquad (8)$$

produce the nitrene (VIII), but would require different stoichiometry. No trace of the fluorocarbon byproducts which would be formed in this process has been detected.

The array of final products obtained in any one experiment was found, as expected, to depend upon the reactant ratio and the order and rate of addition. The reactive intermediate species are capable of interacting in various combinations and products arising from several of these possibilities have been detected.

In each case the hydrocarbon produced by the coupling of two of the radicals derived from the organometallic reagent was a prominent product. Diphenyl and *n*-octane were obtained from phenyllithium and *n*-butyllithium respectively. When an equimolar quantity of phenyllithium was added slowly to *tert*-butyldifluoramine (III), the homogeneous coupling product (V) of the amino radical (VII a) was detected among the products along with the coupling product (IV) of the nitrene (VIII a). The diradical nature of nitrenes, which leads to dimerization and the

$$\underset{\text{VII a}}{2(CH_3)_3C\dot{N}F} \rightarrow \underset{\text{V}}{(CH_3)_3C\overset{F}{\overset{|}{N}}-\overset{F}{\overset{|}{N}}C(CH_3)_3} \quad (9)$$

$$\underset{\text{VIII a}}{2(CH_3)_3C\dot{N}\cdot} \rightarrow \underset{\text{IV}}{(CH_3)_3CN{=}NC(CH_3)_3} \quad (10)$$

production of azo compounds, is well known (*8*). The cross-coupling of VIIIa with the *n*-butyl radical has been observed when an excess of *n*-butyllithium was used.

$$\underset{\text{VIII a}}{(CH_3)_3C\dot{N}\cdot} + 2\ CH_3(CH_2)_3\cdot \rightarrow \underset{\text{VI}}{(CH_3)_3CN(CH_2CH_2CH_2CH_3)_2} \quad (11)$$

In reactions involving triphenylmethyldifluoramine (I), rearrangement of the nitrene (VIII b) appears to be favored energetically, since benzophenone anil (II) was the only product found. II has been reported as the principal product of thermal decomposition of triphenylmethyl, *N*-triphenylmethylhydroxylamine, and a number of related compounds

$$\underset{\text{VIII b}}{Ph_3C\dot{N}\cdot} \rightarrow \underset{\text{II}}{Ph_2C{=}NPh} \quad (12)$$

(*10, 15, 17, 18, 19, 20, 21*) presumably also via the nitrene intermediate. An analogous rearrangement of the *tert*-butyl nitrene (VIII a), if it occurred, would yield the imine (IX) which would be subsequently hydrolyzed to acetone and methylamine. A careful search failed to reveal the presence of any volatile base.

$$\underset{\text{VIII a}}{(CH_3)_3C\dot{N}\cdot} \rightarrow \underset{\text{IX}}{(CH_3)_2C{=}NCH_3} \xrightarrow{H_2O} (CH_3)_2C{=}O + CH_3NH_2 \quad (13)$$

Reactions with Nitric Acid

Since concentrated nitric acid exhibits both oxidative and electrophilic properties, one can anticipate several possible modes of attack on a tertiary alkyldifluoramine: the difluoramine might be protonated and subsequently hydrolyzed; oxidation might produce an amine oxide analog; oxidative cleavage might occur at N–F, C–N, or C–C bonds; or a nitroalkane might be produced. It has been reported, for example, that triphenylmethyldifluoramine is protonated in concentrated sulfuric acid and decomposes with the liberation of difluoramine (*6*). We have confirmed this observation and found, furthermore, that a secondary alkyldifluoramine is similarly protonated but decomposes with the evolution of hydrogen fluoride. Triphenylmethyldifluoramine has been found to dissolve in glacial acetic acid and to be recovered unchanged upon dilution with water. It was not affected by contact with concentrated hydrochloric acid at room temperature.

Publication Date: January 1, 1966 | doi: 10.1021/ba-1966-0054.ch016

The room temperature reactions of *tert*-butyldifluoramine and triphenylmethyldifluoramine with concentrated nitric acid in equimolar quantities and with a large excess of acid have been studied. Table III presents a summary of the products obtained in each case, as determined chiefly by infrared spectral evidence.

Table III. Reactions of Alkyldifluoramines with 70% Nitric Acid

	tert-Butyldifluoramine		*Trityldifluoramine*	
Product	*Equimolar Acid*	*Excess Acid*	*Equimolar Acid*	*Excess Acid*
NO_2	...	Large	Present	Large
N_2O	Present	Present	...	Present
CO_2	...	Large	...	...
NO_3F	Trace	Trace	...	Trace
NOCl or NO_2F	...	...	...	Trace
SiF_4	Present	Present	...	Present
Alkyl nitrate	Present	Present	...	Present
Alkyl nitrite	...	Present	...	Present
Nitroalkane	...	...	...	Present
Carbinol	...	...	...	Major
Alkyldifluoramine	Present	...	Major	...

Several points are worth considering in some detail. The large amount of nitrogen dioxide obtained when excess acid was used is apparently the result of decomposition of nitric acid catalyzed by the difluoramine or one of the reaction products. This interpretation is supported by the fact that the quantities of gas obtained were greatly in excess of stoichiometric, based on the difluoramine, and by the observed exponential pressure rise following a protracted induction period.

The presence of carbon dioxide among the products of the reaction of *tert*-butyldifluoramine with excess nitric acid is a clear indication that C—C bond cleavage occurred. The nitrate and nitrite esters produced in this experiment were mixtures of various alkyl derivatives, and not solely *tert*-butyl derivatives as in the other cases where nitrate esters were detected. The relative stability of trityldifluoramine toward oxidative cleavage is fully in accord with known differences between aromatic and aliphatic systems.

The appearance of silicon tetrafluoride during an investigation of organic fluorine compounds in glass equipment is generally understood to imply the transient formation of hydrogen fluoride; this interpretation should be applied here. An interesting point, not yet fully understood, is the appearance of nitroalkane and carbinol only in the reaction of trityldifluoramine with excess acid.

In general, the results observed are best understood as the consequences of electrophilic attack on the alkyldifluoramines. The fact that such attack did not occur when triphenylmethyldifluoramine was treated with hydrochloric acid, an even stronger electrophile, tends to cloud this

Publication Date: January 1, 1966 | doi: 10.1021/ba-1966-0054.ch016

simple picture. It becomes necessary to invoke the simultaneous participation of an oxidative process in some way which is not yet clear.

Assuming that protonation of the alkyldifluoramine does occur, elimination of difluoramine and formation of a tertiary carbonium ion would logically follow.

$$R_3CNF_2 + H^+ \rightarrow R_3C\overset{+}{N}F_2H \quad (14)$$

$$R_3C\overset{+}{N}F_2H \rightarrow R_3C^+ + HNF_2 \quad (15)$$

The failure of difluoramine to appear among the final products is not particularly surprising. In the presence of nitric acid and/or nitrogen oxides, it might easily be oxidized and may well constitute the source of the silicon tetrafluoride. The formation of a carbonium ion from trityldifluoramine would be favored by resonance stabilization. In the *tert*-butyl case, on the other hand, this driving force is not present and formation of the ion would be expected to occur less readily. In addition, both the *tert*-butyl carbonium ion and the difluorammonium ion from which it is derived would be more subject to a variety of side reactions than the corresponding trityl species.

Reaction of the carbonium ion with water or with nitrate ion would produce the carbinol and the ester, respectively. Alternatively, the

$$R_3C^+ + H_2O \rightarrow R_3COH + H^+ \quad (16)$$

$$R_3C^+ + NO_3^- \rightarrow R_3CONO_2 \quad (17)$$

$$R_3COH + HNO_3 \rightarrow R_3CONO_2 + H_2O \quad (18)$$

carbinol might be esterified by nitric acid. For the reasons cited above these reactions contributed substantially to the overall result only in the triphenylmethyldifluoramine reactions.

Experimental

Materials. The phenyllithium and *n*-butyllithium used in this work were commercial products supplied by Foote Mineral Co. in ether-benzene and hexane solutions, respectively. Triphenylmethyldifluoramine was obtained from Peninsular Chem Research and purified by recrystallization from methanol, m.p., 80°–81.5° C. *tert*-Butyl iodide was obtained from K and K Laboratories, Jamaica, N. Y., and purified before use either by distillation or by washing with aqueous sodium thiosulfate and drying.

Synthesis of *tert*-Butyldifluoramine. A 2-liter bulb, fitted with a freeze-out tip and a vacuum stopcock terminating in a standard ball joint, was charged with 6.0 grams (0.0307 mole) of *tert*-butyl iodide in a nitrogen atmosphere. The liquid was frozen at —78° C., and the bulb was evacuated. After three additional freeze-thaw cycles with intermittent evacuation, the tip of the flask was cooled to —196° C., and 4.16

grams (0.040 mole, measured by volume assuming ideal gas properties) of tetrafluorohydrazine were condensed into the bulb. The bulb was then transferred to a heating jacket and heated to 95° ± 5° C. for 4 hours. Following this, the bulb was cooled to room temperature, the contents were condensed in the tip at —78° C., and any volatile components were removed under vacuum. The crude *tert*-butyldifluoramine was then distilled under vacuum from the bulb at 28° C. into a trap at —78° C. The synthesis was repeated four times, and the combined product was fractionated to yield 5.8 grams (43.3%) of colorless liquid, b.p., 55°–56° C. (760 mm.).

A sample was chromatographed using a Wilkens Autoprep with a 20-ft. by $^3/_8$-inch column packed with 30% SF-96 Silicone on Chromosorb P. Retention time at 35° C. and a flow rate of 100 ml./min. was 40 min.

Analysis showed: calculated for $C_4H_9NF_2$: C, 44.03; H, 8.31; N, 12.84; found: C, 44.46; H, 8.31; N, 12.45.

The infrared spectrum showed very strong absorptions at 880 and 970 cm.$^{-1}$ and a weak band at 930 cm.$^{-1}$, indicative of NF_2 groups. The expected symmetrical and asymmetrical CH_3—C deformation bands (1480 and 1375 cm.$^{-1}$, respectively) and the C—H stretching band (2990 cm.$^{-1}$) were also observed. The mass spectrum, although lacking the molecule ion peak, did show the following significant fragments (*m/e*, assignment, relative intensity): 94, $C_3H_6NF_2^+$, 6.3; 57, $C_4H_9^+$, 100; 33, NF^+, 4.5.

In the photolytic process, a 500-ml. borosilicate glass bulb containing 1.5 grams (8.3 mmole) of *tert*-butyl iodide and 1.58 grams (15.2 mmole) of tetrafluorohydrazine was illuminated with a 300-watt Reflectorflood lamp at a distance of 15 cm. for 24 hours. Upon working up the reaction mixture as described above, 0.4 gram of *tert*-butyldifluoramine was obtained.

Reaction of *tert*-Butyldifluoramine with Phenyllithium. *tert*-Butyldifluoramine (0.55 gram 0.005 mole) was dissolved in 10 ml. of sodium-dried ether, and the solution was cooled to 0°–5° C. In a dropping funnel under nitrogen, 2.5 ml. (0.005 mole) of phenyllithium solution in benzene-ether (Lithium Corp. of America) was diluted with dry ether to 10 ml. This solution was added to the stirred difluoramine solution during 1 hour. A red-brown color appeared and deepened gradually during the addition. A gentle stream of nitrogen was passed through the reaction flask and then bubbled into a standardized solution containing 5.27 meq. of acid while 20 ml. of distilled water were added dropwise to the reaction mixture (20 min.). Stirring was continued for 1 hour. The acid solution was titrated with base, and 5.19 meq. were found. The decrease (1.5%) was not considered to be significant. The aqueous and organic phases of the reaction mixture were separated. The water layer was washed with 15 ml. of ether. The wash and the organic layer were combined and washed with three 10-ml. portions of distilled water. These washes were combined with the aqueous solution which was subjected to analyses as discussed above.

The ether-benzene solution was dried first over Drierite and then over anhydrous sodium sulfate and distilled at atmospheric pressure. The flask was heated in a bath at 55°–60° C. throughout distillation of the bulk of the solvents and raised to 95°–100° C. for 20 min. at the end. The distillate, collected at dry ice temperature, was shown by infrared analysis to consist of unreacted *tert*-butyldifluoramine and ethyl ether. A residue

Publication Date: January 1, 1966 | doi: 10.1021/ba-1966-0054.ch016

weighing 1.10 grams remained. The mass spectrum of this fraction contained peaks at 33 (NF), 41 (C_3H_5), 45 (CNF), and 57 (C_4H_9) mass units. The trace of ether observed ($m/e = 59$) was not sufficient to account for the intensity of the peak at 45. The most probable source of these fragments is the substituted hydrazine (V).

The several components of the less volatile fraction were separated by vapor phase chromatography using a Perkin-Elmer Model 154C instrument. The 6-ft. column was packed with di-*n*-decyl phthalate on firebrick and was maintained at 90° C. with a helium flow rate of 53 ml./min. Since fractions were expected to be too small to be collected individually, the effluent stream was fed directly into the inlet of a Bendix time-of-flight mass spectrometer. In one fraction, mass peaks at 57 (C_4H_9) and 71 ($C_4H_9N_2$) units were observed, in relative intensities identical to those found in azoisobutane (IV).

Reaction of *tert*-Butyldifluoramine with *n*-Butyllithium. A solution of 1.1 grams (0.01 mole) of *tert*-butyldifluoramine in 10 ml. hexane was treated with 26.0 ml. (0.04 mole) of *n*-butyllithium solution, by adding the organometallic reagent dropwise in 1 hour at 5°–10° C. The dark brown mixture was stirred for 2.5 hours at 10°–25° C. and then treated with water. The organic solution was separated and dried over anhydrous Na_2SO_4 while the aqueous solution was analyzed and found to contain 0.197 gram (0.0104 mole, 52.0%) of fluoride ion. The solvent was evaporated from the organic solution, and the residual brown oil was distilled to yield 0.32 gram of a liquid, b.p., 79°–82° C. (0.3 mm.). On the basis of infrared and mass spectral data, the liquid product was identified as *N,N*-di-*n*-butyl-*tert*-butylamine.

Reaction of Triphenylmethyldifluoramine with *n*-Butyllithium. A solution of 5.9 grams (0.02 mole) of triphenylmethyldifluoramine, m.p., 80°–81° C. in 40 ml. of hexane was cooled to 0° C. in a 200-ml. three-neck flask while 25.8 ml. (0.04 mole) of *n*-butyllithium solution was added dropwise with stirring during 1.5 hours. A deep red color developed as the butyllithium came into contact with the hexane solution, but the color changed to a bright yellow on continued stirring at 5°–10° C. At the completion of the addition, the solution was allowed to come to room temperature, and it was stirred at 25° C. for 2 hours. Water was then added to the mixture, the organic phase was separated, washed with water, and dried over anhydrous Na_2SO_4. The solvent was evaporated, leaving 5.72 grams of brown semisolid. The material was kept under 0.5 mm. pressure for 1 hour, a liquid nitrogen trap being employed to collect any liquid distillate. A liquid (0.3 gram) was obtained and submitted for infrared analysis. It showed very strong absorptions indicative of O—H, aliphatic C—H, C—CH_3, C—OH, and $-(CH_2)n$ with $n > 4$. In addition, a medium strength band at 1710 cm.$^{-1}$ (C=O) was also present.

The residue was recrystallized from methanol to yield 2.15 grams (42%) of yellow crystals, m.p., 112°–113° C., which were identified by infrared and elemental analysis as benzophenone anil.

Analysis showed: calculated for $C_{19}H_{15}N$: C, 88.68; H, 5.88; N, 5.44; found: C, 88.85; H, 5.86; N, 5.61.

The physical constants were in excellent agreement with the literature, m.p., 113°–114° C. (*22*).

The methanol solution from the recrystallization was evaporated to dryness to yield 3.3 grams of a mixture of triphenylmethyldifluoramine

and benzophenone anil. In addition, the infrared spectrum of this material showed weak absorptions owing to aliphatic C—H, C=O and C=N or C=C.

A solution of 1.48 grams (0.005 mole) of triphenylmethyldifluoramine in 30 ml. hexane was treated with 6.5 ml. (0.01 mole) of *n*-butyllithium solution as above. Water was added to the reaction mixture, and the organic phase was separated and washed with four 100-ml. portions of distilled water. The combined aqueous washings were transferred to a 500-ml. volumetric flask and adjusted to volume with distilled water. This solution was found to contain 146 mg. F^- (0.0077 mole, 77%) and 0.0028 mole OH^-.

The hexane solution was dried over Na_2SO_4, and the solvent was evaporated. The residue was taken up in CH_2Cl_2 and chromatographed on alumina. The chromatogram was followed by the yellow band which moved down the column. This yellow CH_2Cl_2 eluate was evaporated to dryness, and the residue was recrystallized from ether to yield 0.92 gram (0.0036 mole, 72%) benzophenone anil, m.p., 112°–113° C. The column was eluted with methanol, and the solvent was evaporated to give 0.13 gram of brown solid. The infrared spectrum of this material showed strong absorptions indicative of aliphatic C—H, aromatic C—H, C=N, or C=O (1660 cm.$^{-1}$), a trace of N—F, and substituted aromatic.

***tert*-Butyldifluoramine and Nitric Acid.** *tert*-Butyldifluoramine (1.02 grams, 9.3 mmoles) was condensed under vacuum into a flask containing 10 ml. (150 mmoles) of concentrated HNO_3. The mixture was warmed to room temperature and stirred. The pressure rose to 210–220 mm. and remained constant for 16 hours. After this period, the pressure rose within 1.5 hours to 730 mm. with the evolution of brown gas. On cooling the reaction flask to —70° C. the pressure dropped to 340 mm. A sample of this gas was subjected to infrared analysis and found to contain C—H (3000 and 1480 cm.$^{-1}$), C—CH_3 (1375 cm.$^{-1}$), N_2O (2220 cm.$^{-1}$), N_2O_4 (1750 and 1625 cm.$^{-1}$), N—F (attributed to starting material, 970 and 880 cm.$^{-1}$), NO_3F (920, 790, and 720 cm.$^{-1}$), CO_2 (2300 and 625 cm.$^{-1}$), SiF_5 (1025 cm.$^{-1}$), and NOCl (presumably from attack on NaCl window, 1810 and 1790 cm.$^{-1}$). Mass spectrometric analysis confirmed the presence of starting difluoramine, CO_2 and/or N_2O, SiF_4, and NO_3F, and established the absence of H_2 and O_2. A second gas sample taken at 0° C. was found to contain some of these components but no additional products. The acid solution was extracted with pentane to remove organic products. Infrared analysis of this extract revealed the presence of alkyl nitrite and nitrate (C—H at 2850 and 1450 cm.$^{-1}$, possible C—CH_3 at 1375 cm.$^{-1}$, C—ONO at 1560 cm.$^{-1}$, and C—ONO_2 at 1640 cm.$^{-1}$).

Concentrated nitric acid (0.67 ml., 10.0 mmoles) was delivered by pipet into a 50-ml. round-bottomed flask, fitted with a magnetic stirring bar and a suitable adapter and attached to a vacuum line. The acid was frozen in a liquid nitrogen bath, and the flask was evacuated. The acid was melted and refrozen twice, with evacuation to effect degassification. *tert*-Butyldifluoramine (1.09 grams, 10.0 mmoles) was evaporated into an evacuated calibrated storage bulb to the calculated pressure and then condensed into the flask with liquid nitrogen. The reactor portion of the line with manometer was closed off, and the flask was allowed to warm to room temperature. The mixture was stirred at 26–29° C. for 24 hours, during which the pressure remained essentially constant (186–198 mm.

Publication Date: January 1, 1966 | doi: 10.1021/ba-1966-0054.ch016

Hg). The liquid mixture became yellow, but no brown fumes appeared in the vapor space.

Gas samples for infrared and mass spectral analyses were taken, with the reaction flask at 25° and —78° C. Both samples contained an alkyl nitrate, N_2O, *tert*-butyldifluoramine and some additional N—F material, and a trace of NO_3F.

The liquid reaction mixture was extracted with CCl_4. Infrared analysis of the extract did not indicate any additional products. The aqueous residue was evaporated to dryness at room temperature, and a few needle crystals were recovered. The infrared spectrum of this solid showed only absorptions owing to water. Attempts to dehydrate the small amount of product which remained were unsuccessful.

Triphenylmethyldifluoramine and Nitric Acid. Recrystallized triphenylmethyldifluoramine (1.0 gram, 3.4 mmoles, m.p., 80–81.5° C.) and a small magnetic stirring bar were placed in the bottom of a reaction tube having a small side chamber. Concentrated (70%) nitric acid (2.5 ml., 38 mmoles) was placed in the side chamber and the tube was connected to a vacuum line by means of standard taper joints. The nitric acid was frozen by immersion in a liquid nitrogen bath, and the system was evacuated. The cold bath was removed. Then the tube was rotated so that the nitric acid, as it melted, flowed onto the triphenylmethyldifluoramine.

The resulting slurry was stirred at 22°–25° C. for 24 hours. The reaction mixture bubbled and became progressively darker, and brown fumes were observed in the vapor space. The pressure rose exponentially to reach a maximum of approximately 400 mm. in 2.5 hours (system volume—180 ml.) and then remained constant.

After 24 hours the reaction mixture was cooled to —78° C., and a gas sample was taken for analysis. Infrared and mass spectrometric examination revealed the presence of NO_2, N_2O, SiF_4, and either NOCl or NO_3F.

The reaction tube was then warmed to room temperature, flushed with nitrogen, and opened. The reaction mixture was diluted with distilled water (color changed from dark brown to bright orange), and the solid product was removed by filtration. The filtrate was neutralized with Na_2CO_3 (color changed from pale amber to brown) and extracted with benzene. No residue was obtained when an aliquot of the benzene extract was evaporated. Reacidification of the aqueous layer lightened the color but not to the original shade. The fluoride ion could not be determined because the remaining color was too intense.

The orange solid product was washed with water, dried in vacuum over P_2O_5, and chromatographed on an alkaline alumina column. The first fraction, 420 mg., yellow to pale orange crystals eluted with pentane-benzene, proved to be the principal constituent of the mixture. It was recrystallized from pentane-benzene to give a nearly colorless compound, m.p., 162.5°–163° C. Its infrared spectrum was identical with that of triphenylcarbinol, lit. m.p., 162.5° C. (*11*).

Analysis showed: calculated for $C_{19}H_{16}O$: C, 87.66; H, 6.20; found: C, 87.06/87.21; H, 6.29/6.41.

Triphenylmethyldifluoramine (2.95 grams, 10 mmoles) was placed, along with a small magnetic stirring bar, in a test tube having a standard taper glass joint. The tube was flushed with dry nitrogen and placed in a liquid nitrogen bath. Concentrated HNO_3 (0.67 ml., 10 mmoles) was

introduced slowly and allowed to freeze on the side of the tube without contacting the triphenylmethyldifluoramine. The reaction tube was then connected via a suitable adapter to a vacuum system, evacuated, and allowed to warm to room temperature. After the mixture was stirred for 18 hours at 25°–28° C., a sample of the gaseous products ($p = 55$ mm. in 180 ml.) was taken in an evacuated cell. The system was then filled with nitrogen to atmospheric pressure. The reaction mixture was diluted with distilled water, and the yellow insoluble product was removed by filtration. The yellow aqueous filtrate was extracted three times with methylene chloride; the third extract contained very little color although the aqueous solution remained a strong yellow. On standing, the combined extracts became orange, as did the solid product on the filter.

Infrared analyses of the gas sample and the methylene chloride extract (differential *vs.* solvent) showed no significant absorptions. The aqueous solution was found to contain 7.41 meq. of free acid and 25 mg. (1.3 meq.) of fluoride ion. The infrared absorption spectrum of the bright yellow-orange solid (m.p., 79°–81° C.) was superimposable upon that of triphenylmethyldifluoramine.

Publication Date: January 1, 1966 | doi: 10.1021/ba-1966-0054.ch016

Acknowledgment

This research was supported by the Advanced Research Projects Agency and administered by the Department of the Navy, Office of Naval Research, under Contract Number NOnr 1878(00).

The authors wish to thank Murray S. Cohen of these laboratories for his interest and encouragement during the course of this work. Analytical assistance by Alan Fremmer, John A. Creatura, Raymond N. Storey, Donald Y. Yee, Daniel G. Chowanec, and Donald N. Pregler is gratefully acknowledged.

Literature Cited

(1) Attaway, J. A., Groth, R. H., Bigelow, L. A., *J. Am. Chem. Soc.* **81**, 3599 (1959).
(2) Bigelow, L. A., Terminal Report, Office of Naval Research, AD No. 207549, August 1958.
(3) Coates, G. E., Harris, J., Sutcliffe, T., *J. Chem. Soc.* **1951**, 2762.
(4) Farenhorst, E., Kooyman, E. C., *Rec. Trav. Chim.* **72**, 993 (1953).
(5) Frazer, J. W., *J. Inorg. Nucl. Chem.* **16**, 23 (1960).
(6) Graham, W. H., Parker, C. O., *J. Org. Chem.* **28**, 850 (1963).
(7) Haszeldine, R. N., *Research* **4**, 338 (1951).
(8) Horner, L., Christmann, A., *Angew. Chem.* **2**, 599 (1963).
(9) Johnson, F. A., Colburn, C. B., *J. Am. Chem. Soc.* **83**, 3043 (1961).
(10) Jones, L. W., Fleck, E. E., *J. Am. Chem. Soc.* **50**, 2022 (1928).
(11) Lange, N. A., "Handbook of Chemistry," 6th Ed., p. 370, Handbook Publishers, Inc., Sandusky, 1946.
(12) Pearson, R. K., Dresdner, R. D., *J. Am. Chem. Soc.* **84**, 4743 (1962).
(13) Petry, R. C., Freeman, J. P., *J. Am. Chem. Soc.* **83**, 3912 (1961).
(14) Ruff, O., Giese, M., *Ber.* **69B**, 598 (1936).
(15) Saunders, W. H., Ware, J. C., *J. Am. Chem. Soc.* **80**, 3328 (1958).
(16) Stevens, T. E., *J. Org. Chem.* **26**, 2531 (1961).

(17) Senior, J. K., *J. Am. Chem. Soc.* **38**, 2718 (1916).
(18) Steiglitz, J., *J. Am. Chem. Soc.* **44**, 1293 (1922).
(19) Stieglitz, J., Leech, P. N., *J. Am. Chem. Soc.* **36**, 272 (1914).
(20) Stieglitz, J., Brown, R. L., *J. Am. Chem. Soc.* **44**, 1270 (1922).
(21) Vosburgh, I., *J. Am. Chem. Soc.* **38**, 2081 (1916).
(22) Weston, A. W., Michaels, R. J., Jr., *J. Am. Chem. Soc.* **73**, 1381 (1951).

RECEIVED April 28, 1965.

17

A Survey Study of the Effects of Ionizing Radiation on Volatile Inorganic Compounds of Fluorine, Oxygen, and Nitrogen

R. P. NIELSEN, C. D. WAGNER, V. A. CAMPANILE, and J. N. WILSON

Shell Development Co., Emeryville, Calif.

Publication Date: January 1, 1966 | doi: 10.1021/ba-1966-0054.ch017

A novel radiolysis technique has been used to survey the products from radiolysis of simple covalent inorganic compounds and their mixtures. After exposure to large doses of 3 m.e.v. bremsstrahlung at 77° K., samples were analyzed by distillation directly into a time-of-flight (TOF) mass spectrometer. Interesting reactions observed include formation of N_2, F_2, N_2F_2, and N_2F_4 from NF_3, and O_2, F_2, O_2F_2 and O_3F_2 from OF_2. Fluorochlorocarbons give rise to mass spectrometric peaks tentatively identified as derivatives of ClF_3. In some cases the primary reactions initiated by radiation appear to be reversed by subsequent reactions. Alone, BF_3 is inert; in the presence of NF_3, however, BF_3 forms products tentatively identified as B_2F_2 and BFNF. Evidence has also been found for the formation of species not yet identified.

Very little has appeared in the literature concerning the radiation chemistry of covalent inorganic compounds in condensed phase. In the search for new, high energy oxidizers, it appears plausible that ion fragmentation, electron capture, ion-molecule reactions, and free radical combination reactions at low temperatures may be utilized.

Conversion of several percent of low molecular weight materials by nonchain reactions requires radiation doses of the order of 100 megarads. A 3-m.e.v. Van de Graaff accelerator with a gold target supplies this dose to a small sample in less than 1 hour. The sample can be held at any desired temperature in a Dewar flask. The products, many of them highly reactive, are detected by direct distillation at low temperatures and very low pressure into a time-of-flight mass spectrometer. With this basically simple technique, a survey of radiolysis of many systems,

In Advanced Propellant Chemistry; Holzmann, R.;
Advances in Chemistry; American Chemical Society: Washington, DC, 1966.

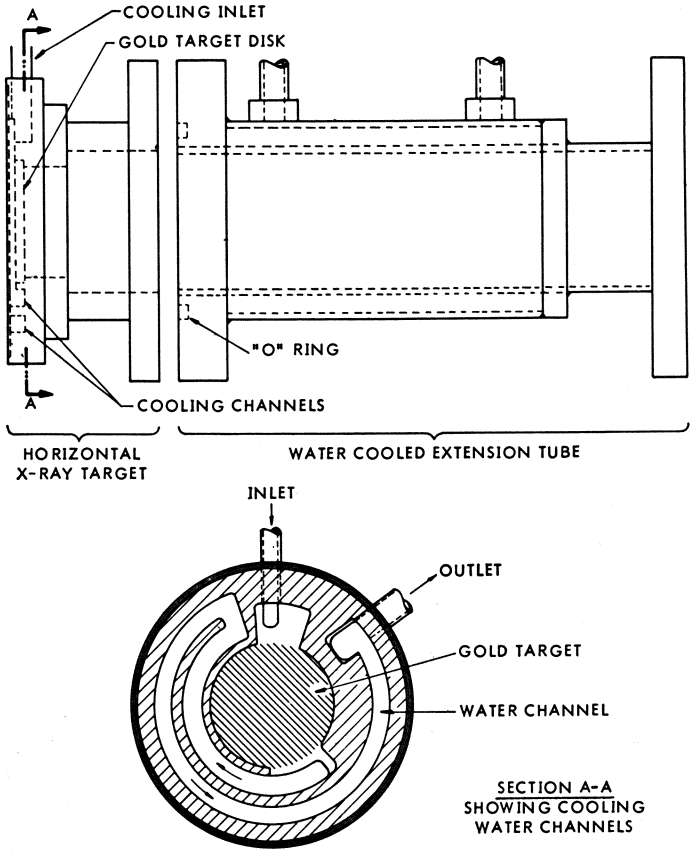

Figure 1. Horizontal x-ray target with water-cooled extension tube

both pure and binary, is under way. This report describes results obtained thus far.

Experimental

Horizontal X-ray Source. Large doses of 2–3 m.e.v. bremsstrahlung (up to 200 megarad/hour) are generated by directing the 3 m.e.v. electron beam from a Van de Graaff accelerator onto a water-cooled gold target (Figure 1). The vertical electron beam is deflected 90°, producing a horizontal beam so that sample placement may be facilitated (Figure 2).

Reaction Vessel. Samples to be irradiated are condensed into the cooled tip of a 4-mm o.d. thin-walled stainless steel tube. A brass slug, silver soldered over the end of the tube, acts as a heat sink. A metering valve (Nupro No. SS-4M) connected to the tube with Swagelok fittings and equipped with a Kel-F O-ring seal and a micrometer handle complete the vessel.

Sample Size. A standardized sample size of 0.075 mmole of reactant was chosen. In a binary reaction system the total sample comprises 0.15 mmole. These amounts provide a convenient sample for analysis and are considered to be safe in the event of an explosion in the 2-ml. reaction vessel.

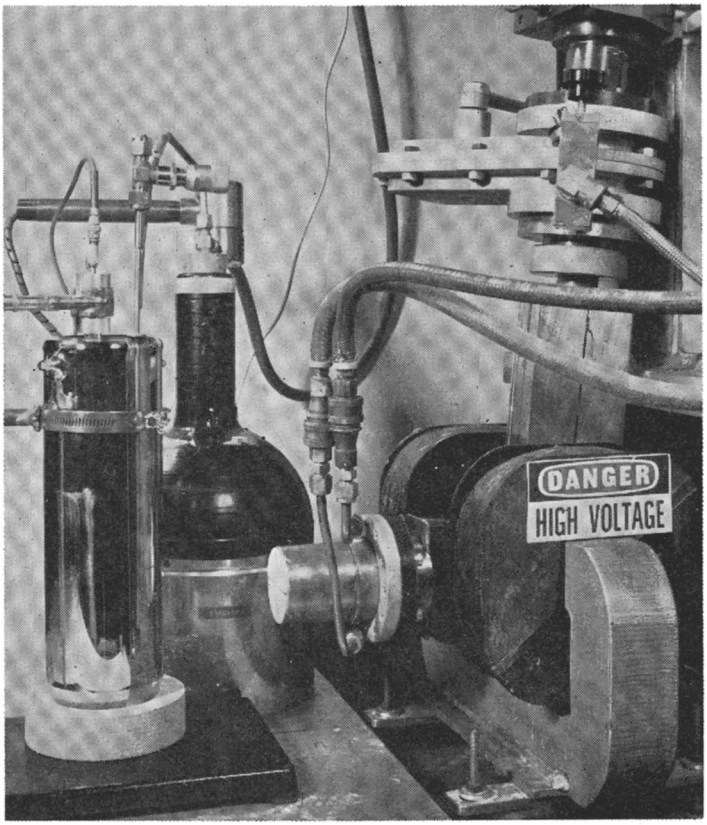

Figure 2. Apparatus for irradiation with high energy photons

Cooling Provisions. The irradiations are carried out at 77° K. by immersing the reaction vessel in liquid nitrogen within a specially constructed vacuum flask (Figure 3) which contains a cooled sidearm that is also convenient for accurately placing the sample tube. A thermocouple and demand system replenishes the liquid nitrogen as necessary.

Dosimetry. Liquid dosimeters are of too large a volume to allow accurate determination of the dose delivered to the small (~50 μliter) samples used in this study. A new cadmium dosimeter based on photoactivation has been developed by one of us (7) and is useful in this study. When cadmium nuclei are irradiated with >1.25 m.e.v. photons, metastable $^{111}Cd^{m}$ nuclei are produced which decay with a 49 minute half-life and emit 149 and 246 k.e.v. photons. A 50 μliter volume

Publication Date: January 1, 1966 | doi: 10.1021/ba-1966-0054.ch017

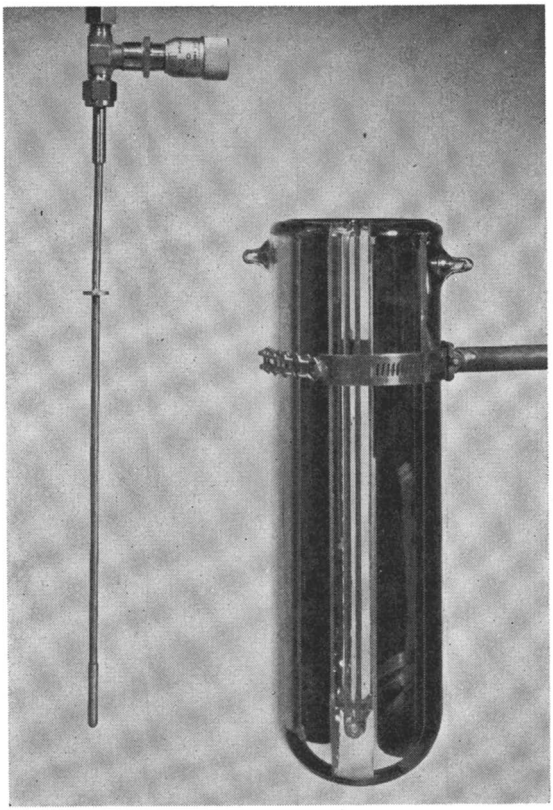

Figure 3. Special Dewar for holding sample during irradiation at −196°K.

(430 mg.) of cadmium metal which has been irradiated for 5 minutes provides a sufficient activity count for accurate dosimetry.

Analysis. The samples under study are maintained at 77° K. before, during, and after irradiation. No warming is allowed until the sample tube has been connected to the mass spectrometer and analysis for noncondensable gases is complete. At 77° F. the gases observed may include F_2, N_2, and O_2. When analysis for the noncondensable gases is complete, these gases are pumped off through another valve until the pressure reaches ~0.05 mm.; at this point analysis for gases which are condensable at 77° K. (but which exert a significant vapor pressure at this temperature) is accomplished. Both NF_3 and OF_2 are among the compounds which may be seen at this point. When these data have been collected, a 77°–350° K. variable cryostat is substituted for the liquid nitrogen bath. The sample is now slowly warmed, and sequential fractions are distilled into the Bendix time-of-flight mass spectrometer. A rough separation is thus accomplished, and the products can be identified more easily. Excess amounts of all components observed in the product mixture are pumped off at the temperature at which they are observed before the temperature is raised and the next fraction is ex-

Publication Date: January 1, 1966 | doi: 10.1021/ba-1966-0054.ch017

amined. The data thus obtained qualitatively indicate the compounds produced in the radiolysis and will serve as a guide for future work on a larger scale.

Results

Irradiations of Pure Substrates. Irradiation of one-component systems is a desirable prerequisite for the study of multi-component systems. The irradiation of a pure compound provides data which may indicate the identity of active intermediates which may then be considered for use as reactants in mixed systems. In addition, products which may be interesting in themselves may result from such treatment. Also, it is necessary to obtain as much product identification data as possible in single-component systems in order to simplify the analytical problems encountered when mixtures are irradiated.

The data in Table I are presented in the following manner: the second column lists the temperature of the sample tube from which the products are distilled into the mass spectrometer at $\sim 8 \times 10^{-6}$ mm.; the third column lists the products as identified by the mass spectra obtained at the respective temperatures, and the fourth column lists ions observed for which no identification has been made.

Table I.

Compound Irradiated	*Temp., °K.*	*Products Tentatively Identified*	*Ions Observed Source Unidentified*
NF_3	77	N_2, F_2 (*see* Figure 4)	
	100	*cis*-N_2F_2, *trans*-N_2F_2	
	134	N_2F_4	
N_2F_4	77	N_2, F_2, NF_3	
	105	*cis*-N_2F_2, *trans*-N_2F_2	
FNO	77	N_2, NO	
	123	N_2O, *cis*-N_2F_2, *trans*-N_2F_2	
	161	O_2F_2, O_3F_2,[c] N_2F_4	
	223	N_2O_4, NO_2F (?)	N_3F^+, O_2^+, N_2O^+, N_2F^+, NOF^+, $N_2O_2F^+$, $N_2OF_2^+$
	[c] 293		$N_3O_2F^+$, plus those observed at 223
ClNO	77	N_2, NO	
	195	N_2O_4, N_2O, Cl_2	
N_2O	77	N_2, O_2	
	244	N_2O_4	
NO	77	N_2	
	124	N_2O	
	243	N_2O_4	
N_2O_4	77	N_2 (no O_2)	
	176	NO, O_2, trace N_2O	
OF_2	77	F_2, O_2	
	107	COF_2,[b] O_2,[a] F_2,[a] OF_2[a]	
	128	O_2,[a] F_2,[a] CO_2[b]	
	176	O_3F_2,[c] O_2F_2, O_2,[a] Cl_2,[b]	
	219	O_2F_2, O_3F_2[c] (trace), O_2,[a] $CClF_3$ (trace)[b]	

Table I. Continued

Compound Irradiated	*Temp., °K.*	*Products Tentatively Identified*	*Ions Observed Source Unidentified*
BF_3		No products observed to 350°	
SO_2		No products observed to 350°	
SF_4		No products observed to 350°	(Note: SOF_2 present as extensive impurity made results inconclusive)
SO_2F_2	83	O_2, OF_2	
	143	CO_2 (trace)[b]	
	253	SOF_4, SF_6	SO_4F^+, $SO_2F_3^+$
SF_6		No products observed to 350°	
SiF_4		No products observed to 350°	
CF_3Cl	77	CF_4	
	293	C_2F_6, CF_2Cl_2, Cl_2, and $C_2Cl_2F_4$ or C_2ClF_5.	
CF_2Cl_2	83	CF_3Cl and possibly CF_4	
	129	Cl_2	
	188	Cl_2F_2 (?), CF_3ClF_2 and/or CF_3Cl_2F	
	293	C_2ClF_5 and/or $C_2Cl_2F_4$, as well as other unidentified C_2 and C_3 species.	
$CFCl_3$	85	CF_3Cl and possibly CF_4	
	130	Cl_2F_2 (?-trace)	
	148	Cl_2, CF_3ClF_2 (?)	
	171	C_2ClF_5 and/or $C_2Cl_2F_4$, CF_2Cl_2	
	293	C_2Cl_6	
CCl_4	208	Cl_2	
	293	C_2Cl_6, plus a C_3 species, probably C_3Cl_8.	
Kel-F No. 90 Grease $\text{-}(CF_2\text{—}CFCl)\text{-}_n$	77	CF_4	
	110	CF_3Cl	
	148	Cl_2	
	175–350	Constant fragment spectrum (see Discussion)	
CO_2		No products observed to 350°	
$(CN)_2$	293	Apparent dimer and decomposition product(s) thereof. (*see* Discussion)	
H—C≡C—H	123	C_2H_4	
	215	C_6H_6, CH_3COCH_3 (impurity), C_4H_2 (diacetylene), C_4H_4 (vinylacetylene)	
$H_2C{=}CH_2$		(*see* reference)	
$H_2C{=}CF_2$	84	H_2	
	211	$(F_2C{=}CH_2)_2$ unidentified dimeric (and trimeric) products, $F_3C\text{—}CH_2F$, HF	

[a] This species evolved from a decomposition at this temperature.
[b] From the action of the sample on the Kel-F grease on the O-ring seal.
[c] Identification uncertain; mass ambiguity with possible silicon compounds.

Irradiations of Binary Mixtures. The low temperature irradiation of binary mixtures is being studied as a unique synthetic method which may produce compounds not previously observed because of their low thermal stabilities. Their synthesis by purely chemical means may be very difficult or perhaps impossible; thus collecting data describing

such structures is a primary aspect of this study. The data below are presented in the same manner as those above (Table II).

Table II.

Compound Irradiated	*Temp., ° K.*	*Products Tentatively Identified*	*Ions Observed Source Unidentified*
NF_3 & O_2	77	N_2	
	100	F_2	NO^+, N_2O^+, NO_2^+, N_2F^+, OF^+
	143	F_2,[a] O_2,[a] FNO, N_2O, *cis*-N_2F_2, *trans*-N_2F_2, NO_2F (?)	
	211	Cl_2,[b] OF_2,[a] O_3F_2,[c] F_2,[a] O_2[a]	
	253	N_2O_4	
NF_3 & OF_2	77	N_2, O_2, F_2,	
	108	*cis*-N_2F_2, *trans*-N_2F_2, COF_2[b]	NO^+
	116	CO_2,[b] N_2O	
	211	O_2F_2	
	253	N_2O_4	
NF_3 & N_2	77	N_2, F_2	
	108	*cis*- and *trans*-N_2F_2	
	134	N_2F_4	
NF_3 & N_2O	77	N_2, O_2, F_2	
	110	*cis*-N_2F_2, *trans*-N_2F_2,	
	179	FNO, Cl_2,[b] NO_2F (?)	
	253	N_2O_4	
NF_3 & NO	77	N_2	
	83		N_2^+, NF^+
	98	*cis*-N_2F_2, *trans*-N_2F_2 (large amounts)	
	113	N_2F_4 (large amounts), N_2O	
	193	N_2O_4, FNO	
NF_3 & N_2O_4	77	N_2, F_2, trace O_2	
	111	*cis*-N_2F_2, *trans*-N_2F_2	
	148	N_2F_4, N_2O, FNO, NFO_2 (?)	O_2^+, N_2^+, NF_2^+
NF_3 & FNO	77	N_2, O_2, F_2, NO (small amount) N_2O, OF_2	
	113	*cis*- and *trans*-N_2F_2, O_2,[a] F_2[a]	
	129	N_2F_4, N_2O, O_2F_2, O_3F_2,[c] O_2,[a] F_2[a]	N_2OF^+
	203	N_2O_4, O_2[a]	
NF_3 & SO_2	77	N_2, F_2	
	99	*cis*-N_2F_2, *trans*-N_2F_2	
	123	N_2F_4, SO_2F_2, SF_4 (trace), CO_2[b]	
	169	SOF_4 (?)	
NF_3 & SO_2F_2	77	N_2, F_2	
	87	NO	
	93	*cis*- and *trans*-N_2F_2	
	108	N_2F_4, N_2O (trace)	
	126	CO_2[b]	
	203	SF_6, SOF_4, SO_4F_2	SF_5O^+, $SF_5O_2^+$, NF_2^+
NF_3 & SF_6		No products other than those of NF_3 alone observed up to 350°	
NF_3 & SiF_4		Same as above	
NF_3 & CO_2		Increased yields of normal NF_3 irradiation products as well as some COF_2	
NF_3 & CCl_4	77	N_2, CF_4	
	128	N_2F_4, *cis*-N_2F_2, *trans*-N_2F_2, CCl_2F_2	
	173	Cl_2, NF_2CCl_3 (?) →	NCl^+, NF_2CCl^+, $NFCCl_2^+$
	195	CCl_3F	
	293	C_2Cl_6	
NF_3 & C_2H_2	77	N_2	
	89	*cis*-N_2F_2, *trans*-N_2F_2	
	156	CHF=CHF	

Table II. Continued

Compound Irradiated	*Temp., ° K.*	*Products Tentatively Identified*	*Ions Observed Source Unidentified*
	186	C_6H_6, $NF_2CH{=}CHF$ (?) →	NF_2^+, CHF^+, $CHNF^+$, $C_2NF_2^+$, $C_2NF_2H^+$, $C_2NF_2H_2^+$
NF_3 & $F_2C{=}CH_2$	77	N_2, CF_4	
	130	N_2F_4, *cis*-N_2F_2, (traces) *trans*-N_2F_2 (traces)	
	293	CF_3CH_2F, $F_2NCH_2CF_3$ (?) →	NF_2^+, CF_3^+, $C_2NF_2^+$, C_2NFH^+, (weak intensities)
NF_3 & $(CN)_2$	77	N_2, F_2, CF_4	
	107	*cis*- and *trans*-N_2F_2	
	129	N_2F_4, CO_2 (impurity)	
	143	FCN (?), CF_3NF_2 (?)	
	293	Complex mixture of unidentified products	$C_4N_2^+/C_2NF_2^+$, $C_4N_2F^+/C_2NF_3^+$, $C_4N_2F_2^+/C_2NF_4^+$, $CN_2F_4^+/C_2N_3F_2^+$, $C_4NF_3^+/C_2F_5^+$, $CNF_5^+/C_3N_2F_3^+$, $CN_2F_5^+/C_3N_3F_3^+$, etc.
NF_3 & BF_3	77	N_2, F_2, B_2F_2 (?), BNF_2 (?)	
	101	*cis*- and *trans*-N_2F_2 (trans in excess)	
	148	N_2F_4, NF_3 (trace)	
	215	*cis*-N_2F_2, BF_3, N_2F_4 (trace), NF_3 (trace)	
NF_3 & Xe	77	N_2, F_2	
	100	*cis*- and *trans*-N_2F_2	
	134	N_2F_4, SiF_4 (trace)	
	243	XeF_2 (?)	
OF_2 & N_2F_4[d] (unirradiated)	77	N_2, NO, NF_3	
	137	N_2O	
	163	FNO, $F_2N{:}NO$ (?)	
	223	N_2O_4	O_2^+, NO_2^+, NO_3^+, N_2F^+, $N_2F_2^+$, N_3F^+, NOF^+, O_2F^+
OF_2 & N_2F_4 (irradiated)	77	N_2, F_2, O_2, NF_3	
	90	*cis*- and *trans*-N_2F_2[a]	
	115	N_2O, O_2,[a] FNO, OF_2,[a] NF_3[a]	
	156	O_2,[a] OF_2[a]	
	170	FNO_2 (?)	
	240	N_2O_4	
OF_2 & N_2	77	O_2, F_2, NF_3	
	107	*cis*-N_2F_2, *trans*-N_2F_2, N_2,[a] O_2,[a] O_2[a]	
	128	N_2O, CO_2, N_2,[a] O_2,[a] NO_2F (?)	N_2F^+
	191	N_2O_4	
OF_2 & O_2	77	(No F_2 observed)	
	93	O_3[c]	
	133	SiF_4[c]	
	173	CO_2,[c] COF_2,[c] O_2,[a] F_2[a]	
	192	O_3F_2,[a,c] O_2F_2, O_2,[a] Fe[a]	
OF_2 & N_2O	77	F_2, N_2, O_2	
	132	COF_2,[b] FNO, NO_2F (?)	
	199	N_2O_4	
OF_2 & NO[d] (unirradiated)	77	O_2, N_2, F_2, OF_2, NF_3	
	158	N_2O, COF_2,[b] SiF_4,[c] FNO, NO_2F (?)	
	193	N_2F_4	N_2F^+
OF_2 & FNO	77	N_2, O_2, F_2	
	143	NF_3, N_2O	
	249	N_2O_4	

Table II. Continued

Compound Irradiated	*Temp., ° K.*	*Products Tentatively Identified*	*Ions Observed Source Unidentified*
OF_2 & N_2O_4	77	O_2, F_2	
	131	O_2,[a] CO_2,[b] COF_2,[b] NO_2F (?)	
	193	O_2F_2, FNO, O_2[a]	
OF_2 & SO_2	77	O_2F, F_2, SF_2 (?) →	*m/q* 70, 51, 32 (weak intensities)
	110	SO_2F_2, SF_4, SOF_4, SF_6	
	143	CO_2[b] (trace)	
OF_2 & SF_6	77	O_2, F_2	
	137	O_2F_2, CO_2,[b] O_2,[a] F_2,[a] OF_2[a]	
	161	SOF_4	
OF_2 & SiF_4		No products other than those of OF_2 alone observed up to 350°	
OF_2 & $(CN)_2$	77	F_2, O_2	
	94	CF_4	
	129	O_2,[a] F_2[a]	
	293	Complex mixture of unidentified products.	Data too ambiguous to assign *m/q* values to specific ions.
OF_2 & CCl_4		Poor data—ambiguity exists in distinguishing OF from ^{35}Cl.	
OF_2 & Xe	77	O_2, F_2	
	98	COF_2[b]	
	107	O_2F_2, O_2[a]	
	128	O_3F_2,[c] O_4F_2,[c] O_2,[a] F_2,[a] CO_2[b]	
	270	O_2,[a] Xe[a]	
	293	XeO_2 (?)	
N_2F_4 & O_2	77	N_2, NF_3, OF_2	
	85	O_3, F_2[a] NO (trace)	
	101	N_2F_2 (both forms)	
	123	N_2O, COF_2,[b] $F_2N{:}NO$(?), FNO_2(?)	
	293	N_2O_4	NO^+, N_2^+, N_2F^+, O_2^+
N_2F_4 & N_2O	77	N_2, O_2, F_2, NO (trace), NF_3	
	93	*cis*-N_2F_2	
	237	N_2O_4	
	293		O_2^+, N_2O^+, N_2F^+, NO_2^+
N_2F_4 & N_2O_4	77	N_2, O_2, F_2, NF_3, NO (trace)	
	97	*cis*- and *trans*-N_2F_2	
	134	O_2[a] N_2O	
	151	FNO, FNO_2(?), N_3F(?)	
N_2F_4 & NO	77	N_2, NF_3	
	106	*cis*- and *trans*-N_2F_2	
	116	$F_2N{:}NO$(?)	
	176	FNO, N_2O	
	242	N_2O_4	
	293	Complex spectrum of fragments	N_2^+, NO^+, NF^+, N_2O^+, NO_2^+, N_2F^+, NF_2^+, $N_2F_2^+$
N_2F_4 & FNO	77	N_2, F_2, NO, NF_3, O_2 (trace)	
	106	*cis*- and *trans*-N_2F_2	
	125	$F_2N{:}NO$ (?)	$N_2O_2F^{3+}$, $N_2O_3F_3^+$
	170	O_2F_2	
	238	N_2O_4, O_2[a]	
N_2F_4 & $(CN)_2$	77	N_2, F_2, NF_3, FCN	
	94	*cis*- and *trans*-N_2F_2	
	159	Complex mixture which may include $CF_3CF_2NF_2$ and $(CF_3)_2NF$.	

Publication Date: January 1, 1966 | doi: 10.1021/ba-1966-0054.ch017

Table II. Continued

Compound Irradiated	*Temp., ° K.*	*Products Tentatively Identified*	*Ions Observed Source Unidentified*
	293	Complex mixture which contains the products of irradiated $(CN)_2$ as well as some unidentified fluorinated material.	
N_2F_4 & CCl_4	85	N_2, F_2, NF_3, CF_3Cl	
	110	*cis*- and *trans*-N_2F_2, CF_2Cl_2	
	148	Cl_2	
	178	$CFCl_3$	
	293	C_2Cl_6	
N_2F_4 & CO_2	87	N_2, F_2, NF_3	
	95	*cis*- and *trans*-N_2F_2, NO (trace)	
	116	O_2,[a] COF_2[b]	
	143	CO_2[b]	
	151	Complex mixture of unidentified products.	
N_2F_4 & SO_2	77	N_2, O_2, F_2, NF_3, NO (trace)	
	98	*cis*- and *trans*- N_2F_2	
	120	N_2O, SO_2F_2	
	163	SOF_4	N_2^+, NF^+, NF_2^+, SOF^+, SO_2F^+
N_2F_4 & SF_6		Only those products observed which are seen for N_2F_4 alone.	
FNO & O_2	77	O_2, N_2	
	87	O_3, O_4 (?)	
	120	N_2O	NO_2^+
	120	O_2F_2, O_3F_2,[c] O_4F_2,[c] O_2,[a] F_2,[a] *cis*- and *trans*-N_2F_2	
	210	N_2O_4	
FNO & $(CN)_2$	83	N_2, NO	
	110	FCN, *cis*- and *trans*-N_2F_2, O_2F_2	
	140	N_2O and/or CO_2	
	215	Complex mixture of unidentified products.	
BF_3 & NO	77	N_2	
	129	N_2O	
	258	FNO, BF_3,[a] *cis*-N_2F_2,[a] N_2O_4, O_2[a]	
BF_3 & N_2O	77	N_2, O_2	
	200	N_2O_4	
	293	N_2O_4,[a] O_2,[a] BF_3,[a] *cis*-N_2F_2,[a] *trans*-N_2F_2 (trace)[a]	
CF_3Cl & Xe	77	CF_4	
	112	Cl_2, C_2F_6, CF_2Cl_2	
	183	$C_2Cl_3F_3$, $C_2Cl_2F_4$, CCl_3F, XeF_2 (?) →	Xe^+ (?) ~132; XeF^+ (?) ~151; XeF_2^+ (?) ~170
Cl & Xe		No products observed up to 350°	

[a] This species evolved from a decomposition at this temperature.
[b] From the action of the sample on the Kel-F grease on the O-ring seal.
[c] Identification uncertain; mass ambiguity with possible silicon compounds exists.
[d] Mixture reacted before irradiation. Products were analyzed in the usual way.
[e] Impurity

Discussion

The basic processes which are responsible for reaction on irradiation of these covalent inorganic systems involve excitation and ionization of the molecules by the secondary electrons generated in the sample by Compton scattering. The primary species produced are excited molecule ions

and excited molecules; these species decompose to fragment ions and radicals and react with the bulk substrate and with one another to give the observed products. At present little is known of the reactions of such species at 77° K., and in this study (which is intended merely to indicate areas for promising further research) little emphasis has been placed on elucidating possible mechanisms of reactions. Such information can only be gained by considering the yields of the various products in a quantitative manner.

Without quantitative yield data one can say little concerning proposed sources of the observed products. It is even difficult without such data to state with certainty which products appear in predominant quantities and whether or not a chain reaction has been found. At this point it appears that the yields are modest and are those which one would expect of nonchain processes with G values of the order of 5–10.

Some of the problems facing the investigator in this kind of study should be mentioned before proceeding to a discussion of the irradiated systems. Many of the experimental difficulties which have been successfully solved are: applying a high dose rate of photons to a small sample, adequate cooling of the samples during irradiation, accurate dosimetry on the geometry of small samples, micro separation of the irradiation products, and analysis of micromolar amounts of highly reactive species via time-of-flight mass spectrometry. Aspects which can be improved include a method for mixing reactants in micro quantities at 77° K. to ensure an intimate mixture and perhaps a mass spectrometric method which would be capable of better identification through higher resolution. The mass spectrometric identification of compounds which are present in the mass spectrometer for a few fleeting seconds in some instances is tenuous. The ambiguity in identifying ions from their m/q values alone is also a constant source of difficulty, as in the case of polyoxygen fluorides where the $O_4F_2^+$ ion and the $HOSiF_3^+$ ion both possess a m/q value of 102, and the difference between these masses amounts to only 0.0015 a.m.u.—an unresolvable difference with a TOF mass spectrometer. Fortunately, most systems lend themselves to TOF mass spectrometry without too much ambiguity. Differences in the volatility of the compounds encountered help one to make rational decisions about the identity of the species observed (Table III).

The data presented may be considered reasonably complete with regard to the proposed identity of the products observed. Aspects of the data interpretation which are not given in the tables are discussed in the following sections which describe the irradiations of groups of related compounds and mixtures thereof.

Nitrogen Trifluoride Systems. The irradiation of NF_3 in the liquid state at 77° K. has been thoroughly studied with respect to its products;

Publication Date: January 1, 1966 | doi: 10.1021/ba-1966-0054.ch017

Table III. Emergence Order of Compounds Observed in the Mass Spectrometer and Their Approximate Distillation Temperatures at P ≅ 8 × 10⁻⁶ Torr.

Compound	*Temperature, ° K.*
H_2	77
N_2	77
O_2	77
F_2	77
NF_3	77
NO	77
OF_2	77
CF_4	77
O_3	90
O_4	90
Xe	90
C_2H_4	90
N_2F_2 (both forms)	100
CH_2CF_2	100
O_2F_2	110
FCN	110
SiF_4	110
CF_3Cl	110
COF_2	120
N_2O	125
C_2H_2	125
CO_2	125
BF_3	125
SiF_4	125
N_2F_4	125
Cl_2	130
FNO_2	140
O_3F_2 (?)	140
CF_2Cl_2	140
$(CN)_2$	150
FNO	150
SO_2	150
SF_4	160
SF_6	160
FNO_3	185
ClNO	195
N_2O_4	200
$CFCl_2$	200
CCl_4	210
C_6H_6	215
C_2Cl_6	275

however, no quantitative data have yet been collected. The following unbalanced equation lists the products:

$$NF_3 \rightsquigarrow N_2 + F_2 + \textit{cis}\text{-}N_2F_2 + \textit{trans}\text{-}N_2F_2 + N_2F_4$$

No species with more than two nitrogen atoms was found among the products. The isothermal distillation of the products observed at 77° K. into the mass spectrometer was followed until these products were largely exhausted. The distillation curves are presented in Figure 4, where it is seen that N_2, with the highest initial partial pressure, diminishes in concentration (as measured by the mass spectrometric peak intensity) with time whereas F_2 appears, and after passing through a maximum, is

quickly exhausted. The NF_3, with the lowest partial pressure initially but which is present in much larger quantities, gradually establishes a pressure steady state as evidenced by constant NF^+, NF_2,+ and NF_3+ mass spectrometric intensities. The fact that the N_2+ intensity does not disappear completely is attributed to the fact that other products—e.g., N_2F_2, contribute a small partial pressure at 77° K. and have N_2+ as the major ion in the cracking pattern.

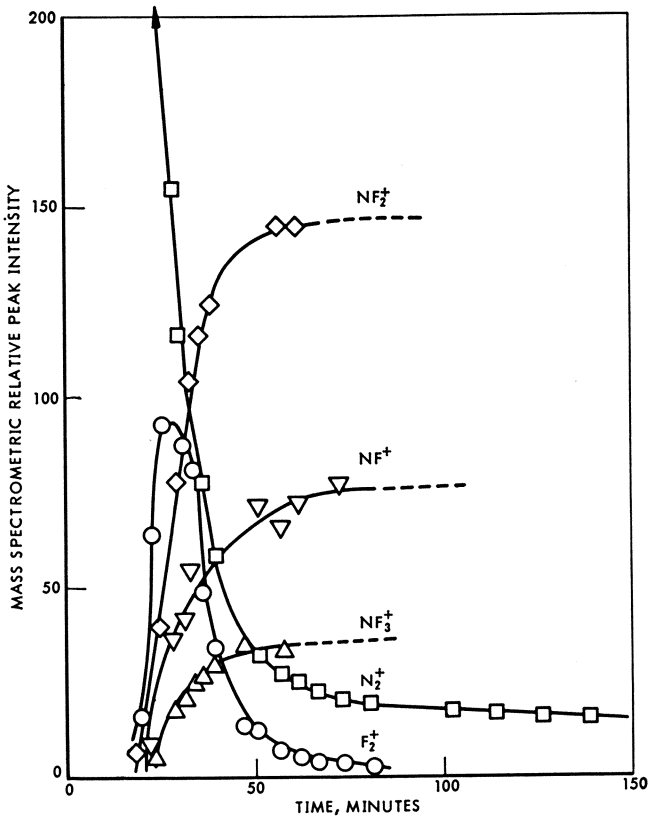

Figure 4. NF_3 irradiation product analysis. Time vs. peak intensity at 77°K.

Some thought has been given to the problem of deciding which primary, transient species are produced on irradiating NF_3. Perhaps one guide to this problem lies in the data available from mass spectrometric studies since the basic processes which occur on electron impact in the mass spectrometer (ionization and fragmentation) are also those which occur during high energy irradiation under impact of Compton electrons. The principal difference in conditions is the contrast between having the sample in a cold, condensed phase instead of in the gas

phase at low pressure. The mass spectrum of NF_3 shows NF_3^+, NF_2^+, and NF^+ as predominant ions with significant yields of N^+ and F^+ as well (*4*). The formation of the fragment ions is presumably accompanied by the production of F_2 and $\cdot F$. Similar products may arise from the initial excitation of NF_3 during radiolysis in the condensed phase, but here the detailed course of events may be modified by collisions between excited or ionized species and surrounding molecules.

The two most easily visualized processes which may occur would involve the loss or capture of an electron:

$$NF_3 + e^- \text{ (fast)} \rightarrow NF_3^+ + 2e^-$$
$$NF_3 + e^- \text{ (thermal)} \rightarrow NF_3^-$$

Subsequent processes would involve the attack of these ions on adjacent molecules, the fragmentation of the initial ion, as shown below:

$$NF_3^+ \rightarrow NF_2^+ + \cdot F$$
$$NF_3^+ \rightarrow NF^+ + F_2$$
$$NF_3^- \rightarrow \cdot NF_2 + F^-, \text{ etc.,}$$

or the eventual neutralization of the ion to produce the starting material in an excited state.

Neutralization of the fragment ions would yield the various free radicals

$$NF_2^+ + e^- \rightarrow \cdot NF_2$$
$$NF^+ + e^- \rightarrow \cdot NF$$

which, by combination reactions could yield the observed products,

$$\cdot NF_2 + \cdot NF_2 \rightarrow N_2F_4$$
$$\cdot NF + \cdot NF_2 \rightarrow \cdot N_2F_3^* \rightarrow N_2F_2 + \cdot F$$

and

$$:NF + :NF \rightarrow N_2F_2^* \rightarrow N_2 + F_2$$

Combination of $\cdot F$ with any of the other radicals would give F_2, NF_3, or $\cdot NF_2$.

Another possibility is the ion-molecule reaction

$$\cdot NF^+ + NF_3 = NF_2^+ + \cdot NF_2$$

which is probably slightly exothermic. The F^- ion could also react with any of the proposed + ions above to give as products either starting material or intermediates.

Experiments designed to demonstrate the existence of $\cdot NF_2$ radicals in the irradiated sample were carried out. A sample of NF_3 was irradiated and immediately distilled through the mass spectrometer; numerous determinations of the NF^+/NF_2^+ and NF_2^+/NF_3^+ ratios were made during

the course of the distillation of 77° K./2 $\times$ 10^{-6} torr until the sample was exhausted. There was no indication that the $\cdot NF_2$ radical was present since normal values of the ratios were obtained throughout the distillation (Table IV). Possible reasons for this result include (1) quantitative reaction of the radicals before detection either on the warm walls of the vessel above the cold region where the bulk of the sample is contained or in the cold liquid NF_3 itself; (2) insufficient volatility of the radicals at 77° K.; (3) irreversible adsorption of the radicals on the sampling system walls. Repetition of the above experiments in the presence of admixed solid xenon (in excess) did not alter the results. In these cases, however, a small amount of XeF_2 was found among the products.

Table IV. Mass Spectrometric Comparison of Irradiated NF_3 With Unirradiated NF_3

Unirradiated NF_3	*Irradiated NF_3*
$NF^+/NF_2^+ = 0.54 \pm 0.03$	$NF^+/NF_2^+ = 0.55 \pm 0.03$
$NF_2^+/NF_3^+ = 4.83 \pm 0.20$	$NF_2^+/NF_3^+ = 4.78 \pm 0.20$

In order to utilize the active intermediate species produced in the irradiation of NF_3, various compounds have been mixed with NF_3 in equimolar amounts (except where otherwise noted), and the mixtures have been irradiated at 77° K. The intent, in general, was to add N—F containing groups to the substrate molecules; it was expected that fluorination of the substrate molecule would be observed as well. Data which are pertinent and supplementary to Table II are given below.

NF_3-Nitrogen Oxide Systems. Several generalizations can be made concerning the radiolysis of these systems, which contain N_2O, NO, or N_2O_4:

(1) N_2, O_2, and F_2 are always produced; however, in the NF_3-NO system both O_2 and F_2 are quantitatively removed by reaction with the substrate:

$$2\ NO + O_2 \rightarrow N_2O_4$$

$$2\ NO + F_2 \rightarrow 2\ F{-}N{=}O$$

(2) N_2O is always produced and displays unusual behavior. Whereas N_2O normally distills at 115°–130° K. in our system, some of the N_2O has appeared at 77° K. This suggests that either N_2O is formed in the gas phase and is trapped there among the noncondensable gases or that a more volatile form of N_2O, possibly a three-membered ring cyclic structure, is generated and distills at a lower temperature than does the linear N_2O.

(3) FNO_2 appears to be a product in the case of N_2O and N_2O_4 but not in the case of NO which apparently accepts most of the available F_2 and $\cdot F$.

(4) N_2O_4 is always produced, and in systems which also yield oxygen a part of the O_2 does not distill at 77° K but appears at elevated temperatures simultaneously with N_2O_4. This behavior suggests that

Publication Date: January 1, 1966 | doi: 10.1021/ba-1966-0054.ch017

either O_2 is trapped in the crystal lattice and is released as the N_2O_4 melts or that a complex has been formed during the irradiation and decomposes as the temperature is raised to give the observed products; some possible complexes could decompose as shown below:

$$2\ O_2 \cdot NO = N_2O_4 + O_2$$

$$2\ O_2 \cdot NO_2 = N_2O_4 + 2\ O_2$$

$$2\ NO_3 = N_2O_4 + O_2$$

(5) the normal products from the irradiation of NF_3 alone are found among the products.

NF_3–BF_3. Although the irradiation of BF_3 alone has not been observed to give products, admixture with NF_3 may lead to the production of new compounds. Mass spectrometric evidence has been obtained for what are thought to be two unique species, B_2F_2 and BFNF. They appear to distill from the product mixture at low temperatures (77° K.), thus indicating high volatility and probable monomeric structures, which might be formulated as shown below:

F—B=B—F F—B=N—F

These structures would be unusual because of boron's great reluctance to form double bonds in normal chemical systems. Doubly bonded boron-oxygen systems have been mentioned in the literature, however (*9*), as have certain hyperconjugated systems (*2*) involving boron and carbon.

A partial separation of the two forms of N_2F_2 which are normally produced in the irradiations of NF_3-containing systems is achieved in the NF_3-BF_3 mixture. Most of the *trans*-N_2F_2 produced is observed to distill at the normal distillation temperature of about 100° K. However, a large part of the *cis*-N_2F_2 does not appear until the temperature is raised to 215° K. The BF_3 is largely removed from the system by distillation at 148° K. A part of this material, however, is also observed at 215° K. This indicates that both species are generated at or around 200° K., and it is logical to assume that the known *cis*-N_2F_2–BF_3 complex (*10*) at that point is undergoing decomposition:

$$(N_2F^+)BF_4^- = cis\text{-}N_2F_2 + BF_3$$

The simultaneous appearance of *cis*-N_2F_2 and BF_3 at a distillation temperature above 200° K. was also observed in the systems NO-BF_3 and N_2O-BF_3.

Small quantities of N_2F_4 and NF_3 which appear along with N_2F_2 at 215° K. suggest that either some reaction involving N—F species is occurring, or that these species were trapped in the BF_3 crystal lattice and are released as the BF_3 melts (146° K.).

NF_3-Olefin Systems. Mixtures of NF_3 with ethylene and 1,1-difluoroethylene (as well as acetylene) were irradiated to see if addition across the olefinic double bond might occur or whether N—F groups might be incorporated into the molecule by some other means. The

data were much too complicated to interpret; the presence of hydrogen in these systems provided a great deal of ambiguity with respect to mass spectrometric m/q values, many of which could be attributed to several ion fragments. It is known that products are formed in these irradiations, but no conclusive identification has been possible. In the case of the irradiation of NF_3 and CCl_4, it is thought that F_2NCCl_3 may be among the products. However, no other carbon-containing NF compound has yet been seen. Data have been obtained for the irradiations of the carbon-containing compounds in the absence of NF_3, however.

Oxygen Difluoride Systems. The irradiation of liquid OF_2 at 77° K. generally follows the lines established for NF_3. The products are as shown below (unbalanced):

$$OF_2 \rightsquigarrow O_2 + F_2 + O_2F_2 + O_3F_2$$

Detecting O_3F_2 was complicated by the decomposition of this species at the temperature at which it is observed. Evidence for the ·OF radical was sought by distilling a freshly irradiated sample of OF_2 directly into the mass spectrometer at 77° K. As the data (Table V) demonstrate, no free ·OF is observed.

Table V. Mass Spectrometric Comparison of Irradiated OF_2 with Unirradiated OF_2

Unirradiated OF_2	*Irradiated OF_2*
$OF^+/OF_2^+ = 2.42 \pm 0.10$	$OF^+/OF_2^+ = 2.40 \pm 0.10$

Adding an excess amount of xenon to this system to provide a solid matrix for possible isolation of the ·OF radical and to make energy transfer more favorable did not affect the ratios reported above. A xenon compound was observed among the products, however, and this species is characterized by three mass spectrometric quintuplets (which characterize the five most abundant Xe isotopes) found at 129, 145, and 161; these are thought to represent Xe^+, and XeO^+, and XeO_{2+}, which would indicate that the product is either XeO_2, a previously unseen oxide, or some higher oxide such as the known XeO_3. Although XeF_6 can be converted to XeO_3 by hydrolysis, similar treatment of a possible source of XeO_2, XeF_4, does not yield XeO_2, but instead gives Xe and XeO_3 according to the following equation (3):

$$3\ XeF_4 + 6\ H_2O = 2\ Xe + XeO_3 + 1.5O_2 + 12\ HF$$

Thus, the possible existence of XeO_2 is interesting in that it does not seem to be easily observed by conventional means. The appearance of the postulated XeO_2 was accompanied by Xe and O_2 in the mass spectrometer, which may indicate a low degree of stability above 200° K.

The intermediate species present in an irradiated sample of oxygen difluoride can presumably be discussed in much the same way as for

those in NF_3, but the nature of the products is somewhat different. Until we have quantitative data concerning the yields of the various higher oxides of fluorine from F_2O, we hesitate to propose a mechanism for their formation.

OF_2-Nitrogen Oxide Systems. Similar products are found in all the irradiations of OF_2 mixed with nitrogen oxides. In the case of NO, the system reacts chemically at 77° K. to such an extent that any radiolysis products that would be obtained from such a mixture would comprise but a small fraction of the total products; hence, no irradiation was performed on this system. The chemical results are reported in Table II. It appears that NO is produced in the radiolysis of both OF_2-N_2O and OF_2-N_2O_4. In the former case no NO is seen as such, but large amounts of FNO are seen, probably as the end chemical product of the NO produced by irradiation. In the case of OF_2-N_2O_4 some NO is observed as such, but only after all of the F_2 produced has been pumped off at 77° K.

A 47 peak was observed in the mass spectrum obtained when an irradiated mixture of N_2O and OF_2 was distilled at 132° K. This peak may be N_2F^+ from N_2F_2 or COF^+ from COF_2; these two ions are indistinguishable in a low resolution mass spectrometer. The latter compound has been observed to result from attack by F_2O or its radiolysis products on the Kel-F grease used to lubricate the O-ring seals in our metering valves; it is usually accompanied by CO_2 at close to the same distillation temperature. In the experiment under discussion, however, any CO_2^+ would be indistinguishable from N_2O^+.

Some O_2F_2 is observed as a product from the irradiated mixture N_2O_4/OF_2 but not from the mixture N_2O/OF_2. Since O_2F_2 is a product from the irradiation of OF_2 alone, we wonder what intermediate species in the OF_2/N_2O system interferes with its formation.

OF_2-O_2 and OF_2-N_2. Little difference is noted between pure OF_2 and the OF_2-O_2 system, other than the production of appreciable amounts of O_3 in the latter case and perhaps some enhancement of the O_3F_2 yield. With N_2 present in tenfold excess, the irradiation of an OF_2-N_2 mixture gives an extraordinary number of nitrogen-containing products, including NF_3, N_2F_2, N_2O, FNO_2, and N_2O_4. This exotic form of "nitrogen fixation" has a parallel in the NF_3-O_2 system, which produces a similarly large number of oxygen-containing products, which is probably more expected.

Sulfur-Containing Systems. Irradiation of SO_2, SF_4, or SF_6 gives no observed volatile products. Sulfuryl fluoride on the other hand was found to produce a number of products; these include O_2, OF_2, SF_6, SOF_4, and some species with the probable stoichiometric formula F_2SO_4 (the compound FSO_2-OOF is known).

Mixtures of either NF_3 or OF_2 with these sulfur compounds have been irradiated to see if the $—NF_2$ or —OF group could be incorporated

into the molecule. In the case of SF_6 no products containing sulfur were observed with NF_3, but a small amount of what is thought to be SOF_4 was formed during the radiolysis with OF_2. The fact that SF_6 gives no products when irradiated alone may demonstrate the reversibility of expected reactions such as these:

$$SF_6 \rightleftharpoons SF_4 + F_2$$

$$2\,SF_6 \rightleftharpoons F_5S{-}SF_5 + F_2$$

In the presence of active oxygen-containing species the SF_4 formed above or some other intermediate may react to form SOF_4, but in the case where only nitrogen-containing species are present attack by fluorine may once again provide a pathway back to SF_6. The SOF_4 is apparently fluorine resistant under these conditions whereas similar nitrogen-substituted compounds are not.

Sulfur dioxide is fluorinated when it is irradiated in the presence of either NF_3 or OF_2, and the products in both cases include SO_2F_2 and SOF_4. Sulfur tetrafluoride itself is observed in the former case but not in the latter, demonstrating some sensitivity of SF_4 towards further oxidation to SF_6 or SOF_4 since both of these are formed in the latter case.

Sulfur tetrafluoride was not studied in detail because of its low purity. The amount of impurities that are difficult to remove from this material probably exceeds the overall radiation yield. The major impurity in commercially available SF_4 is SOF_2. Since one sulfur atom is equivalent to two oxygen atoms in a low resolution mass spectrometer, some confusion results in interpreting the mass spectra, and the system was not studied in detail.

Cyanogen Systems. The cyanogen systems have proved to be very interesting and are an obvious source of many products which probably have not been seen previously. Unfortunately the C–N–F and the

Table VI. Mass Spectrum of Cyanogen at 70 e.v. of Electron Accelerating Voltage[a]

Primary Ions			*Secondary Ions*		
Mass	*Ion*	*Intensity*	*Mass*	*Ion*	*Intensity*
12	C^+	4.0	48	C_4^+	0.0012
14	N^+	0.78	50	C_3N^+	0.051
24	C_2^+	3.8	62	C_4N^+	0.0014
26	CN^+	10.7	64	$C_3N_2^+$	0.026
28	N_2^+	0.1	76	$C_4N_2^+$	0.0008
38	C_2N^+	2.4	78	$C_3N_3^+$	0.024
40	CN_2^+	0.1	104	$C_4N_4^+$	0.004
52	$C_2N_2^+$	100.0			

[a] Taken in an Atlas model CH4 mass spectrometer at a pressure of 1.7 mm. Hg in the gas reservoir (5).

C–N–F–O mass tables of atom combinations up to four atoms each per formula reveal many ions with equivalent mass numbers which makes

Publication Date: January 1, 1966 | doi: 10.1021/ba-1966-0054.ch017

it virtually impossible to identify unknown species. Thus the system $(CN)_2$ and NF_3, $(CN)_2$ and OF_2, and $(CN)_2$ and N_2F_4 will be studied thoroughly only when we are prepared to scale up our operations to the point where we may obtain characterizable amounts of the products. The data collected thus far are listed in Table II.

Cyanogen itself provides a good example of our original ideas concerning the similarities of the processes occurring in the mass spectrometer and those occurring under the influence of ionizing radiation. Consider the reported mass spectrum of cyanogen in Table VI. Here we see that under conditions of high pressure in the mass spectrometer a variety of ion-molecule reactions occur which result in the appearance of secondary ions which may be attributed to an "ionized cyanogen dimer," $C_4N_4^+$, and other ions which result from ion-molecule reactions followed by fragmentation (Table VII). Table VIII shows the mass spectrum of the products of irradiated cyanogen obtained after the more volatile products have been removed by distillation.

A comparison of Tables VI, VII, and VIII shows that the less volatile products of the irradiation of cyanogen resemble the secondary ions

Table VII. Ion-Molecule Reactions in Cyanogen (5)

Secondary Ion	*Reaction*
$C_4N_4^+$	$C_2N_2^+ + C_2N_2 = C_4N_4^+$
$C_3N_3^+$	$C_2N_2^{+*} + C_2N_2 = C_3N_3^+ + CN$
$C_4N_2^+$	$C_2N_2^{+*} + C_2N_2 - C_4N_2^+ + N_2$ (20%)
	$C_2^+ + C_2N_2 = C_4N_2^+$ and/or (80%)
	$C_2N^+ + C_2N_2 = C_4N_2^+ + N$
$C_3N_2^+$	$CN^+ + C_2N_2 = C_3N_2^+ + N$
C_4N^+	$C_2N^+ + C_2N_2 = C_4N^+ + N_2$ and/or
	$C_2^+ + C_2N_2 = C_4N^+ + N$
C_3N^+	$C_2N^+ + C_2N_2 = C_3N^+ + CN_2$ and/or
	$C_2^+ + C_2N_2 = C_3N^+ + CN$
C_4^+	$C_2N^+ + C_2N_2 = C_4^+ + N_2 + N$ and/or
	$C_2^+ + C_2N_2 = C_4^+ + N_2$

* i_s/i_p of the reaction $H_2O + H_2O = H_3O^+ + OH$ was equal to 2.10^{-2} at the same pressure in the gas reservoir and the same repeller field strength.

Table VIII. Fragments Observed in the Mass Spectrum of the Products From the Irradiation of Cyanogen[a]

Mass	*Ion*	*Relative Intensity*
26	CN^+	3.4
28	N_2^+	100.0
36	C_3^+	15.2
38	C_2N^+	50.9
48	C_4^+	25.4
50	C_3N^+	27.2
52	$C_2N_2^+$	44.1
54	CN_3^+	44.1
76	$C_4N_2^+$	86.5
104	$C_4N_4^+$	3.4

[a] This spectrum obtained from products distilled at 293° K/2 × 10^{-6} torr.

produced in the mass spectrometer by ion-molecule interactions. This observation emphasizes the importance of ion-molecule reactions during irradiation. Although specific products have not yet been identified, one of the products appears to be a dimer of questionable stability which, from the mass spectrometric data (which shows the N_2^+ ion and the $C_4N_2^+$ ion as predominant species), seems to decompose into another product with the elimination of nitrogen.

$$C_4N_4 \rightarrow C_4N_2 + N_2$$

There are additional ions in the mass spectrum which probably come from other products of the irradiation; these compounds will be investigated in detail later as we obtain larger amounts of these interesting products.

Nitrosyl Halide Systems. Although some difficulty has been encountered in maintaining the purity of F—N=O and Cl—N=O in our apparatus prior to irradiation studies, we have obtained interesting data both with neat systems and the mixed systems as well. Again, with three or four different atoms in the molecules under study, we find many ambiguities in assigning mass spectrometric m/q values to specific ions; thus we can say little concerning the identity of products from these irradiations.

As in the cases of other unsaturated molecules, such as ethylene (*10*) 1,1-difluoroethylene, and cyanogen, where ion-molecule dimerization seems to play a major role in determining the products of low temperature radiolysis, F—N=O and Cl—N=O also appear to undergo a dimerization and possibly a trimerization in addition to other kinds of reaction.

Among the products of the irradiation of FNO are found all of the nitrogen oxides, the various known polyoxygen fluorides, nitrogen, oxygen, and possibly FNO_3, as well as the proposed dimers and trimers. The evidence for polymeric (FNO) was obtained from the product distillate at 223° K. where the mass spectrometric data shown in Table IX were obtained.

These data obviously represent a number of products observed at this temperature; unfortunately, accurate intensity values were not obtained because of wide pressure fluctuations which occurred during distillation. The amounts of individual products are very small; thus they are quickly exhausted and the mass spectra were of necessity recorded in a minimum of time. Further work is necessary to identify these products with certainty. Data on other nitrosyl halide work are found in Table II.

Halocarbon Systems. The irradiations of CF_3Cl, CF_2Cl_2, $CFCl_3$, and CCl_4 have been studied at low temperatures. In general, the products from CCl_4 are those which have been reported in the literature, namely, Cl_2, C_2Cl_6, etc. (*6*). The fluoromethanes, however, show some very interesting products, which of course require further confirmation. Prob-

Publication Date: January 1, 1966 | doi: 10.1021/ba-1966-0054.ch017

Table IX. Mass Spectrometric Data From the 223°K./2 × 10^{-6} Torr Distillate From the Products of Nitrosyl Fluoride Irradiation

Mass	*Ion*
28	N_2^+
30	NO^+
32	O_2^+
33	NF^+
44	N_2O^+/CO_2^+
46	NO_2^+
47	N_2F^+/COF^+
49	NOF^+
51	OOF^+
52	NF_2^+
61	N_3F^+ (?)
63	N_2OF^+
79	$N_2O_2F^+$
81	NO_3F^+
82	$N_2OF_2^+$
93	$N_3O_2F^+$
95	$N_2O_3F^+$

ably all of these compounds produce CF_4 on irradiation; also the various fluorochloromethanes are interconverted to some extent, and we thus see as products CF_3Cl, CF_2Cl_2, $CFCl_3$, and possibly CCl_4 as well as various C_2 perhalogenated compounds.

More interesting, however, is the observation among the mass spectrometric data of the following ions: 54 (ClF^+), 73 (ClF_2^+); 89 (Cl_2F^+), 108 ($Cl_2F_2^+$) weak; 142 ($CClF_5^+$); 158 ($CCl_2F_4^+$). These groups of ions and their supporting, smaller fragments were observed among different fractions of distillates from irradiated fluorochloromethanes at various temperatures. Suggested molecular sources for these ions are shown below (Table X).

Table X. Fragment Ions Observed in the Mass Spectra of the Products From Irradiation of Fluorochloromethanes

Ion	*Possible Source*
ClF^+, ClF_2^+	ClF and/or ClF_3
Cl_2F^+, $Cl_2F_2^+$	Cl—Cl—F | F
$CClF_5^+$	F_3C—Cl—F | F
$CCl_2F_4^+$	F_3C—Cl—Cl | F

If the proposed structures can be demonstrated to be true products of these irradiation experiments, they will constitute the first members of a new class of compounds where other substituents replace fluorine atoms in the parent molecule chlorine trifluoride.

Kel-F No. 90 grease was irradiated to determine the products formed at room temperature. Since the equipment used in these studies is lubricated with this material and since the grease is irradiated along with

Table XI. Products/Ions From the Irradiation of Kel-F No. 90 Grease, $\leftarrow CF_2CFCl \rightarrow_x$

Products (77°–150° K.)	*Ion Background (175°–350° K.)*
CF_4	69 (CF_3^+)
	85, 87 (CF_2Cl^+)
CF_3Cl	89 (Cl_2F^+)
	93 ($C_3F_3^+$)
Cl_2	101, 103, 105 ($CFCl_2^+$)
	109 ($C_3ClF_2^+$) weak
	116, 118 ($C_2ClF_3^+$)
	135, 137 ($C_3ClF_4^+$)
	152, 154, 156 ($C_2Cl_2F_2^+$)
	164, 166, 168 ($C_2Cl_4^+$) weak

the sample in such a way that the products of the grease may enter the mass spectrometer along with the desired products, it was deemed desirable to determine what background, if any, is contributed by the grease products. Indeed the grease does yield products, and these products fall into two categories: (1) those which immediately enter the mass spectrometer at low distillation temperatures; (2) those which are retained in the grease and are slowly desorbed from the grease during the entire analysis. The latter situation provides the experimenter with a more or less constant background which, once all the ions have been identified, provides "mass markers" in the higher mass regions (Table XI).

Conclusion

The technique described and the results obtained indicate that low temperature radiation synthesis is a tool which may be valuable in studying endothermic oxidizing agents of low thermal stability. Although no quantitative product distribution has been measured, and some of the products are still not identified, the guidelines established by a survey study such as this will be valuable in choosing systems worthy of further study. The mass spectrometric analysis scheme for the product mixtures will provide a monitoring system in guiding the separation of larger amounts of the irradiation products. Other techniques, such as gas chromatography, infrared and ultraviolet spectroscopy, as well as NMR, will, of course, have to be applied to characterize the products.

Acknowledgment

This work was supported by the Advanced Research Project Agency, Department of Defense under contract No. DA-31-124-ARO(D)-54 monitored by the Chemistry Division, U. S. Army Research Office, Durham, N. C.

Literature Cited

(1) ARPA Propellant Contractors Synthesis Conference, IIT Research Institute, Chicago, April 13–15, 1964.
(2) Adams, Roy M., Siedle, A. R., "Boron, Metallo-Boron Compounds and Boranes," R. M. Adams, ed., p. 404, Interscience, New York, 1964.
(3) Appelman, E. H., Malm, J. G., *J. Am. Chem. Soc.* **86**, 2141 (1964).
(4) Colburn, C. B., Kennedy, A. J., *J. Am. Chem. Soc.* **80**, 5004 (1958).
(5) Henglein, A., Jacobs, G., Muccini, G. A., *Z. Naturforsch.* **18A**, 98 (1963).
(6) Johnston, F. J., *et al.*, *J. Phys. Chem.* **65**, 728 (1961).
(7) Wagner, C. D., Shell Development Co., work to be reported elsewhere.
(8) Wagner, C. D., *J. Phys. Chem.* **66**, 1158 (1962).
(9) White, D., Mann, D. E., Walsh, P. N., Sommer, A., *J. Chem. Phys.* **32**, 488 (1960).
(10) Zletz, A. *et al.*, American Oil Co., *Quart. Repts.*, Contract No. DA-31-124-ARO (D)-78, Feb.–May 1964.

RECEIVED April 27, 1965.

18

Synthesis of OF_2 by Electrolysis of Wet HF

JOHN A. DONOHUE, THOMAS D. NEVITT, and ALEX ZLETZ

Research and Development Department, American Oil Co., Whiting, Ind.

Publication Date: January 1, 1966 | doi: 10.1021/ba-1966-0054.ch018

The electrolysis of wet hydrogen fluoride produces a mixture of oxygen difluoride, ozone, and oxygen at the anode. The effects of electrolysis variables on product yields and anode life were studied at water concentrations from 0.2 to 7.8%. Methods were also developed for analyzing the anode products by gas chromatography and for measuring the water content of the hydrogen fluoride in situ by infrared spectroscopy. Brief, periodic interruptions of the cell current during electrolysis give consistent yields of oxygen difluoride at current efficiencies of at least 45% for several hours. No loss of anode material was detected. Potentially, this direct electrolytic synthesis of oxygen difluoride is less expensive and more efficient than the conventional two-step synthesis in which fluorine produced by electrolysis reacts with aqueous alkali.

Oxygen difluoride (OF_2) is an attractive oxidizer for many fuels (*11*, *16*), especially hydrocarbons, because it provides the optimum O/F ratio for hydrocarbon oxidation. Since it is denser than the equimolar O_2-F_2 mixture (Flox), it should be easier to handle and should perform better. However, OF_2 has been expensive to make because the usual preparation from F_2 plus base (*18*) converts half the F_2 to F^-. Consequently, the less attractive but lower cost Flox mixtures have received more attention. A better synthesis for OF_2 would remove this obstacle and justify a more thorough investigation of its performance.

While OF_2 was first identified in the electrolysis of wet HF in 1927 (*7*, *8*, *13*, *14*), this process was not suggested for OF_2 production until 1955 (*10*, *15*). Yields of 60% OF_2 have been claimed for electrolysis of HF containing from 1–20% water (*9*). However, we find that OF_2 yields vary with the water concentration.

In a study to determine whether the OF radical is an intermediate in the electrolysis of wet HF, we have found conditions that ensure

In Advanced Propellant Chemistry; Holzmann, R.;
Advances in Chemistry; American Chemical Society: Washington, DC, 1966.

consistent and satisfactory yields of OF_2. The effects of water, time, and current interruption on product yields and on anode surface are presented. Analyses developed for this work are also presented.

Experimental

Equipment. The electrolysis cell is shown in Figure 1. It is a 300-ml. Kel-F cup equipped with a stainless steel cap and a Teflon gasket. (The liquid level can be observed through the translucent Kel-F.) The cap contains: a thermocouple well and electrode leads; separate ports for introducing electrolyte and water, replacing anodes, and flushing with helium; separate lines for circulating the electrolyte to an infrared cell and for passing the gaseous products through a dry ice (—78° C.) condenser and a NaF scrubber to remove the last traces of HF. During the electrolysis, the cell is immersed in an ice bath.

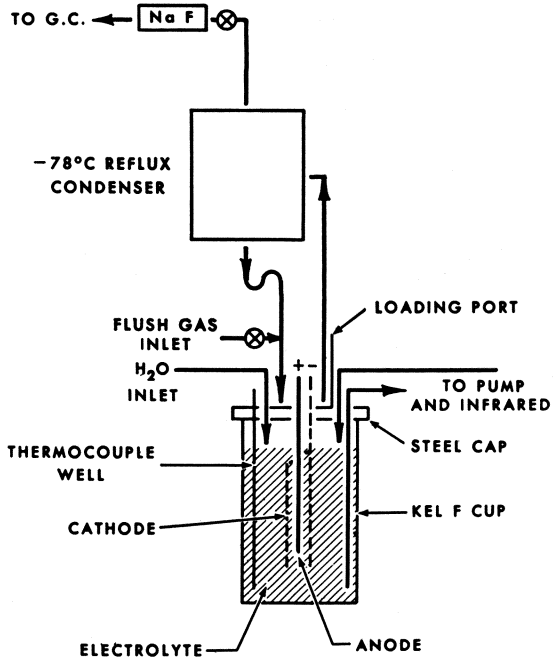

Figure 1. HF electrolysis cell

The power supply is an Electro Products model D-612T. For automatic interrupted operation, it is connected to the electrolysis cell through a mercury relay operated by a Flexopulse timer (Eagle Signal Corp.). Voltages are read at the power supply and corrected for IR drop in the leads to the cell.

Procedure. Incremental amounts of water were added to 250 ml. of HF containing 1 mole % of KF, the solution was electrolyzed with nickel anodes, and the gaseous products were analyzed periodically. In

later experiments water was added continually to replace that lost by electrolysis. Current density was followed continually.

For study of anode surface deposits and weight changes, the anode was removed, rinsed with HF to remove KF, and dried at reduced pressure.

In our earlier runs without continuous infrared analysis, the cell temperature was 0°–3° C. However, when the electrolyte was circulated for infrared analysis, the cell temperature rose to 10°–15° C.

Gas Analysis. Analysis of gaseous products—H_2, O_2, O_3, OF_2, and possibly F_2—has been improved periodically. At first the gaseous products were passed through KI solution, and O_3 and OF_2 were estimated from the amounts of I_2 and F^- produced. Gas chromatography on silica gel (*4, 6*) was used next. Our latest setup is temperature programmed as shown schematically in Figure 2. The apparatus uses only dry, degreased metals and fluorocarbon plastics passivated with OF_2 and O_3. The 6-inch column length is a compromise to minimize O_3 decomposition and still permit separation of H_2 and O_2 at a convenient temperature.

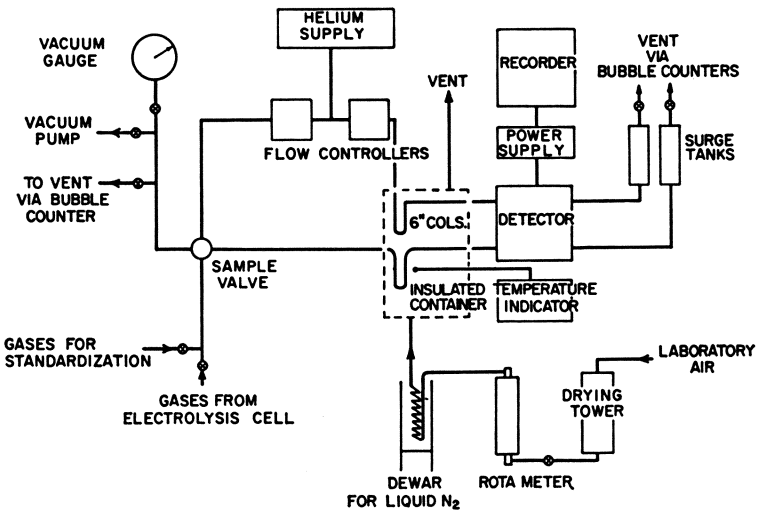

Figure 2. Low temperature programmed gas chromatograph

In a typical analysis the columns are cooled to about —75° C. by dry air precooled by liquid N_2. Then the gas sample is injected into one column by a Perkin-Elmer sampling valve; the second column is for reference. After sampling is complete, the liquid N_2 is removed, and the air flow is continued for about 5 minutes or long enough to warm the columns to about —10° C. and remove the O_3. Yields, as percent of current, are calculated from the gas chromatographic, amperage, sample volume, and total gas flow measurements.

This analysis has limitations. The thermal conductivity detector has a low sensitivity for H_2; yet high concentrations cannot be allowed because response is not linear. Consequently, the flow of helium through the electrolysis cell must be adjusted to keep the H_2 concentration in the sensitive range.

Publication Date: January 1, 1966 | doi: 10.1021/ba-1966-0054.ch018

Even after prolonged passivation, the components of the system still react with F_2 so that only qualitative trace peaks are obtained. However, F_2 production occurs outside the usual range of conditions for OF_2 synthesis. Thus, the F_2 analysis is less important.

Because O_3 decomposes readily (*17*), the true O_3 yields may be higher than found, and the O_2 yields may be correspondingly lower.

Determination and Control of Water Concentration. The water content of the electrolyte is monitored continuously by infrared absorption at 1.95μ (*12*) as shown schematically in Figure 3. The motor-driven syringe (Figure 3) is used to add water to the electrolyte and thus to maintain a constant water concentration during electrolysis. A diaphragm pump (all parts that contact the electrolyte are Teflon except the Hastelloy C balls in the check valves) circulates the electrolyte to an Infracord through FEP Teflon or Kel-F tubing. The cells are made of FEP tubing compressed to a thickness of about 2 mm. between CaF_2 plates. However, gradual fogging of the tubing and the CaF_2 plates causes a slow shift in base line so the usual absorbance *vs.* concentration calibration cannot be used. Instead, a "compensated" transmittance (T_c) *vs.* concentration is calculated from the absorption at 1.12μ where H_2O does not absorb:

$$T_c = \frac{\%T\ 1.95\mu \text{ of electrolyte } vs. \text{ screen}}{\%T\ 1.12\mu \text{ of electrolyte } vs. \text{ air}}$$

Recently, a Kel-F cell without CaF_2 plates has given little if any fogging. To increase the sensitivity, a metal screen is placed at the widest aperture of the reference beam to balance the instrument to near full-scale reading when the cell containing the dry electrolyte is in the same beam.

KF absorbs at 1.95μ but did not interfere because its concentration was held constant.

While hydrogen peroxide is a possible electrolysis product, its concentration never exceeded 0.005 mole %. Added concentrations of 0.05 mole % had a negligible effect on the 1.95μ absorption.

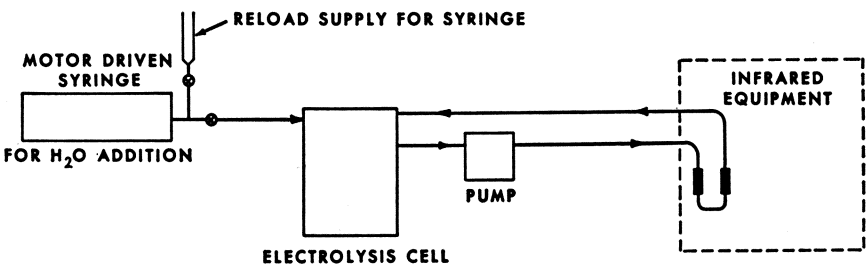

Figure 3. Arrangement for continuous water control and analysis by infrared

Results

The effect of water concentration on the product distribution is shown in Figure 4. Electrolysis was continuous, and water was added incrementally. As water increased beyond about 0.5%, the OF_2 yield

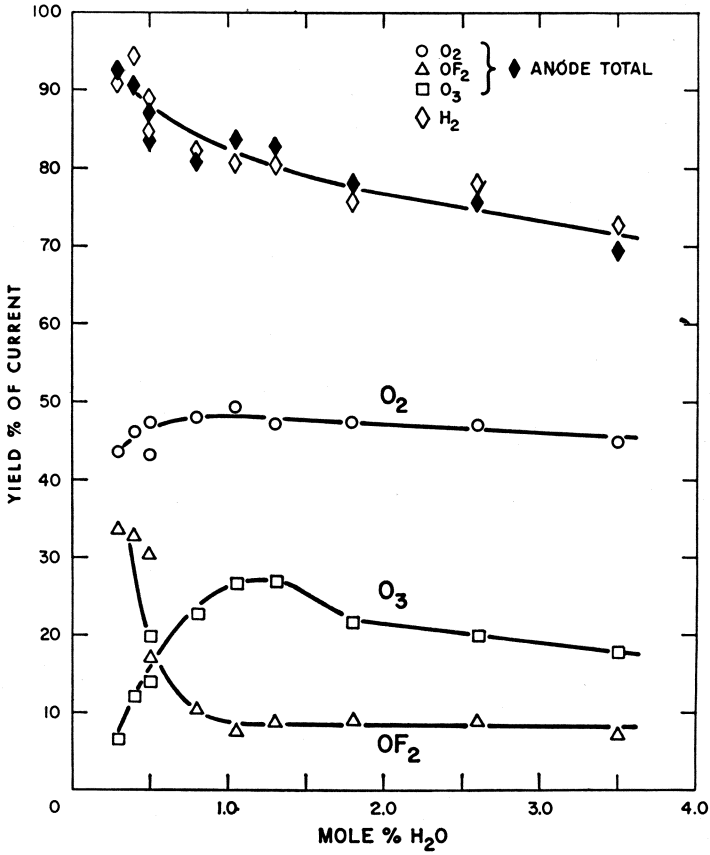

Figure 4. Yields at changing water concentration. KF ≈ 1 mole %, volts = 7.0–7.3, temperature = 2°–3°C.

dropped very rapidly and then leveled out at 7–10% OF_2. Ozone increased as OF_2 decreased and appeared to pass through a broad maximum. Oxygen was constant at 45–50%. Current efficiency for H_2 and total anode gas decreased as water increased, possibly because the cathode was depolarized by dissolved anode products.

Figure 5 shows three sets of data for OF_2 yields. Curve A is the same run shown in Figure 4. Curve B is also a continuous run except that the water concentration was high initially and decreased as water was consumed. Curve C is a run in which electrolysis was stopped after each sample had been taken for gas analysis, and water was added before electrolysis was resumed. The yield of OF_2 was not the same at a given water concentration, but depended on the manner of operation. All three curves show a maximum in OF_2 yield at less than 1 mole % followed by a decrease as water increases. However, interrupting the

current increased the OF_2 yields, at least at intermediate water concentrations.

Figure 6 (run 1) shows the effect of time on OF_2 yield during continuous electrolysis at 0.56 mole % H_2O. A fairly constant (35–36%) yield was obtained for about 3 hours, and then a sharp decline occurred. There was no break in the current density that might indicate an anode surface change. However the 3-hour plateau was not reproducible because in the next run (run 2) the OF_2 yield fell rapidly from the start. Nevertheless, interrupting current again gave higher OF_2 yields. Thus, although run 1 was shut down at 20% OF_2 yield, run 2 started at about 35%. Also, the system showed no permanent effect from a run that

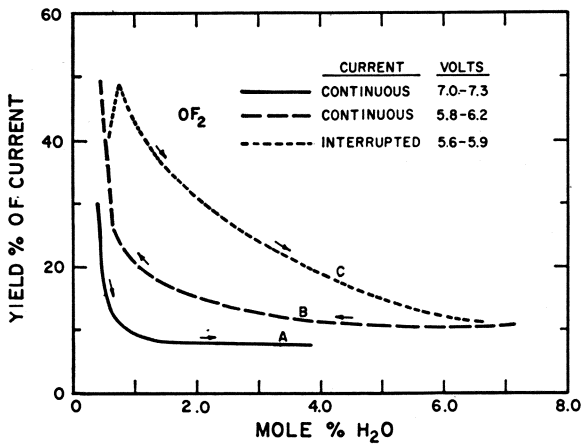

Figure 5. OF_2 yields at changing water concentration. KF ≈ 1 mole %, temperature = 0°–3°C.

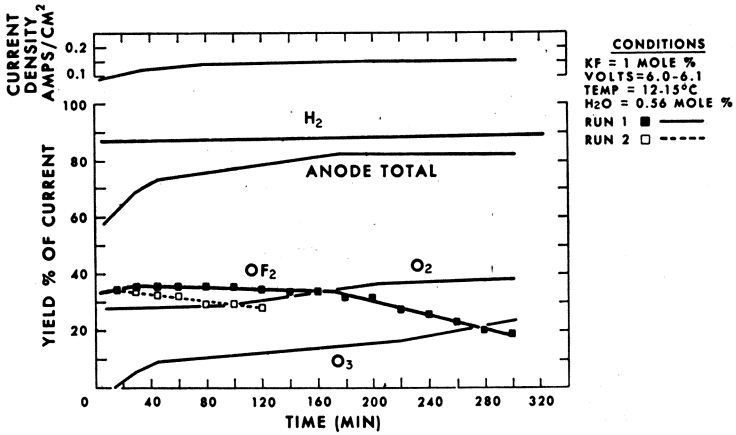

Figure 6. Continuous electrolysis

lasted many hours and ended with a low OF_2 yield. The O_2 and O_3 showed slight increases with time while H_2 was reasonably constant at 85–90%. Since anode total is less than H_2, some unidentified anode products are possible.

The consistent pattern in which off-on operation gives higher OF_2 yields suggested operating with programmed interruption. In Figure 7 a continuous run is compared with two interrupted runs at water levels that bracket the continuous run. Both interrupted runs had higher and more constant OF_2 yields.

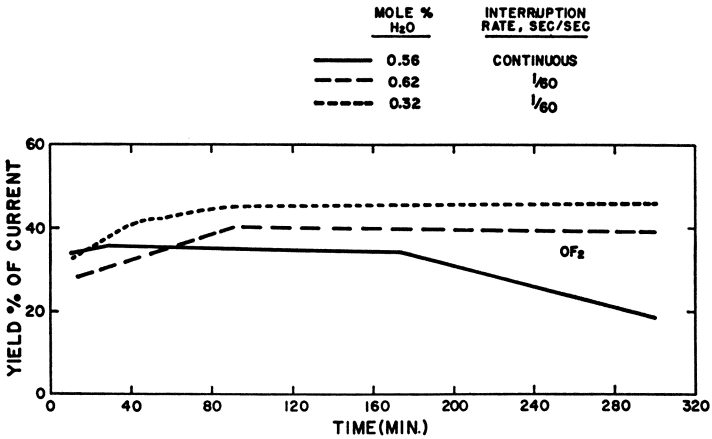

Figure 7. Interrupted electrolysis. KF = 1 mole %, volts = 6.0–6.1, temperature = 10°–14°C.

In addition to yields, current density and anode life are also important in evaluating an electrochemical synthesis. Although the current density should drop as water (a strong electrolyte in HF) is consumed, it does not always do so. Instead, for the first 15–30 minutes of electrolysis it increases in both continuous and interrupted electrolysis. This may be caused by a breakdown in a resistive anode coating. Once a maximum current is reached, the current density remains constant; however, it drops as the last few tenths percent of water are consumed. Also, high water levels (>3%) cause low current densities. The current density maximum was at 0.5–1.0 mole % water.

Nickel anodes lose weight during continuous electrolysis. The loss is large at low water concentration but drops to near zero at higher water (Table I).

The nature of the anode surface depends on the water concentration. At <0.2% H_2O, where F_2 is probably generated, the deposit is flaky and contains both NiF_2 and $KNiF_3$ (by x-ray and electron diffraction). At >0.2% H_2O, where little or no F_2 is made, the deposit is soft, thin, and

Table I

Mole % H_2O	*Volts*	*Faradays/ sq. cm.*	*OF_2 Yield % Current*	*Weight Loss % of Current*
0.2	5.0–8.2	0.0132	6.0	5.0
0.2–0.5	7.6	0.0324	20–47	1.0
0.5–1.5	7.6	0.0670	25–10	0.01

adherent and contains only NiF_2. With interrupted operation no weight was lost at comparable water levels and faradays. However, lower voltages and improved H_2O control may have also contributed to anode stability. While the times here are short (10–30 hours), the data indicate that anode life should be long.

Publication Date: January 1, 1966 | doi: 10.1021/ba-1966-0054.ch018

Discussion

The anode is a key component in the electrolysis. The surface influences product formation and at the same time is influenced by electrolysis reactions. The restoration of high OF_2 yields as excess H_2O is electrolyzed away (Figure 5, curve B) indicates that the surface is formed reversibly. The nickel-nickel fluoride anode is unique and essential to OF_2 formation. Copper and aluminum passivate completely and require very high voltages; platinum disintegrates rapidly (*1*). Only O_2, no O_3 or OF_2, was found with these metals. The nature of changes in the nickel-nickel fluoride anode surface, such as occur during start-up, is still uncertain. Several possibilities exist—i.e., mechanical break-up of the film, different forms of NiF_2 (α, β, γ) (*3*), or mixed oxide-fluoride films.

Speculation (*2*) on electrochemical fluorination considers free F_2 as an unlikely intermediate. Our data also eliminate this route to OF_2. In cases where F_2 is found in the products, adding H_2O does not increase OF_2 yields until the current is interrupted. Another possible route to OF_2 is fluorination of water by K_2NiF_6 or K_3NiF_6 in the film. However, this path is unlikely because K_2NiF_6 and K_3NiF_6 react with water to give only O_2 (*5*).

Formation of O_3 suggests oxygen atoms as an intermediate. Furthermore, increase in O_3 yield when OF_2 yield drops suggests that oxygen atoms are also in intermediate in OF_2 formation and being diverted from OF_2 to O_3 formation. However, only nickel of several metals tested gives O_3 and OF_2 although O_2 was present with the other metals. If O_2 also originates from oxygen atoms, then an added condition on the nickel/nickel fluoride anode surface, lacking on other metal surfaces, contributes to O_3 and OF_2 formation. Further study may reveal the nature of intermediates and how the nickel/nickel fluoride anode contributes to O_3 and OF_2 formation.

The overall current yield of OF_2 and the conversion of HF to OF_2 are higher with the one-step electrolysis than with the two-step process in which F_2 reacts with base (Table II).

Table II

	Current Efficiency for OF_2	Conversion of HF to OF_2
$HF \xrightarrow[\text{elect.}]{98\%} F_2$; $2F_2 + 20H^- \xrightarrow{60\%} OF_2 + 2F^- + H_2O$	30%	30%
$2F_2 + 40H^- \xrightarrow{40\%} O_2 + 4F^- + 2H_2O$		
$HF + H_2O \xrightarrow[\text{elect.}]{} OF_2 + O_3 + O_2 + H_2$	45%	100%

Lower cost OF_2 should result from a development of this electrolysis.

The constant OF_2 yields obtained with current interruptions show we are approaching the consistent operation necessary for pilot plant synthesis or detailed mechanism studies. Our present study provides the necessary analysis, control techniques, and yield data and indicates areas for further possible improvements. However, achieving maximum yields will require study of more variables than we have surveyed here.

The interruption technique may also have applications in preparing other hypofluorite or fluorine compounds by HF electrolysis. Indeed, any electrolysis in which electrode surface changes are important may benefit from interrupted operation.

Publication Date: January 1, 1966 | doi: 10.1021/ba-1966-0054.ch018

Acknowledgment

Research reported in this publication was supported by the Advanced Research Project Agency through the U. S. Army Research Office, Durham, N. C. under contract DA-31-124-ARO(D)-78. This report also discloses proprietary information owned by the American Oil Co., and its use by others is prohibited except as may be provided by the contract.

We thank W. A. Wilson for suggesting the study of wet HF electrolysis and J. Markovich, F. S. Jones, and R. R. Hopkins for help in various parts of the program.

Literature Cited

(1) American Oil Co., *Quart. Repts.*, Contract No. DA-31-124-ARO(D)-78, ARPA Order 402 (1963).
(2) Burdon, J., Tatlow, J. C., *Advan. Fluorine Chem.* **1**, 160, (1960).
(3) Clifford, A. F., Tulumello, A. C., *J. Chem. Eng. Data* **8**, 425 (1963).
(4) Cook, G. A. *et al.*, ADVAN. CHEM. SER. **21**, 44 (1959).
(5) Cotton, F. A., *Prog. Inorg. Chem.* **2**, 200 (1960).
(6) Donohue, J. A., Wilson, W. A., U.S. Patent **3,134,656** (May 26, 1964).
(7) Downing, R. C. *et al.*, *Ind. Eng. Chem.* **39**, 259 (1947).
(8) Emeleus, H., *J. Chem. Soc.* **1942**, 441.

(9) Engelbrecht, A., Nachbaur, E., *Monatsh. Chem.* **90**, 367 (1959).
(10) Grubb, W. T., U.S. Patent **2,716,632** (Aug. 30, 1955).
(11) Haberman, E. G., *Chem. Eng. Prog.* **60**, 72 (1964).
(12) Hyman, H. H., Kilpatrick, M., Katz, J. J., *J. Am. Chem. Soc.* **79**, 3668 (1957).
(13) Le Beau, P. and Damiens, A., *Compt. Rend.* **185**, 652 (1927).
(14) Simons, J. H., *et al.*, *J. Electrochem. Soc.* **95**, 47 (1959).
(15) Schmidt, H., Schmidt, H. D., *Z. Anorg. Chem.* **279**, 289 (1955).
(16) Streng, A. G., *Chem. Rev.* **63**, 607 (1963).
(17) Thorp, C. E., "Bibliography of Ozone Technology," Vol. 1, Armour Research Foundation, Chicago, 1954.
(18) Yost, D. M., Cady, G. H., *Inorg. Syn.* **1**, 109 (1939).

RECEIVED April 19, 1965.

19

Electron Paramagnetic Resonance Spectrum of Liquid Oxygen Difluoride

F. I. METZ, F. E. WELSH, and W. B. ROSE

Midwest Research Institute, Kansas City, Mo.

Publication Date: January 1, 1966 | doi: 10.1021/ba-1966-0054.ch019

When liquid oxygen difluoride (OF_2) is analyzed by electron paramagnetic resonance (EPR) spectroscopy, the shape, line width, and complexity of the resonance signal depend on the purity of the OF_2. The strength of the signal depends on photolysis, and the rate of decay is slow. Pure chromatographed liquid OF_2 prepared in normal room light shows a strong doublet with a peak-to-peak line width of about 2.6 gauss and a doublet separation of 13.5 gauss. The line center of the doublet has a g-value of 2.0039; the line shape closely approximates a Lorentzian curve. The calculated concentration of the paramagnetic species is about 10^{16} unpaired electrons per sample, corresponding to a concentration of about 0.001 mole %.

The electron paramagnetic resonance spectrum of liquid oxygen difluoride has been determined in conjunction with a study of the structure of liquid inorganic oxidizers. The EPR spectra of the higher oxygen fluorides (O_2F_2, O_3F_2, and O_4F_2) have been studied (*5, 6*). Two EPR signals have been observed from samples of O_2F_2 at 77° K. The resonances were assigned to the presence of intermediates in the decomposition $O_2F_2 \rightarrow O_2 + F_2$ rather than to O_2, F_2, or O_2F_2 itself. The stronger of the two signals has been interpreted in terms of the presence of a radical with one unpaired electron, having a hyperfine interaction with only one fluorine nucleus; $O_2F\cdot$ was considered to be a likely possibility. The weaker resonance was associated with the presence of a radical in the triplet state.

The EPR spectrum of O_3F_2 showed (*5, 6*) the same resonances as obtained from O_2F_2 except that the intensity of the stronger signal in the case of O_3F_2 was 50–100 times greater than the intensity of the corresponding resonance in O_2F_2 while the triplet resonance in O_3F_2 is only twice

In Advanced Propellant Chemistry; Holzmann, R.;
Advances in Chemistry; American Chemical Society: Washington, DC, 1966.

as intense as the triplet resonance in O_2F_2. The strong signal in O_3F_2 was also assigned to the $O_2F\cdot$ radical. Contamination of O_2F_2 with O_3F_2 was ruled out by the observation of the resonances after the O_2F_2 sample had been heated above the decomposition temperature of O_3F_2.

O_4F_2 was found to be paramagnetic (*6*). The EPR spectrum at 77° K. consisted of a strong doublet with an average *g*-value of 2.009 and a doublet separation on the order of 13 gauss. In view of the dissimilarity between the spectrum of O_4F_2 and the spectra of O_2F_2 and O_3F_2, it was thought unlikely that the paramagnetic species in O_4F_2 was the $O_2F\cdot$ radical.

The EPR spectrum of O_3F_2 at 90° K. has also been investigated by Maguire (*7*). A doublet with a splitting of 13.6 gauss and a *g*-value of 1.975 was obtained. These results have been interpreted in terms of diradical O_3F_2 as being the paramagnetic species involved. One unpaired electron was thought to be localized near each of the fluorine nuclei. The coupling between the two fluorine nuclei was considered to be weak or zero.

In this study pure liquid OF_2 exhibited no EPR signal when condensed in the absence of light. Upon photolysis, a strong doublet with a hyperfine splitting of 13.5 gauss and a *g*-value of 2.0039 were obtained. Concentrations were on the order of 10^{16} unpaired electrons per sample. Oxygen difluoride is a colorless gas at room temperature and a pale yellow liquid at temperatures below 128° K., its normal boiling point. It is relatively stable, with thermal decomposition beginning at about 200°–250° C. OF_2 is nonlinear with two equivalent O—F bonds having an FOF angle of 104°.

Experimental

Electron Paramagnetic Resonance. EPR measurements were made using a Varian V-4502 X-band spectrometer equipped with a 6-inch magnet and using 100 kc. field modulation. The frequency used was 9.1 Gc. The sample tube was a 3.0 mm. i.d. quartz tube connected to a stopcock and a male ground glass joint by means of a graded seal. Sample volumes were 0.05–0.08 ml. One spectrum was run on a Varian V-4503 K-band spectrometer using a frequency of 34.8 Gc. For measurements at 77° K. the sample tube was placed in a small quartz Dewar which was inserted into the cavity. Measurements in the range 88°–138° K. were made using a V-4557 variable temperature accessory. Peroxylamine disulfonate was used for the scan calibration. The total hyperfine splitting of the spectrum was taken to be 26.0 gauss (*12*). Polycrystalline DPPH (g = 2.0036) in a capillary inside the Dewar was used as the standard for the *g*-value determination. The frequency in the X-band region was determined using a Hewlett-Packard model 5243L electronic counter, a model 5253A frequency converter, and a model 540B transfer oscillator. Concentration measurements were made relative to a Varian 0.1% pitch

Publication Date: January 1, 1966 | doi: 10.1021/ba-1966-0054.ch019

sample in potassium chloride, with the number of spins taken to be $3 \times 10^{+15}$ spins/cm. length of sample. The accuracy of this value is estimated to be ±25% (*13*). Relative values of the intensities of the OF_2 spectra at various temperatures (compared with the pitch standard) are of primary interest while absolute values of the spin concentrations are less important.

Photolysis studies were performed using a PEK-110 100-watt high pressure mercury arc lamp. The 3660-A. line was selected by means of a Bausch and Lomb second-order interference filter.

Purification. A schematic diagram of the purification system is shown in Figure 1. The OF_2 was bled slowly from the storage tank through an HF trap and condensed on the cold vertical column. The HF trap removed hydrogen fluoride and silicon tetrafluoride (*10*) while the cold

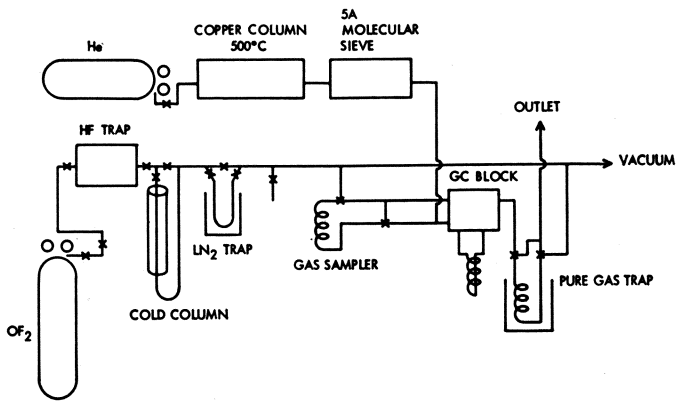

Figure 1. Purification system and vacuum line

column separated any carbon dioxide present. This vertical column was at 77° K. and jacketed with a Dewar. The OF_2 condensed and drained below the cold region of the tube where it refluxed and slowly distilled into the first liquid nitrogen trap. Following Schoenfelder's procedure for N_2F_4 (*9*), the OF_2 was chromatographed. Table I shows the relative elution times of the impurities found to be present. Prior to its introduction, the helium carrier gas was passed through reduced copper oxide wire at 500° C. (*3*) to remove oxygen and through a Linde molecular sieve to remove H_2O.

Table I. Relative Elution Times on $^1/_2''$ x 10′ Silica Gel Column

Flow Rate, 150 ml./min

Substance	*Elution Time of Maximum (min.)*
O_2	4.7
N_2	5.1
OF_2	10.8
F_2	13.0
CF_4	16.5
CO_2	120.0
SiF_4	120.0

Chemicals. The copper oxide wire was Mallinckrodt reagent grade. The molecular sieve was Linde 5A $^1/_{16}$-inch pellets. The OF_2 was obtained from Allied Chemical Corp. and was approximately .93% pure. The silica gel (60/80 mesh) was purchased from Matheson Co.

The $^{17}OF_2$ was prepared in this laboratory. Fluorine (Matheson Co. 98%) reacted with a 0.5*N* potassium hydroxide solution made with $H_2{}^{17}O$ (4.0% ^{17}O) obtained from Yeda Research and Development Co., Since the $^{17}OF_2$ contained impurities (O_2 and F_2), it was purified chromatographically by the procedure above. The enrichment of the oxygen in the final product was on the order of 1% ^{17}O.

Results

No EPR signal was obtained on samples of liquid OF_2 prepared in the absence of light. Liquid OF_2 taken directly from the tank in the presence of room light showed a fairly strong, complex signal with a total line width of about 100 gauss. Similar results were obtained from OF_2 which had been swept through an HF trap and subsequently distilled.

The EPR spectrum of a sample of chromatographed liquid OF_2, prepared in the absence of light, showed a strong doublet (Figure 2) with a

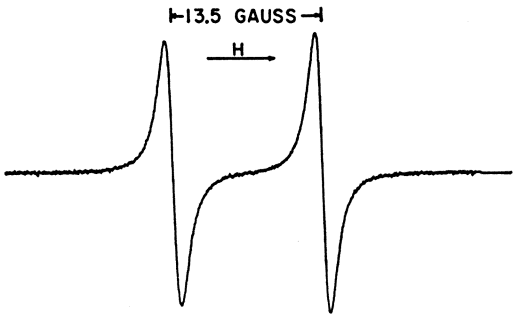

Figure 2. EPR of liquid OF_2 at 9.1 Gc (T = 77°K.), after photolysis

splitting of 13.5 gauss when photolyzed. The line width was temperature dependent with values in the range of 1.6–3.6 gauss. The line center of the doublet had a *g*-value of 2.0039 ± 0.0003, and the line shape closely approximated a Lorentzian curve. The spectra were examined at various modulation amplitudes and microwave power levels to ensure that no distortion owing to overmodulation or power saturation occurred. The intensity of the doublet increased with time during photolysis. The number of paramagnetic species was calculated to be on the order of 10^{16} per sample, corresponding to a concentration of about 0.001 mole %. An EPR spectrum of chromatographed liquid OF_2 prepared in normal room light was similar to the spectrum obtained from the photolyzed samples. In addition to the doublet, a weak anisotropic pattern was ob-

served with outer components 55 gauss on the low field and 42 gauss on the high field side of the center of the doublet pattern.

An EPR spectrum of photolyzed liquid OF_2 obtained at a frequency of 34.8 Gc is shown in Figure 3. A hyperfine splitting of 13.7 gauss was observed in agreement with the value of 13.5 gauss observed at 9.1 Gc. Part of the asymmetry of the signal observed on the high field side of each peak was caused by a recorder malfunction. It is also possible that anisotropies may be observed at the higher frequency used.

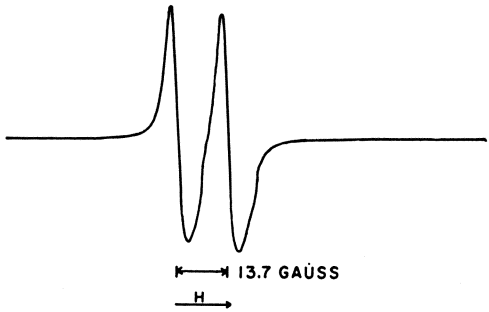

Figure 3. EPR of liquid OF_2 at 35 Gc (T = 77°K.), after photolysis

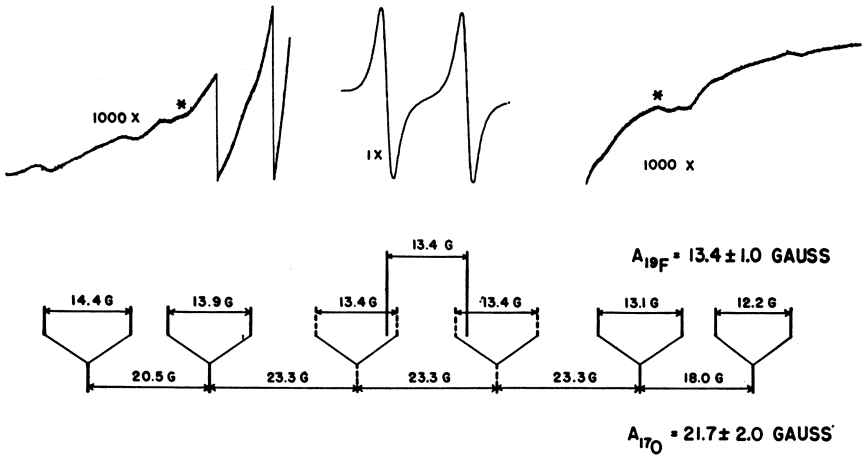

Figure 4. EPR of liquid OF_2, 1% enrichment ^{17}O (temperature = 77°K.), after photolysis

The EPR spectrum of a sample of oxygen difluoride enriched in ^{17}O is shown in Figure 4. A strong central doublet with a hyperfine splitting of 13.4 gauss was observed. In addition, eight low intensity peaks were symmetrically spaced on the wings of the central doublet. At the high gain setting used for these observations, the strong $^{16}OF_2$ doublet was

Publication Date: January 1, 1966 | doi: 10.1021/ba-1966-0054.ch019

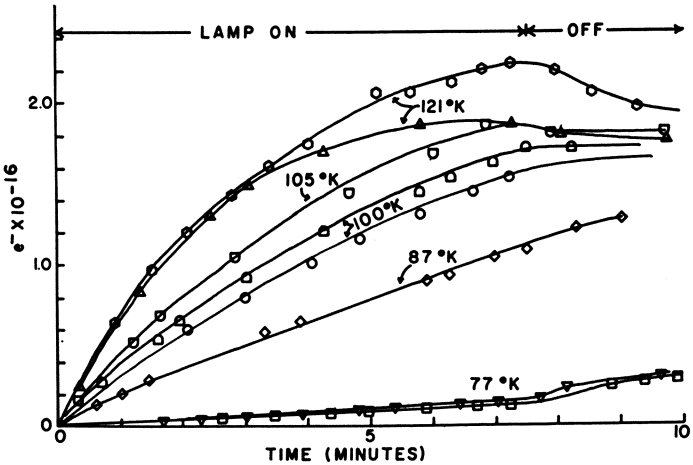

Figure 5. Variation in paramagnetic resonance of photolyzed OF_2 at selected temperatures

off scale, and the innermost peaks are seen only as slight, but observable changes in the slope of the trace. The eight weak $^{17}OF_2$ bands can be resolved into four doublets with a separation on the order of 13.4 gauss, two each on the high and low field side of the strong central doublet. Additional weak components (marked with * in Figure 4) at approximately 40 gauss on each side of the center of the pattern were observed in some of the spectra. It was not possible to determine accurately the intensity of the weak $^{17}OF_2$ hyperfine doublets.

In a series of experiments, EPR spectra of different samples of OF_2 were taken during 7.5 minutes of photolysis and afterwards in the absence of light for sufficient time to observe trends in the signal intensity. The change in signal intensity with photolysis is shown in Figure 5 for a number of temperatures. The calculated intensity at each temperature was corrected for the change in the Boltzmann distribution of radicals in the lowest energy state.

The initial rate of formation of the radical species was temperature dependent. The Arrhenius equation reasonably describes the temperature dependence of the specific rate constants over the temperature range 77°–121° K. The calculated specific rate constants are plotted as a function of temperature in Figure 6; the solid line is the least-squares line through the experimental points. Thus, in the temperature range 77°–121° K., the rate of formation of the paramagnetic entity can be expressed as: $-\log k = 4.5 + \frac{295}{T\,(°\,\mathrm{K.})}$. The overall reaction for the formation of the observed species has an apparent activation energy, E_a, of 1360 cal./mole.

With prolonged photolysis the samples attained a maximum concentration of the resonant species; further photolysis resulted in a diminished signal. The signal intensity at the maximum was also temperature dependent. At 77° K. the signal increased rapidly ($k' = 3.3 \times 10^{-9}$ sec.$^{-1}$) after the lamp was turned off, then more slowly ($k'' = 1.8 \times 10^{-9}$ sec.$^{-1}$). The rate of decay after photolysis did not depend on

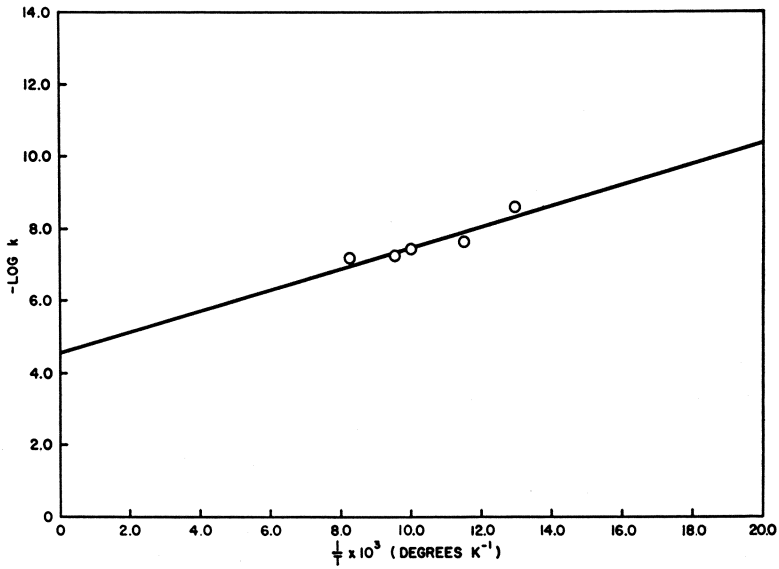

Figure 6. Arrhenius plot for $O_2F\cdot$ formation

temperature; the overall specific rate for the decay processes is 1.1×10^{-9} sec.$^{-1}$ The decay at 77° K. did not proceed to zero intensity but usually reached a value which persisted even after several days storage of the sample in the dark. The signal may be caused to vanish or at least reach a very low level by vaporization and recondensation of the sample in the absence of light.

Figure 7 shows the change in signal strength with continued photolysis at 77° K. for two different intensities of irradiation. With low intensity illumination, a peak concentration was reached at 10 minutes photolysis, after which time additional photolysis produced a diminution of the signal. At 24.5 minutes, the signal strength corresponded to approximately 10^{12} unpaired electrons. After the lamp was extinguished, the concentration immediately increased to a value on the order of 10^{14} unpaired electrons. The concentration continued to increase in the absence of light. If the sample were irradiated again, the signal level rapidly dropped to the previous low value. With high intensity illumination, the signal intensity of a different sample of pure liquid OF_2 reached a maxi-

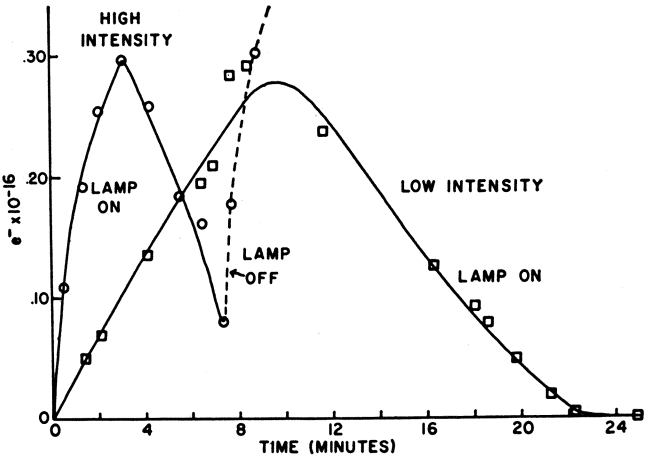

Figure 7. Variation in paramagnetic resonance of OF_2 for high and low intensity irradiation ($\lambda = 3660$ A.)

mum after 3 minutes of photolysis, then rapidly decreased. The lamp was turned off at 7.5 minutes, whereupon the signal intensity increased rapidly. In general, the intensity of the EPR resonance increased with continued photolysis, reached a maximum, and dropped to a very low level.

The dependence of signal strength (radical formation) on intensity of radiation at 3660 A., 77° K. is shown in Figure 8. The relative inten-

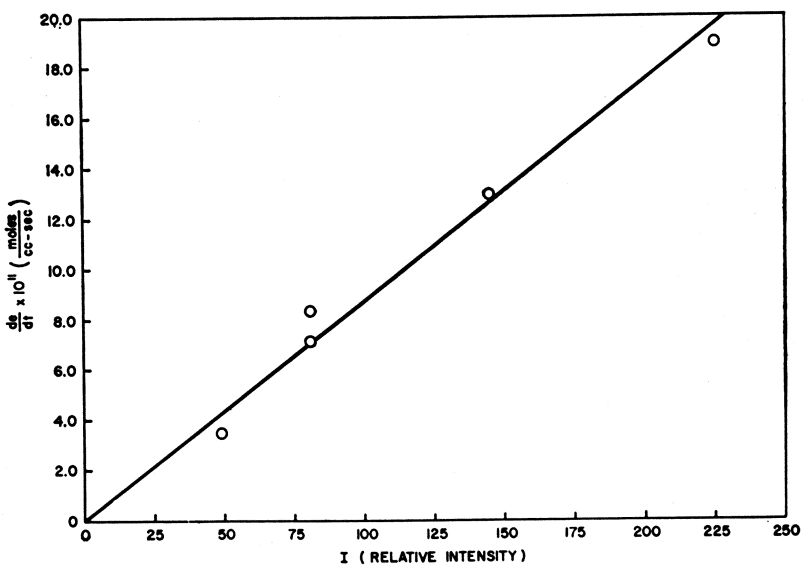

Figure 8. Rate of $O_2F\cdot$ Formation ($\lambda = 3660$ A., $T = 77°$K.) *as a function of relative intensity*

sities used for irradiation were measured spectroscopically for different iris settings of the photolysis lamp. A relative intensity of about 50 was used to obtain the data in Figures 5 and 6. The overall rate constant, 8.7×10^{-13} moles cc.$^{-1}$ sec.$^{-1}$, represents the rate of formation of the resonant species up to the maxima (*see* Figure 7). The kinetic behavior after the maximum has been attained—i.e., during the photolytic decay—is more complex, and no overall rate can be given.

The presence of oxygen may affect the results of these experiments in several ways. Two possible results are a change in the mechanism of the photolytic reactions or a broadening of the EPR signal. Large amounts of oxygen (of the order of 1%) broadened the signal. In experiments in which *ca.* 1% oxygen was added to OF_2, the spectrum was similar to that obtained from pure OF_2 in that the doublet was observed and the radical concentration depended on photolysis. Small amounts of oxygen (0.06%–0.1%) did not change either the rate of formation of the radical or the characteristics of the signal. It is estimated that the amount of oxygen present in the pure OF_2 was 0.03% or less, probably from a slight decomposition of OF_2 accompanying vaporization and recondensation.

Discussion

The lack of an EPR signal in the spectra of samples chromatographed in the absence of light is strong evidence that liquid OF_2 is not paramagnetic. In addition, a hyperfine triplet rather than the observed doublet would be expected from a paramagnetic species such as $OF_2^{\cdot}$. The fact that the separation between the two peaks was caused by hyperfine splitting was demonstrated by the agreement between the separation in gauss observed in spectra taken at frequencies of 9.1 Gc and 34.8 Gc. If hyperfine splitting were not present, the separation would be expected to increase as the ratio (34.8/9.1) of the frequencies of observation.

Considering the system involved, the doublet could arise from $O_xF^{\cdot}$ or $F^{\cdot}$ radicals owing to hyperfine interaction with a fluorine nucleus which has a spin of $^1/_2$. However, the fluorine atom would react via recombination or abstraction much more rapidly than the $O_xF^{\cdot}$ radical. The fluorine radical has not been observed in the condensed phase but has been observed in the gas phase as six well-spaced resonances with a g-value of 4/3. At a frequency of 9.249 Gc, 4159 gauss was the lowest value of the magnetic field at which a resonance occurred (*11*). We have studied the EPR of liquid F_2 at 77° K. Tank fluorine and fluorine run through an HF trap and distilled have exhibited a weak signal with a line width of about 75 gauss and a g-value near 2.0. The signal strength increased with photolysis and seemed to broaden. Probably the observed

Publication Date: January 1, 1966 | doi: 10.1021/ba-1966-0054.ch019

resonance in liquid fluorine was caused by an interaction with impurities. Therefore, it is highly improbable that the resonances observed are caused by F·.

The value of the coupling constant in OF_2 (13.5 gauss) is not what one would expect from hyperfine interaction of an electron with a fluorine nucleus—this interaction usually being much greater. As a comparison, the hyperfine splitting owing to two equivalent fluorine nuclei in NF_2· in liquid N_2F_4 is 64 ± 2 gauss (*2*). Probably the greater electronegativity of the oxygen in O_xF· decreases the unpaired electron density at the fluorine and thus accounts for the small value of the hyperfine splitting.

Four weak doublets symmetrically spaced with respect to the center of the strong $^{16}OF_2$ doublet are observed in the EPR spectrum of $^{16}OF_2$ enriched with $^{17}OF_2$. The average line positions from several spectra are shown in Figure 4. Owing to the low intensity and broadness of the lines, uncertainty in the position of the line centers is on the order of ±1 gauss. The additional two doublets expected to occur toward the center of the pattern were not observed owing to the high intensity of the $^{16}OF_2$ doublet. These two doublets are indicated by dotted lines in Figure 4. As shown in the diagram in Figure 4, the spectrum can be analyzed in terms of six doublets with a spacing of 13.4 gauss owing to a hyperfine interaction of the unpaired electron with one ^{19}F nucleus. Lines drawn in the centers of the four doublets indicate the magnitude of the hyperfine interaction owing to an ^{17}O nucleus. The hyperfine pattern resulting from the interaction with only one ^{17}O nuclear (nuclear spin = $^5/_2$) would be six symmetrically spaced lines of equal intensity. The probable positions of two center components of this pattern are drawn as dashed lines in Figure 4. The magnitude of the splitting owing to ^{17}O is estimated to be 21.7±2 gauss.

Baird (*1*) has reported a value of 19.7 gauss for the hyperfine splitting of ^{17}O in the di-*sec*-butyl nitric oxide radical. The electronegative parts of the two radicals (N,O, and F,O) are similar, so one might expect the hyperfine interaction owing to ^{17}O to be of the same order of magnitude.

The simplicity of the hyperfine patterns obtained from the EPR spectrum of $^{17}OF_2$ shows that there is only one ^{17}O nucleus in the radical. Two ^{17}O nuclei with the same hyperfine interaction would give (instead of six doublets) eleven doublets of intensity 1:2:3:4:5:6:5:4:3:2:1. The intensity of the observed doublets could not be determined accurately, but two ^{17}O nuclei would give a broader pattern than the one observed. No bands were observed outside of the range of the pattern shown in Figure 4. Two ^{17}O nuclei with hyperfine interactions of different magnitudes would produce a complex many-lined spectra, also of greater width than the observed spectrum.

Publication Date: January 1, 1966 | doi: 10.1021/ba-1966-0054.ch019

These studies indicate that the radical observed is $O_xF^{\bullet}$, where $x \geq 1$. A pattern has been observed showing hyperfine interaction with one fluorine nucleus and one ^{17}O nucleus. However, there may be more than one oxygen in the radical.

^{16}O has no hyperfine interaction since its nuclear spin is zero. We conclude that there were one or more oxygens in the radical, and in the present case one of them (if $x \geq 1$) is an ^{17}O.

The two weak bands at approximately 40 gauss on each side of the center of the pattern may be anisotropic components of the strong central doublet. Bands were observed at approximately the same value of the field in the case of other OF_2 spectra run at high gain settings.

The EPR spectrum of O_2F_2 also has been studied in this laboratory. Solid O_2F_2 showed a broad, anisotropic EPR pattern similar to that reported (*5, 6*). In addition, the EPR spectrum of neat liquid O_2F_2 contained a doublet near $g = 2.0$ with a hyperfine splitting of approximately 13 gauss.

The radicals present in the four binary OF compounds (OF_2, O_2F_2, O_3F_2, and O_4F_2) may be $O_2F^{\bullet}$, $O_3F^{\bullet}$, and $O_4F^{\bullet}$. However, radicals with the same hyperfine interaction with a fluorine nucleus (13 gauss) have been observed in all four binary OF compounds. It may be that the same paramagnetic species is present in each compound.

The kinetics of the photolysis suggests possible reactions involved in the formation and decay of the observed fluorine containing paramagnetic entity.

$$OF_2 \xrightarrow{h\nu} (OF_2)^* \tag{1}$$

$$n(OF_2)^* \rightarrow (OF_2)_n \tag{2}$$

$$(OF_2)_n \rightarrow O_xF\cdot + (O_{n-x}F_{2n-1}) \tag{3}$$

In addition, the radicals produced in Reaction 3 may undergo reactions such as:

$$OF_2 + 2O_xF\cdot \rightarrow 2OF_2 + \frac{(2x-1)O_2}{2} \tag{4}$$

$$\left.\begin{array}{ll} 2O_xF\cdot \rightarrow xO_2 + F_2 & (5) \\ 2O_xF\cdot \rightarrow OF_2 + (2x-1)O & (6) \end{array}\right\}\text{Possible } h\nu$$

$$2O \rightarrow O_2 \tag{7}$$

Reaction 5 and/or 6 may proceed photolytically thus accounting for the diminishing signal observed during continued irradiation.

Reaction 1 is the primary photolysis reaction. Visible-ultraviolet spectroscopic studies with liquid OF_2 (*8*) offered evidence for an excited state such as $(OF_2)^*$ in Equation 1. This excited state could dissociate to form $OF^{\bullet}$ and $F^{\bullet}$, but it should readily associate as in Reaction 2. Reaction 3 shows the fragmentation of the associated species to give a

smaller OF polymer and an $O_xF^{\cdot}$ radical. Reaction schemes involving an associated entity could also be written for the higher oxygen fluorides. Thus, one could rationalize the existence of the same $O_xF^{\cdot}$ radical in the four binary OF compounds if the similarity in the hyperfine coupling of the radicals obtained was interpreted in these terms. However, if the fluorine hyperfine coupling is insensitive to the presence of more than one oxygen on the radical, the value of x in $O_xF^{\cdot}$ may be different in the various OF compounds.

Reaction 3 is undoubtedly the rate-controlling step. At 77° K, the overall rate constant for the formation of the paramagnetic species is 2.0×10^{-9} sec.$^{-1}$; the rate constant determined from intensity data is of the same order ($k''' = 2.0 \pm 0.5 \times 10^{-9}$ sec.$^{-1}$) if a quantum yield between 0.5 molecule/$h\nu$ and 1 molecule/$h\nu$ (*4*) is assumed. The overall activation energy, $E_a = 1360$ cal./mole, for the thermal reaction is small as expected for the fragmentation of the associated species.

Reactions 4–7 show possible reactions responsible for the photolytic and nonphotolytic decay of the radical $O_xF^{\cdot}$. Reaction 5 would be more important in the gas phase, and there is evidence (*4*) that light energy is necessary to promote this reaction. However, within limits of detection, ~0.01%, no F_2 has been observed as a product. On the other hand, small increases (0.03–0.05%) in the oxygen content of the samples have been observed. It is felt that the photolytic decay proceeds primarily via Reaction 6, and the nonphotolytic decay is Reaction 4.

The above reactions are not proposed as the only possible ones, but it is felt that they are reasonable in view of the characteristics and intensity behavior of the EPR spectra.

Summary

This study has established that oxygen difluoride dissociates photolytically into a paramagnetic species in which there is a hyperfine interaction between the unpaired electron and one fluorine nucleus. The photolytic rate of formation of the radical species increased with temperature. The decay of the signal intensity in the absence of light after photolysis did not depend on temperature. The kinetics have been interpreted in terms of a photolytic formation scheme. The radical has been characterized by means of the EPR spectrum, but not identified. However, the characteristics of the spectrum show that the radical was $O_xF^{\cdot}$, rather than $F^{\cdot}$.

Acknowledgment

This research was sponsored by the Advanced Research Projects Agency, Washington 25, D. C., and was monitored by Rocket Propulsion

Laboratory, Edwards, Calif., under Contracts Nos. AF 04(611)-9372 and AF 04(611)-10215.

We would like to thank William Landgraf of Varian Associates for his assistance in obtaining the EPR spectra at 34.8 Gc.

Literature Cited

(1) Baird, J. C., *J. Chem. Phys.* **37**, 1879 (1962).
(2) Doorenbos, H. E., and B. R. Loy, *J. Chem. Phys.* **39**, 2393 (1963).
(3) Elliott, K. A. C., *Can. J. Res.*, **27F**, 299 (1949).
(4) Gatti, R., E. Staricco, J. E. Sicre, H. J. Schumacher, *Z. Physik. Chem.* **35**, 343 (1962).
(5) Kasai, P., A. D. Kirshenbaum, *J. Am. Chem. Soc.* **87**, 3069 (1965).
(6) Kirshenbaum, A. D., A. V. Grosse, Temple Research Institute, Contract No. AF 04(611)-9555, *Quart. Progr. Rept.* **1**, **2**, **3** (1963, 1964).
(7) Maguire, R. G., ARL Tech. Rept. **60-287**, Contract No. AF 33(616)-6433, (1960).
(8) Metz, F. I., J. W. Nebgen, W. B. Rose, F. E. Welsh, unpublished data.
(9) Schoenfelder, C. W., *J. Chromatography* **7**, 281 (1962).
(10) Streng, A. G., *Chem. Rev.* **63**, 607 (1963).
(11) Vanderkooi, N., Jr., J. S. Mac Kenzie, ADVAN. CHEM. SER. **36**, 98 (1962).
(12) Varian Associates, EPR at work No. 28.
(13) Varian Associates, Instruction Manual for V-4502 E.P.R. spectrometer system, p. 5-11.

RECEIVED April 23, 1965.

A New Determination of the Heat of Formation of Oxygen Difluoride

WARREN R. BISBEE,[1] JANET V. HAMILTON, RONALD RUSHWORTH, THOMAS J. HOUSER,[2] and JOHN M. GERHAUSER

Rocketdyne Division, North American Aviation, Inc., Canoga Park, Calif.

Publication Date: January 1, 1966 | doi: 10.1021/ba-1966-0054.ch020

The ΔH^0 of reaction at 298.16° K. of oxygen difluoride with hydrogen was measured using a Parr fluorine combustion bomb modified to contain a metal ampoule employing a burst diaphragm. This modification permits heat of reaction measurements on systems where reaction occurs spontaneously upon mixing the reactants. The ΔH^0 of the reaction $OF_2 + 2H_2 \rightarrow H_2O + 2HF$ (infinite dilution) was found to be -223.26 ± 0.38 kcal./mole. From this and existing thermodynamic data, the standard ΔH_f^0 of oxygen difluoride was calculated, and the O—F bond energy was determined. These values are —4.06 and 50.7 kcal./mole, respectively.

The currently accepted value of the O—F bond energy (45 kcal./mole) is calculated from the standard heat of formation of OF_2 (7.6 kcal./mole) which was based on an average of three values obtained in 1930 (7, 8) the precision of which was quite poor. To determine a more reliable heat of formation of OF_2 and thus a better O—F bond energy, the heat of reaction of the following system was measured:

$$OF_2 + 2H_2 \rightarrow H_2O + 2HF \text{ (infinite dilution)}$$

Experimental

Materials. The OF_2, obtained from the Allied Chemical Co., was found to be greater than 99% pure. Active fluoride was analyzed by an iodometric method. By infrared analysis 0.22% CO_2 and 0.02% CF_4 were found; SiF_4 was not detectable; no HF was found.

The hydrogen was a prepurified grade of 99.9% minimum purity obtained from the Mathesoh Co.

[1] Present address, Beckman Instruments, Albuquerque, N. M.
[2] Present address, Western Michigan University, Kalamazoo, Mich.

In Advanced Propellant Chemistry; Holzmann, R.;
Advances in Chemistry; American Chemical Society: Washington, DC, 1966.

Apparatus and Procedure. The thermochemical measurements were made using a Parr fluorine combustion bomb and a National Bureau of Standards (NBS) isothermal calorimeter (No. 63090) manufactured by the Precision Scientific Co. The bomb cylinder and all internal parts of the bomb were Monel. A Monel ampoule was fitted into the top of the bomb to retain the OF_2 sample. The ampoule apparatus reduced the internal volume of the bomb from 380 to 315 cc. The ampoule screws

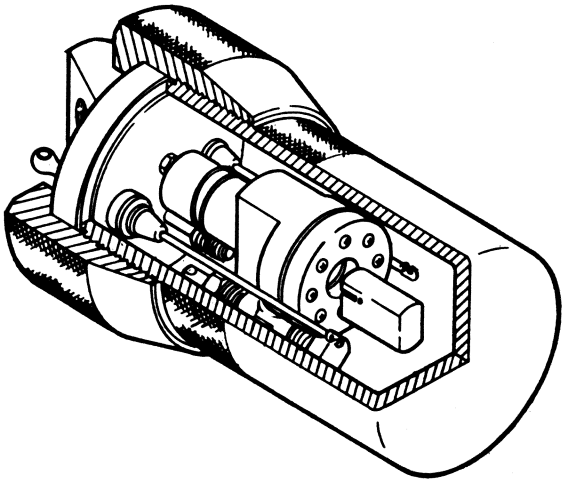

Figure 1. Nickel Parr combustion bomb with ampoule

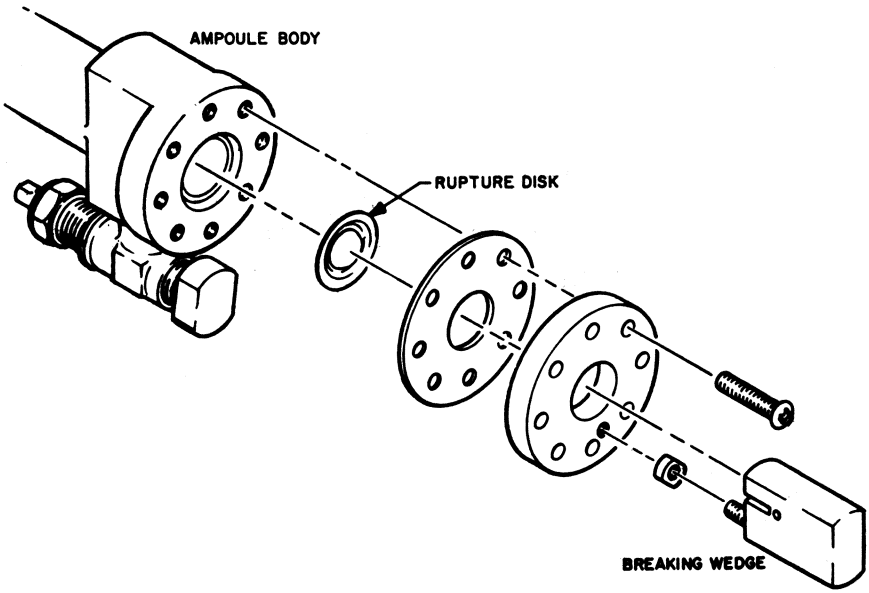

Figure 2. Exploded view of ampoule

Publication Date: January 1, 1966 | doi: 10.1021/ba-1966-0054.ch020

into the bomb head in the position normally occupied by the outlet tube. This prevents the use of the outlet valve. Additional support is provided by a Monel clip which fits around the cylinder body of the ampoule and is attached to the inlet tube. A diagram of the ampoule is given in Figures 1 and 2.

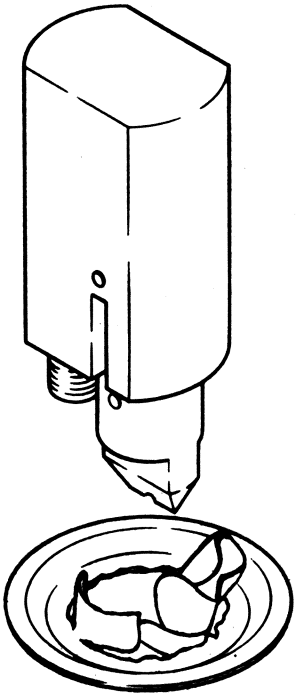

Figure 3. Effect of wedge breaking mechanism on rupture disk

The internal volume of the ampoule was 8.7 cc. The top of the cylinder body and the cylinder head were designed with a 30° angular seat to accommodate a $^1/_2$-inch Monel burst diaphragm. A mechanism, which fits inside the bomb, was designed to rupture the burst diaphragm in the ampoule. This consisted of a piston with a knife-like wedge head (Figure 3) and a small spring made from spring-tempered Monel wire. The piston and spring were held in a compressed position by nickel-chromium alloy fuse wire of known calorific value, which was strung between the two internal electrodes in the bomb. Spring loading of the breaking wedge was accomplished by compressing the piston and spring until the hole in the piston was aligned with that in the breaking mechanism (Figure 3). A pin was then inserted to hold the piston and spring in a compressed position while the fuse wire was attached to the two electrodes. This wire passed through a small indentation in the knife-like wedge head of the piston which is positioned between the two electrodes. The copper pin was then removed, and the piston was held in place with the fuse wire. A pinpoint breaker was also tried;

Publication Date: January 1, 1966 | doi: 10.1021/ba-1966-0054.ch020

however, because it merely punctured a small hole in the diaphragm, it increased the chance of obtaining incomplete reaction and was unsatisfactory.

To solve the problem of loading and weighing a sample in the ampoule, one side exit was designed to accommodate a small 90° angle valve. The weight of the OF_2 samples was determined by weighing the empty ampoule, which had been previously evacuated, and then weighing the filled ampoule.

The OF_2 sample was condensed from a vacuum line into the ampoule, which was weighed on an analytical balance and then attached to the bomb head. Buoyancy corrections were applied only to the weight of the OF_2 sample. A quantity of 50 ml. of water was placed in the bomb to absorb the HF formed during reaction and thus reduce corrosion. The reaction bomb was assembled, pressurized with hydrogen (75.0 p.s.i.g.), and sealed. To start the reaction, the sample was released into the hydrogen by electrically fusing the nickel-chromium alloy wire. This released the piston which ruptured the diaphragm and allowed the reactant gases to mix. Reaction occurred rapidly and completely; the temperature rise of the calorimeter was measured by means of a platinum resistance thermometer, constructed and calibrated by the Leeds and Northrup Co. The thermometer, a four-lead cable type, was used in conjunction with a Leeds and Northrup G-2 Mueller bridge and a high sensitivity galvanometer.

Dickinson's method was used to obtain the corrected resistance change (*3*). This method involves the use of the equation $R_x = R_i + 0.63\ (\Delta R_{obs})$ where R_i is the initial resistance before the reaction is initiated, and R_x is the resistance at t_x, the time on a resistance-time plot where a vertical line drawn through this point will subtend equal areas to the left and to the right of the curve.

To check the mass balance of the reaction, the reaction products were analyzed after each run by a thorium nitrate method for fluoride and by a sodium hydroxide titration for hydrogen ions.

The two methods of analysis agreed within experimental error but were always lower than stoichiometric for each OF_2-H_2 run. It was believed that the approximately 5% of HF unaccounted for was consumed in the slight corrosion of the stainless steel screw heads in the ampoule. Qualitative analysis of the screw heads did show the corroded film on the screws was the metal fluorides. New screws were used in each run, and the necessary thermal corrections were made on the data for this side reaction. The deficiency of HF was used to make these corrections which amounted to the formation of roughly 0.0015 mole of iron and chromium fluorides. Since the ΔH_f^0 of iron and chromium fluorides are nearly the same, the correction was made assuming only the formation of iron fluoride ($\Delta H_f^0 = -177.8$ kcal./mole). As an additional check, an OF_2-H_2 run was made with the stainless steel screws replaced by nickel-plated steel screws. No corrosion was found with the new screws, and the HF was found to be in proper stoichiometric amount within the experimental error of the analytical technique. The heat of reaction, using the nickel-plated steel screws, agreed within experimental error with the results which had been corrected for the small amount of corrosion.

Calibration. The energy equivalent of the calorimeter was determined by burning NBS sample 39h benzoic acid. The combustions were

Publication Date: January 1, 1966 | doi: 10.1021/ba-1966-0054.ch020

carried out with the sample ampoule in place and pressurized to 450 p.s.i.g. with N_2 to prevent collapse of the diaphragm. The NBS benzoic acid was reported to have a heat of combustion of 26,434 abs. j./gram mass (weight in vacuo) under standard conditions at 25° C. with an estimated uncertainty of ±3 j./gram. This value was converted (9) to the bomb conditions (temperature 28° C., pressure of oxygen 30 atm., mass of sample about 1 gram, volume of bomb 0.315 liters, mass of water about 1 gram) used during standardization and found to be 26,432.8 abs. j./gram. To evaluate the energy equivalent of the standard calorimeter, E_s, the following quantities were evaluated for each standardization experiment. The weight of benzoic acid burned was converted to m_s, the weight in a vacuum. The ignition energy, q_i, was calculated from the mass of fuse wire burned times the heat of combustion of the fuse wire, 5.86 j./mg. The energy released by combustion of N_2 to HNO_3 (aq.), q_n, was calculated using 57.8 kj./mole as the energy of the reaction. The deviation, Δe_1, of the energy equivalent from that of the standard calorimeter system was calculated from the summation of the product of the weights and heat capacities of water, oxygen, nitrogen, benzoic acid, and the Hastelloy cup (weight about 9.41 grams) containing the benzoic acid. The summation of these heat capacity corrections multiplied by the reciprocal of the temperature coefficient for the platinum resistance thermometer gave Δe_1. The energy equivalent, E_s, was then calculated according to Equation 1:

$$E_s = [(-\Delta E_b\,(28°\text{ C.})\,m_s + q_i + q_n)/\Delta R_c] - \Delta e_1 \qquad (1)$$

where $-\Delta E_b = 26{,}432.8$ abs. j./gram, and ΔR_c is the corrected temperature rise in ohms.

The standard calorimeter system for this series of experiments was specified as the NBS calorimeter containing the Parr fluorine combustion bomb plus sample ampoule. The standard bomb was defined as the Parr fluorine combustion bomb plus sample ampoule minus the water, the benzoic acid pellet, the Hastelloy cup containing the pellet, the oxygen, and the nitrogen used to pressurize the ampoule.

In a series of five calibration determinations, the mean energy equivalent for the system was 203,063.7 j./ohm or 48,533.4 ± 6.5 cal./ohm. The uncertainty is the standard deviation of the mean.

Results and Calculations

The data are referred to a standard temperature of 25° C. The energy unit used is the calorie which is defined as equal to 4.1840 absolute joules.

The quantity of heat observed during the reaction, Q, was calculated from Equation 2:

$$Q = (E_s + \Delta e_2)\Delta R_c \qquad (2)$$

where E_s is the energy equivalent of the calorimeter; Δe_2 is a correction for deviations from the standard calorimeter system and was computed from the heat capacities of OF_2, H_2, and H_2O; ΔR_c is the corrected temperature rise. The heat capacity values used were 10.35 cal./deg. mole (5),

Table I. Data on OF_2–H_2

Run No.	n (moles OF_2)	Δe_2 cal./ohm	ΔR_c ohm	Q cal.	q_1 cal.
1	0.023042	505.0	0.10417	5108.3	−75.7
2	0.023474	505.0	0.10580	5188.3	−84.1
3	0.025011	505.2	0.11325	5553.6	−80.9
4	0.024748	505.2	0.11174	5479.6	−80.4
5	0.023437	505.0	0.10637	5216.2	−76.9
6	0.014507	504.1	0.06469	3172.2	−51.5

[a] n is the number of moles of OF_2; Δe_2 is the correction for deviations from the standard calorimeter system; ΔR_c is the corrected temperature rise in the calorimeter; Q is the quantity of heat observed during the reaction; q_1 includes corrections for nonideality of the reactant gases, condensation of water in the vapor phase, and heat of dilution of HF solution to infinite dilution; q_2 is the energy supplied by corrosion of the screw heads; $-\Delta E_R$ is the

Publication Date: January 1, 1966 | doi: 10.1021/ba-1966-0054.ch020

6.89 cal./deg. mole (*6*), and 0.999 cal./deg. gram for OF_2, H_2, and H_2O, respectively.

The energy of reaction per mole in the thermodynamic standard bomb process, ΔE_R^0, was calculated at 301° K. for each experiment from Equation 3:

$$-\Delta E_R^0 = (Q - q_1 - q_2)/n \tag{3}$$

where q_1 includes corrections for nonideality of the reactant gases $\partial E/\partial P)_T$, condensation of water from the vapor phase caused by adding HF by the reaction, and heat of dilution of the HF solution to infinite dilution (*10*); q_2 is the energy supplied by the corrosion of the screw heads; n is the number of moles of OF_2. For OF_2 the nonideality is obtained from the critical point ($t_c = -58.0 \pm 0.1°$ C., $P_c = 48.9$ atm.) (*1*) which gives van der Waals constants $a = 0.269$ and $b = 0.0451$ using the following relationships:

$$a = 27R^2T_c^2/64P_c \qquad b = RT_c/8P_c$$

The nonideality correction is then determined from Equation 4:

$$(\partial E/\partial P)_T = -\mu C_p - \left(\frac{\partial[PV]}{\partial P}\right)_T \tag{4}$$

where μ = the Joule-Thompson coefficient $= 1/C_p\ (2a/RT - b)$, and a and b are van der Waals constants. The term $-(\partial[PV]/\partial P)_T$ is determined from the van der Waals equation of state. This value was reduced to the standard heat of reaction at 25° C. Calculating ΔH_R^0 from ΔE_R^0 was done in two steps:

(1) Heats of reaction at 28° C. were calculated from the energy of reaction using the thermodynamic equation $\Delta H_R^0 = \Delta E_R^0 + \Delta nRT$ where Δn is the change in the number of moles of gaseous substances during reaction.

Heat of Reaction[a]

q_2 cal.	$-\Delta E^0_R$ kcal./mole	q_3 kcal./mole	q_4 (ΔT) kcal./mole	$-\Delta H^0_R$ (298.16° K.) kcal./mole
79.2	221.54	−1.80	+0.20	223.14
63.4	221.91	−1.79	+0.19	223.51
87.1	221.80	−1.80	+0.20	223.40
95.0	220.83	−1.79	+0.20	222.42
97.9	221.67	−1.80	+0.19	223.28
0	222.22	−1.79	+0.20	223.81

mean $-\Delta H^0_R$ = 223.26 ± 0.38 kcal./mole[b] was omitted from this table

heat of reaction per mole in the thermodynamic standard bomb process; q_3 is the ΔnRT term to convert energy of reaction to heat of reaction; q_4 is the difference in the heat capacities at constant pressure of the products and reactants; $-\Delta H_R$ is the standard heat of reaction at 25° C.

[b] Uncertainty indicated is twice the standard deviation of the mean.

(2) Heats of reaction at 25° C. were calculated from the equation ΔH_R^0 (298.16° K.) = ΔH_R^0 (301.16° K.) + ΔC_p (298.16–301.16) where ΔC_p is the difference in the heat capacities at constant pressure of the products and reactants. The value for HF (infinite dilution) was taken as −29.5 cal./deg. mole.

The results of the experiments with OF_2-H_2 are given in Table I. The average value of ΔH_R^0 for OF_2-H_2 is −223.26 ± 0.38 kcal./mole.

Discussion

Based on the measured value of the standard heat evolved from the reaction:

$$OF_2\,(g) + 2H_2\,(g) \rightarrow H_2O\,(1) + 2HF\ \text{(infinite dilution)}$$

and combined with the values ΔH_f^0 (HF $_\infty$) = −79.50 kcal./mole, as suggested by Evans (*4*) and ΔH_f^0 (H_2O 1) = 68.32 kcal./mole the calculated standard heat of formation, ΔH_f^0, of OF_2 (g) is −4.06 ± 2.20 kcal./mole.

The uncertainty in the heat of formation was calculated by taking the square root of sum of the squares of the precision error, the accuracy error, and the calibration error. The precision error reflects the reproducibility of the experiments and was taken as twice the standard deviation of the mean. The accuracy error (systematic errors) was obtained by estimating the effect of the various factors on the reaction (such as purity of reactants and limits of error involved in the analyses). This error was estimated to be about 1%.

The heat of formation value, combined with the most recent heats of atomization of fluorine (18.860 kcal.) and oxygen (59.559 kcal.) (*7, 8*) yields a value of 50.7 kcal./mole for the O–F bond energy in OF_2.

Acknowledgment

We wish to acknowledge the assistance of Neal N. Ogimachi who synthesized the OF_2 used in preliminary runs and helped to load the ampoule. The support of the research by the Air Force under contracts AF33(616)-6768 and AF04(611)-7023 is gratefully acknowledged also.

Literature Cited

(1) Anderson, R., Schnizlein, J. G., Toole, R. C., O'Brien, T. D., *J. Phys. Chem.* **56**, 473 (1952).
(2) Chemical Propulsion Information Agency, *CPIA Publ. No. 44*, **1**, 59 (1964).
(3) Dickinson, H. C., *Nat. Bur. Std.* (*U. S.*), Bull. **11**, 189 (1914).
(4) Evans, W. H., Munson, T. R., Wagman, D. D., *J. Res. Nat. Bur. Std.* **55**, 147 (1955).
(5) "JANAF Interim Thermochemical Tables," Dow Chemical Co., Midland, Mich., Sept. 1964.
(6) Ibid., March 1961.
(7) Ibid., June 1961.
(8) Ibid., June 1962.
(9) NBS Certificates for standard sample 39h, benzoic acid.
(10) Rossini, F., *et al.*, *Nat. Bur. Std.* (*U. S.*) *Circ.* **500** (1952).
(11) Ruff, Q., Menzel, W., *Z. Anorg. Allgem. Chem.* **198**, 375 (1931).
(12) VonWartenberg, H., Klinkhott, F., *Z. Anorg. Allgem. Chem.* **193**, 409 (1930).

RECEIVED April 22, 1965.

Chemical Analysis of Corrosive Oxidizers

I. Gas Chromatographic Analysis of Chlorine Trifluoride

V. H. DAYAN and B. C. NEALE

Rocketdyne Division, North American Aviation, Inc., Canoga Park, Calif.

Publication Date: January 1, 1966 | doi: 10.1021/ba-1966-0054.ch021

Chlorine trifluoride (ClF_3) was analyzed quantitatively using a custom built corrosion resistant gas chromatograph with a specially prepared column containing Halocarbon oil 13-21 on Kel-F 300. Retention times for fluorine, chlorine monofluoride, perchloryl fluoride, chlorine, chlorine dioxide, and chlorine trifluoride have been determined. Special sampling techniques, sample handling, and sample introduction techniques are described. A near infrared method for determining hydrogen fluoride is also presented. The combination of gas chromatography and infrared spectrophotometry provides a method for the complete analysis of chlorine trifluoride.

Chlorine trifluoride, a highly corrosive and reactive oxidizer, shows considerable promise as an earth-storable liquid propellant. Since the impurities normally found in chlorine trifluoride are also highly reactive and contain halogens, a direct method of analysis, using a system which is inert to all species, is required.

The quantitative analyses of chlorine trifluoride has been carried out by gas chromatography, using a custom built gas chromatograph with a specially prepared column containing Halocarbon oil on Kel-F. The inlet system of the gas chromatograph is designed so that a liquid sample can be expanded to a gas, and a representative gaseous sample can be taken simultaneously for infrared, near infrared, and gas chromatographic analyses.

Gas liquid chromatography has been used recently for analyzing interhalogens, their impurities, and their degradation products (*1, 2, 3, 4*).

In Advanced Propellant Chemistry; Holzmann, R.;
Advances in Chemistry; American Chemical Society: Washington, DC, 1966.

Lysyj and Newton (*4*) recently described a column which has proved to be very successful for analyzing chlorine trifluoride. A custom built gas chromatograph, utilizing this column, and the use of this instrument to analyze chlorine trifluoride are presented here.

Experimental

Apparatus. A diagram of the custom built gas chromatographic instrument is shown in Figure 1. Because of the highly reactive and corrosive nature of ClF_3, the construction materials for the instrument were stainless steel, Monel, and nickel. The apparatus is best considered as four parts: sample inlet system, column, detector, and detector bypass.

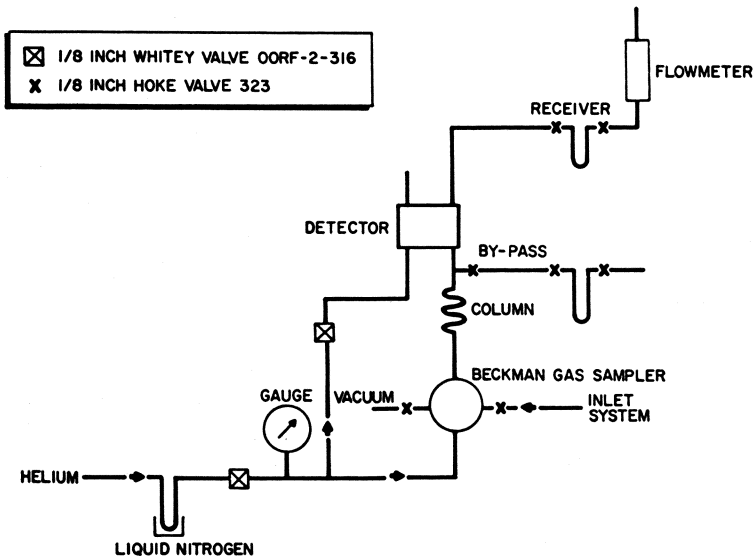

Figure 1. Gas chromatograph for interhalogens

Sample Inlet System. A detailed diagram of the inlet system is shown in Figure 2. All pipework on the system is $^1/_4$-inch stainless steel tubing except where otherwise designated. Valves 1–10 are $^1/_8$-inch stainless steel Hoke valves with V-stems and Teflon packing. Valves 2, 4, 6, and 10 are fitted with $^1/_4$-inch AN-"B" nuts for rapid attachment of samplers. The Beckman two-way gas sampling valve is lubricated with Halocarbon oil 13-21. The sampling loops were replaced by two stainless steel U-tubes of 1.5- and 20-cc. capacity. The expansion bomb is a 1.7-liter stainless steel cylinder. The trap between the helium supply and the Beckman valve is $^1/_4$-inch stainless steel tubing. A null detector is used to measure pressures in the inlet system. Samples are obtained in 10-ml. stainless steel cylinders fitted with a $^1/_8$-inch stainless steel Hoke valve with a V-stem and Teflon packing. When the sample is liquid, it is entirely vaporized into the 1.7-liter expansion bomb, and a gaseous sample is taken for infrared, near infrared, and gas chromatographic analysis.

Publication Date: January 1, 1966 | doi: 10.1021/ba-1966-0054.ch021

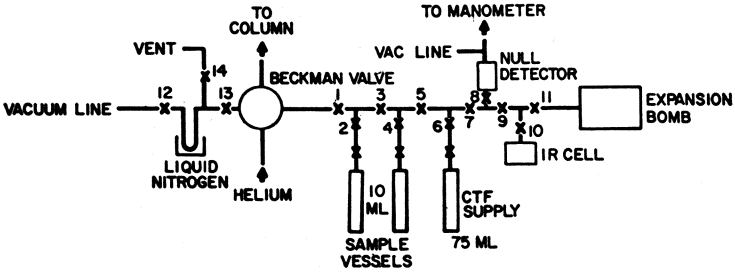

Figure 2. Sample inlet system

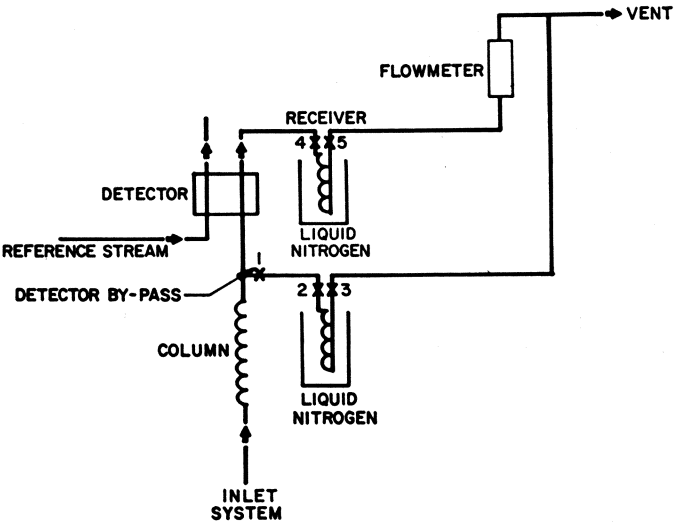

Figure 3. Column, detector, and detector bypass

The infrared cell is fabricated from 5.0-cm. diameter Monel pipe. The windows are silver chloride and are sealed to the body with Halocarbon wax 8-00. The valve for introducing the sample into the cell is a Hoke 417 diaphragm valve.

The near infrared cell is also Monel. The body of the cell is 2.0 cm. in diameter and 7.5 cm. long. The windows are calcium fluoride and are sealed to the nickel body with Halocarbon wax 8-00. The valve is a Hoke 323 stainless steel valve.

Gas Chromatograph Column. The column is a 20-ft. Halocarbon oil 13-21 on Kel-F 300 low density molding powder, 50% w./w. The column was prepared as follows. A known weight of Halocarbon oil 13-21 was dissolved in trichloroethylene. An equal weight of chromatographic grade Kel-F powder, 30–50 mesh, was suspended in the solution. The suspension was refluxed for 30 minutes before removing the solvent by conventional means. The dried material was packed into two 10-ft. sections of $^1/_4$-inch nickel tubing. The packed columns contained 3.5 grams of packing per foot. Prior to use, the column was passivated by allowing approximately 3 ml. of liquid chlorine trifluoride to evaporate

through the column over a 4–8 hour period, after which the column was flushed with helium for 1 hour to remove residual gases.

Detector. A Gow-Mac thermoconductivity cell, model 9285 (pretzel type) with a conventional Wheatstone bridge electrical circuit was used. The cell is a nickel detector block with nickel filaments.

Detector By-pass. A detector bypass was incorporated between the column and the detector. The bypass was used when the inlet system and column were being passivated with chlorine trifluoride. This prevented unnecessary exposure of the cell block and cell filaments to large quantities of corrosive gases. A diagram of the column, detector, bypass, detector, and receiver is shown in Figure 3. All portions of the system are protected from back diffusion of moisture by using the liquid nitrogen traps.

Carrier Gas. Helium was used as a carrier gas. Before entering the instrument, the helium was freed of moisture by passing through a $^1/_4$-inch U-tube immersed in liquid nitrogen.

Analytical Procedure. SAMPLING PROCEDURE. A schematic of the sampling procedure is shown in Figure 4. Representative liquid samples are obtained from storage tanks, run tanks, and cylinders using this system.

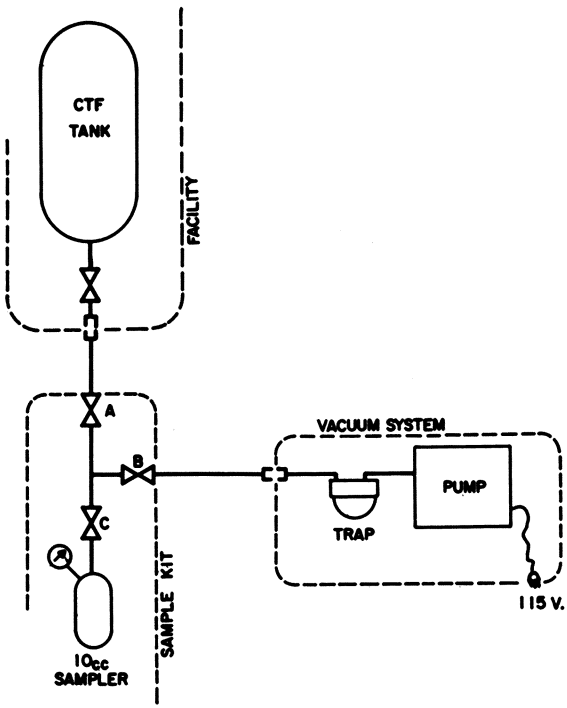

Figure 4. ClF_3 sampling schematic

After evacuating the sampling system, the entire metal line from the valve on the tank to valve B is passivated for 30 minutes with about 1 atm. of chlorine trifluoride vapor. The passivating gas is then condensed into

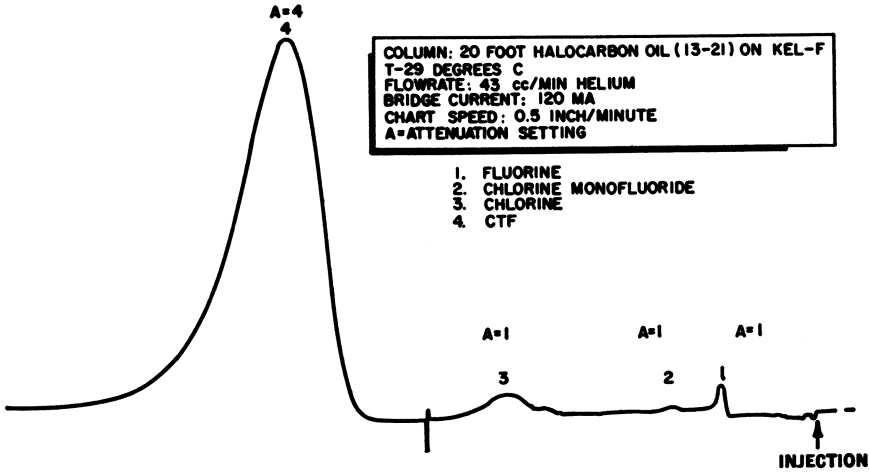

Figure 5. Typical GC curve of ClF_3

the trap and the system is evacuated. Valves B and C are closed, and liquid chlorine trifluoride is dropped into the tee between valves A, B, and C. The tee holds 6–7 grams of chlorine trifluoride. Valve A is closed, and the sample is dropped into the 10-ml. sampler.

INTRODUCTION OF SAMPLE TO THE CHROMATOGRAPH (FIGURE 2). The 10-ml. sampler containing liquid sample is attached to one of the outlets on the manifold. The entire inlet system, including the Beckman valve loop, the expansion bomb, and the infrared cell, is evacuated. Valves 1 and 7 are closed, and then a gaseous sample of ClF_3 is introduced through valve 6 into the inlet systems for passivation. After 30 minutes, the gases are removed from the inlet system by condensing them into a liquid nitrogen trap just before the vacuum pump. By appropriate valve operations, the inlet system is again pumped out, valves 1, 8, and 10 are closed, and the sample to be analyzed is allowed to vaporize into the expansion bomb resulting in a total pressure of 300–500 mm. Valve 11 is then closed, and the remainder of the inlet system is again evacuated. Approximately 100 mm. of vapor are introduced from the expansion bomb into the infrared cell and into the large loop of the Beckman valve. The Beckman valve is rotated, introducing the sample onto the column. The infrared cell is removed and scanned in a spectrophotometer. After each analysis, the gaseous sample is recondensed into the 75-ml. storage bomb by using a liquid nitrogen bath and residual gas removed by the vacuum system. The vacuum pump is protected by the liquid nitrogen trap, but it has been found expedient to change the oil periodically. A typical gas chromatogram is shown in Figure 5. Calculations are based on the assumption that mole percent is proportional to peak area.

The gas chromatograph provides for all expected components except hydrogen fluoride. The infrared spectrum is a cross-check and provides additional information when unexpected species are present.

Hydrogen fluoride (HF) is determined quantitatively by near infrared spectrophotometry. The spectrum of HF is shown in Figure 6. It was obtained on a Beckman DK-2 spectrophotometer. A calibration

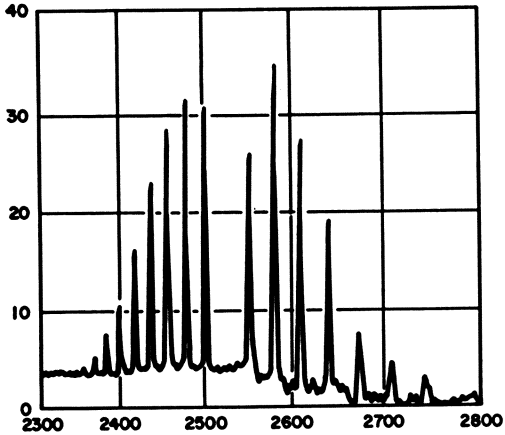

Figure 6. Near infrared spectrum of hydrogen fluoride in ClF_3

curve of the 2580-mμ band was used for the quantitative work. Since HF is normally expected to be present in the 0–5 mole percent range, the sample size normally taken into the calcium fluoride cell is 300–600 mm.

Results and Discussion

The retention times of various components are given in Table I. Because of their extremely reactive nature, several operational problems were encountered in analyzing interhalogens that are not normally experienced with conventional gas chromatography. Whenever a sample was attached to the inlet manifold, the portions of the inlet systems which had been exposed to the atmosphere had serious detrimental effects on the sample when introduced into the inlet. Absorbed surface moisture caused the breakdown of ClF_3. Figure 7 shows a typical chromatogram of a sample of ClF_3 which was introduced through an unpassivated inlet system and allowed to remain in contact with it for

Table I. Retention Times of 20-ft. Column at 25° C.[a]

Component	*Retention Time, Minutes*
Fluorine, air	2.5
Chloryl fluoride	3.0
Chlorine monofluoride	3.5
Perchloryl fluoride	7.0
Chlorine	8.0
Chlorine dioxide	11.5
Chloride trifluoride	13.5–14.0

[a] Helium flowrate: 43 cc./minute

10 minutes. Therefore, the inlet system must be thoroughly passivated with ClF_3 before each sample introduction.

The inlet manifold and the near infrared cell are always maintained fully passivated by keeping 100–200 mm. of chlorine trifluoride in them between analyses. Whenever a sample is to be introduced into the infrared cells, the cells must first be passivated several times with the sample.

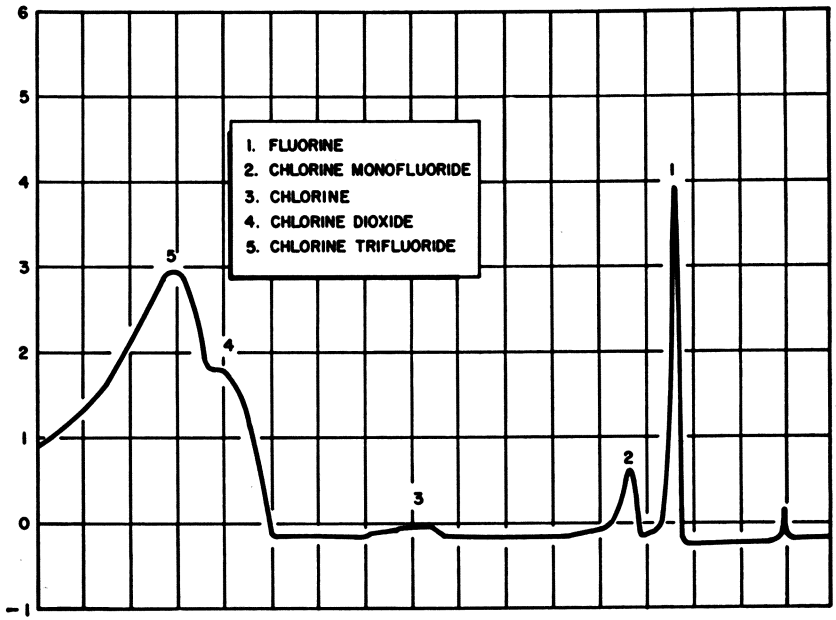

Figure 7. Chromatogram of chlorine trifluoride reaction with unpassivated inlet

Chlorine trifluoride gradually attacks the silver chloride windows of the infrared cell. When the attack is sufficient to cause serious background on the infrared scan, the cell windows are polished best by using a 5% sodium thiosulfate solution on a velvet polishing cloth.

Summary

The analysis of chlorine trifluoride has been routinely performed by a gas chromatographic technique using a specifically designed corrosion resistant instrument. Well-defined chromatographic peaks are obtained for chlorine trifluoride and all normally expected components, except hydrogen fluoride. The hydrogen fluoride content is determined by an independent near infrared method.

Literature Cited

(1) Ellis, J. F., Forrest, C. W., Allen, P. L., *Anal. Chem. Acta.* **22**, 27 (1960).
(2) Ellis, J. F., Forrest, C. W., *J. Inorg. Nucl. Chem.* **16**, 150 (1960).
(3) Iveson, G., Hamlin, A. G., Phillips, T. R., *Pittsburgh Conf. Anal. Chem. Appl. Spectroscopy, Pittsburgh, 1961.*
(4) Lysyj, I., Newton, P. R., *Anal. Chem.* **35**, 90 (1963).

RECEIVED August 9, 1965.

Publication Date: January 1, 1966 | doi: 10.1021/ba-1966-0054.ch021

Chemical Analysis of Corrosive Oxidizers

II. Instrumental Analysis of Nitrogen Tetroxide

N. V. SUTTON, H. E. DUBB, R. E. BELL, I. LYSYJ, and B. C. NEALE

Rocketdyne Division, North American Aviation, Inc., Canoga Park, Calif.

Publication Date: January 1, 1966 | doi: 10.1021/ba-1966-0054.ch022

Since nitrogen tetroxide (NTO) is the most widely used oxidizer in the U.S. space program, it has become necessary to develop sophisticated analytical chemical techniques to ensure the integrity of this system. Commercial NTO consists of N_2O_4, NO_2, N_2O_3, NO, and H_2O (as HNO_3 and HNO_2). The techniques of NMR spectrometry as applied to the proton content are described in detail. Gas-solid chromatography was used to determine the nitrogen oxidizer.

Nitrogen tetroxide is presently the work horse earth-storable oxidizer in liquid propellant systems. Present methods of analysis are wet chemical methods and are nonspecific. In order to fully understand the difficulties encountered in analyzing this compound, a brief review of its chemical and physical properties is presented.

The equilibrium reaction $N_2O_4 \rightleftharpoons 2NO_2$ is one of the fastest chemical reactions known. Nitrogen dioxide, NO_2, is an intensely brown-colored gas. In the liquid state it is largely dimerized to nitrogen tetroxide, N_2O_4, and in the solid state it exists solely as colorless nitrogen tetroxide. The brown color of the liquid is solely the result of the equilibrium quantity of nitrogen dioxide present.

When completely dry, nitrogen tetroxide is not significantly corrosive toward most common metals at room temperature. When it is moist, it becomes highly corrosive because of the formation of nitric acid.

Nitrogen sesquioxide, N_2O_3 (Also called dinitrogen trioxide), is formed by equimolar reaction of NO and NO_2. This oxide is, in turn, in equilibrium with the quite unstable nitrous acid, HNO_2, in the presence of water:

$$NO + NO_2 + H_2O \rightleftharpoons N_2O_3 + H_2O \rightleftharpoons 2HNO_2$$

In Advanced Propellant Chemistry; Holzmann, R.;
Advances in Chemistry; American Chemical Society: Washington, DC, 1966.

N_2O_3 is a dark blue liquid when boiling with decomposition into NO and NO_2 at 38° F. Nitrous acid is a paler blue liquid and is a rather weak acid but a fairly strong oxidizing agent. When the blue N_2O_3 and brown NO_2 are present in N_2O_4, a characteristic dark green color results.

Starting with pure N_2O_4 and pure H_2O, a final solution will be reached through a series of complex equilibrium reactions which may contain all of the species found in Table I.

Table I. Chemical Species in NTO

Species	*State*	*Color*
N_2O_4	Liquid	Colorless
NO_2	Gas and dissolved in liquid	Dark brown
NO	Gas and dissolved in liquid	Colorless
N_2O_3	Liquid	Dark blue
HNO_3	Liquid	Colorless
HNO_2	Liquid	Light blue
H_2O	Liquid	Colorless

Experimental

The military specification for N_2O_4 (Mil. Spec. P-26539A) requires among other things, 99.5% minimum N_2O_4 and 0.1% maximum H_2O equivalent. In the assay, an excess of standard base is added to a known amount of N_2O_4, and the excess is back-titrated with standard acid. Calculations are based upon a milliequivalent weight of 4.6008. If various percentages of the mixed oxides and acids are present, however, they may add or detract from the total acid value calculated as N_2O_4. The water equivalent is determined by evaporating a known amount of N_2O_4 to a residue which is assumed to be a 70% nitric acid solution. This analysis requires an average of 12 hours.

NMR Determination of Protons in NTO. Because of the need for a rapid, reliable method for determining water in N_2O_4, attention was directed to using nuclear magnetic resonance (NMR) as a tool for total proton determination. NMR is advantageous in that only the protons may be observed, and no other nuclei interfere.

In the liquid NTO system, protons are mobile and exchange freely and rapidly with one another. This is an advantage in that only one resonance line will be observed, but it is a disadvantage in that information as to the amounts of the different protons containing species (H_2O, HNO_3, and HNO_2) cannot readily be obtained.

Preparation of Sample. For this determination, a special NMR tube is required. The regular thin-walled NMR tubes are not satisfactory because of the danger of explosion from the pressure of NTO gas and because of the difficulty of any glass blowing with the thin walled tubes. NMR grade, specially sized, borosilicate glass tubing may be purchased from Corning Glass Works. This tubing is 4.80 mm. ±0.004-inch o.d. with 0.8 mm. ±0.005-inch wall. An 8-inch tube is used with a standard taper 12/30 inner joint joined to the open end.

Publication Date: January 1, 1966 | doi: 10.1021/ba-1966-0054.ch022

Approximately 0.5–1.0 ml. of NTO is run into a sample tube, and the tube is quickly capped with a 12/30 outer joint glass cap. Next, the tube is immersed in LN_2 to freeze the NTO. The cap is removed, and the taper joint is attached to a vacuum line as quickly as possible. Still frozen, the tube is pumped out and sealed off with a torch at the junction between the NMR tube proper and the taper joint. Samples so prepared may be stored indefinitely without deterioration or accumulation of moisture.

All of the NTO samples examined so far contained protons in appreciable quantities. To prepare standards, therefore, known amounts of water are added over and above that which is already present, and the calibration curve is extrapolated back to the base line.

Standards are prepared by weighing a special NMR tube together with cap (preferably on an automatic semimicro balance to five places). A measured amount of water is added from a microliter syringe, and the tube, cap, and H_2O are reweighed. NTO is again added, and the tube is weighed. The tube is then frozen, pumped, and sealed off as previously described. If the NTO is first cooled to ice temperature and the tube kept capped, it is perfectly safe to remove the tube from the ice bath long enough to make the second weighing if an automatic balance is used.

NMR Determination. Any NMR instrument capable of detecting protons and equipped with an integrator should be suitable. In the Rocketdyne work, the Varian DP-60 was used, although the Varian A-60 or HA-56/60 would be equally applicable.

After the instrument is warmed up and aligned with an organic proton-containing compound such as acetaldehyde, acetone, or chloroform, integrals are taken consecutively of the unknown and of one or two standards using the same instrumental parameters. Table II and Figure

Table II. Calibration Data for NMR Determination of Protons

Water Added	*Integral (Arbitrary Units)*
0	22
0.078	31
0.36	67

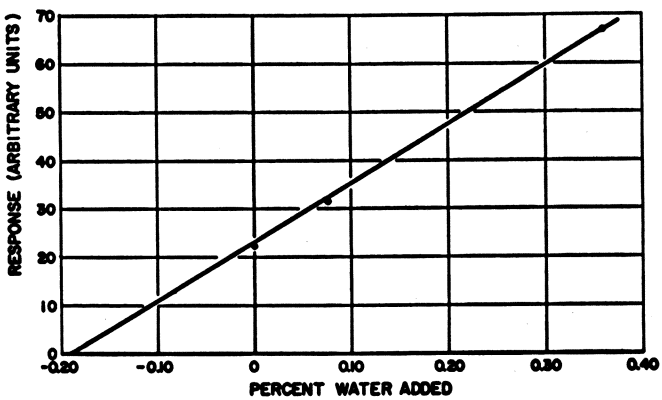

Figure 1. Calibration curve for NMR determination of protons in NTO

Publication Date: January 1, 1966 | doi: 10.1021/ba-1966-0054.ch022

1 show the reading of one unknown and two standards (prepared from the same unknown) all run at +40 decibel RF power and 0.30 X integral output.

In Figure 1, the intercept on the horizontal axis falls at 0.19%. This represents the amount of protons (calculated as water) originally present in the as-received NTO. Thus, the standard to which 0.078% water was added actually contains 0.27% while the second standard actually contains 0.55%.

Results

Comparison of the values obtained from samples by the NMR method and by the military specification method are given in Table III together with a value for H_2O-saturated NTO.

Table III. Percent Water in Unknown

Sample	*NMR, %*	*Military Specification, %*
4-477	0.29	0.17
4-478	0.24	0.14
Bravo	0.19	0.08
5-390	0.16	0.05
6-33	0.26	0.22
6-164	0.20	0.23
Saturated	1.71	1.6 (Ref. *1*)

The value of 1.6% for saturated H_2O is a literature value at 25° C. (*1*). No value is available for the military specification method. The NMR value was taken at 28.3° C., which is the operating temperature of the Rocketdyne magnet. It is felt that this temperature difference could cause the higher value of 1.71%.

Discussion

Insofar as precision of the NMR method is concerned, the small number of samples so far analyzed do not permit a firm statistical analysis. Values so far obtained have agreed within ±0.01%. The NMR values usually run consistently higher than the military specification values by about 0.11%. It will probably be necessary to accumulate more data comparing NMR and military specification results before this discrepancy can be reconciled. However, the NMR results appear to be quite self-consistent, and we suspect that the assumption made in the military specification procedure—that no water is lost during the evaporation—may not be true.

The NMR method appears quite attractive at this time. The reproducibility of results is considerably better than with the military specification method. In addition, the time required per analysis, including the encapsulation of the sample, is no more than $^1/_2$ to $1^1/_2$ hours while the military specification procedure is considerably longer.

Publication Date: January 1, 1966 | doi: 10.1021/ba-1966-0054.ch022

Gas Chromatography Analysis of NTO. As previously mentioned, the presently accepted method for assaying N_2O_4 is really only a total acid value and does not indicate the real composition of nitrogen tetroxide. There were many unsuccessful attempts over the past decade to analyze oxides of nitrogen by gas chromatography; both gas-liquid and gas-solid attempts failed.

The use of gas-liquid chromatography, which utilizes an organic substrate to achieve separation, was precluded by the extreme reactivity of NTO which will react with almost any organic substrate used in chromatography. The conventional gas-solid chromatography uses materials such as silica gel, molecular sieve, alumina, etc. to achieve separation resulting from surface adsorption. Most of the materials mentioned, however, exhibit a high degree of polarity. An attempt to analyze nitrogen oxides using such materials resulted in broad tailing peaks which precluded the possibility of using this approach as a basis for a quantitative analytical technique.

A gas chromatographic analysis of NTO, including separation of NO and N_2O_4, has been accomplished recently. The success of this work was a product of a fundamental study dealing with the principles of high temperature gas-solid chromatography. A number of candidate solid substrates were examined, and the best results were obtained with porous glass. A detailed discussion of porous glass as a gas chromatographic medium, including surface area characteristics (pore volume, pore size, surface area, etc.) was published by MacDonell (*3*) and Lysyj and Newton (*2*). It is sufficient here to state that porous glass shows gas chromatographic separating properties and is inert to the oxides and oxyacids of nitrogen.

As the first step in this investigation, a gas chromatograph was designed and built. The instrument incorporates a universal injection system (made by Microtek Instruments) which can withstand attack by highly reactive specimens.

Two 6-ft. $^3/_{16}$-inch diameter, stainless steel columns packed with 30–40 mesh porous glass (one separating and one reference) are placed in a temperature-programmed oven, which can be programmed at a high temperature rate. The two columns were necessary to provide a uniform change of pressure drop across the separating and reference gas stream, eliminating drifting base line when a temperature program is applied. The detector consists of a thermoconductivity cell with Teflon-clad hot wires (to prevent corrosion of the filaments), housed in a separately heated enclosure. For the read-out, a custom built bridge with potentiometric recorder and a printing integrator are used. The schematic of this system is shown in Figure 2.

Experiments which have been conducted to date indicate that gas

Publication Date: January 1, 1966 | doi: 10.1021/ba-1966-0054.ch022

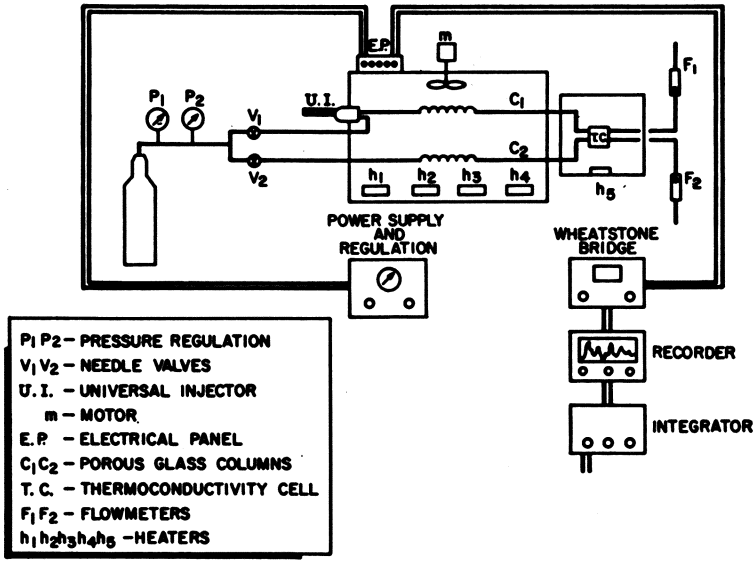

Figure 2. Gas chromatograph for analysis of NTO

chromatographic analysis of nitrogen oxides is feasible, using the high temperature, gas-solid chromatographic principle. In order of elution, the following species appear at room temperature: air, nitric oxide, and nitrogen tetroxide. One temperature programming, an as yet unidentified peak elutes at at temperature of ~ 75° C., followed by water at ~ 165° C. Work is presently being carried out to optimize conditions for the resolution of all of the apparent peaks in N_2O_4.

Acknowledgment

This work was supported, in part, under Contracts AF04(611)7023 and AF04(611)9377, Edwards Air Force Flight Test Center, Edwards, Calif., under the program monitorship of Forrest Forbes.

Literature Cited

(1) Briner, E., Burand, E. L., *Compt. Rend.* 155, 583 (1912).
(2) Lysyj, I., Newton, P. R., *Anal. Chem.* 36, 2514 (1964).
(3) MacDonell, H. L., Noonan, J. M., Williams, J. P., *Anal. Chem.* 35, 1253 (1963).

RECEIVED August 9, 1965.

The Electrical Conductivity of Solid Chlorine and Bromine Trifluorides

MADELINE S. TOY and WILLIAM A. CANNON

Astropower Laboratory, Douglas Aircraft Co., Inc., Newport Beach, Calif.

Publication Date: January 1, 1966 | doi: 10.1021/ba-1966-0054.ch023

The variations of electrical conductivity with temperature of chlorine and bromine trifluorides have been measured from near boiling points to well below melting points. A maximum conductivity below the freezing point of chlorine trifluoride (—83° C.) has been observed, and possible mechanisms for the negative temperature effect are discussed. The electrical conductivities of bromine trifluoride only show little variation with temperature at the liquid state, but on solidification the conductivity is greatly diminished. The conductivity curve of solid bromine fluoride gives two branches similar to silver chloride and bromide and thallium chloride and bromide as described by Lehfeldt. The activation energy for a lower temperature process (between —20° and —196° C.) is 3.81 kcal./gram mole, and the value of higher temperature process (between +8.8° to —20° C.) is 29.8 kcal./gram mole.

The interest in conductivity measurements on fluorinated inorganic compounds at cryogenic temperatures lies in the ability of these compounds to form ions for possible synthesis of potential solid oxidizers. In this study we are concerned with the conductivity measurements of solid chlorine and bromine trifluorides to determine their electrical conductivities and its bearing on structural problems. Specific conductivities of $<10^{-6}$ at 0° C. (*1*) and 10^{-9} $ohm^{-1}cm.^{-1}$ (*3*) have been reported for chlorine trifluoride and 8.0×10^{-8} $ohm^{-1}cm.^{-1}$ at 25° C. (*1*) for bromine trifluoride. In this work a conductivity cell has been developed for measuring fluorine-containing oxidizers at cryogenic temperatures. The variations of conductivity with temperature of chlorine trifluoride have been measured from +11.3° C. (b.p.) to —130° C. (well below m.p., —83° C.) and of bromine trifluoride from +80° C. to —196° C. (m.p., 8.8° C.). Possible mechanisms are discussed.

In Advanced Propellant Chemistry; Holzmann, R.;
Advances in Chemistry; American Chemical Society: Washington, DC, 1966.

Experimental

Materials. Chlorine and bromine trifluorides were obtained from the Matheson Co. Chlorine trifluoride was purified by passing the vapor through a sodium fluoride scrubber to remove possible hydrogen fluoride impurity and then fractionally distilled. Bromine trifluoride was used without additional purification, except the first fraction of the sample was evacuated under reduced pressure at room temperature to remove possible lower boiling impurities.

Conductivity Measurements. Cell resistance measurements were made with a General Radio type 1650-A impedance bridge. It is equipped with an internal, 1000-cycle signal source and tuned null detector. For more sensitive balance at high resistances, a Hewlett Packard 400L vacuum tube voltmeter is used as an external null detector.

Publication Date: January 1, 1966 | doi: 10.1021/ba-1966-0054.ch023

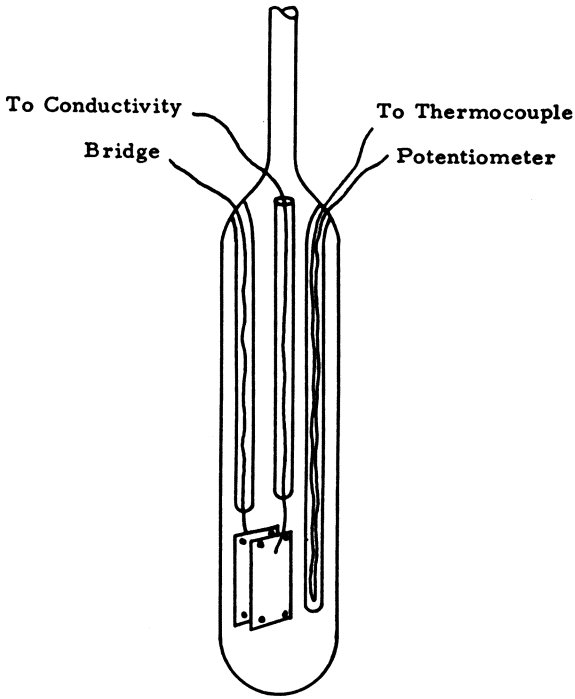

Figure 1. Conductivity cell

The conductivity cell is modified from a conventional type. It is made of borosilicate glass, which resists the attack of anhydrous chlorine and bromine trifluorides, and is equipped with two smooth platinum electrodes to minimize electrode corrosive effects. These electrodes are approximately 12×25 mm. in size, held 1.5 mm. apart with borosilicate glass spacers. The arrangement of electrodes and leads is shown in Figure 1. An internal thermocouple well leads from the top of the cell to a point near the electrodes and contains a copper constantan thermocouple. The cell constant is determined by measuring the cell resistance

while the cell is filled with 0.001*N* KCl solution at 25° C. (cell constant = specific conductivity × observed resistance, where specific conductivity of 0.001*N* KCl at 25° C. = 0.00014695 $ohm^{-1}cm.^{-1}$). The change in cell constant owing to changes in cell and electrode dimensions has been calculated to be insignificant to as low as −195° C. and is therefore ignored in this work.

The possibility of imperfect contact of the solid with the electrode does not seem to be a problem in view of the uniformity of the curves and reproducibility as indicated below.

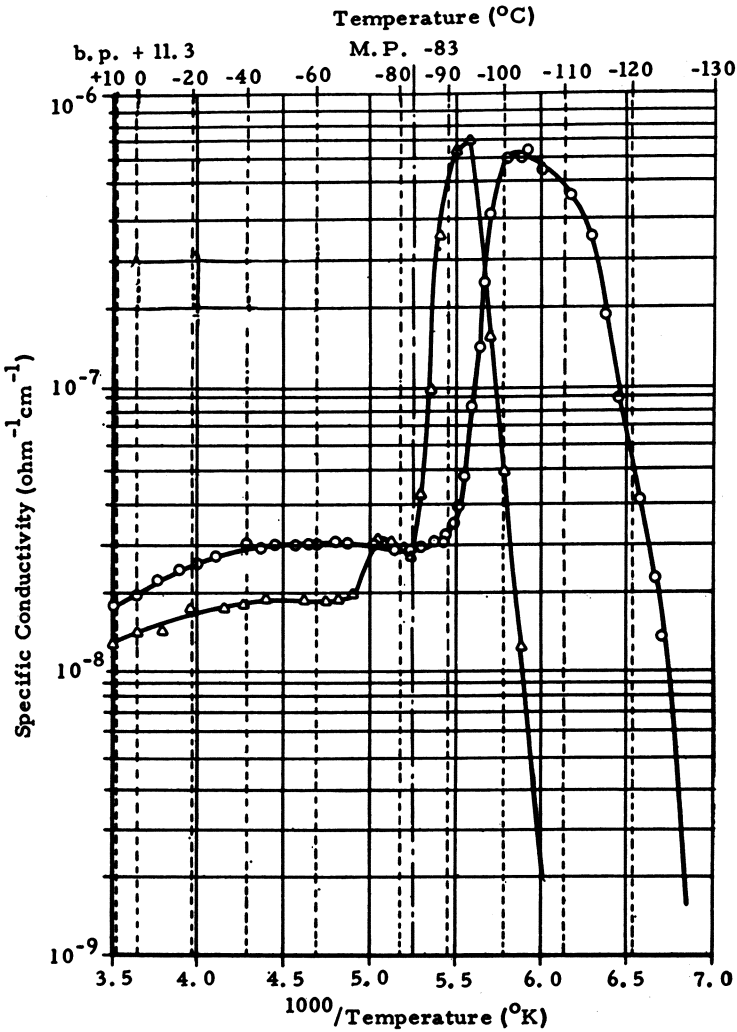

Figure 2. Conductivity of chlorine trifluoride as a function of temperature. Δ—before low temperature fractionation; 0—after low temperature fractionation

Results and Discussion

Conductivity *vs.* Temperature of Chlorine Trifluoride. The conductivity of chlorine trifluoride has been measured over the temperature range from near the boiling point (+11.3° C.) to —130° C. Figures 2 and 3 are plots of the conductivity as a function of temperature as the sample of chlorine trifluoride is cooled from the boiling point at a rate of approximately 2°–3° C. per minute. The conductivity increases slightly

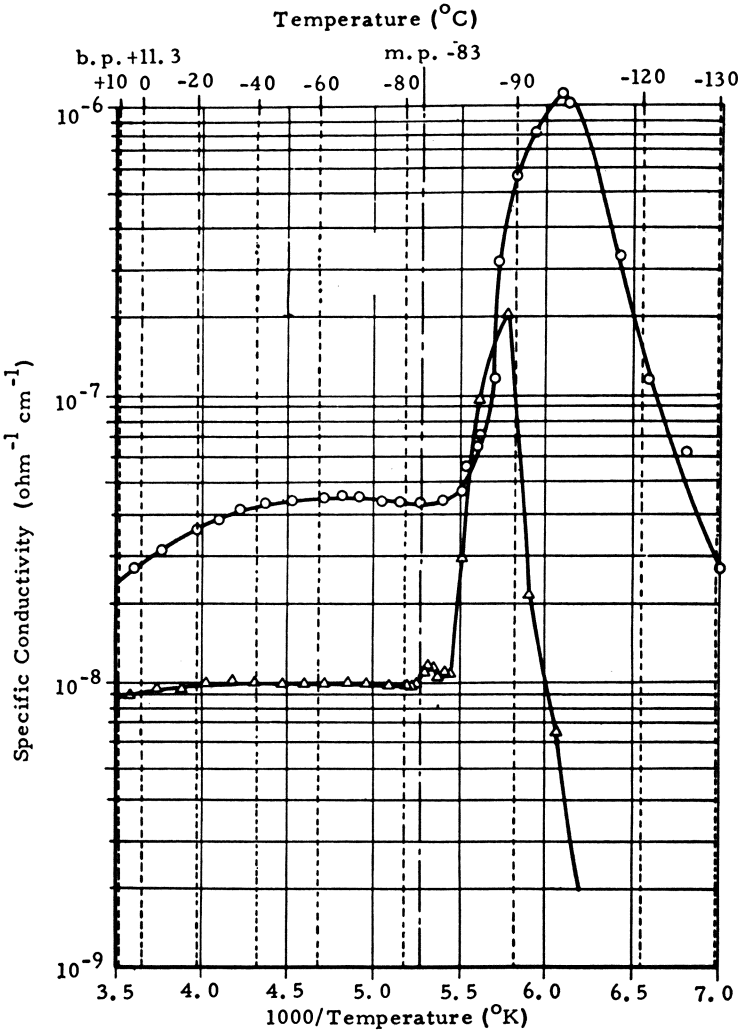

Figure 3. Conductivity of chlorine trifluoride as a function of temperature. Δ—before low temperature fractionation; 0—after low temperature fractionation

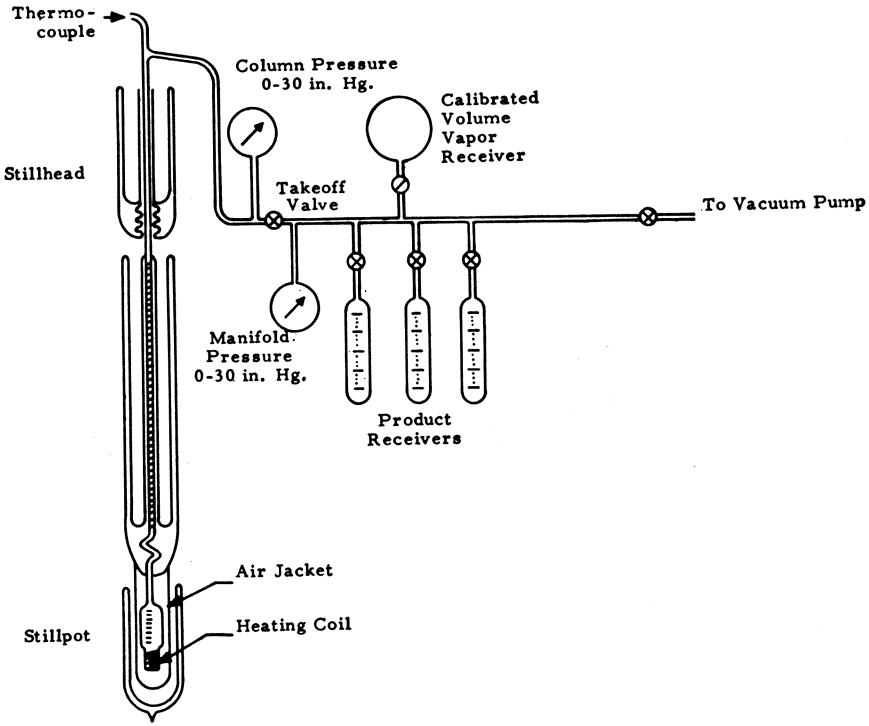

Figure 4. Schematic diagram of low temperature fractionation and gas chromatography apparatus

as the sample is cooled and displays a small maximum before the freezing point (m.p. —83° C.) is reached. Below the freezing point the conductivity increases rapidly to a sharp maximum. The temperature *vs.* conductivity plot (Figure 2) for a sample purified by low temperature fractionation (*9*) no longer has the small maximum occurring just above the freezing point, and the maximum peak has been broadened and displaced to a lower temperature.

It was thought that the broadening of the peak may reflect the presence of trace carbon or silicon halides or chlorine impurities which might have been introduced through reaction of chlorine trifluoride with Kel-F grease used on the stopcocks in the distillation apparatus. Therefore, the distillation manifold was rebuilt using stainless steel needle valves in place of stopcocks. No grease was used at any part of the distillation equipment or manifold (Figure 4). When the experiment was repeated, the same general trend was noted—i.e., the disappearance of the small discontinuity above the freezing point and the displacement to lower temperature and broadening of the conductivity maximum. The results are plotted in Figure 3. It is likely that the necessarily long residence

time in glass (*ca.* 24 hours) required for the distillation results in pickup of ionic impurities. This could account for the enhanced conductivity in both the solid and liquid after low temperature fractionation.

Solid chlorine trifluoride has a negative temperature coefficient for the conductivity within a narrow temperature range below the freezing

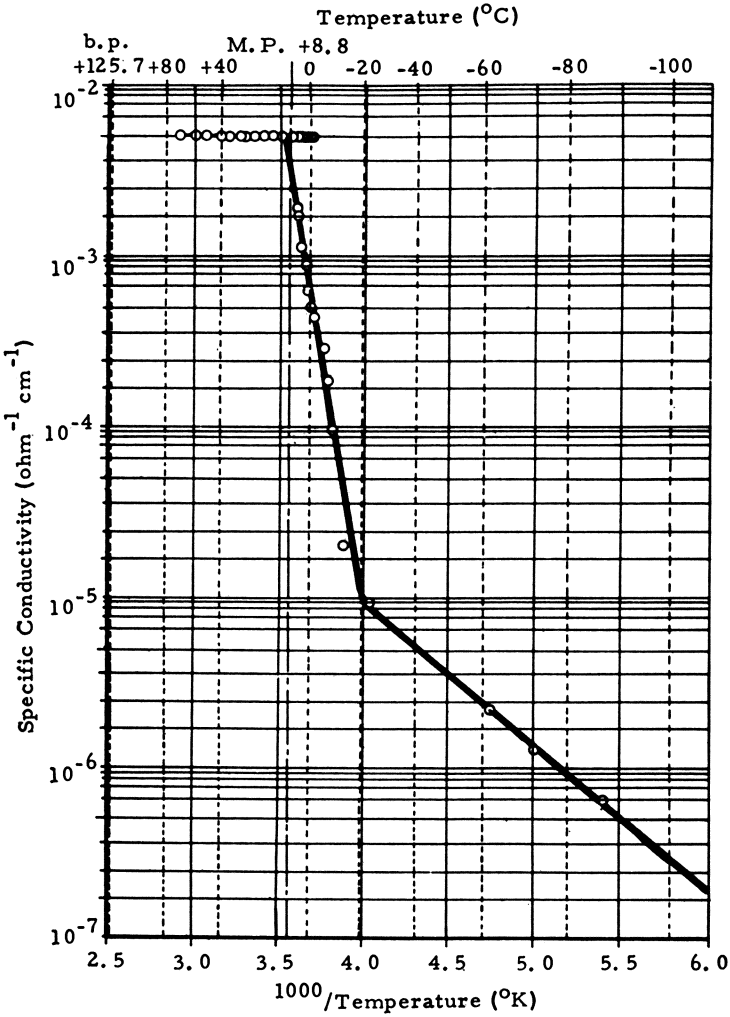

Figure 5. Conductivity of bromine trifluoride as a function of temperature

point. This negative temperature effect is likely caused by a decrease in stability of one or both of the postulated ionic species (ClF_2^+ and ClF_4^-) with increasing temperature rather than electronic conduction. Indirect

evidence for the existence of ClF_2^+ cation is supported by the isolation of the compounds ClF_2AsF_6 and ClF_2SbF_6 by Seel and Detmer (*5,6*) and ClF_2BF_4 by Selig and Shamir (*7*). The existence of ClF_4^- anion is supported by the isolation of the compounds $KClF_4$, $RbClF_4$ and $CsClF_4$ *(10)*. An alternative possibility is that the solid is polycrystalline and that conduction depends on grain boundary surface. Such a solid would be molecular, and conduction would occur in surface and grain boundary films where ClF_3 is slightly ionized. The portion of ions in such absorbed films is greater than in the bulk liquid since ionization would favor absorption on the possibly dipolar solid. The decrease in conductivity with increasing temperature is then caused by a decrease in inner surface.

Conductivity *vs.* Temperature of Bromine Trifluoride. The conductivity of bromine trifluoride has been measured over a range of 80° to −196° C. (Figure 5). There is little variation of conductivity with temperature in the liquid state; the liquid has a tendency to supercool. The value of specific conductivity at 25° C. is 5.03×10^{-3} $ohm^{-1}cm.^{-1}$; literature value is 8×10^{-3} $ohm^{-1}cm.^{-1}$ (*1*). The discrepancy is caused by polarization and the shunting effect of the relatively high capacitance cell used. When the same sample is introduced into a cell of higher cell constant (0.5 $cm.^{-1}$) and corrected for the frequency effect, the value agrees with the literature. This is only significant at high conductive range ($10^{-3}ohm^{-1}cm.^{-1}$) and becomes insignificant as specific conductivity decreases.

The ions accounting for the conductivity are probably BrF_2^+ and BrF_4^-. Woolf and Emeléus (*11*) reported the existence of the ionic equilibrium

$$2BrF_3 \rightleftharpoons BrF_2^+ + BrF_4^-$$

in liquid bromine trifluoride by isolating the compounds BrF_2SbF_6 and $(BrF_2)_2SnF_6$ for BrF_2^+ cation and $KBrF_4$, $AgBrF_4$ and $Ba(BrF_4)_2$ for BrF_4^- anion.

Conductivity of solid bromine trifluoride decreases rapidly with temperature leading to a marked discontinuity around the melting point (+8.8° C.). Another discontinuity is observed at *ca.* −20° C. (Figure 5). There are two curves with different slopes, a higher temperature portion and a lower temperature portion. This is similar to the behavior of AgCl, AgBr, TlCl, and TlBr as described by Lehfeldt (*4*) and suggests that solid bromine trifluoride may have an ionic lattice of BrF_2^+ and BrF_4^- ions. Phosphorus pentachloride, which conducts to a small extent in the solid, has been shown to possess a lattice of PCl_4^+ and PCl_6^- ions (*2*). Electrolytic conduction is expressed as the exponential

$$\sigma = \sigma_0 e^{-Q/kT} \quad (1)$$

where σ_0 is a constant that can be expressed in terms of mobilities, and Q

is the activation energy (*8*). For the solid BrF_3 curve shown in Figure 5 it is to be expected that

$$\sigma = \sigma_0 e^{-Q_1/kT} + \sigma'_0 e^{-Q_2/kT} \quad (2)$$

since two processes are operating. The activation energy Q_1 for the lower temperature process (between —20° and —196° C.) is of the order of 3.81 Kcal./gram mole, or one-eighth the value of Q_2, 29.8 Kcal/gram mole (between +8.8° to —20° C.), whereas σ_0 (2.13×10^{-11} ohm^{-1}cm.$^{-1}$) is many orders of magnitude greater than σ'_0 (1.73×10^{-29} ohm^{-1}cm.$^{-1}$).

Acknowledgment

We wish to thank the Advanced Research Projects Agency for its support through Contract No. DA-31-124-ARO(D)-115. The authors are indebted to N. A. Tiner, W. D. English, and M. J. Plizga for helpful discussions and S. Miranda for assistance.

Literature Cited

(1) Banks, A. A., Emeléus, H. J., Woolf, A. A., *J. Chem. Soc.* **1949**, 2861.
(2) Clark, D., Powell, H. M., Well, A. F., *J. Chem. Soc.* **1942**, 642.
(3) Clark, H. C., *Chem. Rev.*, **58**, 869 (1958).
(4) Lehfeldt, W., *Z. Physik* **85**, 717 (1933).
(5) Seel, F., Detmer, O., *Angew. Chem.* **70**, 163 (1958).
(6) Seel, F., Detmer, O., *Z. Anorg. Allgem. Chem.* **301**, 113 (1959).
(7) Selig, H., Shamir, J., *Inorg. Chem.* **3**, 294 (1964).
(8) Sinnott, M. J., "The Solid State for Engineers," p. 356, John Wiley and Sons, New York, 1958.
(9) Toy, M. S., Cannon, W. A., English, W. D., Douglas Aircraft Co., *Quart. Rept.* **144-Q4** March 10–June 15, 1964.
(10) Whitney, E. D., MacLaren, R. O., Fogle, C. E., Hurley, T. J., *J. Am. Chem. Soc.* **86**, 2583 (1964).
(11) Woolf, A. A., Emeléus, H. J., *J. Chem. Soc.* **1949**, 2865.

RECEIVED April 12, 1965.

Hydrolysis of the Nitrogen Fluorides

GERALD L. HURST[1] and S. I. KHAYAT

Harshaw Chemical Co., Cleveland, Ohio

Hydrolytic reactions of the nitrogen fluorides, NF_3, N_2F_4, and cis- and trans-N_2F_2 are discussed. Nitrogen trifluoride is inert to pure water at 133° C. but react slowly with aqueous base at 100° C. to give nitrite and fluoride. The mechanism involves nucleophilic attack by the hydroxyl ion. N_2F_4 is hydrolyzed slowly with water at 60–100° C. yielding nitric oxide and hydrofluoric acid. At higher temperatures (133° C.) appreciable amounts of elementary nitrogen and nitrate are produced. Long induction periods are observed at 60° C. followed by a steadily increasing rate as a result of autocatalysis by nitric oxide. Cis- and trans-N_2F_2 are hydrolyzed with water at 74° C. and 89° C., respectively. In each case the reaction is first order with respect to N_2F_2, and the major products are elementary nitrogen and oxygen.

Publication Date: January 1, 1966 | doi: 10.1021/ba-1966-0054.ch024

Considerable data have been assembled concerning the physical and chemical properties of the nitrogen fluorides (*6*), yet a review of the literature revealed no systematic study of the reactions of these compounds with water. Although some isolated experiments relating to the hydrolysis of these gases have been reported (*6*), the results have not been critically analyzed. Usually these hydrolytic reactions were reported as observations noted during the investigation of other properties.

Basic Hydrolysis of NF_3

Nitrogen trifluoride is extremely resistant to chemical attack by water and aqueous acid; the compound can be recovered quantitatively after one week in contact with excess dilute acid (HNO_3, H_2SO_4, $HClO_4$) or pure water at 133° C. In the presence of aqueous base, however, slow hydrolysis occurs at 100° C. yielding nitrite and fluoride.

[1] Present address: Aerojet-General Corp., Azusa, Calif.

In Advanced Propellant Chemistry; Holzmann, R.;
Advances in Chemistry; American Chemical Society: Washington, DC, 1966.

$$NF_3 + 4OH^- \xrightarrow{100^\circ\ C.} NO_2^- + 3F^- + 2H_2O \qquad (1)$$

This behavior differs sharply from that of nitrogen trichloride, which is hydrolyzed to give ammonia and hypochlorite under similar conditions (*4*). The latter products are readily explained in terms of nucleophilic attack directed at the chlorine atoms, a mechanism which appears reasonable in view of the fact that the electronegativities of N and Cl are very nearly the same and that the halogen may easily expand its valence shell. Obviously, these considerations cannot be applied to the nitrogen trifluoride molecule since fluorine is considerably more electronegative than nitrogen and it has no available *d* orbitals. Although the nitrogen atom also has no free orbitals, the relatively low electron density would at least offer less resistance to the approach of a nucleophile.

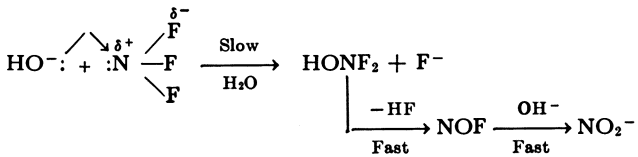

(2)

The proposed intermediate, $HONF_2$, would be expected to be unstable with respect to the loss of HF, as is apparently the case with the unknown perfluoro alcohols (*10*).

Two other reaction modes worth considering include the formation of an intermediate activated complex with water

$$NF_{3(aq.)} \xrightarrow{\text{Slow}} NF_3{}^*{}_{(aq.)} \xrightarrow[\text{Fast}]{OH^-} \text{products} \qquad (3)$$

and the intriguing but unlikely reversible ionization of NF_3.

$$NF_{3(aq.)} \underset{}{\overset{\text{Slow}}{\rightleftharpoons}} NF_2{}^+{}_{(aq.)} + F^-{}_{(aq.)} \xrightarrow[\text{Fast}]{OH^-} \text{Products} \qquad (4)$$

or

$$NF_{3(aq.)} \overset{\text{Fast}}{\rightleftharpoons} NF_2{}^+{}_{(aq.)} + F^-{}_{(aq.)} \xrightarrow[\text{Slow}]{OH^-} \text{Products} \qquad (5)$$

Preliminary experiments indicated that the rate of reaction of gaseous NF_3 with caustic soda solution in a static system was first order with respect to NF_3 with little dependence on the initial concentration of the base. Although these observations are apparently consistent with the first-order Equations 3 and 4, more detailed studies show that these results are misleading.

If the reactions were first order in NF_3 only, the rate of decrease of the partial pressure (P) of NF_3 with time (T) in a closed system should be given by the following equations:

$$\frac{dP}{dT} = \frac{KV_c}{V_o} \qquad \frac{V_o}{V_c} \log \frac{P_o}{P} = KT$$

where V_o is the volume available to gaseous NF_3, V_c is the volume of the caustic soda solution, and P_o is the initial pressure of NF_3. The assumption is made that a Henry's law equilibrium is established between gaseous and dissolved NF_3.

Figure 1 shows the results of several experiments plotted according to the integrated form of the rate equation. The points of line B and

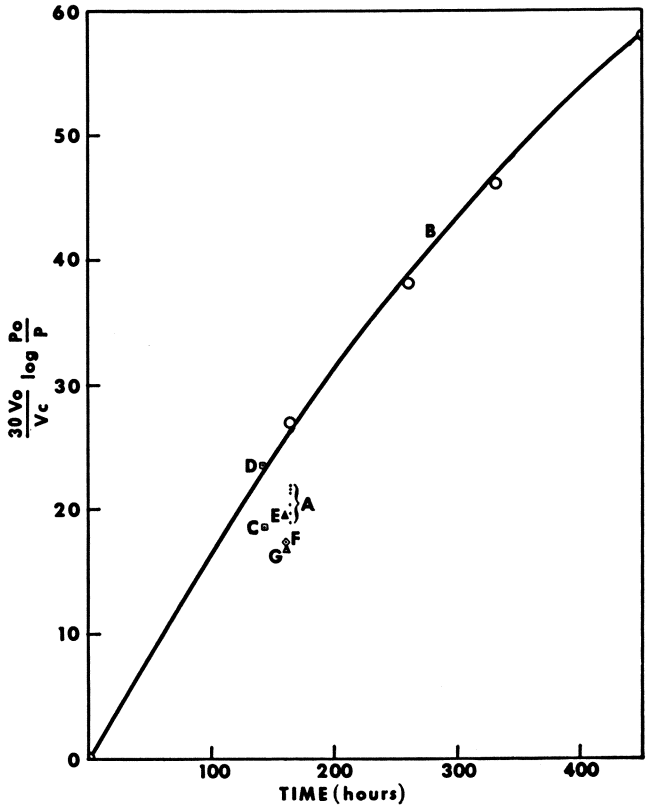

Figure 1. Reaction of NF_3 with NaOH solution at 100°C.

(A) 30 ml. 0.5N NaOH
P_o = 0.25–2.0 atm.
(B) 20 ml. 0.5N NaOH
P_o = 1 atm.
(C) 20 ml. 0.5 NaOH
Surface area reduced from 10.8 to 4.4 sq. cm.
P_o = 1 atm.
(D) 20 ml. 0.5N NaOH
Surface area reduced from 10.8 to 8.0 sq. cm.
P_o = 1 atm.
(E) 30 ml. 1.0N NaOH
P_o = 1 atm.
(F) 30 ml. 0.5N NaOH + 15 mmole NaF
P_o = 1 atm.
(G) 30 ml. 0.5N NaOH + 15 mmole $NaNO_3$
P_o = 1 atm.

group A were calculated from data furnished by Bronaugh (*1*). The line B was obtained from a series of experiments in which samples of NF_3 (4.83–7.16 mmole) at a constant initial pressure of 1 atm. were allowed to react with 20 ml. of 0.5*N* NaOH for varying lengths of time. The curvature of the line clearly suggests that the steadily decreasing hydroxyl ion concentration (up to 90% neutralization) does indeed tend to decrease the reaction rate, but the effect is much less than would be expected for the second-order equation:

$$NF_3 + OH^- \rightarrow \text{Products} \tag{6}$$

The group of points A was derived from reactions involving samples of NF_3 at initial pressures ranging from 0.25 to 2 atm. (1.7–8.7 mmole) and 30 ml. of 0.5*N* NaOH. The positions of the top four points of this group, which were obtained from simultaneous runs, again indicate that the extent of conversion of NF_3 depends on the concentration of OH^-. Thus, the height of the individual points decreases inversely with the corresponding degree of neutralization of the caustic soda. More important, however, is the fact that group A lies well below B, showing that the reactions involving 20 ml. of base were more than $^2/_3$ as fast as those with 30 ml. Since the solutions were contained in upright Teflon cups of identical diameter in each case, the data indicate that the rate of conversion of NF_3 was significantly influenced by the available surface area. Presumably, the NF_3 failed to reach an equilibrium concentration in solution in spite of the long reaction times. The dependence of the reaction rate on the area of the gas-liquid interface was confirmed in the experiment represented by points D and C in which the surface area of the solutions (20 ml. 0.5*N* NaOH) were reduced from 10.8 sq. cm. to 8.0 and 4.4 sq. cm., respectively.

The apparently small effect of the initial OH^- concentration on the rate of hydrolysis of NF_3 is probably caused not only by the surface area phenomenon described above but also by a reduction in the solubility of the gas resulting from increased ionic strength. The proposed salting-out effect is demonstrated in the experiments represented by points E, F, and G. In E, 1.0*N* NaOH (30 cc.) was used in place of the 0.5*N* caustic soda employed by Bronaugh (*1*) for group A; yet the extent of reaction was approximately the same. A concentration of 0.5*N* NaOH was also used in F and G, but the total ionic strength of the solutions was increased to the equivalent of 1.0*N* NaOH by adding NaF and $NaNO_3$, respectively. In each of the latter experiments the reaction rate was significantly lowered, indicating that inhibition caused by rising ionic strength tends partly to offset the acceleration associated with increasing OH^- concentration. In this connection it should be noted that concentrated NaOH (12*N*) reacts extremely slowly with NF_3.

The rate of basic hydrolysis is decreased to exactly the same extent

Publication Date: January 1, 1966 | doi: 10.1021/ba-1966-0054.ch024

(within the experimental accuracy) by equivalent amounts of NaF or $NaNO_3$. If the reaction involved the mechanism shown in Equation 5, NaF would be expected to act as an inhibitor by shifting the equilibrium to the left. Thus, it is possible that the reaction may proceed via the nucleophilic mechanism given in Equation 2.

Reaction of NF_3 with Aqueous HCl

Additional support for the proposed nucleophilic mechanism of the basic hydrolysis has been provided by a study of other aqueous systems such as hydrochloric acid. Although NF_3 is unaffected by prolonged contact with either pure HCl or pure water at 133° C., the compound reacts slowly with aqueous HCl at this temperature, yielding products which vary with the concentration of the acid. Nitric oxide and nitric acid are formed by the dilute solution (0.5*N*):

$$3NF_3 + 6H_2O \xrightarrow[133^\circ\ C.]{\text{Dil. HCl}} 3HNO_2 + 9HF \qquad (7)$$
$$\xrightarrow{H^+} 2NO + HNO_3 + H_2O$$

while the more highly concentrated reagent (4*N*) yields elementary nitrogen and chlorine.

$$2NF_3 + 6HCl \xrightarrow[133^\circ\ C.]{H_2O} N_2 + 3Cl_2 + 6HF \qquad (8)$$

As in the case of the basic hydrolysis the rate of conversion of NF_3 was found to vary only slightly with the strength of the solution. The fact that NF_3 reacts with aqueous HCl but not with the pure compound clearly suggests that ionic attack is involved. The active species in the reaction is almost undoubtedly Cl^- since it has been shown that while NF_3 is inert to many acids, it reacts readily with hot, neutral sodium chloride solution (4*N*).

$$NF_3 \xrightarrow[H_2O]{NaCl} N_2, NO_3^-, F^-, Cl_2 \qquad (9)$$

Reaction of NF_3 with Aqueous Nucleophiles

Further indirect evidence for the postulated nucleophilic behavior of Cl^- and OH^- has been obtained from a series of experiments in which NF_3 was allowed to react with solutions containing anions of varying nucleophilic strength. It was found that for those species tested the extent of reaction within a given time and temperature range increased monotonically with the accepted value (5) of the nucleophilicity of the anion. Furthermore, although NF_3 did not react with acid solutions of weak nucleophiles, the reaction rate with halides was increased by the

presence of hydronium ion, as would be expected for an S_N2 mechanism involving the loss of fluoride:

$$\begin{cases} F_2N{-}F + H_3O^+ \rightleftharpoons F_2N{-}FH^+ + H_2O \\ X{:}^- + F_2N{-}FH^+ \rightarrow XNF_2 + HF \rightarrow \ldots \end{cases} \quad (10)$$

The results of a number of experiments involving nucleophilic reagents are listed in Table I. In the strictest sense it is not possible to

Table I. Reactions of NF_3 with Nucleophiles in Aqueous Solution

Reagent	*Molarity Volume ml.*	*Temp. °C.*	*Reaction Time hrs.*	*Initial NF_3 mmole*	*P_oNF_3 at Reaction Temp. atm.*	*NF_3 Reacted %*	*Product mmoles*
$HClO_4$	0.5–20	133	159	2.14	0.585	1.0	...
HNO_3	0.5–20	133	159	2.10	0.574	1.0	...
H_2SO_4	0.5–20	133	159	3.34	0.99	1.0	...
H_2SO_4	4.0–20	133	159	3.52	1.02	1.0	...
HCl	0.5–20	133	235	3.00	1.00	54.4	NO(0.73); NO_2^-(0.12); NO_3^-(0.81); F^-(4.74)
HCl	4.0–20	133	235	3.16	1.02	63.6	N_2(1.06); Cl_2(2.75); F^-(5.38)
HCl	0.5–20	133	159	2.14	0.636	13.5	Cl_2(0.12)
NaCl	4.0–20	133	306	4.37	1.047	24.7	N_2(0.33); NO_3^-(0.42)
HBr	0.5–20	133	159	1.98	0.633	67.7	N_2(0.31); N_2O(0.06); Br_2(2.44); F^-(3.84)
NaCl	0.5–30	100	160	2.97	0.936	1.0	...
HCl	0.5–30	100	160	2.98	0.939	1.0	N_2; Cl_2
NaBr	0.5–30	100	160	3.07	0.957	14.0	NH_4^+(0.44); F^-(1.37)
HBr	0.5–30	100	160	3.01	0.938	22.6	N_2(0.1); NH_4^+(0.33); F^-(1.74); Br_2(0.94)
NaOH[a]	0.5–30	100	160	3.01	0.939	38.2	NO_2^-(1.15); F^-(3.35)
NaI	0.5–30	100	160	2.97	0.91	50.8	N_2(0.50); N_2O(0.05); NH_4^+(0.72); F^-(4.84)
HI	0.5–30	100	160	3.15	0.952	71.8	NH_4^+(2.11); I_2(5.05)
$Na_2S_2O_3$	0.5–30	100	160	2.79	0.837	61.3	S(5.1); F^-(3.75); NH_4^+(1.50)

[a] NaOH reaction data were calculated.

compare the relative degrees of reaction solely on the basis of the nucleophilicity of the starting material because reactive intermediates may influence the overall conversion rate. The varying stoichiometries also impose restrictions for those experiments which involve small quantities of aqueous reagent and are thus subject to unequal changes in concentration for a given amount of NF_3 reacted. In spite of these limitations the data clearly indicate that the reaction rates increase with nucleophilic strength in the order:

$$NO_3^-, ClO_4^-, SO_4^{-2} \ll Cl^- < Br^- < OH^- < I^- < S_2O_3^{-2}$$

Reaction of NF_3 with Electrophiles

In his early work on NF_3 Ruff (*13*) reported that the compound was stable to $AlCl_3$ at red heat. Investigations in this laboratory show that

NF_3 does react with $AlCl_3$ under mild conditions (80° C., 4 days) to produce nitrogen and chlorine. Chlorine is liberated rapidly at 135° C. The reaction presumably involves coordination of a fluorine atom of NF_3 to the vacant orbital of the aluminum atom, as is believed to be the case with the chlorination of fluorocarbons by $AlCl_3$. Reactions conducted in a Teflon infrared cell gave no evidence for the formation of gaseous intermediates such as NF_2Cl.

Nitrogen trifluoride is readily converted to ammonium ion by acidic or neutral ferrous sulfate solution at 60° C.

$$4H^+ + 6Fe^{+2} + NF_3 \rightarrow NH_4^+ + 3F^- + 6Fe^{+3} \tag{11}$$

In a typical experiment, NF_3 (3.18 mmoles, $P_o = 0.69$ atm.) was maintained in contact with the aqueous salt (20 ml., 0.5*N*) for 12 days, resulting in the destruction of about 44% of the NF_3.

Ferric chloride solutions react very slowly with NF_3 at 100° C.; the $FeCl_3$ acts as a hydrolysis catalyst, yielding nitric oxide and nitrate. This catalysis is not a general property of the transition metal ions as shown by the total inertness of NF_3 to solutions of $CoCl_2$, $MnSO_4$, $CuSO_4$, and $NiSO_4$ at 100° C. over periods up to 7 days.

Hydrolysis of N_2F_4

Tetrafluorohydrazine reacts more readily than NF_3 with aqueous solutions; at 133° C. it is rapidly destroyed by contact with acidic, basic, and neutral solutions. The reaction with caustic soda produces mainly nitrous oxide and nitrite along with a trace of nitrogen.

$$\begin{cases} N_2F_4 + 4OH^- \xrightarrow{133^\circ\ C.} 2NO + 4F^- + 2H_2O \\ 4NO + 2OH^- \xrightarrow{133^\circ\ C.} N_2O + 2NO_2^- + H_2O \end{cases} \tag{12}$$

With water and aqueous HCl, significant quantities of nitrogen and nitrate are formed in addition to nitric oxide. Surprisingly, the amount of nitrogen produced was found to be greater with water than with 4*N* HCl, and in neither instance was as much N_2 formed as in the corresponding reaction of NF_3 with 4*N* HCl. At lower temperatures (60°–100° C.) N_2F_4 is nearly quantitatively converted to NO by water and dilute HCl (0.5*N*).

The results of a number of experiments on the kinetics of the N_2F_4-H_2O system are shown in Table II and depicted in Figure 2. The hydrolytic mechanism is obviously complex as indicated by the long induction periods and the subsequent exponential increase in the reaction rates. The total time required to destroy completely the N_2F_4 shows a difficult-to-reproduce inverse dependence on the initial pressure of this compound. The effect of N_2F_4 pressure on the overall reaction rate has been con-

firmed in other experiments. In a typical series, N_2F_4 samples at concentrations of 0.65, 1.27, 2.53, 3.85, and 5.22 mmole/100 ml. were heated with water for 5 days at 35° C., 6 days at 50° C., and 6 days at 60° C. The first three samples (low pressures) were recovered quantitatively while the fourth and fifth samples reacted to the extent of 6% and 100%, respectively.

Table II. Hydrolysis of N_2F_4 at 60° C.

Exp. No.	*Initial N_2F_4, mmole*	*Concentration N_2F_4, mmole/100 ml.*	*Reagents*	*Reaction Time, days*	*N_2F_4 Reacted, %*	*Products, mmoles*
1	13.23	9.01	H_2O (5 ml.)[a]	5.1	0	
				7.8	1.7	
				11.8	17.6	
				15.5	100.0	NO(26.0); NF_3(0.09)
2	7.07	6.82	H_2O (5 ml.)	1.7	0	
				3.5	0	
				6.2	0	
				12.3	7.3	NO(1.04)
3	5.06	4.57	H_2O (5 ml.)	4.7	0	
				7.5	0.2	
				14.7	5.9	
				16.0	9.6	NO(0.95)
4	4.95	4.55	H_2O (5 ml.)	4.0	0	
				6.5	0	
				10.2	0.3	
				21.4	41.9	NO(4.10)
5	5.09	4.55	H_2O (5 ml.)	3.7	0	
				5.6	0.6	
				18.9	100.0	NO(10.00); NF_3 (trace)
6	6.59	4.56	H_2O (5 ml.)	10.8	3.6	
				14.6	33.5	
				17.3	100.0	NO(12.88); NF_3(0.05)
7	3.17	2.27	H_2O (5 ml.)	19.7	8.5	
				24.5	49.5	
				26.1	89.0	
				27.0	100.0	NO(6.10)
8	6.20	4.58	H_2O (5 ml.)[a]	15.7	100.0	NO(12.23); NF_3 (trace)
9	2.99	2.22	H_2O (5 ml.)[a]	9.9	0.3	
				16.7	4.5	NO(0.13)
10	3.01	2.23	0.5*N* HCl (5 ml.)	9.9	100.0	NO(5.92)
11	3.06	2.23	0.5*N* HF (5 ml.)	10.0	14.0	
				16.7	100.0	NO(6.01)
12	3.03	2.27	2*N* NaOH (5 ml.)	7.1	11.0	
				14.7	17.2	N_2O(0.50)
13	3.06	2.25	H_2O (5 ml.) + O_2 (0.05 mmole)	6	100.0	NO_2, NO_3^-
14	6.22	4.56	H_2O (5 ml.) + NO (0.61 mmole)	5.8	53.2	
				10.0	100.0	NO(13.00)
15	2.86	3.14	1*N* H_2SO_4 (10 ml.)	5.6 at 35° C.		
				13 at 50° C.	24.5	NO(1.26)
16	2.87	3.14	1*N* H_2SO_4 (10 ml.)	5.6 at 35° C.		
				16 at 50° C.	47.0	NO(2.65)

[a] Normal laboratory distilled water from two different batches was used in Experiments 8 and 9; in all other experiments involving pure water trace impurities were removed by deionization, triple distillation, and filtration through a 4.5μ millipore filter.

The marked acceleration of the hydrolysis with time is apparently a result of secondary reactions initiated by the product nitric oxide. The fastest and slowest reactions (E and D) illustrated in Figure 2 were conducted under identical conditions except for adding 10 mole % of nitric oxide to the N_2F_4 in E. The hydrofluoric acid formed also exerts a positive influence on the rate but to a lesser degree than nitric oxide.

Both hydrochloric acid (0.5*N*) and sodium hydroxide (2*N*) profoundly alter the reaction. The halide causes the complete destruction of N_2F_4 at low pressures in less than 10 days while the hydroxide produces a slow, steady reaction with no indication of an induction period or increasing rate with time (line F).

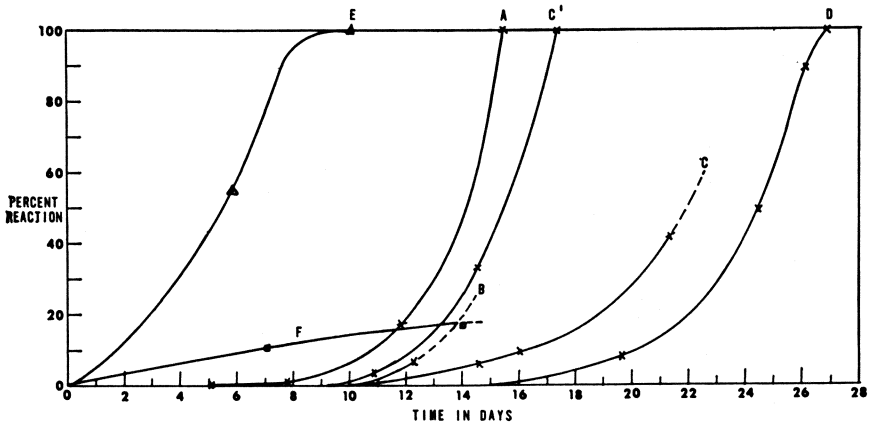

Figure 2. Hydrolysis of N_2F_4 at 60°C.

(A) N_2F_4 (9.01 mmole/100ml.) + H_2O (5 ml.)
(B) N_2F_4 (6.82 mmole/100ml.) + H_2O (5 ml.)
C, C' } N_2F_4 (4.56 mmole/100ml.) + H_2O (5 ml.)
(D) N_2F_4 (2.27 mmole/100 ml.) + H_2O (5 ml.)
(E) N_2F_4 (4.56 mmole/100 ml.) + 10% NO + H_2O (5 ml.)
(F) N_2F_4 (2.27 mmole/100 ml.) + NaOH (2N) (5 ml.)

Experimental results on the N_2F_4-H_2O reaction were very difficult to duplicate; the lines C and C′, which are vastly different, were obtained from supposedly identical runs, using N_2F_4 and water from the same sources. The large variations in reaction rate are believed to be caused by minute amounts of oxygen remaining in the starting materials even after careful purification, including boiling and vacuum degassing of the water. In control experiments, oxygen was found to be at least 10 times as effective as nitric oxide in promoting the reaction; adding about 1 mole % of the gas (based on N_2F_4) to the mixture reduced the total conversion time by a very conservatively estimated factor of 4.

The above observations are consistent with the following reaction scheme:

$$N_2F_4 + 2H_2O \xrightarrow{\text{Slow}} 2NO + 4HF \quad (13)$$

$$NO \xrightarrow[N_2F_4,\ H_2O]{\text{Slow}} NO_2 \quad (14)$$

$$NO + NO_2 + H_2O \rightleftharpoons 2HNO_2 \xrightleftharpoons{+\,{}^2/_3H_2O} {}^4/_3HNO_3 + {}^2/_3NO \quad (15)$$

$$2NO_2 + N_2F_4 \xrightarrow{\text{Fast}} 4NOF \quad (16)$$

$$2NOF + H_2O \xrightarrow{\text{Fast}} NO_2 + NO + 2HF \quad (17)\ (3)$$

$$4NOF + SiO_2 \xrightarrow{\text{Fast}} 2NO_2 + 2NO + SiF_4 \quad (18)\ (14)$$

The formation of some nitrogen dioxide (Equation 14) at 60° C. appears likely in view of the fact that large quantities of this gas were observed in the products of similar reactions at higher temperatures (133° C.). Experiments in this laboratory have confirmed that N_2F_4 is readily attacked by NO_2 (Equation 16) giving NOF, which would in turn rapidly hydrolyze (Equation 17) or react with the glass (Equation 18) and thus regenerate the NO_2. Increasing acidity would favor higher concentrations of free NO_2 by shifting the equilibrium (Equation 15) to the left. By analogy to the chemistry of NF_3, caustic soda might be expected to be more efficient than water in the direct (nucleophilic) attack on N_2F_4, but secondary reaction would be inhibited by the removal of NO_2. Obviously oxygen would immediately convert any NO present to NO_2.

Hydrolysis of cis- and trans-N_2F_2

Both isomers of N_2F_2 were found to be unaffected by water at 60° C. over a period of 15 hours. The cis isomer hydrolyzes slowly at 74° C. (30% in 17 hours) while the trans isomer reacts at a similar rate at 89° C. In each case the major products are elementary nitrogen and oxygen in addition to hydrofluoric acid.

$$2N_2F_2 + 2H_2O \rightarrow 2N_2 + O_2 + 4HF \quad (19)$$

Nitrous oxide is also formed, but only in minor quantities ($<3\%$).

The results of a number of hydrolytic experiments with *cis*- and *trans*-N_2F_2 are summarized in Figures 3 and 4. The data in Figure 3 were obtained by allowing samples of *trans*-N_2F_2 at 89° C. to react with 5 ml. portions of water, aqueous NaOH ($2N$), or aqueous HCl ($0.5N$) in borosilicate glass ampoules. The line A, drawn through the circled points, shows the logarithmic rate of change in the number of millimoles of *trans*-N_2F_2 in contact with water. Line B was derived by plotting the function log $(N_o - {}^2/_3\, n)$ where N_o is the initial concentration of *trans*-N_2F_2, and

Publication Date: January 1, 1966 | doi: 10.1021/ba-1966-0054.ch024

n is the total amount of noncondensable gas produced at any given time. The lines C and D were obtained from experiments involving aqueous NaOH ($2N$) and aqueous HCl ($0.5N$), respectively and were plotted on the same basis as line A.

If the reaction proceeded quantitatively according to Equation 19, lines A and B should be superimposed. The difference between these lines is at least partly caused by the formation of nitrous oxide. Also,

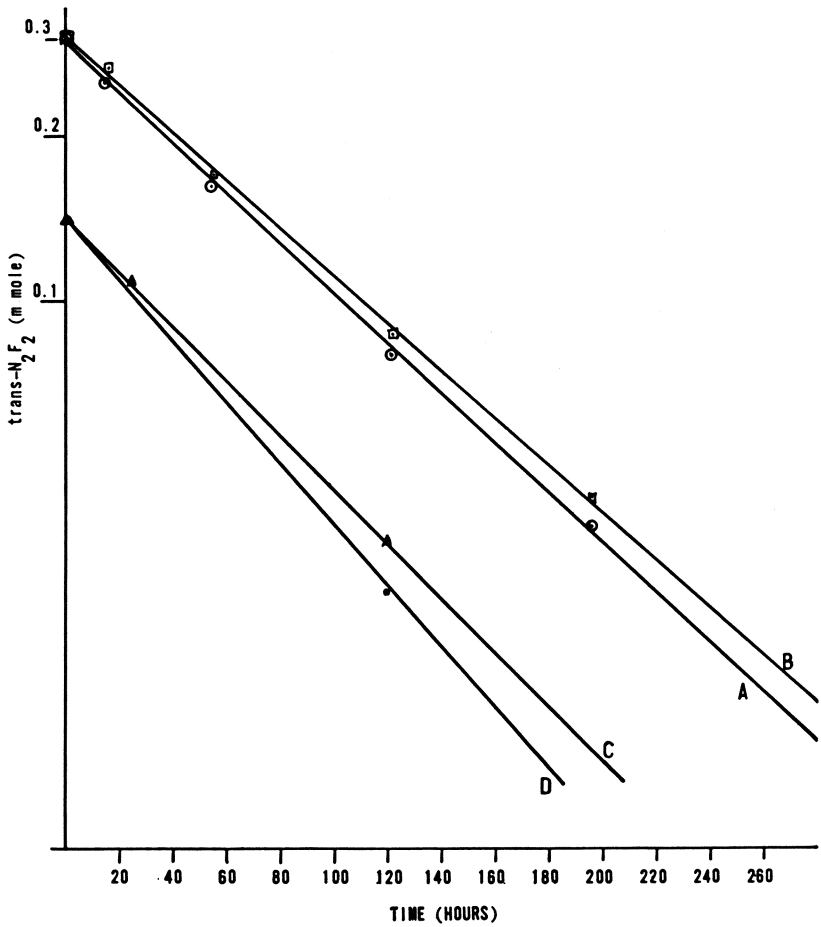

Figure 3. Hydrolysis of trans-N_2F_2 at 89°C.

(A) trans-N_2F_2 + H_2O (5 ml.)
(B) trans-N_2F_2 + H_2O (5 ml.)
Ordinate = $N_0 - 2/3n$
where N_0 = initial N_2F_2
n = total noncondensable gas produced.
(C) trans-N_2F_2 + NaOH (5 ml. 2N)
(D) trans-N_2F_2 + HCl (5ml. 0.5N)

infrared spectroscopic studies on the original and partially reacted *trans*-N_2F_2 suggest that the material may have contained a small amount of undetectable impurity which would have caused a slightly but proportionally consistent overestimation of the amount of N_2F_2 present.

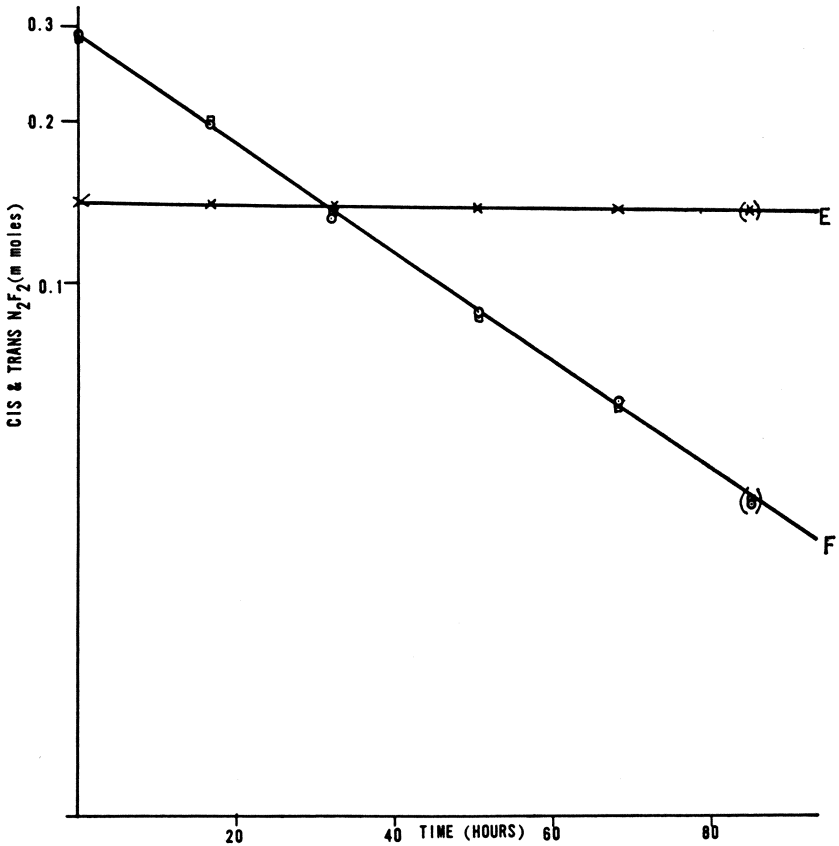

Figure 4. Hydrolysis of a mixture of cis- and trans-N_2F_2 at 74°C.

(E) trans-N_2F_2
(F) ⊙ cis-N_2F_2
⊡ N_o — (2/3n—Δ)
n = total noncondensable gas produced
Δ = total trans-N_2F_2 reacted
Points in parentheses refer to reaction with 2N NaOH in place of water

A similar set of experiments involving a mixture of *cis*- and *trans*-N_2F_2 (67% cis) at 74° C. is recorded in Figure 4. The reaction rates of *trans*- and *cis*-N_2F_2 are given by lines E and F, respectively. The points enclosed by squares express the rate of formation of noncondensable gases (N_2 and O_2) from *cis*-N_2F_2 in terms of the function log $[N_o - (^2/_3 n - \Delta)]$ where N_o is the initial amount of the cis isomer, n is the total amount of noncondensable gas produced in the given time, and Δ is the amount of

trans isomer reacted as calculated from line E. The excellent agreement between the noncondensable function and line F is probably somewhat fortuitous since detectable quantities of N_2O were also formed.

After the completion of the preceding experiment, the remaining isomeric mixture was allowed to react with 2*N* NaOH under similar conditions of temperature and pressure. No change in the reaction rate occurred as is indicated by the points in parentheses in Figure 4.

The above data suggest two important conclusions:

(1) The reactions of *cis*- and *trans*-N_2F_2 with water are each first order with respect to the nitrogen fluoride.

(2) The hydrolyses do not proceed via nucleophilic attack on N_2F_2.

The second conclusion is based on the observations that the strong nucleophile OH^- does not significantly accelerate the reactions and on the fact that very little nitrous oxide is produced.

From the above it can be seen that the hydrolytic behavior of N_2F_2 is quite different from those of the other binary nitrogen fluorides discussed earlier. Difluorodiazine is strongly endothermic (*12*) and thermodynamically unstable (*11*); this makes it necessary to consider not only direct chemical attack by water but also the thermal decomposition to the elements. The reactivity of *cis*-N_2F_2 toward glass (*2*) presents an additional question of possible competing reactions with the container walls.

In an effort to resolve these problems a study was made of the decomposition of N_2F_2 in glass, both alone and in the presence of elementary nitrogen. The experimental results given in Table III indicate that both isomers decompose slowly at the previously established hy-

Table III. Decomposition of *cis*- and *trans*-N_2F_2 in Glass

Initial N_2F_2 mmole	*Initial Partial Pressure of N_2F_2 at Reaction Temp. mm. Hg*	*Partial Pressure of N_2 mm. Hg*	*Surface Area / Volume* $cm.^{-1}$	*Reaction Temp. °C.*	*Time hrs.*	*Decomposition %*
trans (0.240)	40	500	1.8	89	18	9
trans (0.246)	40	500	1.8	89	16	11
trans (0.229)	40	nil	1.8	89	16	5
trans (0.217)	36	nil	1.9	89	18	5
trans (0.412)	69	nil	1.8	89	16	5
trans (0.412)	69	500	1.9	89	16	10
trans (0.040)	67	500	6.7	89	16.5	11
cis (0.028)	cis (6)	300	1.9	75	18	cis (5)
trans (0.137)	trans (29)					trans (nil)
cis (0.024)	cis (5.1)	nil	1.9	75	18	cis (8)
trans (0.437)	trans (29)					trans (nil)
cis (0.104)	cis (18)	nil	6.7	75	18	cis (9)
trans (0.063)	trans (10)					trans (nil)
trans[a] (0.246)	37	500	1.8	25	18	nil

[a] Control run to establish efficiency of recovery technique.

drolysis temperatures and that the reaction rates increase with the total pressure of the system. Variations in the area of the available glass surface apparently do not alter the rates significantly.

Hydrolytic attack, in the form of water vapor, was found to be approximately twice as effective as a comparable pressure of nitrogen in destroying the isomers. Furthermore, nitric oxide was considerably more active than water under similar conditions.

Although the rate of decomposition of *cis*-N_2F_2 in glass is virtually independent of the initial surface area, changes occurring in the nature of the surface during the course of the reaction have a profound effect. Lines C, E, and G in Figure 5 indicate that the decomposition rate increases rapidly as etching occurs. The sharp break in line C shows the result of transferring the gas to a fresh ampoule. The activation of the

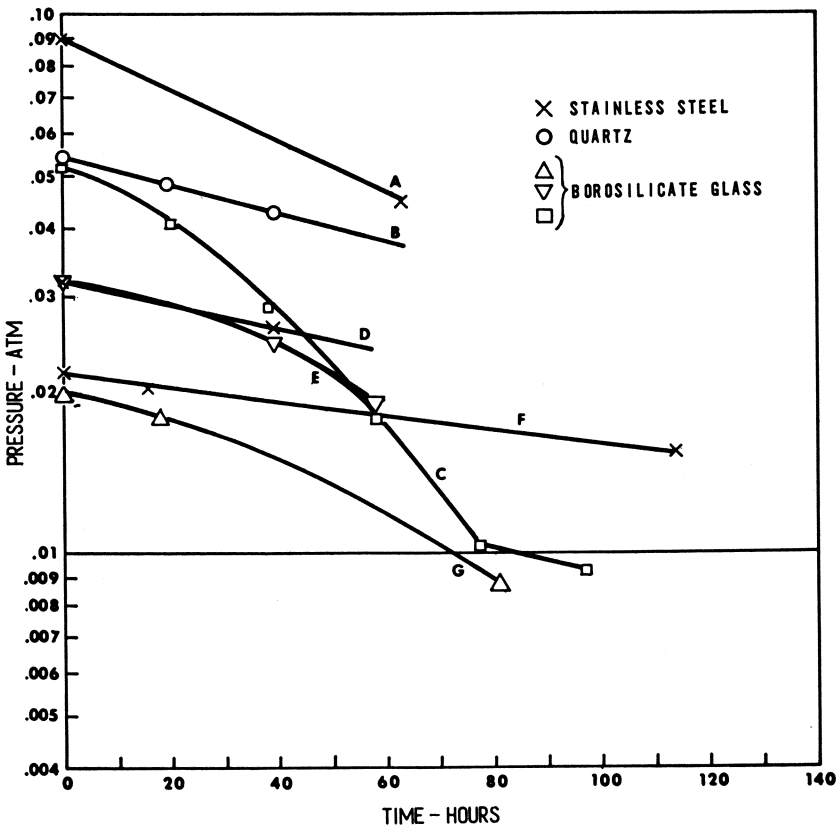

Figure 5. Decomposition of cis-N_2F_2 at 74°C.

glass walls apparently does not occur in the presence of water since the hydrolytic reactions remain first order over a long period of time. It is also significant that the rate of reaction with activated dry glass is

substantially greater than that in the presence of water. Approximately 25% of the *cis*-N_2F_2 is converted to N_2O in dry glass as compared with less than 3% in similar experiments involving water.

The results of experiments on the aging of *cis*-N_2F_2 in glass, quartz, and stainless steel are shown in Figure 5. The data indicate that the initial rate of decomposition at a given pressure is approximately the same in each of the materials tested.

The varying slope of lines A, D, and F (Figure 5) shows that the reaction rate in stainless steel increases proportionally more rapidly than the pressure. Additional experiments at pressures up to 12 atm. have demonstrated that the reaction is approximately second order with respect to the nitrogen fluoride (*7*), and similar results have been obtained with copper at 175° C. (*8*). Studies of the stainless steel system are complicated by the fact that the metal catalyzes the isomerization of N_2F_2 (*7*). No detectable isomerization occurs in either glass or quartz.

Experimental

Sealed borosilicate glass ampoules (*ca.* 135 ml.), equipped with one or more break seals, were used for all hydrolytic reactions. In the experiments involving NF_3 and caustic soda, the base was contained in loose-fitting Teflon cups within the ampoules to prevent attack on the glass. Infrared spectroscopy was generally used for the analysis of gaseous products.

Nitrogen trifluoride and tetrafluorohydrazine were obtained from Peninsular ChemResearch, Inc., and Air Products Inc., respectively. Difluorodiazine was prepared by the reaction of N_2F_4 with $AlCl_3$ at −78° C. (*9*).

Acknowledgment

This research was supported by the Advanced Research Projects Agency through the U.S. Army Research Office (Durham) under Contract No. DA-31-124-ARO-(D)-76.

Literature Cited

(1) Bronaugh, H. J., *ARPA Quart. Tech. Summ. Rept.* **HQ-76-4** (1964).
(2) Colburn, C. B., Johnson, F. A., Kennedy, A., McCallum, K., Metzger, L. C., Parker, C. O., *J. Am. Chem. Soc.* **81**, 6397 (1959).
(3) George, J. W., "Progress in Inorganic Chemistry," F. A. Cotton, ed., p. 41, Interscience Publishers, Inc., New York, 1960.
(4) Gould, E. S., "Inorganic Reactions and Structure," p. 216, H. Holt and Co., New York, 1956.
(5) Hine, J., "Physical Organic Chemistry," p. 137, McGraw-Hill, New York. 1956.

(6) Hoffman, C. J., Neville, R. G., *Chem. Rev.* **62**, 1, (1962).
(7) Hurst, G. L., Khayat, S. I., unpublished work.
(8) Hurst, G. L., Khayat, S. I., *ARPA Quart. Tech. Summ. Rept.* **HQ-76-7**, 5–7 (1964).
(9) Hurst, G. L., Khayat, S. I., *J. Am. Chem. Soc.* **87**, 1620 (1965).
(10) Lovelace, A. M., Rausch, D. A., Postelnek, W., "Aliphatic Fluorine Compounds," p. 137, Reinhold, New York, 1958.
(11) Lustig, M., *Inorg. Chem.* **4**, 104 (1965).
(12) Pankratov, A. V., Fercheninon, A. N., Talakin, O. G., Sokolov, O. M., Knyazeva, N. A., *Zh. Fiz. Khim.* **37**, 1399 (1963); *C. A.* **59**, 8191*c* (1963).
(13) Ruff, O., *Z. Anorg. Chem.* **197**, 283 (1931).
(14) Simon, J. H., "Fluorine Chemistry," Vol. I, p. 89, Academic Press Inc., New York, 1950.

RECEIVED August 6, 1965.

Measurement of Impact Sensitivity of Liquid Explosives and Monopropellants

DONALD LEVINE and CARL BOYARS

U. S. Naval Ordnance Laboratory, White Oak, Silver Spring, Md.

Publication Date: January 1, 1966 | doi: 10.1021/ba-1966-0054.ch025

Instrumentation of a standard drop-weight tester to give pressure-time records and further modification to permit high speed photography have allowed intimate study of the impact initiation-explosion process in nitroglycerin. A plot of peak impact pressure vs. concentration of conventional desensitizer (in nitroglycerin) gives a continuous, nearly linear relationship. The ratio of peak impact pressure to initial pressure is a most significant factor in determining probability of explosions of nitroglycerin. This is consistent with quasi-adiabatic compression of air bubbles as a step in the mechanism of initiation. The photographic studies support this mechanism, showing compression, breakdown of bubble structure (thereby causing more efficient heat transfer to the surrounding liquid), an induction period, and ignition starting in hot spots at the site of the bubble.

Because of the importance of knowing what mechanical shocks a liquid explosive will withstand, the relative order of sensitivity for different liquid explosives and monopropellants, and the effectiveness of those additives considered desensitizers, much work has gone into developing standard methods for determining impact sensitivity. Bowden and Yoffe (2) pointed out that initiation of explosives is generally a thermal process; mechanical energy supplied is converted to heat in a small region, forming a hot spot. For liquids, they considered adiabatic compression of small entrapped bubbles of gas and friction to be the two most important methods of generating hot spots. In initiation of liquids by impact, they showed that the absence of gas bubbles required much higher energies, and the necessary heating of the liquid was then attributed to viscous flow. To support the adiabatic compression hypothesis, they quoted data to show that increasing the initial gas pressure decreased the probability of initiation of explosion by impacts of the same kinetic energy.

In Advanced Propellant Chemistry; Holzmann, R.;
Advances in Chemistry; American Chemical Society: Washington, DC, 1966.

Bowden and Yoffe and others (*14*) have commented on the effect of γ (the specific heat ratio), the thermal diffusivity, and the reactivity of the trapped gas or vapor.

Johansson and co-workers (*7, 8, 9*) have shown that heat transfer from a compressed spherical bubble does not increase the temperature of its liquid surface sufficiently to account for the impact sensitivity of liquid explosives; the high sensitivity of nitroglycerin is postulated as arising from the fact that small droplets are readily formed by the impact and ignited by the compressed air. Bolkhovitinov (*1*) postulated crystallization of the liquid under the impact pressure, with the phase transition causing the temperature increase which causes explosions. Bowden (*3*) favors the adiabatic compression of gas bubbles combined with the dispersion of the explosive into fine particles as the mechanism for initiation by mechanical impact.

Starting with Bowden and Yoffe's adiabatic compression hypothesis, a method and apparatus (the Olin-Mathieson (O-M) drop-weight tester) were adopted by a committee on test methods (*11*). The technique was

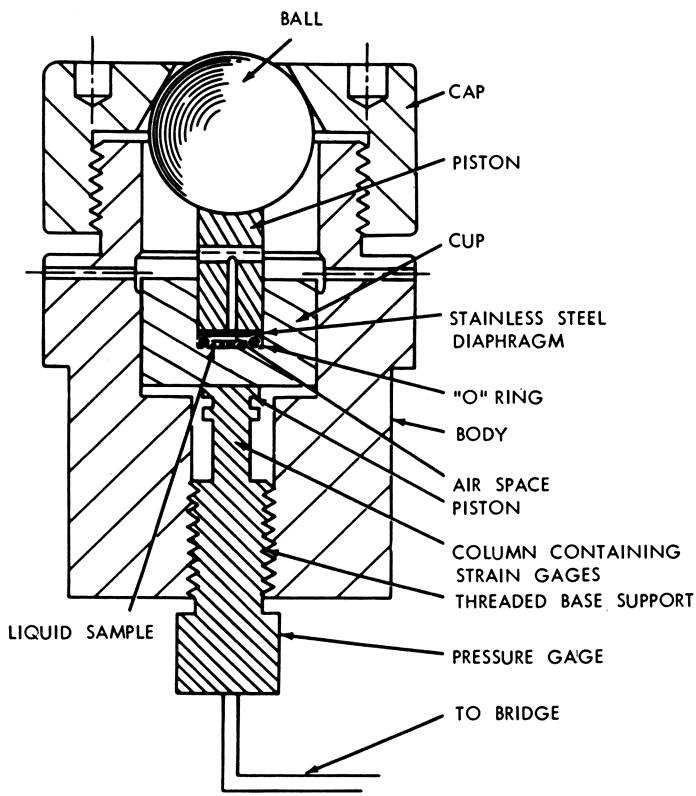

Figure 1. Details of sample cup assembly containing pressure gage

Publication Date: January 1, 1966 | doi: 10.1021/ba-1966-0054.ch025

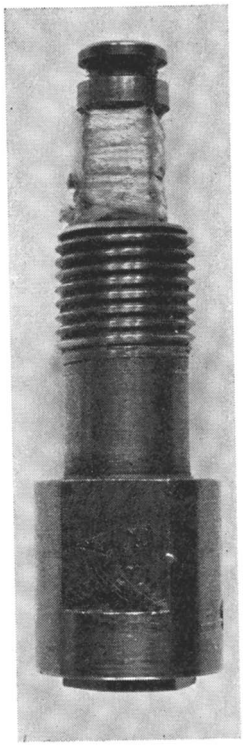

Figure 2. Pressure gage

later modified somewhat (*12*). Mason and co-workers (*13*) have emphasized the importance of supports for stabilizing the apparatus.

While investigating the effect of desensitizers on nitroglycerin (*10*), the authors introduced certain significant modifications in the O-M tester. The published results of that investigation describe the instrumented drop-weight apparatus but perhaps in insufficient detail. The modification does not affect the measured values of impact sensitivity of nitroglycerin solutions (comparing data obtained on the same apparatus prior to incorporating instrumentation), and a fuller description of the apparatus may be useful to other workers. In addition, further work has revealed certain interesting phenomena related to measuring impact sensitivity and the mechanism of initiation by impact which will be discussed here. These phenomena were studied by pressurization measurements and by photographing the compression-initiation-explosion process.

Pressure-Time Measurement

The original O-M apparatus has been adequately described (*11, 12*). The modifications which permit determination of pressurization rate,

maximum pressure, and impulse owing to impact have been briefly described (*10*). Figure 1 shows details of the sample cup assembly containing the pressure gage. The piston-type pressure gage has now been calibrated over the range 1–6800 atm. A photograph of the gage is shown in Figure 2. It is machined from a single piece of metal and consists of a piston, column, and a threaded base which serves to anchor the gage firmly to the sample cup assembly. The sensing elements are Baldwin strain gages (BLH FAB 12-12) which are bonded to the surface of the column with an adhesive; they are protected with a cloth covering. The strain of the column is directly proportional to the applied pressure. Calibration with a Tinius Olsen dead-weight tester showed the response of the pressure gage to be linear over the entire range. Placing the two strain gages on opposite faces of the pressure gage compensates for any bending of the column.

Publication Date: January 1, 1966 | doi: 10.1021/ba-1966-0054.ch025

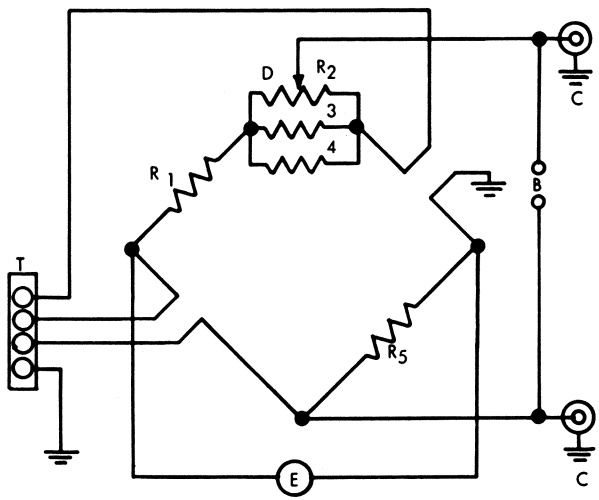

Figure 3. Bridge circuit. $R_1 = R_5 = 120$ *ohms;* $R_2 = 100$ *ohms (10 turns);* $R_3 = R_4 = 10$ *ohms; B = zero balance checkpoint to galvanometer/potentiometer; C = signal output to oscilloscope; D = balance control; E = 6-volt power supply; T = to pressure gage*

A line filter removes any extraneous signals generated from other electrical equipment in the area. The three-conductor, shielded cable from the gage to the Wheatstone bridge (Figure 3) is about 6 feet long. Type D Tektronix plug-ins are used in their differential mode with the oscilloscopes. The bridge is balanced accurately by means of variable resistance R_2, using a Leeds and Northrup potentiometer or a calibrated galvanometer. Alternatively, it can be balanced (less accurately) by

changing the input setting from a.c. to d.c. at the oscilloscope until there is no deflection of the beam when switching from a.c. to d.c.

The sample cup is then precompressed by means of a spanner wrench. The resistance change of the strain elements unbalances the bridge current, providing a deflection of the potentiometer, galvanometer, or oscilloscope beam. The same electrical equipment was used to calibrate the gage. In this way, the initial precompression and pressure *vs.* time during impact and explosion are accurately measured.

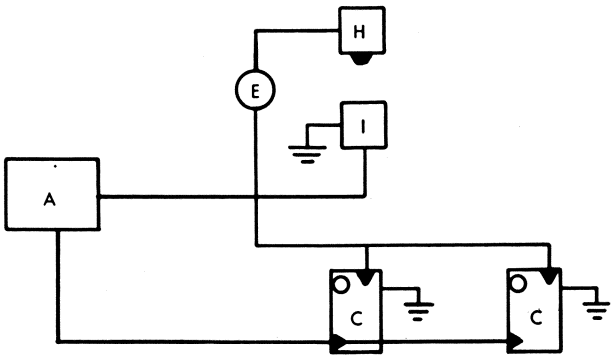

Figure 4. Block diagram of instrumentation on drop-weight apparatus. A = Wheatstone bridge; E = 22-volt battery; H = drop-weight hammer; I = assembly containing sample cup and pressure gage; C = oscilloscopes

The pressure developed in the initial precompression is measured with the more sensitive galvanometer or potentiometer; the higher pressures caused by impact and explosion are read as a function of time on the oscillograph. The oscilloscope sweep is triggered by the falling weight when it contacts the ball and piston of the sample cup assembly. Figure 4 is a block diagram of the apparatus.

Gray (*4, 5*) has made some measurements of the pressure-time relationship caused by impact and explosion of nitroglycerin, using the piezoelectric effect of a quartz crystal. Griffin (*6*) has described a pressure cell designed specifically for the O-M tester. It contains the standard sample holder components. Pressure from the impacted sample cup is transmitted through a system of pistons with O-rings and hydraulic fluid to a transducer. In that system, considerable energy loss occurs; greater impact energies were required for initiating explosives in the instrumented as compared with the uninstrumented apparatus. Griffin attributes this to compressibility of the hydraulic fluid and O-ring seals. One may expect that a system in which O-ring seals are used to prevent hydraulic fluid leakage around the pistons will also be subject to frictional losses and binding. Griffin also stated that the compressibility is responsible for a

downward movement of the pressure cell's anvil piston during an explosion ($\sim 3 \times 10^{-4}$ inch per 1000 p.s.i.g.); this causes an increase in volume of the sample cavity, reducing the maximum pressure sufficiently to prevent the sample cell diaphragm from rupturing. Rupture of this diaphragm is a normal event when a standard size sample (0.03 cc.) explodes.

The pressure-measuring apparatus described in this paper apparently does not affect the impact sensitivity of the nitroglycerin solutions tested. Tests have not been carried out on comparatively insensitive materials requiring high impulse and high energy for initiation, and it is possible that under such conditions differences in sensitivity might be shown between the instrumented and uninstrumented apparatus. However, the rugged, single-piece metal construction of the pressure gage and the fact that its linear deflection is only $\sim 2 \times 10^{-5}$ inch per 1000 p.s.i.g. should tend to minimize the differences.

Photographic Apparatus

Using a transparent plastic (Plexiglas) sample cup, motion pictures have been made of the impact and explosion processes of nitroglycerin in the O-M tester. The Dynafax model 326 camera can provide framing rates from 200–26,000 frames/sec. The maximum framing rate used in this study was 18,000 frames/sec. The camera was equipped with a magnetic pick-up, and its speed was controlled by means of a Variac. The output of the magnetic pickup supplied an input signal to a Berkeley electronic counter, accurately measuring the framing rate; therefore, no timing marks were needed on the film.

Strips of Kodak Tri-X and high speed Ektachrome 35 mm. film were used. The film length was $33^7/_8$ inches, cut with a specially designed cutter from a 100-ft. length of film.

A 6-inch, f/3.8 objective lens with coated optics was used in conjunction with a $4^1/_2$-inch extension tube. Three No. 5 medium peak flash bulbs connected in series provided the proper background lighting. The Dynafax capping shutter is equipped with a synchromatic delay which provided synchronization for this type of lamp.

The experimental setup is shown in Figure 5. A solenoid is mechanically connected to the arm of the release mechanism by means of an $11^1/_2$-inch length of metal tubing. It is connected electrically to a triggering switch through which the camera and a delay mechanism are also connected (Figure 6). When the switch is triggered, the electromagnet is energized, causing the weight to fall. The delay mechanism is also activated, postponing the energizing of the capping shutter and flash bulbs until 20 msec. before impact. A 20-msec. period was necessary for the flash bulbs to build up to peak intensity. The delay time—i.e., time be-

Publication Date: January 1, 1966 | doi: 10.1021/ba-1966-0054.ch025

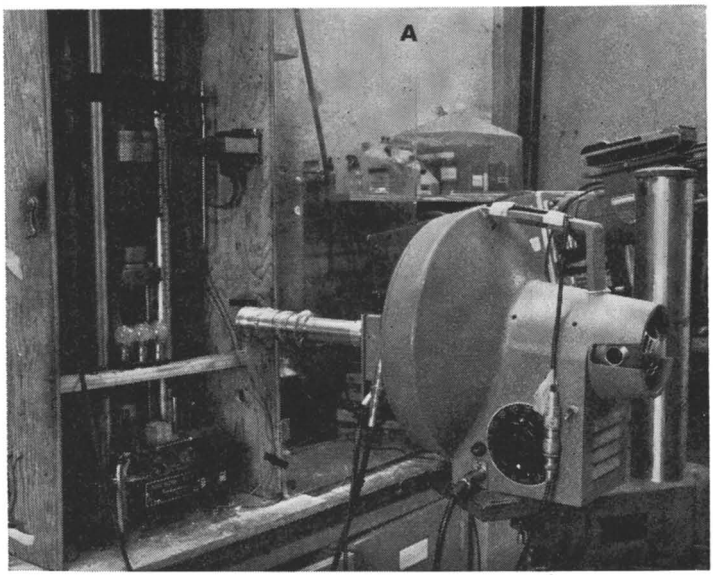

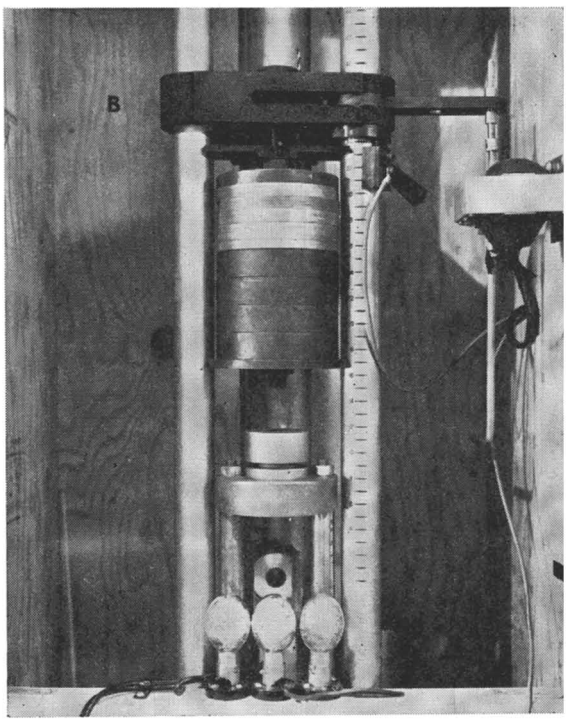

Figure 5. Apparatus for photographic studies, (A) showing location of camera, (B) showing location of posts, flashbulbs, and mirror below sample assembly; weights, release, and solenoid above

Publication Date: January 1, 1966 | doi: 10.1021/ba-1966-0054.ch025

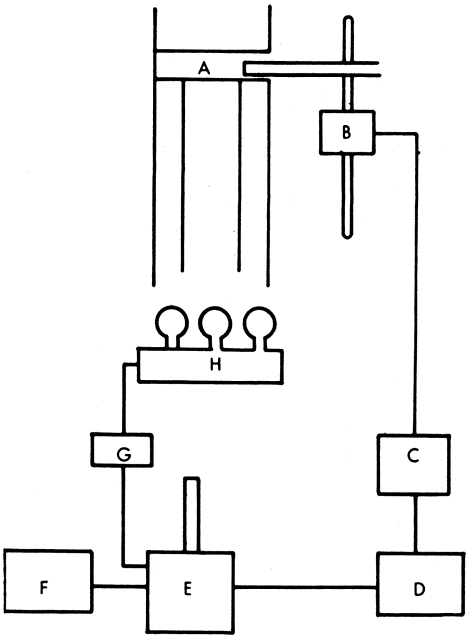

Figure 6. Block diagram of apparatus for photographic studies. (A) drop-weight tester, (B) solenoid, (C) triggering unit, (D) delay unit, (E) camera, (F) counter, (G) 22.5-volt battery, (H) flash unit.

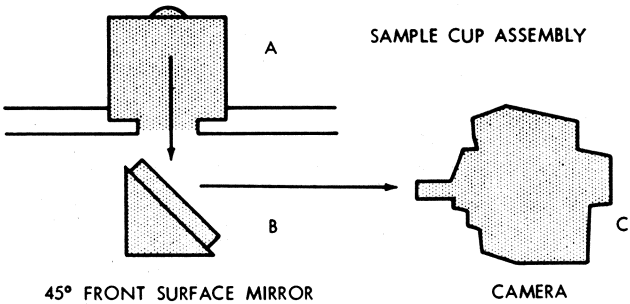

Figure 7. Front surface mirror arrangement; arrows indicate light path. (A) sample cup assembly, (B) 45° front surface mirror, (C) camera.

tween triggering the electromagnet which releases the weight and energizing the flash bulbs, was set by causing the switch to trigger a type 551 Tektronix dual beam oscilloscope and observing the time between the start of the sweep and the signal produced when the weights made con-

tact with the ball of the sample cup assembly. By connecting the delay unit to the second input of the oscilloscope, the delay time could be observed and varied, depending upon the height from which the weight was dropped. With this unit, delays from 30 to 200 msec. after release time could be achieved.

The plastic sample cup was polished and machined to the same dimensions as the standard metal cup. To contain the plastic cup, the standard body assembly was used except that one $^{11}/_{16}$-inch hole was made in the bottom of the assembly to permit the sample to be photographed. Two $^{3}/_{4}$-inch steel rods were screwed to the base of the tester. They had a 1-inch thick recessed plate to support the sample cup assembly and to provide space for the front surface mirror which was used to reflect the image to the camera (Figure 7).

Publication Date: January 1, 1966 | doi: 10.1021/ba-1966-0054.ch025

Results and Discussion

The earlier paper (*10*) reported impact pressure, rate of pressurization, ignition delay time, and pressure-time relationships during explosion as a function of concentration of desensitizers in nitroglycerin. Those data helped to explain the difficulty in getting reproducible test results on liquid explosives when the impacting weight is small; it was found that excessive pressure oscillation occurred during impact when a 1-kg. weight was used. The oscillographic data also illuminated several phenomena associated with impact testing—e.g., the effect of impacting weight and of drop height on the efficiency of conversion of momentum to impulse delivered to the sample and also on the pressurization rate of the sample. It was concluded that in order to eliminate differences in rate of impact pressurization, weights should be dropped from a constant height, as far as practicable, so that variation in the energy delivered is obtained by varying the weight only. The paper reported the decreases in deflagration rate and the increases in initiation delay time, in impulse delivered to the sample, and in impact weight required for 50% probability of initiation as a function of increasing desensitizer concentration. No difference was detected in effectiveness of the common desensitizers, triacetin, dibutyl phthalate, and dimethyl phthalate. A plot of impact weight at the 50% point *vs.* desensitizer concentration showed a much lower slope for the region 0–16% desensitizer (by weight) than for 16–30%. A "memory effect" was found—i.e., repeating the drop test with the same weight and height on a sample which had previously failed to ignite at or near the 50% point resulted in a positive test every time.

We have now found that a plot of peak impact pressure (rather than impacting weight) *vs.* desensitizer concentration gives a continuous, nearly linear relationship. Figure 8 is a plot of peak impact pressure *vs.* impacting weight from a height of 1 cm. Figure 9 is the plot of peak

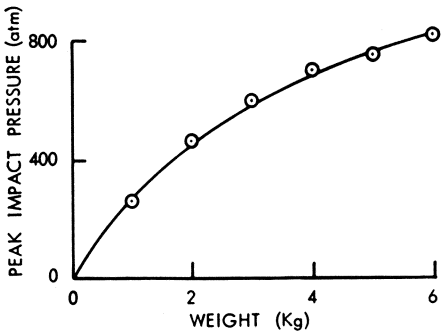

Figure 8. Peak pressure owing to impacting weight from a height of 1 cm.

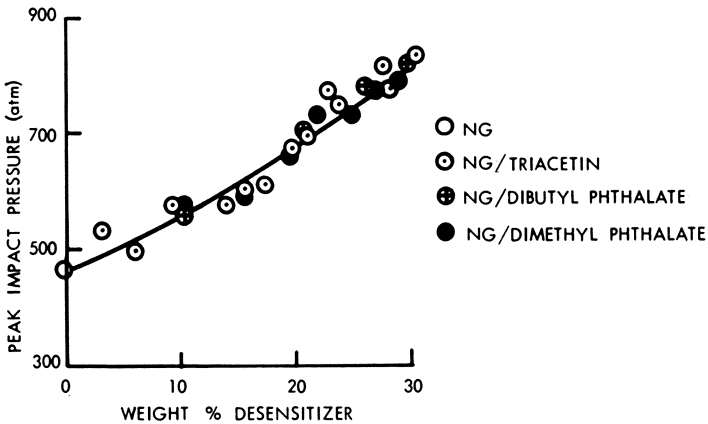

Figure 9. Impact pressure necessary to cause explosion (50% point) of nitroglycerin solutions when impacted from a height of 1 cm. with varying weights

Publication Date: January 1, 1966 | doi: 10.1021/ba-1966-0054.ch025

impact pressure *vs.* desensitizer concentration. These data were obtained using samples precompressed by the technique specified in the standard procedure (*12*)—i.e., by tightening the sample assembly cap with a torque wrench to a reading of 7 inch-lbs. This procedure we have found to give an initial pressure (before impact) of 18.5 ± 2 atm.

In order to get better reproducibility of initial pressure, we have changed the precompression technique, using a spanner wrench and controlling pressurization by reading the galvanometer or potentiometer. This is important for obtaining reproducible data for it has been shown (*2*) that the percent of impacts which result in explosion is decreased when initial pressure is increased. We have also found that the ratio of peak impact pressure to initial (precompressed) pressure is a most significant factor in determining probability of explosion of nitroglycerin. This is consistent with quasi-adiabatic compression as a step in the initia-

tion mechanism. Figure 10 shows probability of explosion as a function of compression ratio for nitroglycerin impacted from a height of 1 cm. with varying weights, using precompression to various initial pressures. The measurements of probability of explosion in Figure 10 are rather crudely performed (from a statistician's viewpoint); for each point, 10 nitroglycerin samples were prepared, the sample cups precompressed to identical initial pressures, the same weight dropped on each sample, and the number of positive tests recorded. Although the limit of precision of each impact pressure reading is estimated at ± 3 to ± 5%, a correlation between compression ratio and probability of explosion is apparent.

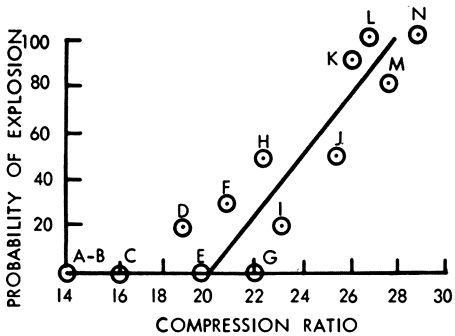

Figure 10. Probability of explosion vs. compression ratio for nitroglycerin impacted from a height of 1 cm. with varying weights using precompression to various initial pressures

Sample	*Weight kg.*	*Pressure atm.*
A	*4.8*	*51.2*
B	*2.3*	*37.6*
C	*2.8*	*36.9*
D	*4.8*	*38.4*
E	*1.5*	*18.5*
F	*2.3*	*25.6*
G	*1.7*	*18.5*
H	*6.0*	*38.4*
I	*1.8*	*18.5*
J	*2.0*	*18.5*
K	*4.8*	*27.8*
L	*6.0*	*32.0*
M	*2.2*	*18.5*
N	*2.3*	*18.5*

The data of Figure 10, incidentally, do not show that the probability of explosion of nitroglycerin on impact depends solely on compression ratio. The distribution of data points suggests that those samples at lower initial pressures require a somewhat higher compression ratio for the same probabilities of explosion than do those samples at higher initial pressures. If this observation is proved to be correct by further experiments, it could

Publication Date: January 1, 1966 | doi: 10.1021/ba-1966-0054.ch025

be explained by more efficient heat transfer from the compressed gas bubble in the case of higher initial pressures. The smaller gas volume containing the same amount of gas and the increased dispersion of liquid droplets accompanying the increased impact momentum both favor more efficient heat transfer to the liquid.

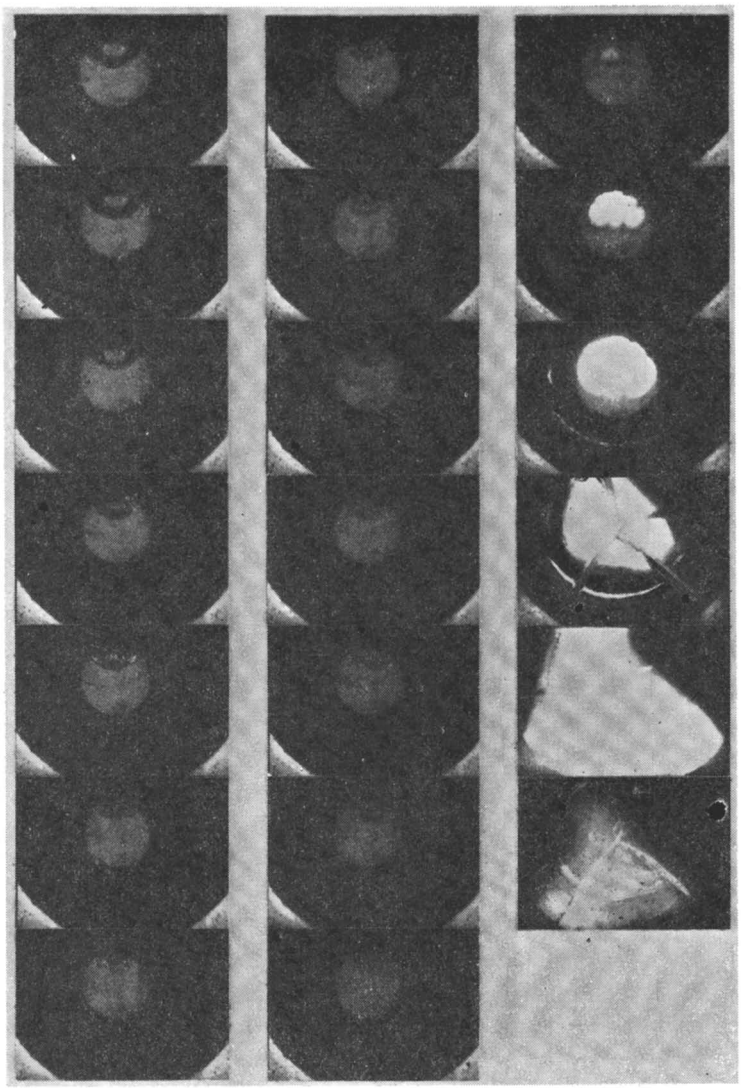

Figure 11. Photographic sequence of compression and subsequent explosion owing to impact momentum and energy corresponding to 50% probability of explosion; interframe time—100 μsec. Sequence is top to bottom, left to right

Publication Date: January 1, 1966 | doi: 10.1021/ba-1966-0054.ch025

The "memory effect" noted in our earlier paper is caused by the fact that pressurization within the sample cup decreases following an impact which does not produce explosion. A set of 20 samples initially pressurized to 18.5 atm. averaged 12.0 atm. after impact without explosion. On subsequent impact of the same sample cup with the same weight, the pressure ratio is substantially higher, and explosion results.

A significant conclusion from the data on the importance of compression ratio in initiating explosion of nitroglycerin is that processing or handling liquid explosives and monopropellants under reduced pressure may introduce a hazard by sensitizing the liquid to weak impacts.

In photographic studies, no initiations were observed with standard size, normally precompressed samples of nitroglycerin impacted with 2 kg. from a height of 1 cm. These impact conditions give 50% probability of initiation in the standard steel cup. Presumably, this is caused by the deformation of the plastic sample cup on impact and to the method of supporting it. It was found that a 5-kg. weight falling 1 cm. approximated the 50% initiation point, using the standard 30μl sample and a precompression of 7 inch-lb. torque. Figure 11 is a typical photograph of the impact and subsequent explosion of the nitroglycerin when struck with this weight falling 1 cm. The time between the separation of the frames is 100 μsec. The light region covering the major portion of the area in Figure 11 is liquid nitroglycerin while the dark area represents the interface of the gas bubble. The precompressed gas bubble appears not as a thin disk of air 9.30 mm. wide and 0.23 mm. thick as Mason and coworkers (*13*) postulated, but as a stationary, nonspherical bubble which adheres to the O-ring and sample container. Two much smaller bubbles are also visible. As the impacting weight contacts the steel ball, the gas begins to be compressed. Following this, droplets of liquid appear, and the structure of the bubble is destroyed and replaced by a turbulence area. After an induction period, initiation occurs in the region where the large bubble was located.

The velocity of the propagation of the luminous front is about 20 meters/sec. The maximum velocity which could be detected with this camera is about 100 meters/sec.

To determine the effect of impact energies above the 50% probability point, a 5-kg. weight was dropped from 2 cm. onto a 30-μl sample of nitroglycerin precompressed to 7 inch-lb. The camera speed was increased to 18,000 frames/sec., a frame separation of 55.6 μsec. Figure 12 shows the effect of the additional impact momentum and energy. The initiation this time appears to begin in more than one place in the region of the bubble breakup. The velocity of propagation increased from 20 to 36 meters/sec. In addition, the time between the impact and the first signs of luminous reaction decreased from 1.2 to 0.67 msec.

Publication Date: January 1, 1966 | doi: 10.1021/ba-1966-0054.ch025

Figure 13 shows the effect of increasing the torque to 15 inch-lb. and impacting the sample from a height of 1 cm. with 8 kg. With this increased precompression, the bubble appeared to be mobile; it shifted position when the cup was tilted (upon removal of the sample cup assembly from the drop-weight apparatus for observation). Subsequent to

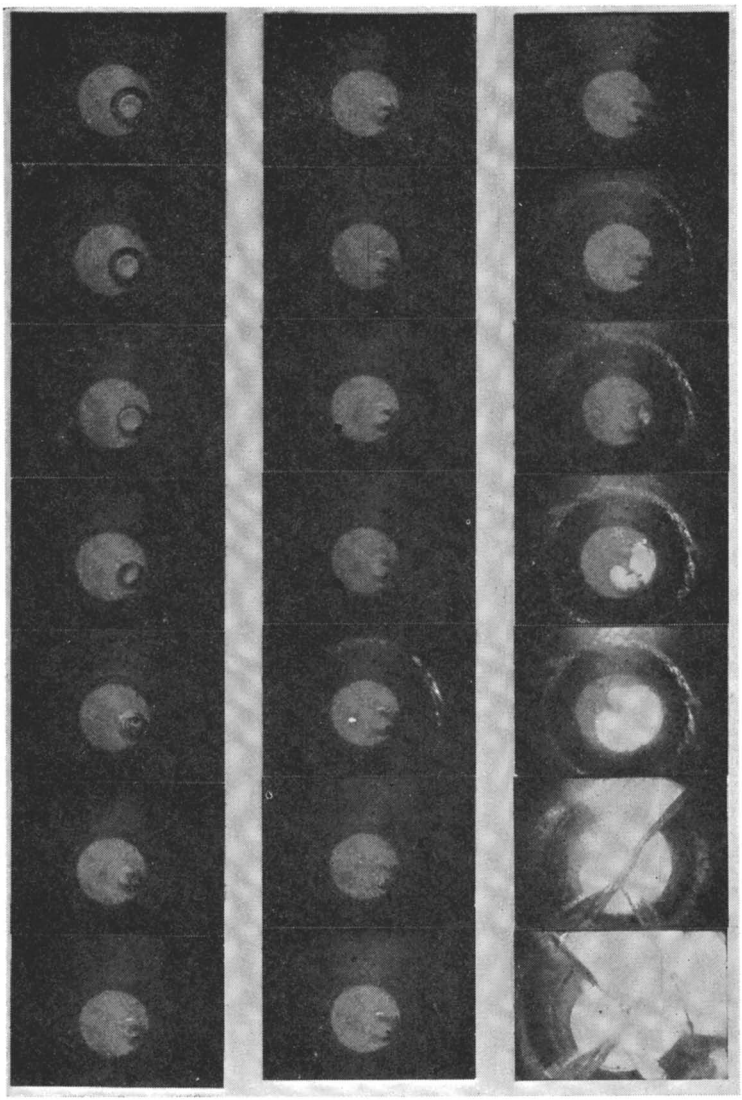

Figure 12. Photographic sequence of compression and subsequent explosion owing to impact momentum and energy well above 50% probability of explosion; interframe time—55.6μsec. Sequence is top to bottom, left to right

Publication Date: January 1, 1966 | doi: 10.1021/ba-1966-0054.ch025

Publication Date: January 1, 1966 | doi: 10.1021/ba-1966-0054.ch025

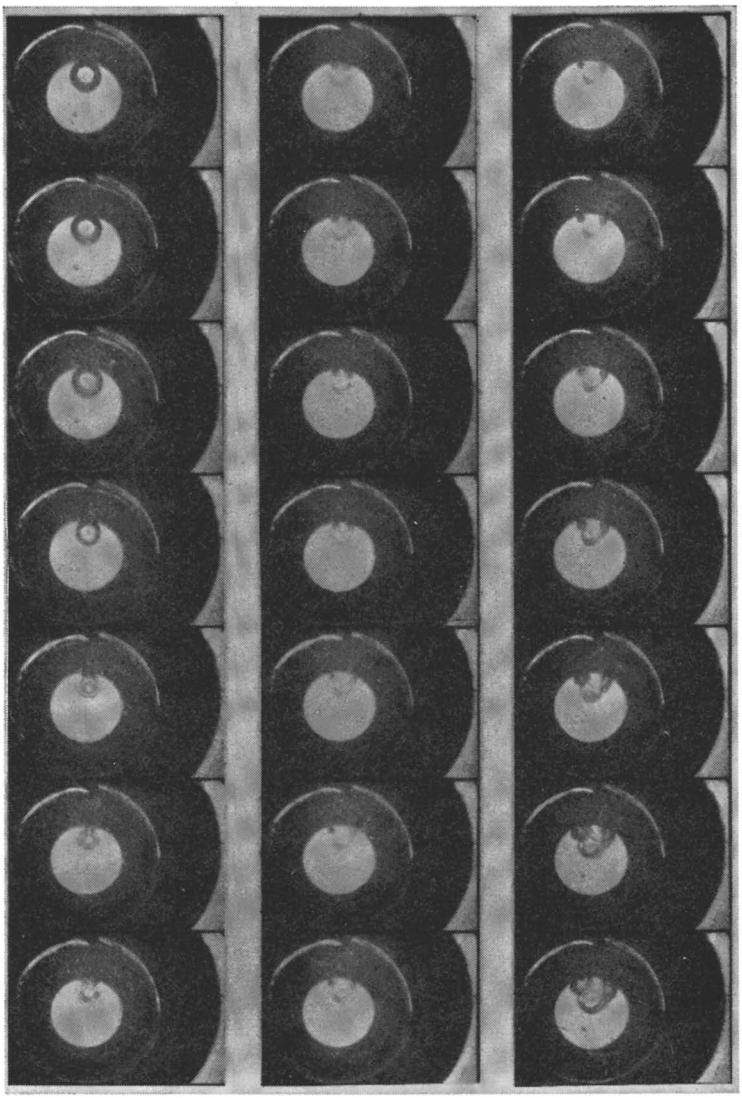

Figure 13. Photographic sequence showing impact compression and failure to explode because of high initial pressure; interframe time—111 μsec. Sequence is top to bottom, left to right

the impact without initiation, the bubble volume appeared to increase. This is caused by loosening of the cap. Presumably, if the sample were again impacted without tightening the cap, it would explode. However, this experiment was precluded by the fact that the plastic cup fractures on second impact. No initiations were observed on 30 μl samples pre-

compressed to 15 inch-lb. torque when impacted from a height of 3 cm. with 8 kg.

Figure 14 shows the results of increasing the sample volume, thereby decreasing the bubble volume. Instead of the usual 30 μl, 50 μl were used. The samples were compressed to 7 inch-lb. torque, and an 8-kg.

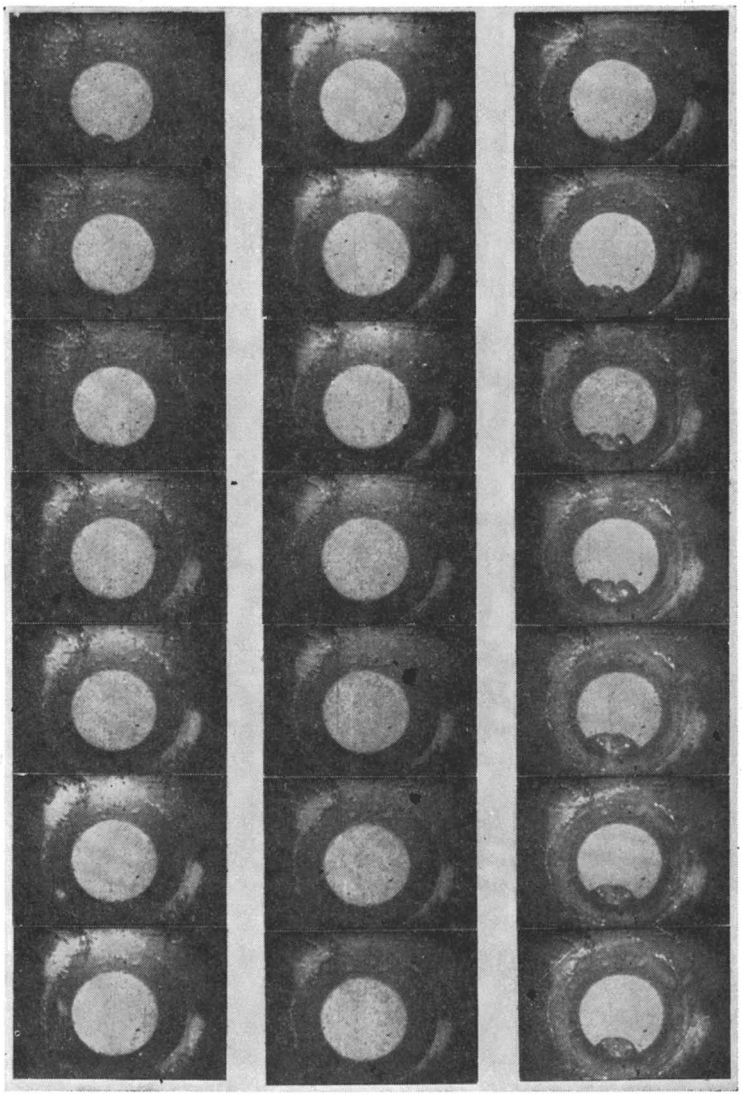

Figure 14. Photographic sequence showing impact compression and failure to explode because of increased sample size and corresponding decrease of air bubble volume; interframe time—222μsec. Sequence is top to bottom, left to right

Publication Date: January 1, 1966 | doi: 10.1021/ba-1966-0054.ch025

weight was dropped from 4 cm. Of five tests, only one ignition was observed, and this occurred after considerable delay; the explosion did not show on the film while the compression and expansion were observed. It may have occurred on a second impact of the rebounding weight, striking a much larger and lower pressure gas bubble.

Summary

Of the approximately 12 motion pictures we made of the impact initiation process, all show that the structure of the air bubble is broken down and replaced by a turbulence area. Ignition occurs at the former site of the bubble after an induction period. The compression ratio of the air bubble appears to be the major factor determining probability of initiation by impact. The mechanism for impact initiation of nitroglycerin therefore appears to be a quasi-adiabatic compression of the gas, with heat transfer accelerated by spray formation. Hot spots formed at the former site of the bubble undergo an accelerating exothermic reaction which proceeds to a deflagration. The possibility that liquid explosives under reduced pressure may be sensitized to weak impacts must be considered.

Acknowledgment

We wish to acknowledge H. Cleaver's assistance in electronic design and T. Stengel's assistance with the photographic apparatus.

Literature Cited

(1) Bolkhovitinov, L. G., *Dokl. Akad. Nauk. S.S.S.R.* **126**, 322 (1959), *C.A.*, **55**, 20433C (1961).
(2) Bowden, F. P., Yoffe, A. D., "Initiation and Growth of Explosion in Liquids and Solids," pp. 1–2, 28–55, Cambridge, University Press, New York, 1952.
(3) Bowden, F. P., *Symp. Combust., 9th, Cornell Univ., Ithaca, N. Y., 1962*, 499, 514 (1963).
(4) Gray, P., *Research (London)* **2**, 392 (1949).
(5) Gray, P., *Trans. Faraday Soc.* **46**, 849 (1950).
(6) Griffin, D. N., *ARS Propellants, Combust., Liquid Rockets Conf., Palm Beach, Fla., 1961*, Paper No. 1706–61.
(7) Johansson, C. H., Selberg, H. L., *Appl. Sci. Res.* **A5**, 439 (1955).
(8) Johansson, C. H., Persson, A., Selberg, H. L., *Symp. Combust. 6th, Yale Univ., 1956*, 606 (1957).
(9) Johansson, C. H. *et al.*, *Proc. Roy. Soc. (London)* **246**, 160 (1958).
(10) Levine, D., Boyars, C., *Combust. Flame* **9**, 131 (1965).
(11) "Liquid Propellant Test Methods Recommended," Chemical Propulsion Information Agency, The Johns Hopkins University Applied Physics Laboratory, Silver Spring, Md., 1959.

(12) "Liquid Propellant Test Methods, Test No. 4, Drop-Weight Test," Chemical Propulsion Information Agency, The Johns Hopkins University Applied Laboratory, Silver Spring, Md., 1964.
(13) Mason, C. M. *et al.*, *Intern. Conf. Sensitivity Hazards Explosives, London, 1963.*
(14) Moyle, M. P., Fedor, A. J., "The Mechanism of Explosion Initiations in the Standard Impact Sensitivity Tester," Institute of Research, Lehigh University, Bethlehem, Pa., 1964.

RECEIVED April 13, 1965. Released by the Commander, U. S. Naval Ordnance Laboratory.

Physical Properties of the Liquid Ozone–Fluorine System

A. J. GAYNOR and CHARLES K. HERSH

IIT Research Institute, Chicago, Ill.

Publication Date: January 1, 1966 | doi: 10.1021/ba-1966-0054.ch026

The density, viscosity, and surface tension of liquid ozone-fluorine mixtures were determined at —183° and —195.8° C. At the two temperatures investigated, the density can be determined from the following equations: $\rho_{-183°C.} = 0.1009$ *(wt. fraction* O_3*)* $+ 1.4704$ *and* $\rho_{-195.8°C.} = 0.0534$ *(wt. fraction* O_3*)* $+ 1.5611$. *The viscosity of solutions at —183° C. varies linearly (on a log scale) with the composition from 1.55 cp. for 100% ozone to 0.208 cp. for 100% fluorine. A similar relationship exists at —195.8° C., where the viscosity varies from 4.15 cp. for 100% ozone to 0.344 cp. for 100% fluorine. The ozone-fluorine mixtures are Newtonian fluids. Vapor pressure and vapor liquid equilibria data are also presented for pressures up to 20 atm.*

Utilizing the energetic oxidizers—ozone and fluorine—has been an aim of rocket technologists for many years. The physical properties of pure ozone and pure fluorine have been characterized well. Mixtures of ozone with oxygen (*1*) and fluorine with oxygen have also been characterized. The latter system is ideal while the former is not. It occurred to us that the physical properties of ozone-fluorine mixtures should be characterized so that this system could be evaluated more completely by liquid propellant technologists. Further, we expected that the mixtures might have superior properties.

With this intent we measured the density, surface tension, viscosity, and vapor pressure of the ozone-fluorine system at liquid oxygen and liquid nitrogen temperatures.

Experimental

Density. An apparatus and procedure similar to that described elsewhere (*1*) was used for the density measurements. A borosilicate glass

In Advanced Propellant Chemistry; Holzmann, R.;
Advances in Chemistry; American Chemical Society: Washington, DC, 1966.

U-tube, 4 mm. i.d. and 10 cm. long, was used for the density measurement. The volume of the U-tube was determined as a function of the distance from a reference mark at the bottom of the tube. Calibrations were made at room temperature, initially with water and carbon tetrachloride, and again at cryogenic temperatures with liquid oxygen. A measured amount of liquid ozone was transferred to the U-tube, and the procedure was repeated with enough liquid fluorine to result in a solution of the desired concentration.

Two techniques were used to aid in mixing the ozone and fluorine. One technique consisted of bubbling helium through the mixture. The second technique consisted of closing the valves separating the legs of the U-tube, raising the temperature of the gas slightly (less than 5 degrees), equalizing the pressure, and repeating the procedure.

Equilibrium between the liquid and vapor was noted by observing the pressure and color of the solution. Fluorine is pale yellow-green while liquid ozone is blue-black, and the color can therefore give a fair measure of solution uniformity. Pressure equilibrium was usually achieved with three heatings on alternate arms.

The fourth heating was used to give the pressure differential for manometrically determining the density. The temperatures of the liquid oxygen and nitrogen were obtained using an oxygen vapor-pressure thermometer. The densities obtained in this way are given in Table I; they represent an average of at least four independent measurements.

Table I. Density of Liquid Ozone-Fluorine Mixtures

Temperature °C.	*Ozone Concentration wt. %*	*Density, grams/cc.*	
		Measured	*Calculated*[a]
−183	0.0	1.472	1.470
	31.0	1.499	1.502
	84.6	1.557	1.556
	100.0	1.571	1.571
−195.8	0.0	1.561	1.561
	23.0	1.573	1.573
	61.8	1.595	1.594
	100.0	1.614	1.615

[a] From Equations 1 and 2.

These data were then reduced to straight-line functions on a Univac 1105 computer by the method of least squares. Equations 1 and 2 were used to determine the density of liquid ozone-fluorine mixtures at the two temperatures investigated.

$$\rho_{-183°C.} = 0.1009 \text{ (wt. fraction } O_3) + 1.4704 \quad \text{(deviation} = \pm 0.0013) \tag{1}$$

$$\rho_{-155.8°C.} = 0.0534 \text{ (wt. fraction } O_3) + 1.5611 \quad \text{(deviation} = \pm 0.0024) \tag{2}$$

Viscosity. The viscosity of ozone-fluorine mixtures was determined in a modified Ostwald viscometer (*1*) which was used with a variable volume of liquid. The viscometer was made from precision-bore glass tubing (4 mm. i.d.) with a capillary section 0.203 mm. in diameter and 12 cm. long.

Publication Date: January 1, 1966 | doi: 10.1021/ba-1966-0054.ch026

To force the liquid to a convenient height above the capillary section, either helium pressure was used or the metal tubes containing the equilibrium vapor over each leg were heated after the valves had been closed. Then the valve isolating the two arms of the viscometer was opened, and the readings of the height, h, of liquid as it fell through the capillary were taken as a function of time. The driving pressure was proportional to the difference between the liquid and the equilibrium levels $(h - h_e)$ and in uniform bore tubing the rate of flow was proportional to dh/dt. Hence, for a liquid following Poiseuille's law, log $(h - h_e)$ should be proportional to the time of flow. In every case a linear relation between log $(h - h_e)$ and time was obtained, which showed that ozone-fluorine solutions are Newtonian fluids.

The half time $(t_{1/2})$, which is the time required for the liquid to fall one-half the distance from the initial level to the equilibrium level, was determined from graphs of the time-height functions. The viscosity was calculated from Equation 3.

$$\eta = C\rho t_{1/2} L \tag{3}$$

where η = viscosity, ρ = density of the fluid, grams/cc., and C = an apparatus constant determined with liquids of known viscosity (1.289×10^{-2} centipoise-cc./sec.-gram).

Calibration fluids were water, ethylene glycol, and liquid oxygen. The results shown in Table II represent at least two independent measurements for each viscosity reported.

Table II. Viscosity of Ozone-Fluorine Mixtures

Ozone Concentration, mole	*Viscosity, cp.*	
	−183°C.	*−195.8°C.*
100.0	1.55 ± 0.01	4.15 ± 0.04
79.1	0.905 ± 0.01	
70.5		1.95 ± 0.01
30.5	0.343 ± 0.03	
26.8		0.682 ± 0.02
0.0	0.208 ± 0.01	0.344 ± 0.01

Surface Tension. The surface tension of various ozone-fluorine mixtures was determined by the capillary rise method in the apparatus used for the viscosity measurements (*1*) using Equation 4.

$$T = \frac{rhpq}{2} \tag{4}$$

where:

T = surface tension
r = radius of capillary, cm.
h = capillary rise, cm.
ρ = density of solution, grams/cc.
g = gravitational constant, cm./sq. sec.

Results at −183° and −195.8° C. are given in Table III. Again, the procedure and equipment are calibrated by determining the surface tension of known materials—e.g., liquid oxygen.

Publication Date: January 1, 1966 | doi: 10.1021/ba-1966-0054.ch026

Table III. Surface Tension of Ozone-Fluorine Mixtures

Ozone Concentration, mole %	*Surface Tension*	
	−183°C.	*−195.8°C.*
100.0	39.9	43.5
79.1	30.2	
70.5		35.6
30.5	19.1	
26.8		22.4
0.0	12.3	15.5

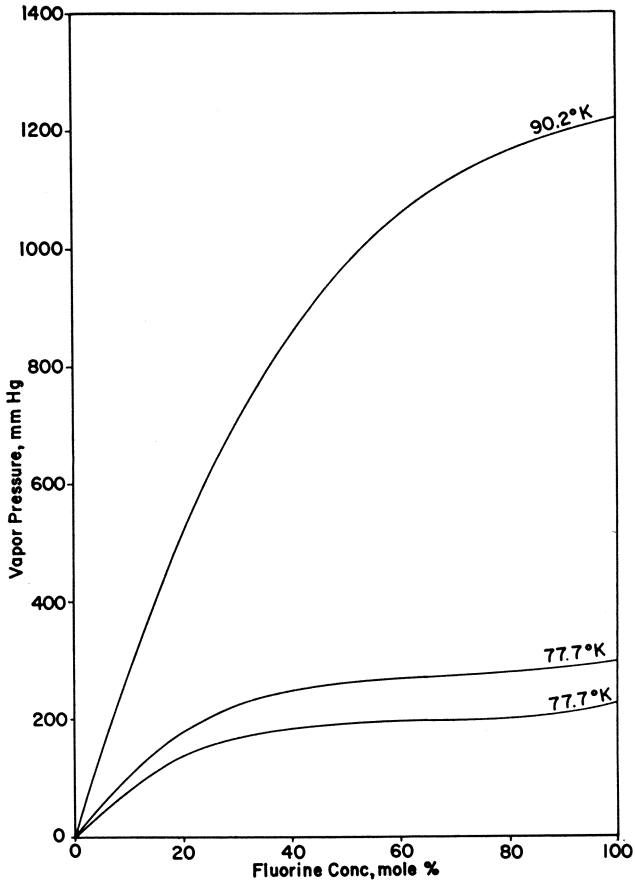

Figure 1. Vapor pressure of liquid ozone-fluorine mixtures

Vapor Pressure. Two different techniques (*1, 2*) were used to determine the vapor pressure of various liquid ozone-fluorine mixtures, depending on the pressures to be measured. The first technique was developed

Publication Date: January 1, 1966 | doi: 10.1021/ba-1966-0054.ch026

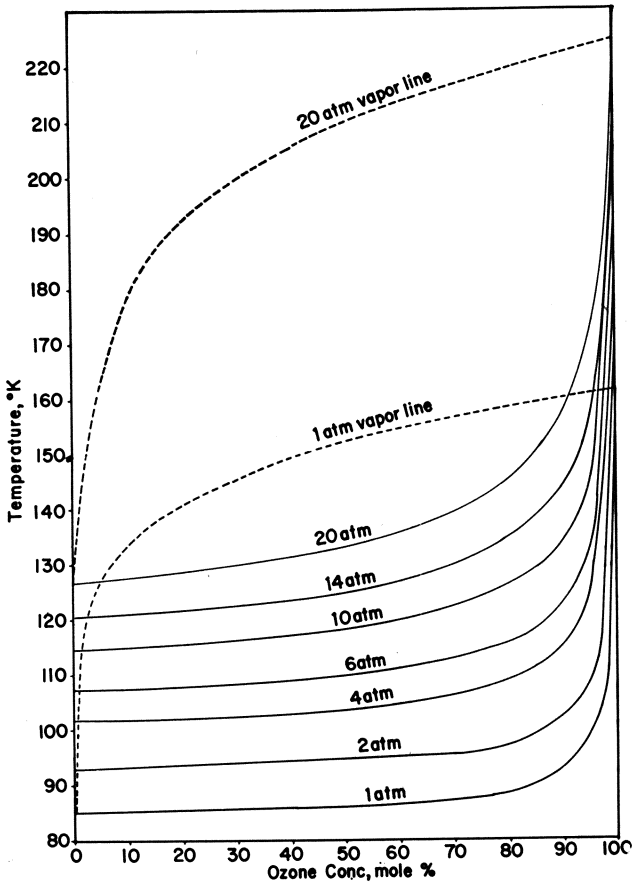

Figure 2. Vapor-liquid equilibrium diagram of ozone-fluorine system

for measurements at low pressures (1.5 atm.). The liquid ozone, which was condensed at liquid oxygen temperature (—183° C.) into a calibrated glass tube, was pumped on at reduced pressure to remove any residual oxygen; then the total volume was measured with a cathetometer. The measured amount of ozone was then transferred quantitatively to a glass tube by distillation. The above procedure was repeated with liquid fluorine condensed at liquid nitrogen temperature, and the two liquids were allowed to come to equilibrium before a vapor pressure reading was taken. In this apparatus both color and constant pressure were used to determine equilibrium. Readings were taken at bath temperatures of 75.7°, 77.7°, and 90.2° K. These temperatures were measured with an oxygen vapor pressure thermometer. After the initial values had been determined, additional known amounts of fluorine were admitted to the U-tube, and vapor pressure readings were taken again. The data obtained in this way

for a series of ozone-fluorine mixtures are given in Figure 1. A total of 16 experimental points were used to determine each curve.

It was thought that a stirring bar would ensure a homogeneous solution of the two liquids in the modified apparatus. However, in each of the three attempts to use a Teflon-coated stirring bar on the greater than 90 mole % ozone mixtures, the apparatus was destroyed by an explosion. Apparently, the mixtures which have high ozone concentrations are as sensitive to the wiping action of the stirring bar along the glass surface of the reservoir as is 100% ozone (from previous experience).

In the second technique (to 20 atm.), the apparatus was an all-metal system similar to that used for measurements on ozone-oxygen mixtures (*2*). The test chamber was constructed of stainless steel. It consisted of 1-inch bar stock (1-$^1/_2$ inches long), Swagelok fittings, a pressure gage, and a copper-constantan thermocouple. The system had a volume of 20.1 cc.

The experimental procedure consisted of determining the liquid lines. The results are shown in Figure 2. When the volume of vapor in a closed system is kept small relative to the volume of liquid, the amount of liquid that must be vaporized to give a 20-atm. pressure is small. Thus, the composition of the liquid will be changed by only a negligible amount. For these determinations the composition of the ozone and fluorine charge was known accurately, and a provision was made for agitating the test bomb. Over 100 separate measurements were used to obtain the liquid lines.

As determined by this method, the vapor pressure of pure fluorine agreed with the value reported by Landau (*4*), and the vapor pressure of oxygen agreed with the value reported by Hilsenrath *et al.* (*3*). This verified the fact that the pressure and temperature indicators were correct relative to each other.

Results and Conclusions

These studies indicate that liquid ozone-fluorine mixtures are homogeneous and do not form a two-phase region as does the ozone-oxygen system. Mixtures of 30% ozone in fluorine require very few handling precautions over those observed with 100% liquid fluorine.

The 1- and 20-atm. vapor lines, as shown in Figure 2, were constructed from the liquid data and the vapor pressure of pure ozone using Equation 5:

$$y = xP/P_t \tag{5}$$

where y is the mole fraction of ozone in the vapor, x is the mole fraction of ozone in the liquid, P is the vapor pressure of ozone, and P_t is the total pressure. Thus, Figure 2 represents the vapor-liquid equilibrium diagram of the ozone-fluorine system although the diagram is of course subject to the errors associated with the use of Raoult's and Dalton's laws.

The viscosity of the solution decreases rapidly as fluorine is added. A semilog plot of viscosity of the mole fraction gives a straight line at both temperatures which is typical of a nonassociated liquid. The surface tension of ozone is approximately three times that of oxygen.

Publication Date: January 1, 1966 | doi: 10.1021/ba-1966-0054.ch026

Acknowledgment

This work was supported at IIT Research Institute by the National Aeronautics and Space Administration under Contract No. NASw-76.

Literature Cited

(1) Hersh, C. K., Berger, A. W., Brown, J. R. C., ADVAN. CHEM. SER. **21**, 22 (1959).
(2) Hersh, C. K., Brabets, R. I., Platz, G. M., Swehla, R. J., Kirsh, D. P., *ARS J.* **30**, 264 (1960).
(3) Hilsenrath, J. *et al. Nat. Bur. Std. (U.S.), Circ.* **564** (1955).
(4) Landau, R., Rosen, R., "Preparation, Properties, and Technology of Fluorine and Organo-Fluoro Compounds," Chap. 7, C. Slesser, ed., McGraw-Hill Book Co., New York, 1951.

RECEIVED May 3, 1965.

Publication Date: January 1, 1966 | doi: 10.1021/ba-1966-0054.ch026

INDEX

Publication Date: January 1, 1966 | doi: 10.1021/ba-1966-0054.ix001

In Advanced Propellant Chemistry; Holzmann, R.;
Advances in Chemistry; American Chemical Society: Washington, DC, 1966.

O

P

Q

R

S

T

V

Publication Date: January 1, 1966 | doi: 10.1021/ba-1966-0054.ix001